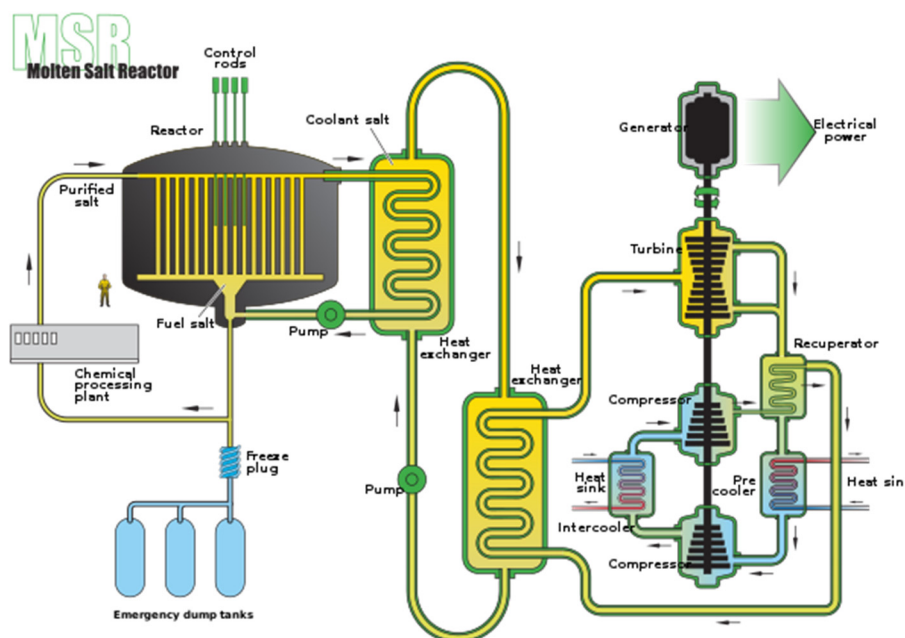


# Molten Salt Reactor Salt Processing – Technology Status

Guy Fredrickson, Guoping Cao,  
Ruchi Gakhar, and Tae-Sic Yoo

August 2018

The INL is a  
U.S. Department of Energy  
National Laboratory  
operated by  
Battelle Energy Alliance



#### **DISCLAIMER**

This information was prepared as an account of work sponsored by an agency of the U.S. Government. Neither the U.S. Government nor any agency thereof, nor any of their employees, makes any warranty, expressed or implied, or assumes any legal liability or responsibility for the accuracy, completeness, or usefulness, of any information, apparatus, product, or process disclosed, or represents that its use would not infringe privately owned rights. References herein to any specific commercial product, process, or service by trade name, trade mark, manufacturer, or otherwise, does not necessarily constitute or imply its endorsement, recommendation, or favoring by the U.S. Government or any agency thereof. The views and opinions of authors expressed herein do not necessarily state or reflect those of the U.S. Government or any agency thereof.

# **Molten Salt Reactor Salt Processing – Technology Status**

**Guy Fredrickson, Guoping Cao, Ruchi Gakhar, and Tae-Sic Yoo**

**August 2018**

**Idaho National Laboratory  
INL ART Program  
Idaho Falls, Idaho 83415**

**<http://www.inl.gov>**

**Prepared for the  
U.S. Department of Energy  
Office of Nuclear Energy  
Under DOE Idaho Operations Office  
Contract DE-AC07-05ID14517**





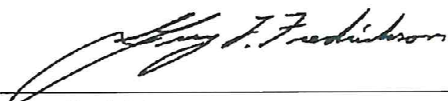
INL ART Program

# Molten Salt Reactor Salt Processing – Technology Status

INL/EXT-18-51033  
Revision 0

August 2018

Author:

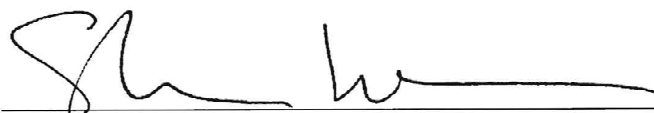


Guy Fredrickson  
Researcher, Pyrochemistry and Molten Salt Systems Department

8/29/2018

Date

Technical Reviewer:



Stephen Warman  
Project Manager, Pyrochemistry and Molten Salt Systems  
Department

8/29/2018

Date

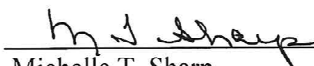
Approved by:



Diane V. Croson  
INL ART Deputy Director

8/29/18

Date



Michelle T. Sharp  
INL Quality Assurance

8/29/18

Date

## REVISION LOG

[illegible]

## SUMMARY

This report presents a summary of 752 citations related to molten salt reactor development at Oak Ridge National Laboratory (ORNL). This effort was initiated with a focused purpose of locating technical information related to the chemical processing of fluoride salts to support the Th-232/U-233 fuel-cycle molten salt breeder reactor (MSBR). However, it soon became apparent that technical information on chemical processing was spread throughout numerous reports spanning decades of time. Therefore, the search effort was broadened to include any information deemed relevant to molten salt reactor development at ORNL.

In addition, this report provides an overview of the engineering requirements for a chemical processing plant to support the Th-232/U-233 fuel-cycle MSBR. This includes descriptions of the unit operations and flowsheets developed at ORNL. The transition from the two-fluid MSBR to the single-fluid MSBR was largely due to the development of new separations technologies for the management of uranium, protactinium, and fission products in fluoride molten salts. The development and refinement of chemical processing plant flowsheets continued throughout the entirety of the MSBR program at ORNL. A great deal of experimental and theoretical work was performed in support of the unit operations and flowsheets described here.

The report also summarizes the literature on thermo-physical properties and phase diagrams for salts (both fuel and coolant salts) considered for various designs discussed as part of molten salt reactor development at ORNL. In addition, properties for several salt-mixtures (binary and ternary) identified for application as coolant salts for molten salt reactors, advanced high-temperature reactors, and other advanced reactor designs, are included. The consolidated data help identify the current knowledge and the relevant literature gap for a particular system of interest.

MSBR and molten chloride fast reactors (MCFR) can use the fuel elements from the spent nuclear fuels. To recycle the spent nuclear fuels for preparing the fuels for MSBR and MCFR, two head-end processes, fluorination and chlorination, for reprocessing the spent nuclear fuels were reviewed. To make the fluoride salts for MSBR, the majority of the spent fuels including uranium oxide, uranium nitride, and metal fuels can be fluorinated by using fluorine gas ( $F_2$ ) or other fluorinating gases such as  $HF$ ,  $ClF_3$ ,  $BrF_3$ ,  $2NH_4HF_2$ ,  $NF_3$ . During the fluorination process, the volatile  $UF_6$  can be separated easily by chemical reaction between spent fuel and fluorination reagent, followed by sorption and then desorption.  $UF_6$  can be further easily reduced to the  $UF_4$  suitable for MSBR. To make the chloride salts for MCFR, the spent oxide fuels can be chlorinated by  $CCl_4$ ,  $COCl_2$ ,  $Cl_2-CCl_4$ ,  $NH_4Cl$ , or  $Cl_2$  gas with carbon presence, and  $MoCl_5$  etc.  $CCl_4$  appears a widely used chlorination reagent. Due to the solid gas reaction characteristic, powders with higher surface areas were preferred for improving the efficiency and chlorination reaction kinetics. In recent years, by using non-corrosive  $ZrCl_4$  as chlorinating reagents and employing a liquid phase (for example  $LiCl-KCl$  at  $500^\circ C$ ) chlorination process, the spent oxide fuels ( $UO_2$ ,  $PuO_2$ ) were reportedly chlorinated effectively.

Materials corrosion (which is strongly affected by the molten salt chemistry, among others) is a significant issue and needs to be well-controlled for long-term operation of a molten salt reactor. The purification of and materials corrosion in both fluoride and chloride salts are reviewed. Owing to the molten salt reactor experiment program in 1960s and recent U.S. Department of Energy supported programs in fluoride salts (particularly FLiBe salt), a large data base of molten salt chemistry (including salt purification and materials corrosion control) exists. The purification of the fluoride salt can be achieved by  $H_2/HF$  gas mixture sparging followed by hydrogen sparging and filtering. Other non-corrosive fluorination reagents were also reported for purification of fluoride salts. If the salt is controlled at a slightly reducing redox potential, by controlling the  $UF_4/UF_3$  ratio at a desired value, the corrosion of the candidate alloys, such as Hastelloy N and 316SS, is expected to be minimized.

The available data for corrosion of materials in fluoride salts is limited, and even less data is available for chloride salts. The purification of chloride salt is not as established as that of fluoride salt, and the oxide impurity in the chloride salts is more difficult to be removed by HCl sparging.  $CCl_4$  gas sparging is found much more effective than the HCl sparging. To make high quality, impurity free chloride salts, a standardized purification process is desired. Current results on the corrosion of materials in chloride salts are not consistent, probably due to different experimental conditions and the unknown impurity in the tested chloride salts. For example, the effects of chromium content in the alloy and temperature on the corrosion of materials in the chloride salts are not clear. An improved understanding on chloride salt corrosion mechanism is needed. To select the most suitable materials for long-term service in chloride fast reactors, further systematic study is needed.

The attempts to adopt the electrochemical separation processes to the molten salt reactor system are relatively new, and few literature results on this effort are available. The motivation of this effort is that a well-designed electrochemical separation process for the treatment of the involved salt in the MSR can be beneficial in terms of cost, simplicity, and waste minimization. From the perspective of electrochemically treating the salt for separating undesirable constituents, the relative stability of salt species plays an important role. Ideally, one may want to have a salt system with the least stable species that needs to be separated as a neutron poison fission product. Thus, with a reactor system requiring molten salt reprocessing to maintain reactor performance, the choice of salt species allowing a simple separation process should be another important requirement. This requirement can be systematically approached by examining the relative stability of the candidate species expressed with the standard state free energy formation. Given the preliminary information on the relative stability of the salt species, the pertinent challenges associated with the treatment of the molten salt in supporting the molten salt reactor operation are discussed.

# CONTENTS

SUMMARY .....	vii
ACRONYMS .....	xvii
1. SUMMARY OF TECHNICAL DOCUMENTS RELATED TO MOLTEN-SALT REACTOR DEVELOPMENT AT OAK RIDGE NATIONAL LABORATORY .....	1
1.1 Introduction .....	1
1.2 Aircraft Nuclear Propulsion Program .....	2
1.3 Early Development of Civilian Power Liquid-Fuel Reactor Technologies .....	6
1.4 Fluorination and Fluoride Volatility Processing .....	6
1.5 Two-Fluid Molten Salt Breeder Reactor .....	7
1.6 Molten Salt Reactor Experiment .....	9
1.7 Molten Salt Reactor Experiment Decommissioning .....	10
1.8 Molten Salt Converter Reactor .....	10
1.9 Molten Salt Breeder Experiment .....	10
1.10 Molten Salt Reactor Demonstration .....	11
1.11 Single-Fluid Molten Salt Breeder Reactor .....	11
1.12 Denatured Molten Salt Reactor .....	11
1.13 Subsequent Reports .....	13
1.14 Annual, Semiannual, and Quarterly Reports .....	13
1.15 Technology Evaluation Reports .....	13
1.16 External Publications by Oak Ridge National Laboratory Research Staff .....	13
1.16.1 Information Resources .....	13
2. FUNCTIONAL ENGINEERING REQUIREMENTS OF A CHEMICAL PROCESSING PLANT TO SUPPORT A 1,000 MWE TH-232/U-233 FUEL-CYCLE MOLTEN-SALT BREEDER REACTOR .....	15
2.1 Introduction .....	15
2.2 Breeding .....	16
2.2.1 Th-232/U-233 Fuel Cycle .....	16
2.2.2 Brief Note on the U-238/Pu-239 Fuel Cycle .....	18
2.3 Comparison of Performance Characteristics of Three Reactors .....	18
2.4 Management of Pa-233 in the Th-232/U-233 Fuel-Cycle MSBR .....	23
2.5 Modeling of the MSBR and the Chemical Processing Plant .....	25
2.6 Chemical Processing Plant Studies .....	27
2.7 Chemical Processing Unit Operations .....	33
2.8 Fluorination .....	33
2.9 UF <sub>6</sub> Purification .....	35
2.10 UF <sub>6</sub> Reduction .....	35
2.11 Vacuum Distillation .....	36
2.12 Reductive Extraction .....	37
2.13 Multistage Contactors .....	39

2.14	Hydrofluorination.....	39
2.15	Metal Transfer Process.....	40
2.16	Electrolytic Oxidizer/Reducer.....	44
2.17	Oxide Precipitation .....	47
2.18	Selective Crystallization .....	47
2.19	Process Gas Purification .....	47
2.20	Fates of Fission Products .....	48
2.21	Chemical Processing Plant Flowsheets.....	48
3.	HEAD-END PROCESSES .....	54
3.1	Fluorination.....	54
3.2	Key Findings and Future Research and Development Needs for Fluorination.....	60
3.3	Chlorination .....	61
3.4	Key Findings and Future Research and Development Needs for Chlorination .....	67
4.	MOLTEN SALT CHEMISTRY MANAGEMENT.....	68
4.1	Fluoride Salt Purification.....	68
4.2	Corrosion in Fluoride Salt.....	68
4.2.1	Intrinsic Corrosion .....	68
4.2.2	Impurity Driven Corrosion.....	68
4.2.3	Temperature Gradient Driven Corrosion .....	71
4.2.4	Dissimilar Materials Effects.....	72
4.2.5	Stress Corrosion Cracking .....	72
4.2.6	Corrosion Data in FLiBe Salt.....	72
4.3	Chloride Salt Purification.....	74
4.4	Corrosion in Chloride Salt .....	74
4.5	Key Findings and Future Research and Development Needs.....	78
5.	LITERATURE REVIEW ON THERMO-PHYSICAL PROPERTIES AND PHASE DIAGRAM OF MOLTEN SALTS FOR MSR APPLICATIONS.....	79
5.1	Introduction.....	79
5.2	Fuel Salts.....	79
5.2.1	Fluoride Salts .....	79
	<i>Aircraft Nuclear Propulsion</i> .....	80
5.2.2	Chloride Salts.....	87
5.3	Coolant Salts .....	91
5.3.1	Alkali Fluorides.....	92
5.3.2	ZrF <sub>4</sub> Containing Salts.....	96
5.3.3	BeF <sub>2</sub> Containing Salts .....	101
5.3.4	Chloride Salts.....	106
5.3.5	Fluoroborate Salts .....	110
5.4	Conclusions.....	113
6.	APPLICATION OF ELECTROCHEMICAL TECHNIQUES FOR EMERGING MOLTEN SALT REACTOR SYSTEMS.....	115
6.1	Introduction.....	115

6.2	Chemical Stability of Fluoride and Chloride Species .....	115
6.3	Related Literature Results and Challenges .....	119
7.	REFERENCES .....	122
	Appendix A Citation Tables .....	130

## FIGURES

Figure 1-1.	Schematic of the ARE reactor vessel (ORNL-1845). .....	4
Figure 1-2.	Schematic of the Aircraft Reactor Test reactor vessel (ORNL-2095).....	5
Figure 1-3.	Schematic of the proposed two-fluid MSBR reactor vessel (ORNL-3996).....	8
Figure 1-4.	Schematic of the MSRE reactor vessel (ORNL-TM-728). .....	9
Figure 1-5.	Photograph of the MSRE assembled reactor system (ORNL-TM-728). .....	10
Figure 1-6.	Schematic of the proposed single-fluid MSBR reactor vessel (ORNL-4812). .....	12
Figure 2-1.	Depiction of a two-fluid MSBR. ....	15
Figure 2-2.	Depiction of a single-fluid MSBR. ....	16
Figure 2-3.	Fissile consumption as a function of energy production. ....	19
Figure 2-4.	Mass flowrate of coolant. ....	20
Figure 2-5.	Volumetric flowrate of coolant ( $\text{m}^3 \text{s}^{-1}$ ).....	21
Figure 2-6.	Volumetric flowrate of coolant (gpm).....	21
Figure 2-7.	Coolant cycle time.....	22
Figure 2-8.	Pa-233 management in the single-fluid MSBR.....	24
Figure 2-9.	Steady state Pa-233 concentration and extraction rate as a function of cycle time.....	25
Figure 2-10.	Conceptual performance space.....	26
Figure 2-11.	Schematic of a “frozen-wall” fluorinator [8]. ....	34
Figure 2-12.	Flowsheet for $\text{UF}_6$ purification flowsheet [8].....	35
Figure 2-13.	Schematic of a continuous $\text{UF}_6$ reduction column [8].....	36
Figure 2-14.	Schematic of a vacuum distillation still [8].....	37
Figure 2-15.	Ellingham diagram of select fluorides.....	38
Figure 2-16.	Gibbs free energies of select fluorination and hydrofluorination reactions. ....	40
Figure 2-17.	Gibbs free energies of select lithium reduction reactions. ....	41
Figure 2-18.	Gibbs free energies of select thorium reduction reactions. ....	42
Figure 2-19.	Gibbs free energies of select lithium reduction reactions. ....	42
Figure 2-20.	Gibbs free energies of select thorium reduction reactions. ....	43
Figure 2-21.	Illustration of the metal transfer process. ....	44
Figure 2-22.	Flowsheet for the metal transfer process [9]. ....	44

Figure 2-23. Schematic of the electrochemical oxidizer/reducer [10].	46
Figure 2-24. Flowsheet including an electrolytic cell in a reductive extraction circuit [11].	47
Figure 2-25. Flowsheet of chemical processing plant supporting a two-fluid MSBR caustic scrubber [12].	49
Figure 2-26. Flowsheet of chemical processing plant supporting a two-fluid MSBR NaF and $MgF_2$ [13].	49
Figure 2-27. Flowsheet of chemical processing plant supporting a two-fluid MSBR protactinium [14].	50
Figure 2-28. Flowsheet of chemical processing plant supporting a single-fluid MSBR no metal transfer [14].	51
Figure 2-29. Flowsheet of chemical processing plant supporting a single-fluid MSBR fuel salt and salt blanket [14].	51
Figure 2-30. Flowsheet of chemical processing plant supporting a single-fluid MSBR with metal transfer process [16].	52
Figure 2-31. Flowsheet of chemical processing plant supporting a single-fluid MSBR, Variation 1 [17].	53
Figure 2-32. Flowsheet of chemical processing plant supporting a single-fluid MSBR, Variation 2 [17].	53
Figure 3-1. A typical process flow-sheet of the spent fuel processing by fluorination [23].	56
Figure 3-2. Relationships between rate of fluorination of uranium oxides with $BrF_3$ or fluorine [17].	57
Figure 3-3. Scheme of a fluorination reactor inserted in a horizontal tube furnace [16].	58
Figure 3-4. A schematic of the flame fluorination reactor used by D. Watanabe et al. [25].	59
Figure 3-5. Schematic Fluorination Facility by $BrF_5$ [30].	60
Figure 3-6. Vapor pressures of chlorides versus temperature [36].	62
Figure 3-7. Photos of uranium metal fuels and chlorination product: uranium metal pellet (left) and chlorination product (right) [39].	63
Figure 3-8. Uranium chlorinated versus time using different salt media [41].	64
Figure 3-9. Chlorination process by using $Cl_2$ , carbon and LiCl-KCl salt media [42].	65
Figure 3-10. A flow sheet proposed by Elysium on utilizing the recovered fuels from chlorination of spent fuels for their fast reactors [45]. The liquid chlorination in the flowsheet is shown in [44].	66
Figure 4-1. $U^{3+}/U^{4+}$ in the MSRE fuel salt runs 5-14 [57].	70
Figure 4-2. Nickel base alloys after immersion in LiF-ThF <sub>4</sub> -UF <sub>4</sub> -UF <sub>3</sub> molten salt at 800°C for two compositions of UF <sub>4</sub> /UF <sub>3</sub> ratios: left UF <sub>4</sub> /UF <sub>3</sub> = 80-100, and right UF <sub>4</sub> /UF <sub>3</sub> = 500 [56].	70
Figure 4-3. Temperature gradient driven corrosion in MSRE: left high corrosion in hot leg and Cr was dissolved into the molten salt persistently, and right, the Cr was deposited on the surface of the coldest area [58].	71
Figure 4-4. Depth of corrosion attack, in terms of maximum Cr depletion depth, as a function of corrosion time [64].	73



Figure 4-5. Chromium concentration in the fuel salt with and without Zr redox stabilization. Higher Cr concentration means higher corrosion rate [34].	77
Figure 4-6. Chromium concentration in the coolant salt with and without 2% ZrF <sub>2</sub> redox stabilization. Higher Cr concentration means higher corrosion rate [34].	78
Figure 5-1. NaF-ZrF <sub>4</sub> -UF <sub>4</sub> system.	81
Figure 5-2. Two-fluid MSBR fuel salt – LiF-BeF <sub>2</sub> -UF <sub>4</sub> system.	82
Figure 5-3. Two-fluid MSBR blanket salt – LiF-BeF <sub>2</sub> -ThF <sub>4</sub> system.	83
Figure 5-4. Calculated liquid surface of LiF-BeF <sub>2</sub> -ThF <sub>4</sub> , LiF-BeF <sub>2</sub> -UF <sub>4</sub> , LiF-ThF <sub>4</sub> -UF <sub>4</sub> and BeF <sub>2</sub> -ThF <sub>4</sub> -UF <sub>4</sub> , combined to a quaternary system. Melting temperatures are labeled in K and isotherms with an interval of 25 K are shown [89].	84
Figure 5-5. LiF-BeF <sub>2</sub> -ThF <sub>4</sub> system.	85
Figure 5-6. Phase diagram for PuCl <sub>3</sub> -NaCl and UCl <sub>3</sub> -NaCl systems.	88
Figure 5-7. Phase diagram for KCl-UCl <sub>4</sub> system.	88
Figure 5-8. Phase diagram for LiCl-UCl <sub>4</sub> system.	89
Figure 5-9. Phase diagram for NaCl-UCl <sub>4</sub> system.	89
Figure 5-10. Phase diagram for KCl-UCl <sub>3</sub> system.	90
Figure 5-11. Phase diagram for LiCl-UCl <sub>3</sub> system.	90
Figure 5-12. Phase diagram for NaCl-UCl <sub>3</sub> system.	91
Figure 5-13. LiF-KF phase diagram.	92
Figure 5-14. LiF-RbF system.	93
Figure 5-15. LiF-NaF-KF ternary system phase diagram	95
Figure 5-16. LiF-ZrF <sub>4</sub> system.	97
Figure 5-17. NaF-ZrF <sub>4</sub> system.	98
Figure 5-18. NaF-LiF-ZrF <sub>4</sub> system.	99
Figure 5-19. RbF-ZrF <sub>4</sub> system.	100
Figure 5-20. KF-ZrF <sub>4</sub> system.	101
Figure 5-21. LiF-BeF <sub>2</sub> system.	103
Figure 5-22. NaF-BeF <sub>2</sub> system.	104
Figure 5-23. LiF-NaF-BeF <sub>2</sub> system.	105
Figure 5-24. LiCl-KCl system.	107
Figure 5-25. LiCl-RbCl system.	108
Figure 5-26. NaCl-MgCl <sub>2</sub> system.	109
Figure 5-27. KCl-MgCl <sub>2</sub> system.	110
Figure 5-28. NaF-NaBF <sub>4</sub> system.	111
Figure 5-29. KF-KBF <sub>4</sub> system.	112
Figure 5-30. RbF-RbBF <sub>4</sub> system.	113

Figure 6-1. Ellingham diagram of fluoride species.....	117
Figure 6-2. Bi-Be phase diagram. ....	117
Figure 6-3. Ellingham diagram of chloride species. ....	119
Figure 6-4. Conceptual salt treatment flowsheet of a single-fluid MSR [139]. ....	120
Figure 6-5. Conceptual fuel cycle scenario for a fast spectrum molten chloride salt reactor [137].....	121

## TABLES

Table 2-1. Performance characteristics of three reactor types. ....	19
Table 2-2. Thermal and physical properties of the coolant liquids. ....	23
Table 2-3. Series of progress reports on MSBR chemical processing technologies. ....	27
Table 3-1. Boiling points of typical volatile, semi-volatile, and non-volatile fluorides during the fluorination of spent fuels [25]. ....	55
Table 3-2. Calculated reactions enthalpies and free energies for fluorination by $\text{NF}_3$ of uranium oxides and plutonium oxide at $300^\circ\text{C}$ [31]. ....	57
Table 3-3. Comparison between $\text{COCl}_2$ and $\text{Cl}_2\text{-CCl}_4$ as chlorinating agents for $\text{PuO}_2$ [38]. ....	63
Table 3-4. Chlorination reactions of $\text{UO}_2$ and $\text{PuO}_2$ when $\text{ZrCl}_4$ is used as a chlorination reagent. ....	65
Table 3-5. Gibbs free energy of the chlorination reactions when $\text{HCl}$ is used as chlorination reagent [46]. ....	66
Table 4-1 Equilibrium level of dissolved metals for pure elements in contact with $\text{FLiNaK}$ and $\text{FLiBe}$ salts [59]. ....	72
Table 4-2. Summary of corrosion data of Inconel and Hastelloy N tested in forced-circulation loops operated at maximum temperature $704^\circ\text{C}$ with $\text{LiF-BeF}_2$ salts at ORNL forced-circulation loop tests operated with $\text{LiF-BeF}_2$ salts at ORNL [63]. ....	72
Table 4-3. Corrosion rates of several high chromium steels in chloride salts in ORNL loop tests [67]. ....	75
Table 4-4. Corrosion of several alloys in $\text{KCl-MgCl}_2$ at $850^\circ\text{C}$ for 100 hours in quartz crucible and graphite crucible [60, 73, 74]. ....	75
Table 4-5 Weight changes for the alloys exposed in molten $\text{NaCl-KCl-MgCl}_2$ (33–21.6–45.4 mol%) under $\text{N}_2$ atmosphere at $700^\circ\text{C}$ for 100 h. [75].....	76
Table 5-1. Aircraft Reactor Experiment, 2.5 MWt operated. ....	80
Table 5-2. Aircraft Reactor Test, 60 MWt proposed. ....	81
Table 5-3. MSBR 1,000 MWe design for fuel salt. ....	82
Table 5-4. MSBR 1,000 MWe design for blanket salt.....	83
Table 5-5. MSRE 8 MWt operated. ....	84
Table 5-6. 1,000 MWe design.....	85
Table 5-7. 150 MWt proposed. ....	86
Table 5-8. 1,000 MWe design for fuel salt. ....	86

Table 5-9. 1,000 MWe design for coolant salt.....	87
Table 5-10. Molten chloride fast breeder reactor (2,000 MWth).....	87
Table 5-11. LiF-KF (50-50 mol%). .....	92
Table 5-12. LiF-RbF (43-57 mol%).....	93
Table 5-13. LiF-NaF-KF (46.5-11.5-42.0 mol%), FLiNaK.....	94
Table 5-14. LiF-NaF-RbF (42-6-52 mol%). .....	96
Table 5-15. LiF- ZrF <sub>4</sub> (51-49 mol%). .....	96
Table 5-16. NaF-ZrF <sub>4</sub> (59.5-40.5 mol%). .....	97
Table 5-17. LiF-NaF-ZrF <sub>4</sub> (26-37-37 mol%).....	98
Table 5-18. RbF-ZrF <sub>4</sub> (58-42 mol%). .....	99
Table 5-19. KF-ZrF <sub>4</sub> (58-42 mol%).....	100
Table 5-20. LiF-BeF <sub>2</sub> (67-33 mol%), FLiBe. ....	101
Table 5-21. NaF-BeF <sub>2</sub> (57-43 mol%). .....	104
Table 5-22. LiF-NaF-BeF <sub>2</sub> (31-31-38 mol%). .....	105
Table 5-23. LiCl-KCl (59.5-40.5 mol%). .....	106
Table 5-24. LiCl-RbCl (58-42 mol%).....	107
Table 5-25. NaCl-MgCl <sub>2</sub> (58-42 mol%). .....	108
Table 5-26. KCl-MgCl <sub>2</sub> (68-32 mol%). .....	109
Table 5-27. NaF-NaBF <sub>4</sub> (8-92 mol%).....	110
Table 5-28. KF-KBF <sub>4</sub> (25-75 mol%). .....	111
Table 5-29. RbF-RbBF <sub>4</sub> (31-69 mol%).....	112
Table A-1. ORNL technical reports for the Aircraft Nuclear Propulsion Program. ....	130
Table A-2. ORNL progress reports for the Aircraft Nuclear Propulsion Program. ....	132
Table A-3. General Electric Company comprehensive technical reports for the Aircraft Nuclear Propulsion Program. ....	134
Table A-4. ORNL progress reports for the homogeneous reactor experiment/project/program. ....	135
Table A-5. ORNL technical reports for the early development of molten salt power reactors. ....	137
Table A-6. ORNL technical reports on fluorination and fluoride volatility processes. ....	139
Table A-7. ORNL technical reports for the two-fluid molten salt breeder reactor. ....	141
Table A-8. Special series of ORNL technical reports for the two-fluid molten salt breeder reactor. ....	141
Table A-9. ORNL technical reports for the Molten Salt Reactor Experiment.....	142
Table A-10. Special series of ORNL technical reports for the Molten Salt Reactor Experiment.....	144
Table A-11. ORNL technical reports for the MSR experiment decommissioning. ....	145
Table A-12. ORNL technical reports for the MSCR. ....	145
Table A-13. ORNL technical reports for the molten salt breeder experiment. ....	145

Table A-14. ORNL technical reports for the MSR demonstration. ....	145
Table A-15. ORNL technical reports for the single-fluid molten salt breeder reactor. ....	146
Table A-16. Special series of ORNL technical reports for the single-fluid molten salt breeder reactor. ....	148
Table A-17. ORNL technical reports for the denatured MSR. ....	149
Table A-18. Recent ORNL technical reports on MSR technologies. ....	149
Table A-19. ORNL progress reports for the MSR Program. ....	151
Table A-20. ORNL progress reports for the Chemical Technology Division, Unit Operations Section. ....	154
Table A-21. Annual progress reports for the ORNL Chemical Technology Division. ....	160
Table A-22. Annual progress reports for the ORNL Reactor Chemistry Division. ....	161
Table A-23. Reports evaluating nuclear reactor technologies. ....	162
Table A-24. External publications on MSR technologies by ORNL research staff. ....	163
Table A-25. Bibliographies related to MSR technologies. ....	166

## ACRONYMS

AEC	Atomic Energy Commission
ANL	Argonne National Laboratory
ANP	Aircraft Nuclear Propulsion
ARE	Aircraft Reactor Experiment
ART	Advanced Reactor Technologies
DMSR	denatured molten salt reactor
gpm	gallons per minute
HF	hydrogen fluoride
HTRE	Heat Transfer Reactor Experiments
MCFR	molten chloride fast reactor
MSBR	molten salt breeder reactor
MSCR	molten salt converter reactor
MSR	molten salt reactor
MSRD	molten salt reactor demonstration
MSRE	molten salt reactor experiment
NACA	National Advisory Committee for Aeronautics
NEPA	Nuclear Energy for Propulsion of Aircraft
ORNL	Oak Ridge National Laboratory
PWR	pressurized water reactor
SFBR	sodium-cooled fast breeder reactor
TF	tritium fluoride
USAF	United States Air Force



# **Molten Salt Reactor Salt Processing – Technology Status**

## **1. SUMMARY OF TECHNICAL DOCUMENTS RELATED TO MOLTEN-SALT REACTOR DEVELOPMENT AT OAK RIDGE NATIONAL LABORATORY**

*Guy L. Fredrickson*

### **1.1 Introduction**

The Manhattan Project was the first program to exploit nuclear energy for the purpose of atomic weapons development. Though formally established in 1942 with U.S. Army Colonel Leslie R. Groves as the director, the beginnings of the program date back to 1939 when President Franklin D. Roosevelt established an advisory committee to assess the feasibility and potential capabilities of atomic weapons. This, of course, was in direct response to the threats imposed on the U.S. by World War II.

Upon the conclusion of World War II in 1945, the veil of secrecy surrounding the Manhattan Project began to lift. The successful deployment of atomic weapons was a reality known to all, and this spawned pursuits to find other applications of nuclear energy. In addition to continued weapons development, new applications included: aircraft nuclear propulsion, naval nuclear propulsion, civilian power production, medical and industrial isotope production, and Project Plowshare (the use of nuclear explosives for construction purposes). Specifically, molten salt reactor (MSR) technologies were developed in the U.S. in support of aircraft nuclear propulsion and civilian power production.

The foundations for the development of MSR technologies lie within the historical and continued work performed at the Oak Ridge National Laboratory (ORNL). The purpose here is to present a summary of 752 citations related to MSR development at ORNL. This effort was initiated with a focused purpose of locating technical information related to the chemical processing of fluoride salts to support the Th-232/U-233 fuel-cycle molten salt breeder reactor (MSBR). However, it soon became apparent that technical information on chemical processing was spread throughout numerous reports spanning decades. This presented a challenge in that understanding the rationales behind the various proposed chemical processing schemes requires an understanding of the rationales for the chosen paths of MSR development. Therefore, the search effort was broadened to include any information deemed relevant to MSR development at ORNL.

As the list of citations grew, the history of MSR development at ORNL came into focus. Based on a review of technical content, chronological order, and mission context, the citations are partitioned (albeit imperfectly) into 15 (albeit overlapping) categories as follows.

- Aircraft Nuclear Propulsion Program (1949–1961)
  - Aircraft Reactor Experiment, 2.5 MWt Operated
  - Aircraft Reactor Test, 60 MWt Proposed
- Early Development of Civilian Power Liquid-Fuel Reactor Technologies (1950–1962)
  - Homogeneous Aqueous Reactor Program (1950–1961)
  - Molten Salt Reactor Program (1957–1976)
- Fluorination and Fluoride Volatility Processing (1954–1976)
  - Molten Salt Reactor Salt Treatment

- Uranium Recovery from Zirconium and Aluminum Clad Fuels
- Two-Fluid Molten Salt Breeder Reactor (1961–1970)
  - MSBR 1,000 MWe Design
- Molten Salt Reactor Experiment (1960–1975)
  - Molten Salt Reactor Experiment 8 MWt Operated
- Molten Salt Reactor Experiment Decommissioning (1971–Present)
  - Extended Storage-In-Place
- Molten Salt Converter Reactor (1961–1965)
  - 1,000 MWe Design
- Molten Salt Breeder Experiment (1969–1970)
  - 150 MWt Proposed
- Molten Salt Reactor Demonstration (1972)
  - 350 MWe Proposed
- Single-Fluid Molten Salt Breeder Reactor (1969–1978)
  - 1,000 MWe Design
- Denatured Molten Salt Reactor (1977–1980)
  - 1,000 MWe Design
- Subsequent Activities (1995–2017)
- Annual, Semiannual, and Quarterly Reports (1955–1976)
- Technology Evaluation Reports (1959–1977)
- External Publications by ORNL Research Staff (1957–2017).

What follows is a brief description of each category, including a list of citations most closely associated with that category. The vast majority of citations were prepared by ORNL staff in direct support of MSR development. However, there are exceptions. These include citations prepared outside of ORNL that support or independently evaluate work performed at ORNL. In some select cases, include citations related to the development of other reactor technologies occurring at the same time.

## **1.2 Aircraft Nuclear Propulsion Program**

Investigations into the use of nuclear reactor technologies to power flight began in May 1946 when the United States Air Force (USAF) and the Atomic Energy Commission (AEC) initiated the Nuclear Energy for Propulsion of Aircraft (NEPA) Project.

This led to the creation of the Aircraft Nuclear Propulsion (ANP) Program in September 1949. The ANP Program was a collaboration between the Department of Defense, National Advisory Committee for Aeronautics (NACA), and AEC. Department of Defense managed work through the NEPA Division of Fairchild Engine and Aircraft Corporation; NACA through its Cleveland Laboratory; and AEC through ORNL. General Electric Company, under contract with the USAF and AEC, joined the ANP Program in 1951. The entire ANP Program was abruptly terminated in June 1961.



ORNL developed liquid-fueled reactor technologies for the ANP Program. The Aircraft Reactor Experiment (ARE) was operated November 3–12, 1954 for a total of 96 MWh. It was a molten-salt fueled reactor and attained a peak power of 2.5 MWt. The nominal composition of the fuel salt was NaF-ZrF<sub>4</sub>-UF<sub>4</sub> (53.09-40.73-6.18 mole %). The Aircraft Reactor Test (a.k.a., the “fireball”) was proposed as a 60 MWt molten-salt fueled reactor. The nominal composition of the fuel salt was NaF-ZrF<sub>4</sub>-UF<sub>4</sub> (50-46-4 mole %). It was well under construction when the ANP Program was terminated. In both designs, the fuel salts were moderated by beryllium oxide (i.e., beryllia ceramic) cores.

Schematics of the ARE and Aircraft Reactor Test reactor vessels are shown in Figures 1-1 and 1-2, respectively. ORNL technical reports for the ANP Program are listed in Appendix A, Table A-1. Accompanying programmatic progress reports are listed in Table A-2.

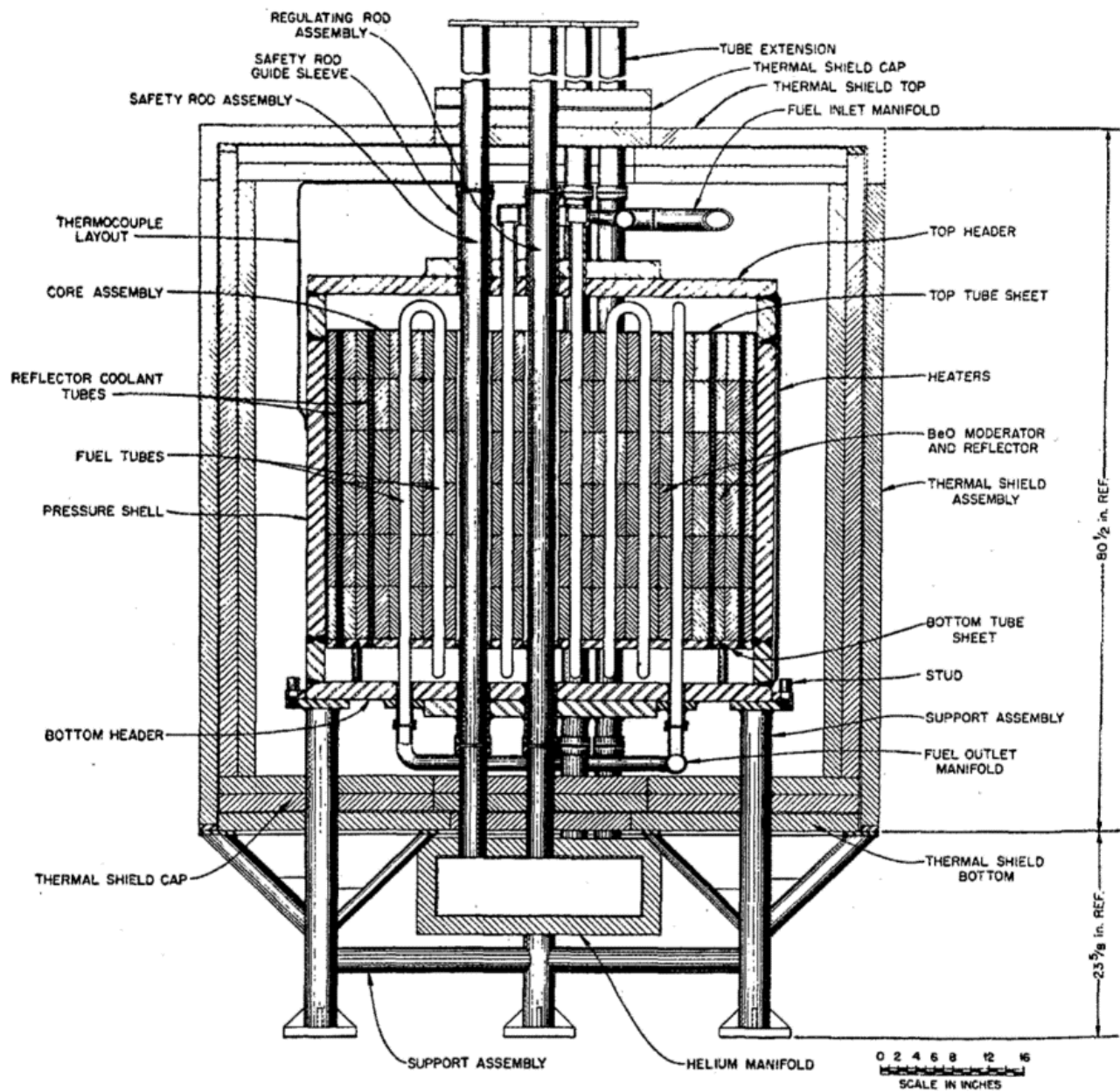


Figure 1-1. Schematic of the ARE reactor vessel (ORNL-1845).

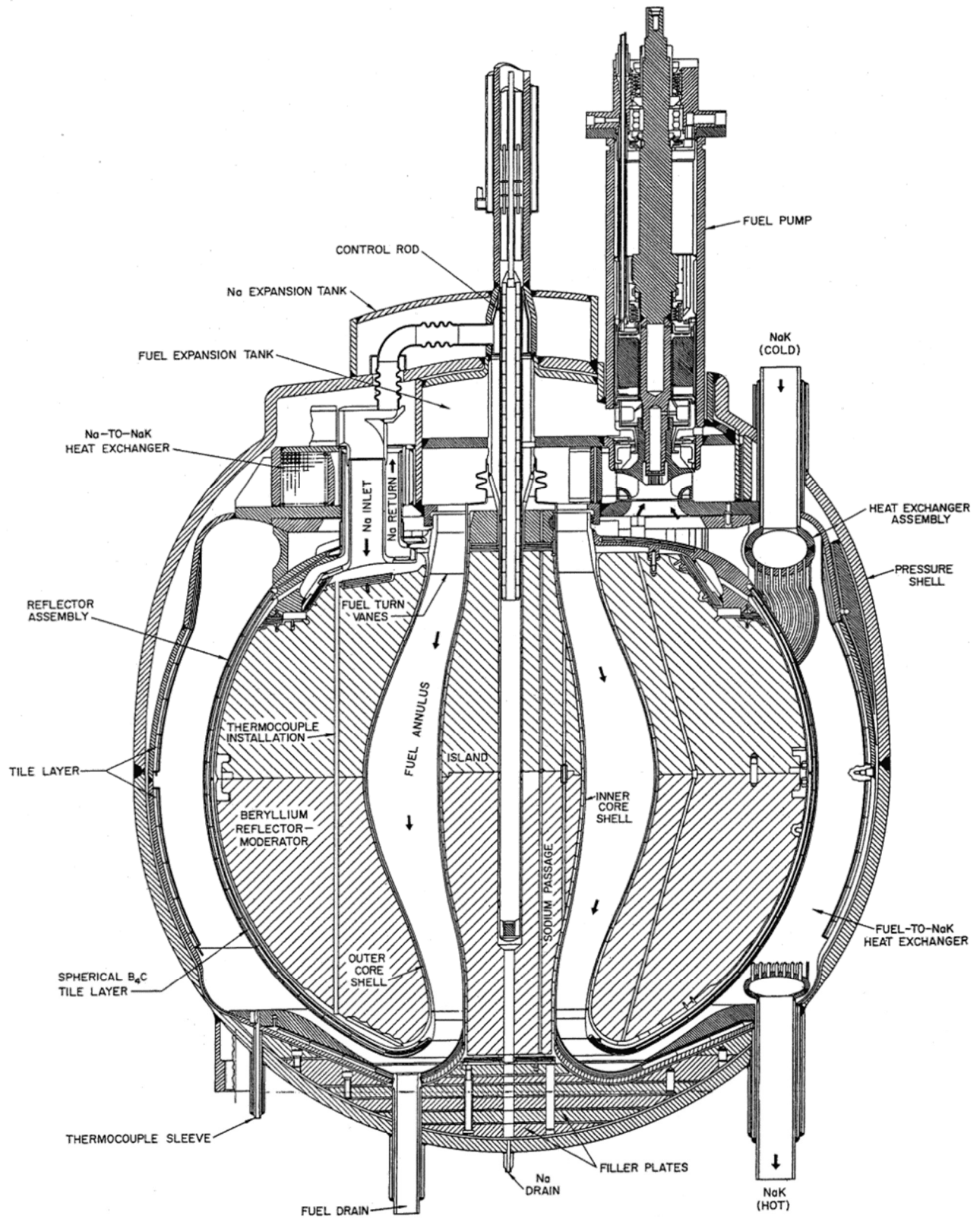


Figure 1-2. Schematic of the Aircraft Reactor Test reactor vessel (ORNL-2095).

General Electric Company developed solid-fueled reactor technologies for the ANP Program. These included Heat Transfer Reactor Experiments (HTREs) No. 1 to No. 4. HTRE No. 1 used nickel-chromium uranium-oxide-dispersion fuel. It accumulated 151-h of operation in 1956. HTRE No. 2 was a modification of HTRE No. 1 intended to serve as a test bed for development of, among other things, high-temperature ceramic-based fuels. It accumulated 1299-h of operation between July 1957 and the termination of the ANP Program. HTRE No. 3 was a full-scale aircraft reactor based on metallic dispersion fuel. It accumulated 126-h of operation in 1959. HTRE No. 4 intended to use beryllium-oxide uranium-oxide ceramic fuel. Its deployment was abandon in favor of direct prototype testing that never came to fruition. A series of comprehensive technical reports prepared by General Electric Company following the termination of the ANP Program are listed in Table A-3.

### **1.3 Early Development of Civilian Power Liquid-Fuel Reactor Technologies**

The ANP Program was one of many programs at that time seeking to marry nuclear reactor technologies with applications and vice versa. It was a period of discovery in nuclear reactor sciences, and fluid-fuel reactors for civilian power production were gaining attention. This family of reactor design concepts included aqueous fueled, liquid-metal fueled, and molten-salt fueled systems. The aqueous fueled systems are known as aqueous homogeneous reactors because the fluid-fuel contains both the fuel and the moderator. The mission for the development of liquid-metal fueled reactors was shared by Los Alamos National Laboratory, Argonne National Laboratory (ANL), Ames Laboratory, and others. The missions for the development of aqueous homogeneous reactors and molten-salt reactors were primarily performed by ORNL.

Based on the best available information of the day, it was believed that (1) there would be an increasing reliance on nuclear energy to provide for an increasing demand for civilian electrical power, and (2) the known uranium reserves were insufficient to meet this demand without the implementation of breeder reactor technologies. Therefore, emphasis was placed on the development of fast-spectrum breeder reactors based on the U-238/Pu-239 fuel cycle and thermal-spectrum breeder reactors based on the Th-232/U-233 fuel cycle. As the cost/benefit analyses of the various technologies matured, ultimately the Homogeneous Reactor Program was terminated and ORNL focused its attentions on the Th-232/U-233 fuel cycle MSBR.

ORNL progress reports for the homogenous reactor program are listed in Table A-4. ORNL technical reports during the early development of molten salt power reactors are listed in Table A-5. From a technical perspective, there was overlap between MSR technologies intended for aircraft propulsion and those intended for civilian power production. Therefore, it was not always clear if a particular report was better suited for inclusion in Table A-1 or Table A-5. Generally, the reports in Table A-1 appeared to be technically related to, or programmatically sponsored by, the ANP Program. Such an exacting distinction is not imposed on the reports in Table A-5.

### **1.4 Fluorination and Fluoride Volatility Processing**

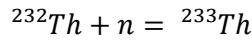
Studies on fluorination and fluoride volatility were performed for at least three distinct technical objectives, including (1) preparation and purification of fluoride salts, (2) chemical separation of uranium from irradiated fluoride salts, and (3) chemical separation of uranium from irradiated zirconium-clad and aluminum-clad fuels. Reports in the first two categories are generally related to chemical processing of salts to support MSR operations. Reports in the third category, though not directly related to MSR operations, are of interest as a potential means of providing a source for uranium-bearing salts fluoride for MSR operations. ORNL technical reports on fluorination and fluoride volatility processes are listed in Table A-6. Additional reports on this subject are listed in Tables A-1, A-7, and A-9, based on their specific technical objectives.

## 1.5 Two-Fluid Molten Salt Breeder Reactor

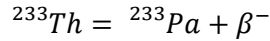
This MSR was a design concept for a 1,000 MWe Th-232/U-233 fuel-cycle two-fluid MSBR. It is only a design study, never proposed for construction. The two-fluids refer to blanket salt (a.k.a. fertile salt) and fuel salt. The blanket salt is the carrier salt for the fertile isotope Th-232, the nominal composition is LiF-ThF<sub>4</sub>-BeF<sub>2</sub> (71-27-2, mole %), and the fuel salt is the carrier salt for the fissile isotope U-233. The nominal composition is LiF-BeF<sub>2</sub>-UF<sub>4</sub> (68.5-31.3-0.2, mole %) moderated by a graphite core. Both salts are separately, independently, and simultaneously circulated through the reactor core for the dual purposes of fueling the reactor and extracting the heat. The capability for this design to be a breeder relies on the careful management of neutron economy.

The most efficient neutron economy is that which provides the highest yield of fissile isotopes per release of fission neutrons. Consider the following series of reactions.

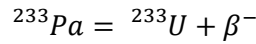
Fertile Th-232 is transmuted to Th-233:



Th-233 has a half-life of 21.83 min and decays to Pa-233:



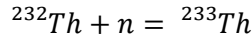
Pa-233 has a half-life of 26.967 d and decays to fissile U-233:



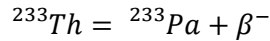
In this series, only one neutron is required to convert Th-232 to U-233. This is the most preferred path for breeding U-233 from Th-232 because it provides the best neutron economy. All other fates of Th-232 are to be minimized as much as possible within the constraints of practical engineering.

For example, consider the following series of reactions.

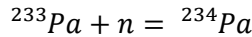
Fertile Th-232 is transmuted to Th-233:



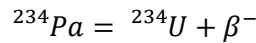
Th-233 has a half-life of 21.83 min and decays to Pa-233:



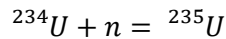
Fertile Pa-233 is transmuted to Pa-234:



Pa-234 has a half-life of 6.75 h and decays to U-234:



Fertile U-234 is transmuted to fissile U-235:



In this series, three neutrons are required to convert Th-232 to U-235. Under these circumstances of poor neutron economy, the reactor would be a converter and not a breeder. Therefore, in order for the reactor to have a positive breeding ratio, protactinium must be continuously removed from the blanket salt, for the purpose of maintaining a sufficiently low concentration of protactinium in the blanket salt, for the purpose of maintaining a sufficiently high neutron economy.

In this context, isotopes of protactinium are not the only isotopes to consider. All high neutron-cross-section fission product isotopes and daughters thereof must also be managed accordingly to maintain a positive breeding ratio. The most notable of these are Xe-135 and Sm-149.

The general chemical processing scheme for this type of breeder reactor is as follows.

- Separate and recover the Pa-233 from the blanket salt.
- Isolate the Pa-233 in a salt reservoir (separate from the blanket and fuel salts).
- Harvest daughter U-233 from the salt reservoir as the Pa-233 decays.
- Return harvested U-233 to the fuel salt as required.
- Store excess U-233 as required (available when the breeding ratio is greater than one).
- Add fresh Th-232 to the blanket salt as required.

A schematic of the proposed two-fluid MSBR reactor vessel is shown in Figure 1-3. ORNL technical reports on the two-fluid MSBR design are listed in Table A-7. A special series of ORNL reports on this subject are listed in Table A-8. Section 1.14 "Annual, Semiannual, and Quarterly Reports" lists additional reports describing designs for two-fluid MSBRs.

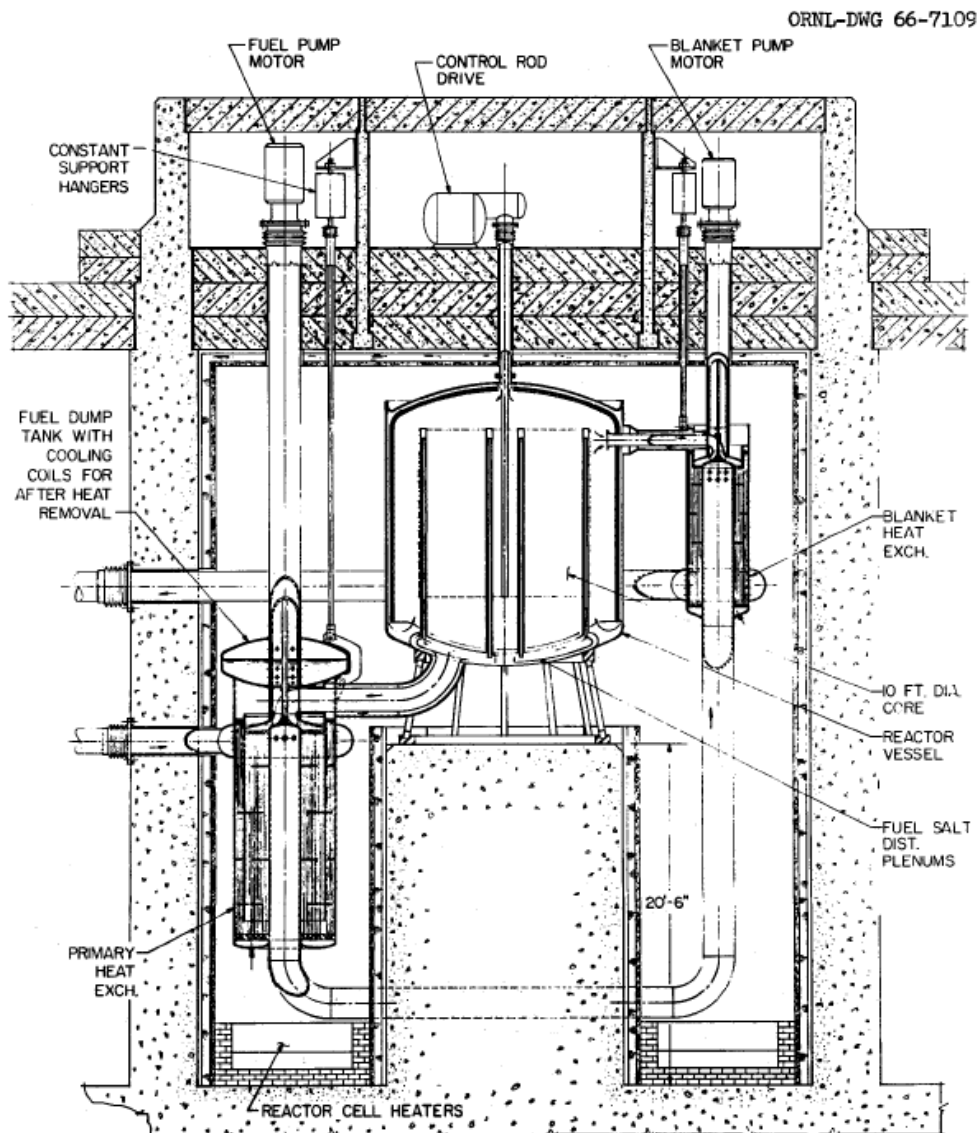


Figure 1-3. Schematic of the proposed two-fluid MSBR reactor vessel (ORNL-3996).

## 1.6 Molten Salt Reactor Experiment

The molten salt reactor experiment (MSRE) at ORNL was the most comprehensive study of an operating MSR ever performed. Although the MSRE was not a breeder reactor, it demonstrated many features of a breeder reactor. It was operated between June 1, 1965 and December 12, 1969 for a total of 105 GWh. The maximum design power was approximately 8 MWt. This energy was not converted to electricity; it was dissipated to the atmosphere. It operated with a single fuel salt, the nominal composition was  $\text{LiF-BF}_2\text{-UF}_4\text{-ZrF}_4$  (65-29.2-0.8-5 mole %) moderated by a graphite core. It did not demonstrate the Th-232/U-233 fuel cycle; Th-232 was never added to the fuel salt, and it did not demonstrate on-line chemical processing to manage the protactinium. It was operated in two distinct phases. During Phase I program operations, U-235 provided the fissile inventory in the fuel salt. At the conclusion of Phase I, the U-235 was removed from the fuel salt by the fluoride volatility process. The resulting barren salt was recharged with U-233 and during Phase II program operations, U-233 provided the fissile inventory in the fuel salt. During the later stages of Phase II, Pu-239 was added to the fuel salt.

A schematic of the MSRE reactor vessel is shown in Figure 1-4 and a photograph of the assembled reactor system is shown in Figure 1-5. ORNL technical reports on the MSRE are listed in Table A-9. A special series of ORNL reports on this subject are listed in Table A-10.

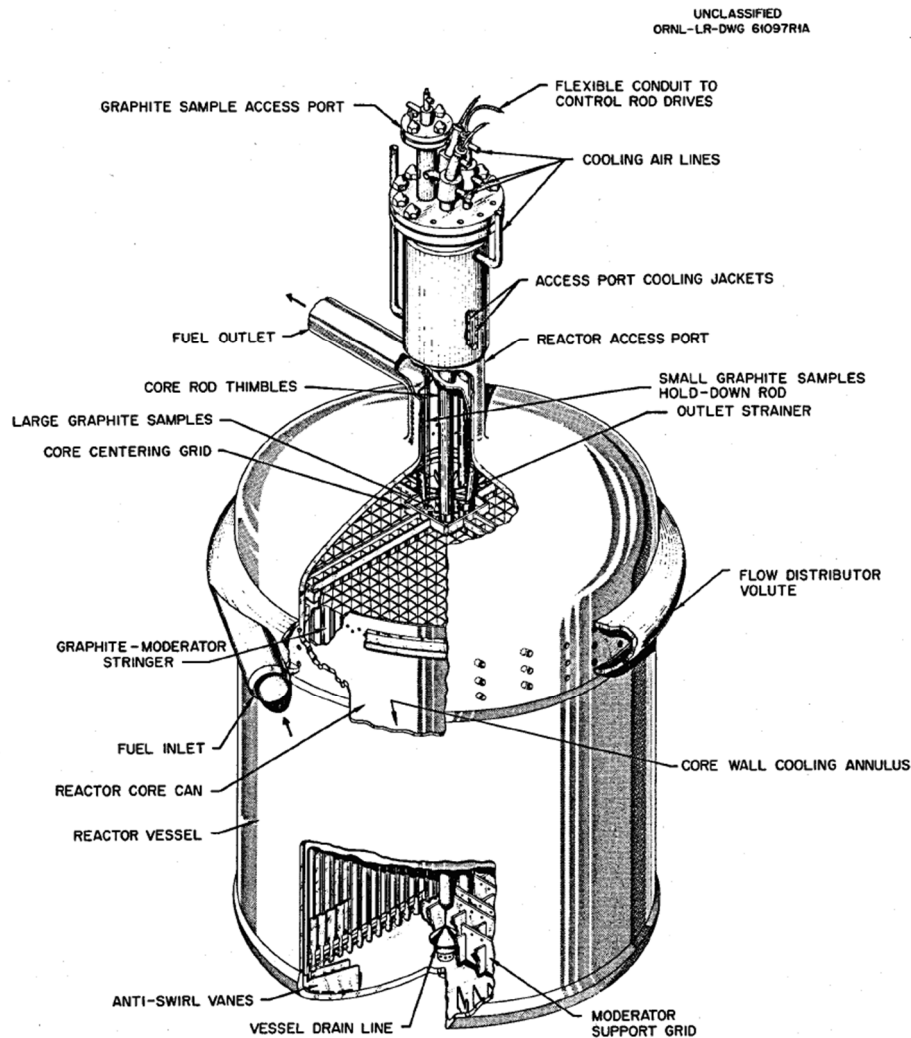


Figure 1-4. Schematic of the MSRE reactor vessel (ORNL-TM-728).



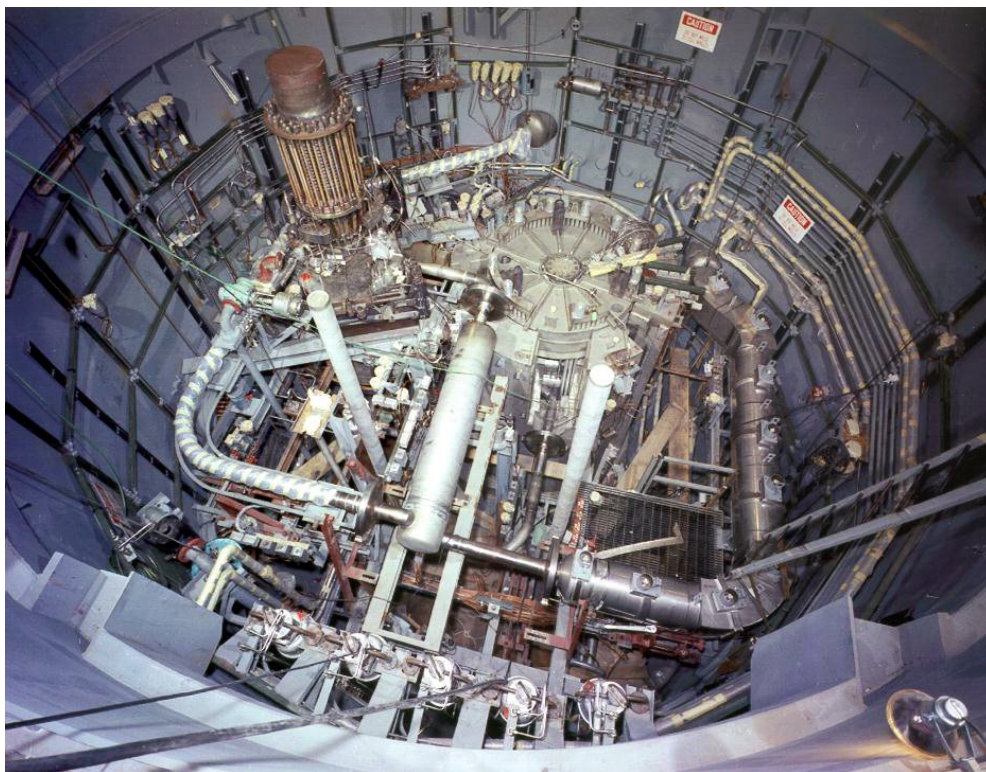


Figure 1-5. Photograph of the MSRE assembled reactor system (ORNL-TM-728).

## 1.7 Molten Salt Reactor Experiment Decommissioning

Following the shutdown of the MSRE in 1969, the fuel salt was drained into two criticality-safe storage tanks and the flush salt was drained into a third tank. There are 4,650 kg (1.9 m<sup>3</sup>) of fuel salt and 4,265 kg (1.9 m<sup>3</sup>) of flush salt. The bulk composition of the fuel salt is LiF-BeF<sub>2</sub>-ZrF<sub>4</sub>-UF<sub>4</sub>-PuF<sub>4</sub> (42.3-36-20.6-1.1-0.02 wt%) and the bulk composition of the flush salt is LiF-BeF<sub>2</sub>-ZrF<sub>4</sub>-UF<sub>4</sub>-PuF<sub>4</sub> (53.1-47.8-0.89-0.015-0.0004 wt%). These drain tanks and many of the MSRE components remain in place awaiting final disposition. ORNL technical reports on the decommissioning of the MSRE are listed in Table A-11

## 1.8 Molten Salt Converter Reactor

This reactor was a design concept for a 1,000 MWe Th-232/U-235 fuel-cycle single-fluid molten salt converter reactor (MSCR). The nominal composition of the fuel salt was LiF-BeF<sub>2</sub>-ThF<sub>4</sub>-UF<sub>4</sub> (68-22-9-1 mole %) moderated by a graphite core. It is only a design study, never proposed for construction. It was based on design and experience gained during the MSRE Program. As a converter reactor, the breeding ratio is less than one. Compared to breeder technologies, the chemical processing of the salt for this converter design required only the separation and recovery of uranium. Discharge salt thus stripped of uranium was disposed. ORNL technical reports on the MSCR are listed in Table A-12.

## 1.9 Molten Salt Breeder Experiment

This reactor was a design concept for a 150 MWt Th-232/U-233 fuel-cycle single-fluid MSBR. The nominal composition of the fuel salt is LiF-BeF<sub>2</sub>-ThF<sub>4</sub>-UF<sub>4</sub> (71.5-16-12-0.5 mole %) moderated by a graphite core. The molten-salt breeder experiment (MSBE) was proposed as a follow-on study to the MSRE. Its stated purpose was “to demonstrate on an intermediate scale the solutions to all the technical



problems of a high-performance MSBR”. The MSBE was never constructed. ORNL technical reports on the MSBE are listed in Table A-13.

### **1.10 Molten Salt Reactor Demonstration**

The molten salt reactor demonstration (MSRD) tested a design concept for a 350 MWe Th-232/U-235 fuel-cycle single-fluid MSCR. The nominal composition of the fuel salt was LiF-BeF<sub>2</sub>-ThF<sub>4</sub>-UF<sub>4</sub> (71.5-16-12-0.5 mole %) moderated by a graphite core. The MSRD was proposed as a follow-on study to the MSRE. Its stated purpose was “to demonstrate the molten-salt reactor concept on a semi-commercial scale, while requiring little development of basic technology beyond that demonstrated in the MSRE”. The MSRD was never constructed. An ORNL technical report on the MSRD is listed in Table A-14.

### **1.11 Single-Fluid Molten Salt Breeder Reactor**

This reactor was a design study never proposed for construction. The design concept was for a 1,000 MWe Th-232/U-233 fuel-cycle single-fluid MSBR. The nominal composition of the fuel salt was LiF-BeF<sub>2</sub>-ThF<sub>4</sub>-UF<sub>4</sub> (71.7-16-12-0.3 mole %) moderated by a graphite core. Outside all other design concepts, the single-fluid MSBR received the most attention and the most recent attention.

The single-fluid MSBR design is considered an improvement over the two-fluid MSBR design. Advances in the chemical processing technologies used to treat the salt for the management of protactinium and fission products allowed a single-salt to perform the functions of both the blanket and fuel salts. Allowance for the flow of only a single salt stream through the reactor core (rather than the flow of two independent salt streams) greatly simplified the design requirements of the core and supporting mechanical equipment.

A schematic of the proposed single-fluid MSBR reactor vessel is shown in Figure 1-6. ORNL technical reports on the single-fluid MSBR design are listed in Table A-15. A special series of ORNL reports on this subject are listed in Table A-16. Section 1.14 “Annual, Semiannual, and Quarterly Reports” lists additional reports describing designs for single-fluid MSBRs.

### **1.12 Denatured Molten Salt Reactor**

The denatured molten salt reactor (DMSR) was a design concept for a 1,000 MWe Th-232/U-235 fuel-cycle single-fluid MSCR. The initial fuel salt composition is similar to that of the single-fluid MSBR, but the initial composition changes significantly over time as transuranics accumulate. It is only a design study, never proposed for construction. The denaturant is U-238 that is added to manage the enrichment level of the uranium fraction of the salt. The DMSR design was considered more proliferation resistant than the MSBR design.

ORNL technical reports on the single-fluid DMSR design are listed in Table A-17.

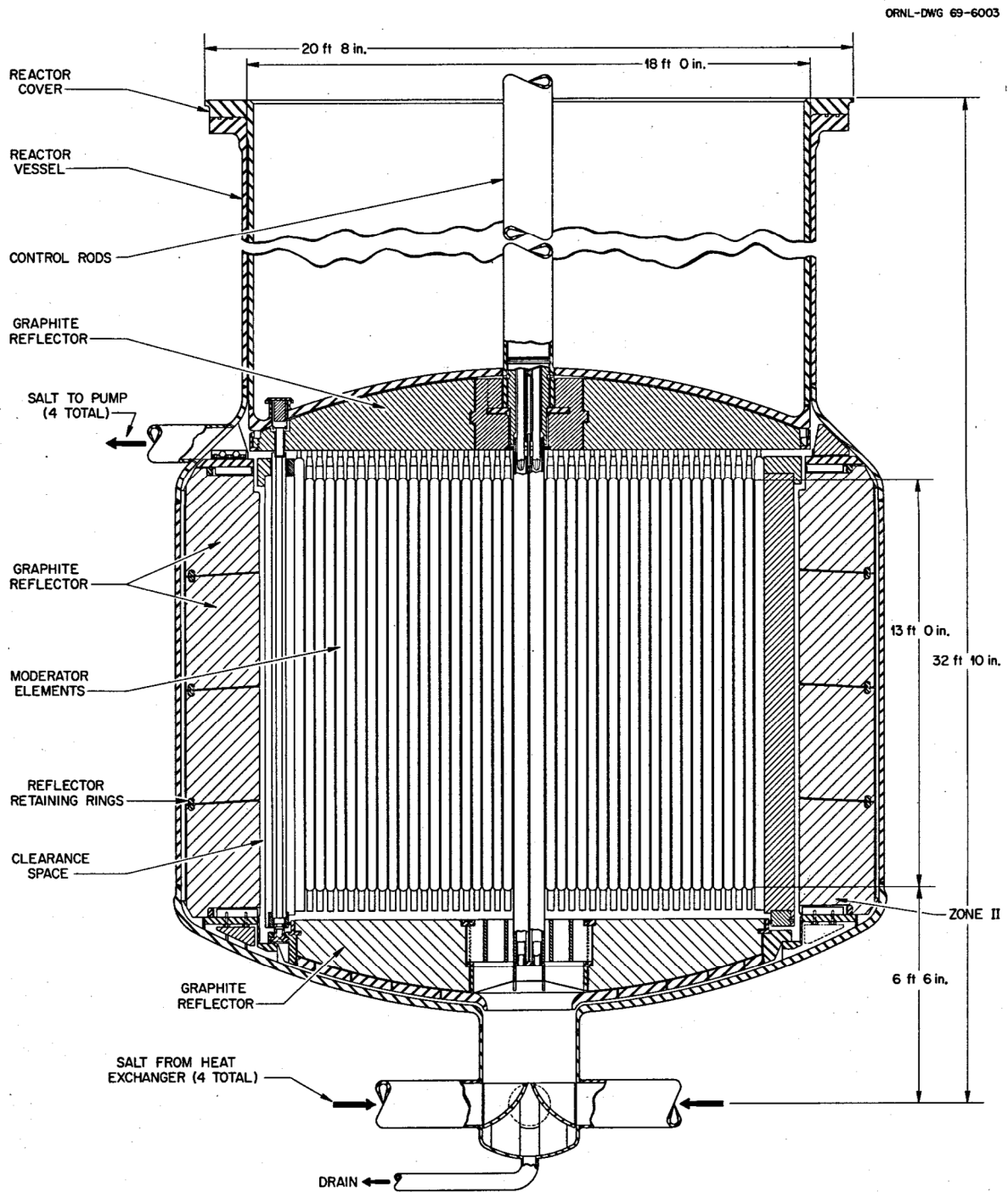


Figure 1-6. Schematic of the proposed single-fluid MSBR reactor vessel (ORNL-4812).

### **1.13 Subsequent Reports**

It appears there was relatively little activity on MSR technologies at ORNL between 1980 and 1995. Subsequent reports focused on various nuclear applications of molten salts, including accelerator-driven reactors and next generation high-temperature reactors. These later reports are listed in Table A-18.

### **1.14 Annual, Semiannual, and Quarterly Reports**

A great deal of technical information on all aspects of MSR development resides in the various series of ORNL programmatic progress reports published between 1955 and 1979.

The Molten Salt Reactor Program, Quarterly and Semiannual Progress Reports (1957-1976) are listed in Table A-19. The Chemical Technology Division, Unit Operations Section, Monthly and Quarterly Progress Reports (1955-1968) are listed in Table A-20. The Chemical Technology Division, Annual Progress Reports (1959-1979) are listed in Table A-21. The Reactor Chemistry Division Annual Progress Reports (1960-1972) are listed in Table A-22. In each instance where the report number is absent, the citation was presumed to exist based on the logical chronological continuation of the report series.

Design concepts for two-fluid MSBRs are described in Molten Salt Reactor Program, Semiannual Progress Reports: ORNL-3708 (Jul 1964), and ORNL-3936 (Feb 1966) through ORNL-4254 (Feb 1968).

Design concepts for single-fluid MSBRs are described in Molten Salt Reactor Program, Semiannual Progress Reports: ORNL-4344 (Aug 1968) through ORNL-4728 (Aug 1971).

The MSRE is described in MSR Program, Semiannual Progress Reports: ORNL-3014 (Jul 1960) through ORNL-4676 (Feb 1971).

Chemical processing of molten salts in support of the MSBR is described in MSR Program, Semiannual Progress Reports: ORNL-3936 (Feb 1966) through ORNL-5132 (Feb 1976).

### **1.15 Technology Evaluation Reports**

Technology evaluation reports are often prepared by committees of technical experts (from commercial and government organizations) for the benefit of decision making within the executive and legislative branches of government. These reports are particularly useful for capturing the context and rationale that drove the technical recommendations at the time the reports were prepared. Reports evaluating nuclear reactor technologies are listed in Table A-23.

### **1.16 External Publications by Oak Ridge National Laboratory Research Staff**

External publications include journal articles, conference proceedings, and books. These contributions span the entire history of MSR research at ORNL. Of all the citation lists provided in this summary, this is undoubtedly the most incomplete. External publications by ORNL research staff are listed in Table A-24. And bibliographies related to MSR technologies are listed in Table A-25.

#### **1.16.1 Information Resources**

A great many of these reports and publications can be found on the internet. Useful resources include:

- Google: <https://www.google.com/>.
- Google Scholar: <https://scholar.google.com>.
- ORNL Library: <https://ornl.gov/content/research-library>.
- U.S. Department of Energy, Office of Scientific and Technical Information: <https://www.osti.gov/>.

- Thorium Manufactured Reactors: <http://www.thmfgres.com/>.
- Energy from Thorium Blog: <http://energyfromthorium.com/>.
- Molten Salt Energy Technologies: <http://molten salt.org/>.

## 2. FUNCTIONAL ENGINEERING REQUIREMENTS OF A CHEMICAL PROCESSING PLANT TO SUPPORT A 1,000 MWE TH-232/U-233 FUEL-CYCLE MOLTEN-SALT BREEDER REACTOR

*Guy L. Fredrickson*

### 2.1 Introduction

Over its history, ORNL performed engineering design studies of several conceptual MSRs with various configurations. This section focuses on two of these studies: the two-fluid [1] and the single-fluid [2] 1,000 MWe Th-232/U-233 fuel-cycle molten salt breeder reactors (MSBR).

In the two-fluid MSBR design, the two-fluids refer to blanket salt and fuel salt. The blanket salt is the carrier salt for the fertile isotope Th-232; the nominal composition is  $\text{LiF-ThF}_4\text{-BeF}_2$  (71-27-2, mole %). And the fuel salt is the carrier salt for the fissile isotope U-233; the nominal composition is  $\text{LiF-BeF}_2\text{-UF}_4$  (68.5-31.3-0.2, mole %) moderated by a graphite core. Both salts are separately, independently, and simultaneously circulated through the reactor core for the dual purposes of fueling the reactor and extracting the heat. The coolant salts are  $\text{NaBF}_4\text{-NaF}$  (92-8, mole %), which carry the thermal energies from the blanket and fuel salts to other heat exchangers for steam production. A two-fluid MSBR is depicted in Figure 2-1.

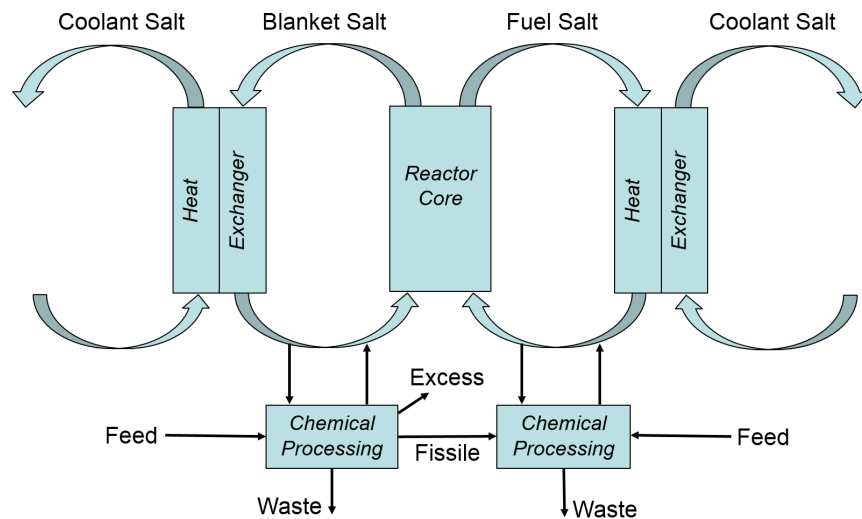


Figure 2-1. Depiction of a two-fluid MSBR.

In the single-fluid MSBR design, the functions of the blanket salt and fuel salt are combined into a single fuel salt. The nominal composition of the fuel salt is  $\text{LiF-BeF}_2\text{-ThF}_4\text{-UF}_4$  (71.7-16-12-0.3 mole %) moderated by a graphite core. The coolant salt is the same as specified for the two-fluid MSBR design. Allowance for the flow of only a single salt stream through the reactor core (rather than the flow of two independent salt streams) greatly simplified the design requirements of the core and supporting mechanical equipment. The two-fluid MSBR is an earlier design than the single-fluid MSBR. The ability to propose the single-fluid MSBR design was made possible through technology improvements with respect to separations chemistry during chemical processing. A single-fluid MSBR is depicted in Figure 2-2.

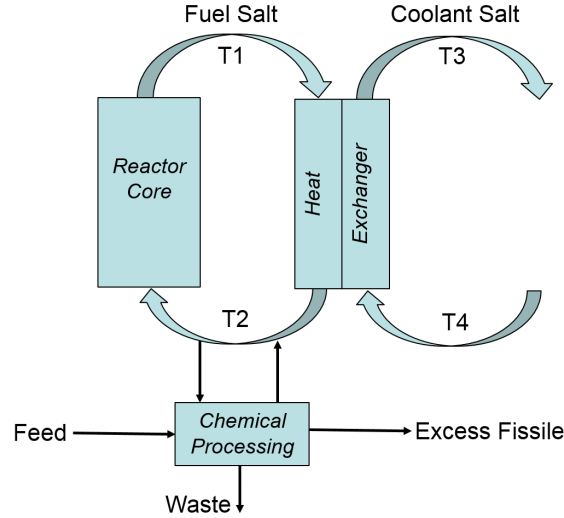


Figure 2-2. Depiction of a single-fluid MSBR.

In Figure 2-2, the heat gained by the fuel salt as it passes through the reactor is transferred to the coolant salt as both the fuel and coolant salts pass through the heat exchanger. Therefore,  $T1 > T2$ , where  $T1$  and  $T2$  are outlet and inlet temperatures, respectively, of the fuel salt passing through the reactor core. Likewise,  $T3 > T4$ , where  $T3$  and  $T4$  are the outlet and inlet temperatures, respectively, of the coolant salt passing through the heat exchanger. The unique characteristics of coolant salts are not discussed in this report.

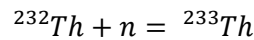
## 2.2 Breeding

A breeder reactor is capable of producing excess fissile material that, in theory, is harvested and used to fuel additional reactors. There are two breeder fuel cycles: U-238/Pu-239 and Th-232/U-233. These breeder fuel cycles are often initiated with natural uranium or U-235 enriched uranium. The only isotopes mined and extracted from the earth's crust are the fissile isotope U-235 and the fertile isotopes U-238 and Th-232. In addition to the presence of fertile material, the capacity for breeding relies on careful management of the neutron economy within the reactor core through engineering design and operation. A converter reactor can be very similar to a breeder reactor. It too generates fissile material, but less than it consumes. Therefore, these same two fuel cycles can apply to converter reactors.

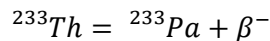
### 2.2.1 Th-232/U-233 Fuel Cycle

The most efficient neutron economy is that which provides the highest yield of fissile isotopes per release of fission neutrons. Consider the following series of reactions.

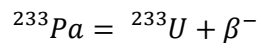
Fertile Th-232 is transmuted to Th-233 by capturing a neutron:



Th-233 has a half-life of 21.83 min and decays to Pa-233:



Pa-233 has a half-life of 26.967 d and decays to fissile U-233:

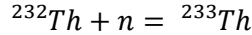


In this series, only one neutron is required to convert Th-232 to U-233. This is the most preferred path for breeding U-233 from Th-232 because it provides the best neutron economy. All other fates of Th-232,

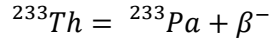
and all other fates of neutrons, are to be minimized as much as possible within the constraints of practical engineering.

For example, consider the following series of reactions.

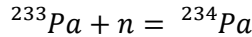
Fertile Th-232 is transmuted to Th-233 by capturing a neutron:



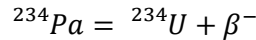
Th-233 has a half-life of 21.83 min and decays to Pa-233:



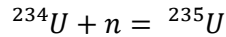
Fertile Pa-233 is transmuted to Pa-234 by capturing a second neutron:



Pa-234 has a half-life of 6.75 h and decays to U-234:



Fertile U-234 is transmuted to fissile U-235 by capturing a third neutron:



In this series, three neutrons are required to convert Th-232 to U-235. Under these circumstances of poor neutron economy the reactor would be a converter and not a breeder. Therefore, in order for the reactor to have a positive breeding ratio, protactinium must be continuously removed from the salt, for the purpose of maintaining a sufficiently low concentration of protactinium in the salt, for the purpose of maintaining a sufficiently high neutron economy.

In this context, isotopes of protactinium are not the only isotopes to consider. All high neutron-cross-section fission product isotopes and daughters thereof must also be managed accordingly to maintain a positive breeding ratio. The most notable of these are Xe-135 and Sm-149.

The general chemical processing scheme for the two-fluid MSBR (see Figure 2-1) is as follows.

- Separate and recover the Pa-233 from the circulating blanket salt.
- Isolate the Pa-233 in a salt reservoir (separate from the blanket and fuel salts).
- Harvest daughter U-233 from the salt reservoir as the Pa-233 decays.
- Return harvested U-233 to the fuel salt as required.
- Store excess U-233 as required (available when the breeding ratio is greater than one).
- Add fresh Th-232 to the blanket salt as required.

The general chemical processing scheme for the single-fluid MSBR (see Figure 2-2) is as follows.

- Separate and recover the Pa-233 from the circulating fuel salt.
- Isolate the Pa-233 in a salt reservoir (separate from the fuel salt).
- Harvest daughter U-233 from the salt reservoir as the Pa-233 decays.
- Return harvested U-233 to the fuel salt as required.
- Store excess U-233 as required (available when the breeding ratio is greater than one).
- Add fresh Th-232 to the fuel salt as required.

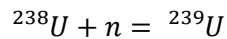
Where chemical processing (i.e., reprocessing) of nuclear fuel is practiced, it is always decoupled from reactor operations. For example, consider the pressurized water reactor (PWR) fleet in France. Spent

oxide fuels are removed from the reactors and transferred to water storage pools where they are allowed time to cool and decay. The fuels are then treated in aqueous reprocessing plants to recover purified actinide oxides, which are used to make new fuels. In this scenario, the only factor coupling reprocessing with reactor operations are the in-process inventories of spent and new fuels. This is not the case for MSBRs. The ORNL design studies cited in this report rely on the chemical processing of a salt stream that is continuously withdrawn from the bulk-inventory of salt circulating through the reactor. Because the proposed cycle times for processing the entire bulk-inventory of salt are short, ranging from 3 to 10 days, decoupling as described above is not a viable option. This relationship between chemical processing and MSBR operations will be made clearer in sections that follow.

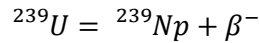
### 2.2.2 Brief Note on the U-238/Pu-239 Fuel Cycle

There are design concepts for U-238/Pu-239 fuel-cycle MSBRs. Consider the following reactions.

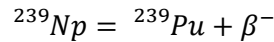
Fertile U-238 is transmuted to Np-239 by capturing a neutron:



U-239 has a half-life of 23.45 min and decays to Np-239:



Np-239 has a half-life of 2.356 d and decays to fissile Pu-239:



These reactions are analogous to the transmutation of Th-232 to U-233 describe earlier. The half-lives of Th-233 and U-239 are very similar, 21.83 and 23.45 min, respectively. However, the half-lives of Pa-233 and Np-239 are quite different, 26.967 and 2.356 d, respectively. It is this difference that fundamentally explains why breeder reactors based on the Th-232/U-233 fuel cycle require more timely management of intermediate and fission product isotopes than do breeder reactors based on the U-238/Pu-239 fuel cycle.

## 2.3 Comparison of Performance Characteristics of Three Reactors

All nuclear reactors used for the production of civilian power have this in common: thermal energy is extracted from the core via the flow of a heat transfer fluid, which in turn is used to make steam, which in turn is used to spin electrical turbines. In the sodium-cooled fast breeder reactor (SFBR) design, the fuel is stationary and liquid sodium is the heat transfer fluid. Likewise in the PWR design, the fuel is stationary and pressurized liquid water is the heat transfer fluid. What is unique about the MSBR design, is that the fuel and the heat transfer fluid are one-in-the-same, namely molten salt. What follows is a comparison of select performance characteristics of the three reactors described in Table 2-1.



Table 2-1. Performance characteristics of three reactor types.

	ORNL Single-Fluid MSBR	Orano Super-Phenix	Westinghouse AP1000
Reactor Type	MSBR	SFBR	PWR
Status	Conceptual	Decommissioned	Operating
Thermal Power, MWt	2,250	3,000	3,415
Electrical Power, MWe	1,000	1,200	1,117
Power Efficiency, %	44.4	40.0	32.7
Liquid Coolant	Molten Salt	Sodium	Pressurized water
Liquid Coolant Inventory, MT	160	3,500	178
Fuel Type	Molten salt	Mixed oxide	Uranium oxide
Breeder Fuel Cycle	Th-232/U-233	U-238/Pu-239	-
Neutron Spectrum	Thermal	Fast	Thermal
Reference: [2, 3, 4]			

Order-of-magnitude calculations of fuel consumptions are shown in Figure 2-3 for the normalized production of 1,000 MWe for the reactors listed in Table 2-1. The thermal energy (MWt) curves in Figure 2-3 for U-235 and U-233 are based on fission energies of 202.5 and 197.9 MeV, respectively. The net consumption rate of fissile metal (based on U-233 for the MSBR and U-235 for the SFBR and PWR) is shown as a function of the thermal-to-electrical conversion efficiency of each reactor to produce 1,000 MWe. This is a particularly important consideration for the MSBR because the fission products report directly to the fuel salt. In other words, for this example, the MSBR fuel salt is accumulating approximately  $2.375 \text{ kg d}^{-1}$  of fission product elements in the production of 1,000 MWe. (As a rule-of-thumb approximation,  $1 \text{ kg d}^{-1}$  of fissile metal is consumed per 1,000 MWt produced. And generally, there are not large differences in thermal energies released during the fission the different fissile isotopes.)

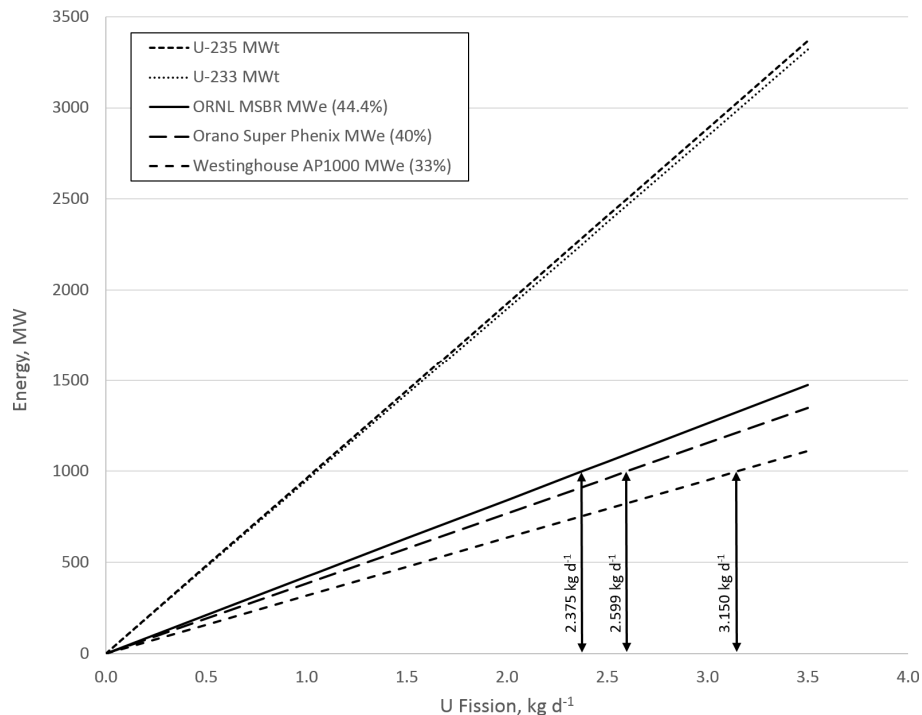


Figure 2-3. Fissile consumption as a function of energy production.

As discussed previously, a reactor core is essentially a heat exchanger. In the core, thermal energy is produced by fission (and other nuclear processes) and extracted by coolant flow. As a consequence, the coolant temperature increases as it flows through the reactor core. At steady state, the rate of thermal energy production equals the rate of thermal energy extraction, and the temperature at any fixed point is (to a first approximation) unchanging. Therefore, there are fundamental relationships between the thermal and physical properties of the reactor core and coolant. These relationships are expressed in terms of a mass flowrate ( $\text{MT s}^{-1}$ ) of coolant in Figure 2-4, a volumetric flowrate ( $\text{m}^3 \text{s}^{-1}$ ) of coolant in Figure 2-5, and a volumetric flowrate (gallons per minute [gpm]) of coolant in Figure 2-6, all as a function of the temperature increase of the coolant as it flows through the reactor core. Both sets of units,  $\text{m}^3 \text{s}^{-1}$  and gpm, are presented here because they are commonly encountered in the various reactor design studies.

In each case, the range of coolant temperature increase is 30 K; which is +15 K and -15 K on either side of the specified design coolant temperature increase. The purpose for including a range of temperatures was to improve the illustrations of the relationships. It is not meant to imply that the reactor designs have this degree of tolerance.

Each of the three reactors has a fixed inventory of coolant. Based on the respective flow rates and inventories, the times to cycle the coolant inventories through the reactors are shown in Figure 2-7.

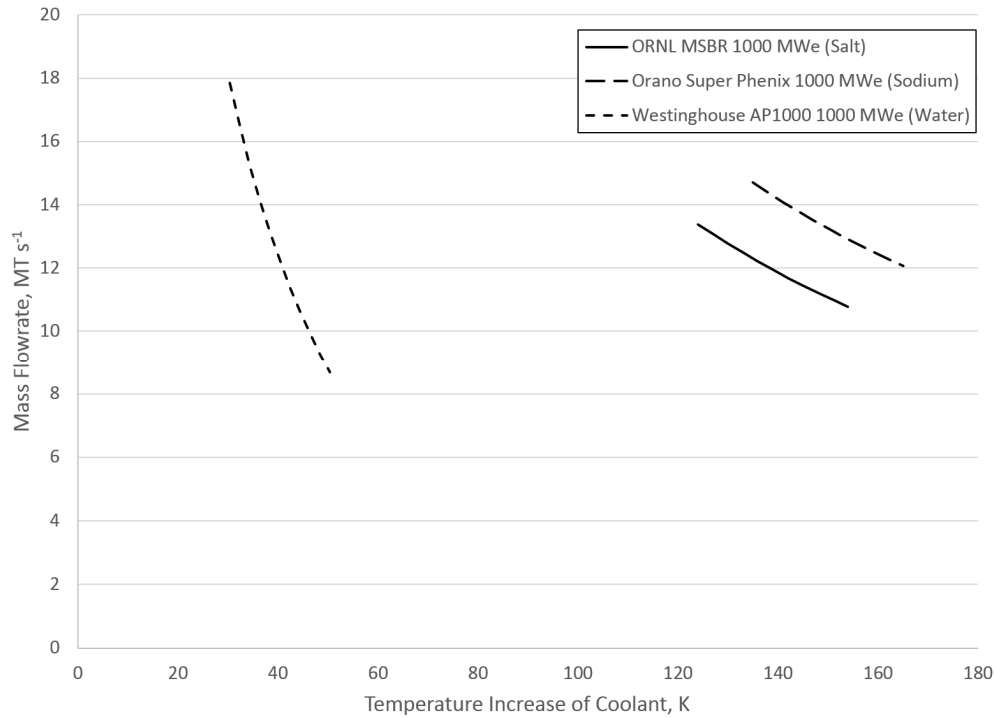


Figure 2-4. Mass flowrate of coolant.

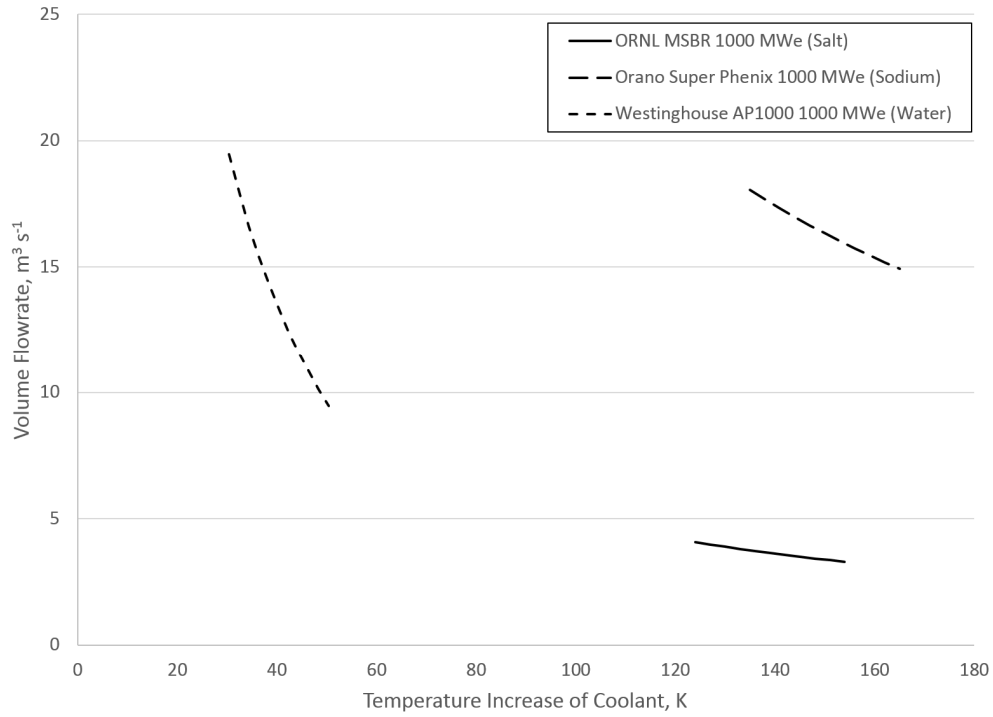


Figure 2-5. Volumetric flowrate of coolant ( $\text{m}^3 \text{s}^{-1}$ ).

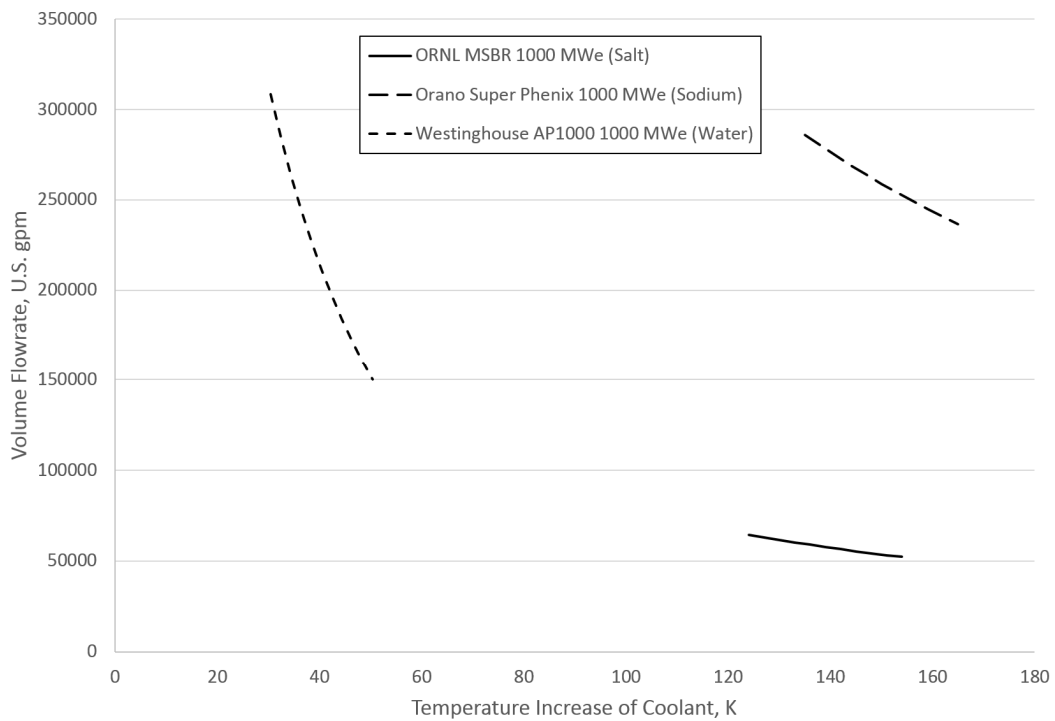


Figure 2-6. Volumetric flowrate of coolant (gpm).

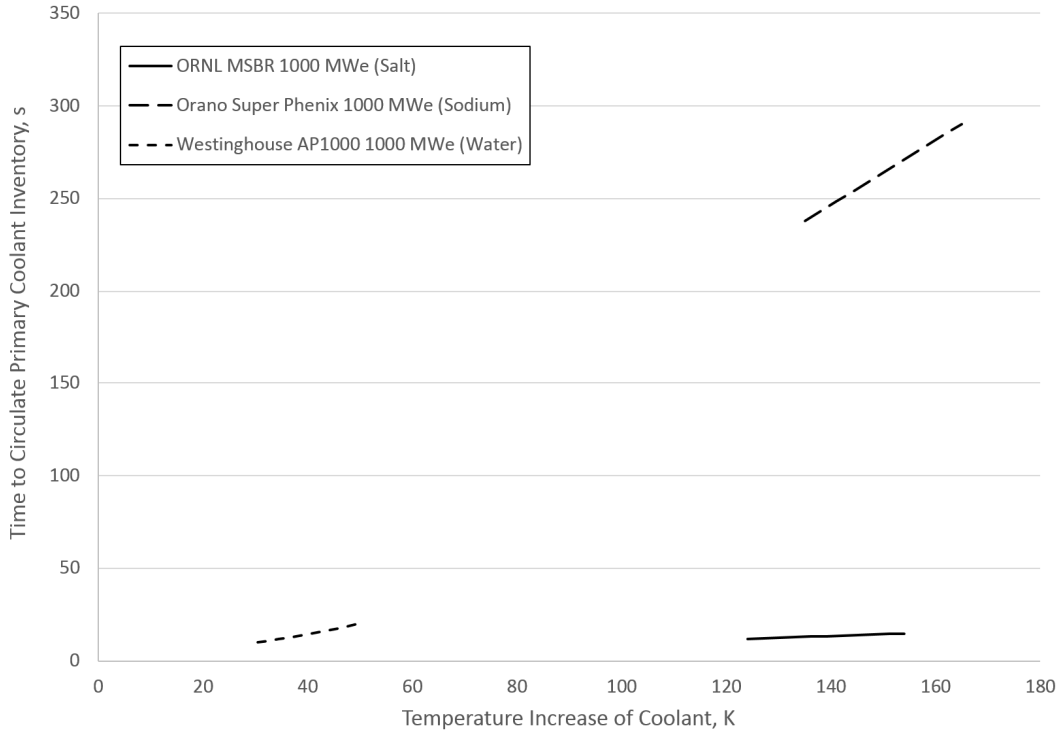


Figure 2-7. Coolant cycle time.

The thermal and physical properties used to construct Figures 2-4 through 2-7 are summarized in Table 2-2. The actual design specifications are highlighted in grey; these data were used as the midpoints in the accompanying figures. Heat capacities of salt [2], sodium [5], and water [6] were taken from the literature. Densities of salt [2], sodium [7], and water [6] were taken from the literature. For liquid water to exist at the temperatures of interest in Table 2-2, the water must necessarily be pressurized to approximately 120 bar. Correspondingly, the vapor pressures of salt and sodium at the temperatures of interest were well below one bar.

In Table 2-2, notice the similarities and the differences between the three reactors and the three coolant liquids. The following observations are of particular interest.

- The temperature increase of coolant through the PWR is much less than the MSBR and SFBR.
- The temperature increase of coolants through the MSBR and SFBR are comparable.
- The heat capacity of water is much greater than that of salt and sodium.
- The heat capacities of salt and sodium are comparable.
- The density of salt is much greater than that of sodium and water.
- The densities of sodium and water are comparable.
- The mass flowrates in Figure 2-4 are all within a comparable range of each other. The design-basis mass flowrates for the MSBR, SFBR, and PWR are 11.95, 13.25, and 12.22 MT s<sup>-1</sup>, respectively. That the MSBR and SFBR have similar mass flowrates is expected because these reactors share similar properties; namely the temperature increases of the coolants, and the heat capacities of salt and sodium. That the PWR has a similar mass flowrate, even though the temperature increase of the coolant is much lower, is a consequence of the much greater heat capacity of water.

Table 2-2. Thermal and physical properties of the coolant liquids.

Coolant Inlet Temperature, °C											
MSBR	566	566	566	566	566	566	566	566	566	566	566
SFBR	395	395	395	395	395	395	395	395	395	395	395
PWR	281	281	281	281	281	281	281	281	281	281	281
Coolant Outlet Temperature, °C											
MSBR	690	693	696	699	702	705	708	711	714	717	720
SFBR	530	533	536	539	542	545	548	551	554	557	560
PWR	311	313	315	317	319	321	323	325	327	329	331
Coolant Increase in Temperature, °C											
MSBR	124	127	130	133	136	139	142	145	148	151	154
SFBR	135	138	141	144	147	150	153	156	159	162	165
PWR	30	32	34	36	38	40	42	44	46	48	50
Heat Capacity, J g <sup>-1</sup> K <sup>-1</sup>											
Salt	1.357	1.357	1.357	1.357	1.357	1.357	1.357	1.357	1.357	1.357	1.357
Sodium	1.259	1.259	1.258	1.258	1.258	1.258	1.257	1.257	1.257	1.257	1.257
Water	5.582	5.676	5.779	5.889	6.009	6.137	6.274	6.421	6.579	6.746	6.924
Density, kg L <sup>-1</sup>											
Salt	3.291	3.289	3.287	3.285	3.283	3.281	3.279	3.277	3.275	3.273	3.271
Sodium	0.815	0.814	0.814	0.813	0.812	0.811	0.811	0.810	0.809	0.808	0.807
Water	0.917	0.917	0.917	0.917	0.917	0.917	0.917	0.917	0.917	0.917	0.917

The volumetric flowrates in Figures 2-5 and 2-6 are not all within a comparable range of each other. The design-basis volumetric flowrates for the MSBR, SFBR, and PWR are 3.64, 16.33, and 13.33 m<sup>3</sup> s<sup>-1</sup>, respectively; and 57,680, 258,900, and 211,300 gpm, respectively. The SFBR and PWR have similar volumetric flowrates because sodium and water have similar densities. The MSBR has a much lower volumetric flowrate because salt has a much higher density than sodium and water.

The circulation times in Figure 2-7 are not all within a comparable range of each other. The design-basis circulation times for the MSBR, SFBR, and PWR are 13.4, 264, and 14.6 s, respectively. Because the SFBR is a pool-type reactor, it has a particularly large reservoir of sodium coolant. Therefore, the time to circulate the primary coolant inventory through the SFBR is much longer than the times required for the MSBR and PWR, which have much smaller coolant inventories.

These comparisons have demonstrated that the flow of salt through the MSBR is perfectly consistent with the flow of sodium through the SFBR and the flow of water through the PWR. Nevertheless, the magnitudes of the coolant flowrates are astonishingly high. In the case of the MSBR, the fuel salt is flowing through the reactor core at a rate of 15 MT s<sup>-1</sup>, which is equivalent to 3.64 m<sup>3</sup> s<sup>-1</sup> (57,680 gpm). And the entire 160-MT inventory of fuel salt is circulated through the reactor core every 13.4 s.

## 2.4 Management of Pa-233 in the Th-232/U-233 Fuel-Cycle MSBR

The management of Pa-233 is certainly one of the major factors necessary to maintain a positive breeding ratio in the Th-232/U-233 fuel-cycle MSBR. Pa-233 must be continuously extracted from the blanket salt (in the two-fluid design) or the fuel salt (in the single-fluid design). A simplified extraction scheme for a single-fluid MSBR is shown in Figure 2-8.

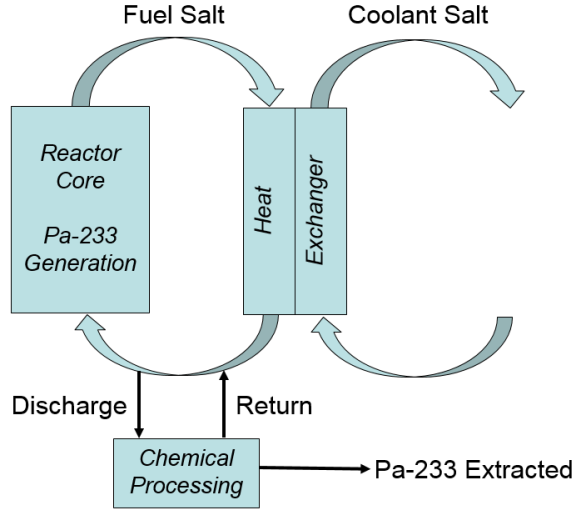


Figure 2-8. Pa-233 management in the single-fluid MSBR.

The rate of Pa-233 generation in the reactor core is a function of the entire system performance and cannot be accurately calculated by simple methods. This system dependence will be discussed again shortly, but it can be well imagined that under a specific set of reactor performance characteristics Pa-233 is generated within the core at some rate (i.e., kg d<sup>-1</sup>). If the system is at steady state, the following constraints apply.

- There is no net accumulation of Pa-233 in the fuel salt. Meaning that the concentration of Pa-233 in the fuel salt remains constant.
- In order for there to be no net accumulation in the fuel salt, the rate of generation of Pa-233 in the reactor core is equal to the rate of extraction of Pa-233 by chemical processing.

This steady state condition is described by the following equation.

$$R_{GEN} = R_{EXT} = R_D * C_D - R_R * C_R \approx R_D * (C_D - C_R) \approx R_D * (C_D * EFF_{EXT})$$

where,

$R_{GEN}$  = Rate of Generation of Pa-233 in the Reactor Core, kg d<sup>-1</sup>

$R_{EXT}$  = Rate of Extraction of Pa-233 by Chemical Processing, kg d<sup>-1</sup>

$R_D$  = Flowrate of Salt Discharge from the Fuel Salt to Chemical Processing, kg d<sup>-1</sup>

$C_D$  = Concentration of Pa-233 in Discharge Salt, kg kg<sup>-1</sup>

$R_R$  = Flowrate of Salt Return from Chemical Processing to the Fuel Salt, kg d<sup>-1</sup>

$C_R$  = Concentration of Pa-233 in Return Salt, kg kg<sup>-1</sup>

$EFF_{EXT}$  = Efficiency of Chemical Processing to Extract Pa-233 from the Salt Discharge, fraction

The above equation is recast by introducing a term for *cycle time*, which is the time required to cycle the entire inventory of fuel salt through chemical processing.

$$R_{GEN} = R_{EXT} \approx R_D * (C_D * EFF_{EXT}) \approx \frac{M_{FS}}{T_{CYC}} * (C_D * EFF_{EXT})$$

Where,

$M_{FS}$  = Total Mass of Fuel Salt, kg

$T_{CYC}$  = Cycle Time, d

With regards to the ORNL single-fluid 1,000 MWe MSBR design study, the steady state concentrations of Pa-233 in the fuel salt was calculated for the 3-d and 10-d cycle times as 45 parts per million [8] and 130 parts per million [9], respectively. Based on a total fuel salt volume of 48.7 m<sup>3</sup> with a density of 3291 kg m<sup>3</sup> [2], the mass of fuel salt in the reactor system is 160 MT. Therefore, for a 3-d cycle time the salt discharge rate to chemical processing is 53.4 MT d<sup>-1</sup> (2.98 gpm), and for a 10-d cycle time the rate is 16.0 MT d<sup>-1</sup> (0.89 gpm).

The relationships described above are shown in Figure 2-9. The steady state Pa-233 concentration is assumed to be linear between the two modeled concentrations for the 3-d and 10-d cycle times. The Pa-233 extraction rate is based on an extraction efficiency ( $EFF_{EXT}$ ) of 0.99. From this small window into the performance characteristics of the single-fluid MSBR as modeled by ORNL, it is apparent that the Pa-233 extraction rate is inversely proportional to the cycle time. In simple terms, the shorter the cycle time, the greater the breeding ratio.

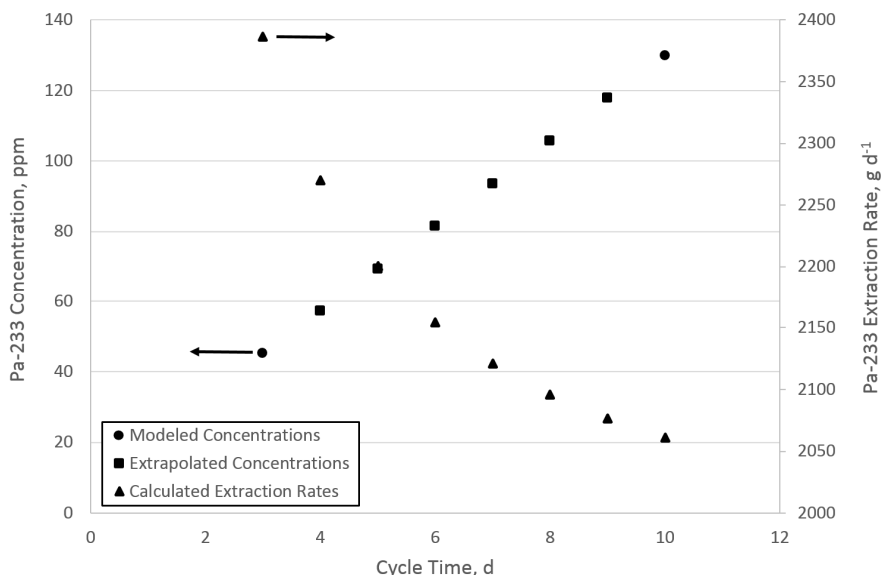


Figure 2-9. Steady state Pa-233 concentration and extraction rate as a function of cycle time.

Of course, the performance described in Figure 2-9 is not a rigorous interpretation because it is based on two sets of modeled results from two separate ORNL reports. There is much more performance intricacy in the ORNL models than that described in Figure 2-9. For example, it is necessary to consider the unique fates of each of the many products of fission, transmutation, and corrosion; as well as the neutronics performance of the reactor core. For example, fission product gases and some noble metal fission products are managed by means other than the chemical processing flowsheet. The neutronics performance of the core is influenced by every aspect of the chemical composition of the fuel salt.

## 2.5 Modeling of the MSBR and the Chemical Processing Plant

The preceding discussion was intended to provide a single technical illustration (not a complete description) of the point made earlier, that reactor performance and chemical processing performance are intimately and complexly coupled. An attempt is made in Figure 2-10 to further illustrate the nature of such a relationship. In nonspecific terms, performance in Figure 2-10 exists as a three-dimensional space within the XYZ coordinates, where X, Y, and Z are three independent measures of performance. For some nonspecific actual process under consideration, ideal performance is defined as any point within Space A, the smallest space. Such ideal performance could imply a degree of perfection that cannot be realized by the actual process. Space B represents acceptable performance. Certainly, ideal performance lies within the realm of acceptable performance, which is why Space A lies within Space B. Space C

represents the modeled performance of the actual process. A modeled performance based on realistic process assumptions is required to overlap with Space B if there is any hope of the actual process performing acceptably. Finally, to be useful, the modeled performance should bound the actual performance with some measure of statistical uncertainty, which is why Space D lies within Space C.

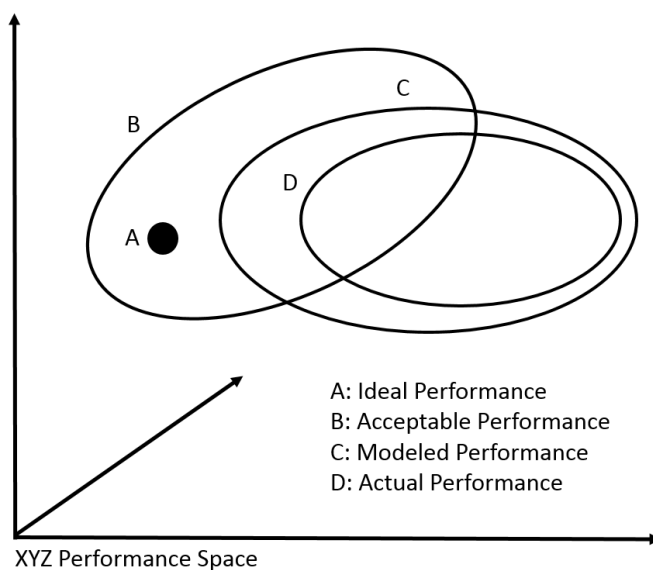


Figure 2-10. Conceptual performance space.

In the context of the MSBR discussion at hand, Space A represents the performance of an idealized chemical processing plant. The expression *idealized* is meant to imply performance measures such as perfect chemical separations, no process losses, no corrosion, no down-time, etc. In such a case, though unrealistic, the performance of the chemical processing plant is rendered a nonissue with respect to the success of the reactor concept as a whole.

Space B represents acceptable performance of the chemical processing plant. For example, if the chemical processing plant can meet or exceed these performance requirements, the reactor concept remains viable. Space B does not represent an analysis of the performance capabilities of the chemical processing plant (that follows next). Instead, it strictly represents an analysis of the performance requirements imposed by the reactor technology. In other words, Space B is not an analysis of how the chemical processing plant will achieve such performance, it is only an analysis of what performance the chemical processing plant must achieve.

Space C represents the performance of the modeled chemical processing plant. It is based on the selection of a specific flowsheet (and all of the process parameters and assumptions that go along with the engineering analysis of the flowsheet). In order to be useful, the performance of the modeled chemical process plant must be a probabilistic measure of the performance of the actual chemical processing plant. In other words, the modeled performance must bound the actual performance. The modeled performance takes into account that chemical separations are not perfect, there are process losses, there is corrosion, there is down-time, etc.

In summary, Spaces A and B are most closely associated to the performance of the reactor, and Spaces C and D are most closely related to the performance of the chemical processing plant. However, none of these performance measures are completely independent of each other, and the relationships are intimately and complexly coupled.



## 2.6 Chemical Processing Plant Studies

The performance concepts discussed above were well understood early in the development of MSR technologies. However, the design a chemical processing plant capable of achieving acceptable performance (modeled, actual, or otherwise) took a great deal of time and effort and, in the end, was never demonstrated in concert with an operating reactor. The operation of a chemical processing plant is described by a chemical/engineering flowsheet, which is described by an assemblage of chemical/engineering unit operations, whose interrelationships with each other obey chemical/engineering principles such as mass and energy balances, thermodynamics, kinetics, thermal/physical properties, materials compatibility, etc. These challenges were certainly recognized from the earliest stages. However, the most significant advances in chemical processing plant designs accompanied the two-fluid and single-fluid 1,000 MWe MSBR design studies.

There are many ORNL reports containing technical information on chemical processing of molten salts. An example of a series of progress reports dedicated to this topic is summarized in Table 2-3. Earlier reports prior to ORNL-TM-3053 contained additional technical information unrelated to MSBR chemical processing technologies (i.e., the progress reports were shared by different programs). Reports beginning with ORNL-TM-3053 and later were dedicated to MSBR chemical processing technologies.

Table 2-3. Series of progress reports on MSBR chemical processing technologies.

Date	Report Number	Table of Contents (Abridged)
Feb-68	ORNL-4094	7. Molten-Salt Reactor Processing
		7.1 Relative Volatilities of Rare-Earth Fluorides in LiF
		7.2 Buildup of a Concentration Gradient in a Semicontinuous Still
Feb-68	ORNL-4139	5. Molten-Salt Reactor Processing
		5.1 Molten-Salt Distillation Studies
May-68	ORNL-4204	7. Molten-Salt Reactor Processing
		7.1 Molten-Salt Distillation Studies
Jul-69	ORNL-4234	5. Molten-Salt Reactor Processing Studies
		5.1 Vapor-Liquid Equilibrium Data in Molten-Salt Mixtures
		5.2 Circulation Rates and Heat Transfer in Molten-Salt Stills
		5.3 Distillation of MSRE Fuel Carrier Salt
Dec-67	ORNL-4235	Not yet available for public release.
Oct-69	ORNL-4364	2. Molten-Salt Reactor Processing Studies
		2.1 MSRE Distillation Experiment
		2.2 Removal of Protactinium from a Single-Fluid MSBR
		2.3 Continuous Fluorination of Molten Salt
		2.4 Removal of Nickel, Iron, and Chromium Fluoride from Simulated MSRE Fuel Carrier Salt
Feb-70	ORNL-4365	3. Molten-Salt Reactor Processing Studies
		3.1 MSRE Distillation Experiment
		3.2 Frozen-Wall Corrosion Protection
		3.3 Studies of a Simulated Molten-Salt Liquid-Bismuth Contactor

Date	Report Number	Table of Contents (Abridged)
		3.4 Electrolytic-Cell Development
Apr-70	ORNL-4366	3. Molten-Salt Reactor Processing Studies
		3.1 Distillation of Molten Salt
		3.2 Gas-Lift Pumping of Liquid Metals
		3.3 Simulated Salt-Metal Contactor Studies
Nov-70	ORNL-TM-3053	1. Introduction
		2. Semicontinuous Engineering Experiments on Reductive Extraction
		3. Electrolytic Cell Development
		4. Separation of Rare Earth From Thorium by Fractional Crystallization from Bismuth
		5. Material Balance Calculations for an MSBR
		6. References
Feb-71	ORNL-TM-3137	1. Introduction
		2. Proposed Flowsheet for Processing a Single-Fluid MSBR by Reductive Extraction
		3. MSBR Material-Balance Calculations
		4. Removal of Protactinium from a Single-Fluid MSBR
		5. Use of the Protactinium Isolation System for Controlling the Uranium Concentration in the Blanket of a Single-Fluid MSBR
		6. Removal of Rare Earths from a Single-Fluid MSBR
		7. Semicontinuous Engineering Experiments on Reductive Extraction
		8. Electrolytic Cell Development
		9. MSRE Distillation Experiment
		10. References
May-71	ORNL-TM-3138	1. Introduction
		2. Removal of Protactinium from a Single-Fluid MSBR
		3. Effect of Chemical Processing on the Nuclear Performance of an MSBR
		4. Reductive Extraction Experiments in a Mild-Steel Flow-Through Facility
		5. Digital Simulation of the Flow Control Systems for the Reductive Extraction Facility
		6. Electrolytic Cell Development
		7. Analysis of Mass Transfer in Electrolytic Cells
		8. Axial Mixing in Packed Columns with High-Density Fluids
		9. Removal of Heat from Packed-Column Contactors used for Isolating Protactinium
		10. MSRE Distillation Experiments

Date	Report Number	Table of Contents (Abridged)
		11. References
Aug-71	ORNL-TM-3139	1. Introduction
		2. Semicontinuous Reductive Extractions Experiments in a Mild-Steel Facility
		3. Measurement of Axial Dispersion Coefficient in Packed Columns
		4. A Simplified Method for Estimating the Effect of Axial Dispersion on Countercurrent Column Performance
		5. Effect of Axial Dispersion in Packed Column Contactors used for MSBR Processing
		6. Axial Dispersion in an Open Bubble Column
		7. Electrolytic Cell Development: Static Cell Experiments
		8. Design and Installation of the Flow Electrolytic Cell Facility
		9. Calibration of an Orifice-Head Pot Flowmeter with Molten Salt and Bismuth
		10. Bismuth-Salt Interface Detector
		11. Stripping of ThF <sub>4</sub> from Molten Salt by Reductive Extraction
		12. References
Oct-71	ORNL-TM-3140	1. Introduction
		2. Rare-Earth Removal Using the Metal-Transfer Process
		3. Protactinium Isolation Using Fluorination-Reductive Extraction
		4. Axial Dispersion in Open Bubble Columns
		5. Semicontinuous Reductive Extraction Experiments in a Mild-Steel Facility
		6. Simulation of the Flow Control Systems for the Reductive Extraction Facility
		7. Calibration of an Orifice-Head Pot Flowmeter with Molten Salt and Bismuth
		8. Electrolytic Cell Development: Static Cell Experiments
		9. Electrolytic Cell Development: Formation of Frozen Films with Aqueous Electrolytes
		10. Development of a Bismuth-Molten Salt Interface Detector
		11. Continuous Salt Purification
		12. MSRE Distillation Experiment
		13. Recovery of <sup>7</sup> Li from <sup>7</sup> Li-Bismuth Rare-Earth Solutions by Distillation
		14. Prevention of Axial Dispersion in Packed Columns
		15. Hydrodynamics of Packed Column Operation with High-Density Fluids
		16. References
Dec-71	ORNL-TM-3141	1. Introduction
		2. MSBR Fuel Processing using Fluorination-Reductive Extraction and the Metal Transfer Process
		3. Axial Dispersions in Open Bubble Columns

Date	Report Number	Table of Contents (Abridged)
		4. Considerations of Continuous Fluorination and Their Applicability to MSBR Processing
		5. Use of Radio-Frequency Induction Heating for Frozen-Wall Fluorinator Development Studies
		6. MSRE Distillation Experiment
		7. Development of the Metal Transfer Process
		8. Electrolytic Cell Development: Static Cell Experiments
		9. Study of the Purification of Salt by Continuous Methods
		10. Semicontinuous Reductive Extraction Experiments in a Mild-Steel Facility
		11. References
Feb-72	ORNL-TM-3257	1. Introduction
		2. Analysis of the Fluorination-Reductive Extraction and Metal Transfer Flowsheet
		3. Development of a Frozen-Wall Fluorinator: Design Calculations for Induction Heating of a Frozen-Wall Fluorinator
		4. Development of the Metal Transfer Process
		5. Study of the Purification of Salt by Continuous Methods
		6. Semicontinuous Reductive Extraction Experiments in a Mild-Steel Facility
		7. Measurement of Axial Dispersion Coefficients in Packed Columns
		8. References
May-72	ORNL-TM-3258	1. Introduction
		2. Analysis of the Fluorination-Reductive Extraction and Metal Transfer Flowsheet
		3. Analysis of Uranium removal from Fuel Salt by Oxide Precipitation
		4. Development of a Frozen-Wall Fluorinator: Installation of a Simulated Fluorinator for Studying Induction Heating
		5. Measurement of Axial Dispersion Coefficients and Gas Holdup in Open Bubble Columns
		6. Development of the Metal Transfer Process
		7. Semicontinuous Reductive Extraction Experiments in a Mild-Steel Facility
		8. Prevention of Axial Dispersion in Packed Columns
		9. Electrolytic Reduction of LiCl using a Bismuth Cathode and a Graphite Anode
		10. Study of the Purification of Salt by Continuous Methods
		11. Electrolytic Oxidation of $\text{Pa}^{4+}$ to $\text{Pa}^{5+}$ in MSBR Fuel Salt
		12. References
Dec-72	ORNL-TM-3259	1. Introduction
		2. Flowsheet Analysis: Isolation of Protactinium by Oxide Precipitation

Date	Report Number	Table of Contents (Abridged)
		3. Flowsheet Analysis: Reference Processing Plant Flowsheet Based on Fluorination, Reductive Extraction, and the Metal Transfer Process
		4. Flowsheet Analysis: Importance of Uranium Inventory in an MSBR Processing Plant
		5. Flowsheet Analysis: Removal of Rare-Earth Fission Products from LiCl in the Metal Transfer Process
		6. Frozen-Wall Fluorinator Development: Experiments on Induction Heating in a Continuous Fluorinator Simulation
		7. Predicted Corrosion Rates in Continuous Fluorinators Employing Frozen-Wall Protection
		8. Predicted Performance of Continuous Fluorinators
		9. Measurement of Axial Dispersion Coefficients and Gas Holdup in Open Bubble Columns
		10. Semicontinuous Reductive Extraction Experiments in a Mild-Steel Facility
		11. Development of the Metal Transfer Process: Operation of Experiment MTE-2
		12. Development of the Metal Transfer Process: Design of Experiment MTE-3
		13. Development of Mechanically Agitated Salt-Metal Contactors
		14. Hydrodynamics of Packed-Column Operation with High-Density Fluids
		15. Analysis of Multicomponent Mass Transfer Between Molten Salts and Liquid Bismuth During Countercurrent Flow in Packed Columns
		16. Study of the Purification of Salt by Continuous Methods
		17. References
Dec-72	ORNL-TM-3352	1. Introduction
		2. Frozen-Wall Fluorination Development: Experiments on Induction Heating in a Continuous Fluorinator Simulation
		3. Semicontinuous Reductive Extraction Experiments in a Mild-Steel Facility
		4. Development of the Metal Transfer Process: Inspection of Experiment MTE-2
		5. Development of the Metal Transfer Process: Agitator Tests for Experiment MTE-3
		6. Distribution of Radium Between LiCl and Li-Bi Solutions
		7. Development of Mechanically Agitated Salt-Metal Contactors
		8. Analysis of Multicomponent Mass Transfer Between Molten Salts and Liquid Bismuth During Countercurrent Flow in Packed Columns
		9. Engineering Studies of Uranium Oxide Precipitation
		10. Study of the Purification of Salt by Continuous Methods
		11. References
Mar-75	ORNL-TM-4698	1. Introduction
		2. Salt-Metal Contactor Development

Date	Report Number	Table of Contents (Abridged)
		3. Development of the Metal Transfer Process: Continuation of Engineering-Scale Experiments
		4. Continuous Fluorinator Development
		5. References
Jul-75	ORNL-TM-4863	1. Introduction
		2. Development of the Metal Transfer Process
		3. Salt-Metal Contactor Development: Experiments with a Mechanically Agitated, Nondispersing Contactor using Water and Mercury
		4. Salt-Metal Contactor Development: Experiments with a Mechanically Agitated, Nondispersing Contactor in the Salt-Bismuth Flowthrough Facility
		5. Fuel Reconstitution Development: Design of a Fuel Reconstitution Engineering Experiment
		6. References
Jan-76	ORNL-TM-4870	1. Introduction
		2. Continuous Fluorinator Development: Autoresistance Heating Test AHT-3
		3. Development of the Metal Transfer Process
		4. Salt-Metal Contactor Development: Experiments with a Mechanically Agitated, Nondispersing Contactor in the Salt-Bismuth Flowthrough Facility
		5. Salt-Metal Contactor Development: Experiments with a Mechanically Agitated, Nondispersing Contactor using Water and Mercury
		6. Fuel Reconstitution Development: Installation of Equipment for a Fuel Reconstitution Engineering Experiment
		7. References
Mar-76	ORNL-TM-4894	1. Introduction
		2. Continuous Fluorinator Development: Autoresistance Heating Test AHT-4
		3. Development of the Metal Transfer Process
		4. Salt-Metal Contactor Development: Experiments with a Mechanically Agitated, Nondispersing Contactor in the Salt-Bismuth Flowthrough Facility
		5. Salt-Metal Contactor Development: Experiments with a Mechanically Agitated, Nondispersing Contactor using Water and Mercury
		6. Fuel Reconstitution Development: Installation of Equipment for a Fuel Reconstitution Engineering Experiment
		7. References
Jun-76	ORNL-TM-5041	1. Introduction
		2. Continuous Fluorinator Development: Autoresistance Heating Test AHT-4 and Conceptual Design of the Continuous Fluorinator Experimental Facility
		3. Development of the Metal Transfer Process: Experiment MTE-3B
		4. Salt-Metal Contactor Development: Experiments with a Mechanically Agitated, Nondispersing Contactor in the Salt-Bismuth Flowthrough Facility

Date	Report Number	Table of Contents (Abridged)
		5. Salt-Metal Contactor Development: Experiments with a Mechanically Agitated, Nondispersing Contactor using Water and Mercury
		6. Fuel Reconstitution Development: Analytical Instrumentation and Alternatives for Gold-Lining of Equipment for the Second Fuel Reconstitution Engineering Experiment
		7. References

## 2.7 Chemical Processing Unit Operations

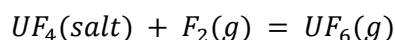
Chemical processing flowsheets were studied at ORNL for three different scenarios.

- *Two-Fluid MSBR*. The reactor is operated with distinct blanket salt and fuel salt heat-exchanger circuits. The reactor core and the chemical processing plant are designed such that the blanket and fuel salts always remain separated from each other. Slip streams of each salt are treated separately in the chemical processing plant. The thorium-containing blanket salt is treated to remove uranium and protactinium; while the uranium-containing fuel salt is treated to remove fission products. The blanket and fuel salts have markedly different LiF:BeF<sub>2</sub> ratios.
- *Single-Fluid MSBR (Version 1)*. As above, the reactor is operated with distinct blanket salt and fuel salt heat-exchanger circuits. However, there is no longer a strict requirement to keep the two salts separated from each other. Slip streams of each salt are mixed with each other (hence, *single-fluid*) upon entering the chemical processing plant, which returns a thorium-containing salt (with low concentrations of uranium and protactinium) to the reactor's blanket salt circuit, and a uranium-containing salt (with low concentrations of thorium and protactinium) to the reactor's fuel salt circuit. Otherwise, the blanket and fuel salt shared the same LiF:BeF<sub>2</sub> ratio.
- *Single-Fluid MSBR (Version 2)*. Unlike the examples above, the reactor is operated with a single fuel salt heat-exchanger circuit. The single fuel salt serves both functions as fuel and blanket. A single slip stream of the fuel salt is treated in the chemical processing plant, which manages the concentrations of thorium, protactinium, uranium, and fission products in the fuel salt returned to the reactor.

Brief descriptions are provided below of a variety of unit operations that appear in the various chemical processing flowsheets proposed by ORNL to manage MSBR salts. The process descriptions are intended to be generalized. The flowsheets themselves changed significantly over time and become quite complex through the interrelationships of unit operations with each other and the inherent control strategies required to make the processes function. Process descriptions with greater detail are better reserved for discussions of specific flowsheets.

## 2.8 Fluorination

Fluorination has a key role in all of the proposed chemical processing flowsheets. The primary purpose of fluorination is to separate uranium from bulk salt by exploiting the selective fluorination of uranium tetrafluoride (UF<sub>4</sub>) and the high vapor pressure of uranium hexafluoride (UF<sub>6</sub>). The UF<sub>4</sub> in the salt is converted to UF<sub>6</sub> by the action of fluorine gas. The UF<sub>6</sub> then enters the gas and is effectively separated from the bulk salt.



Fluorination was studied as a batch and continuous process. A continuous fluorinator is essentially a counter-current contactor with molten salt and fluorine gas flowing in opposite directions to each other while intermixing. Unfortunately, fluorine gas is highly corrosive to all practical materials of construction

such as steels and nickel-based alloys. To overcome this challenge, it was proposed that all wetted components in the reaction vessel be protected against corrosion by a frozen-layer of salt. This was called the “frozen-wall” technology. A schematic of a “frozen-wall” fluorinator is shown in Figure 2-11.

Fluorinators appear in the chemical processing flowsheets as separate unit operations applied to blanket salt, fuel salt, reservoir salt (i.e., in-storage salt where time is allowed for Pa-233 to decay to U-233), and intermediate process salts depending on which variant of the MSBR and chemical processing flowsheet are being considered.

Analogous to volatile  $\text{UF}_6$ , some fission products likewise form volatile fluorides during fluorination. For example, candidate fission products in this category include Br, I, Cs, Se, Mo, Tc, Ru, Sb, Zr, and Te. Therefore, if these fission products are entrained in the fuel salt entering the fluorinator, then some fraction will report to the  $\text{UF}_6$ -containing gas stream leaving the fluorinator. However, the chemistries that determine the ultimate fates of fission products generated within the MSBR is a highly complex subject that is touched upon later. But suffice it to say for now that there are no materials that contact the fuel salt with which certain fission products cannot react.

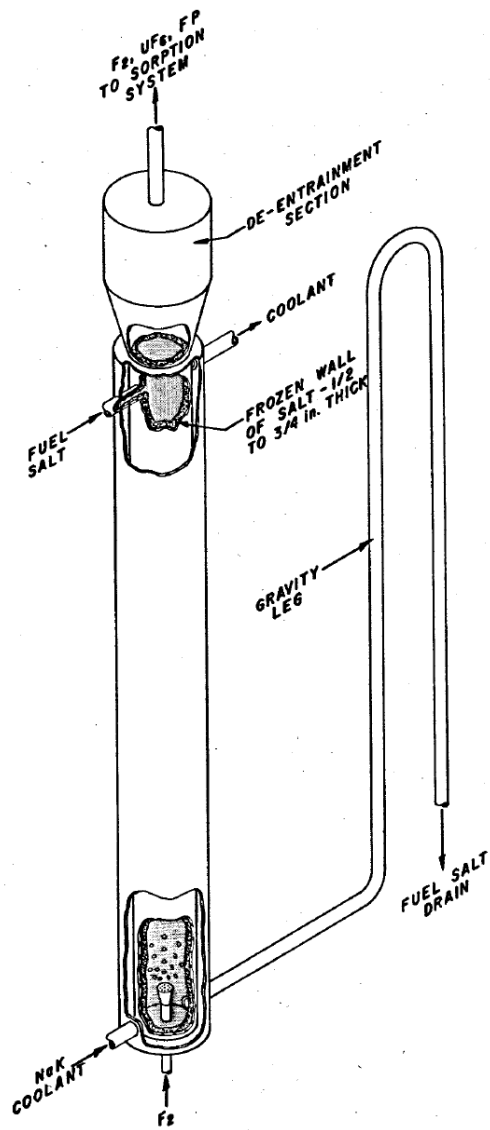


Figure 2-11. Schematic of a “frozen-wall” fluorinator [8].



## 2.9 UF<sub>6</sub> Purification

The UF<sub>6</sub>-containing gas stream emanating from the fluorinator is purified of volatile fission products by selective sorption and desorption reactions with beds of NaF and MgF<sub>2</sub> pellets. The first sorption bed is NaF at 400°C, which irreversibly captures Nb and Zr fluorides from the gas stream. The second sorption bed is NaF at 100°C, which reversibly captures U and Mo fluorides from the gas stream. The remaining volatile fission products pass through the second sorption bed and continue on to be captured as waste. With the U and Mo fluorides thus isolated, the second sorption bed is subsequently heated to >150°C to desorb the U and Mo fluorides into a clean gas stream. The third sorption bed is MgF<sub>2</sub> at 150°C, which captures the Mo fluorides allowing the UF<sub>6</sub> to pass through as a purified gas stream. A detailed flowsheet for UF<sub>6</sub> purification is shown in Figure 2-12.

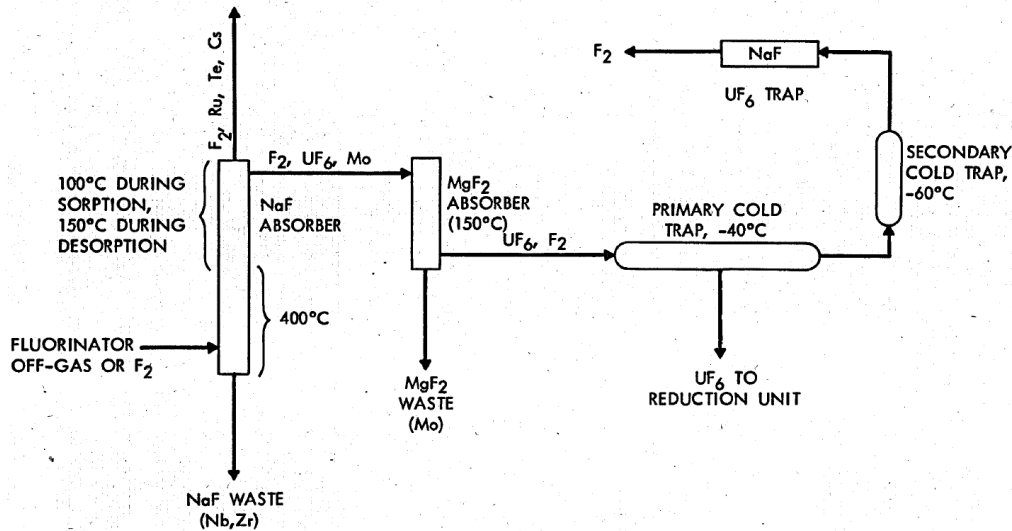
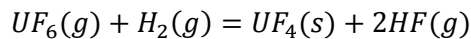


Figure 2-12. Flowsheet for UF<sub>6</sub> purification flowsheet [8].

## 2.10 UF<sub>6</sub> Reduction

The purified UF<sub>6</sub> gas is captured in cold-traps and reduced to UF<sub>4</sub> salt by the action of hydrogen gas.



The reduction of UF<sub>6</sub> was studied as a dry process as indicated by the above reaction, and as a wet process in which the UF<sub>6</sub> was first dissolved into LiF-BeF<sub>2</sub> salt before being reduced to UF<sub>4</sub>. As with fluorination, materials compatibility was again a challenge. Here too, it was proposed that all wetted components be protected against corrosion by a frozen-layer of salt (i.e., "frozen-wall" technology). That fraction of UF<sub>4</sub> required to sustain reactor operation is returned to the fuel salt. The general processes of returning UF<sub>4</sub> to the fuel salt are called *fuel reconstitution*. The excess UF<sub>4</sub>, made possible by the breeding aspect of the reactor operation and the separation and recovery efficiencies of the chemical processing plant, is retained as a commodity for future reactor fuel. A schematic of a continuous UF<sub>6</sub> reduction column is shown in Figure 2-13.

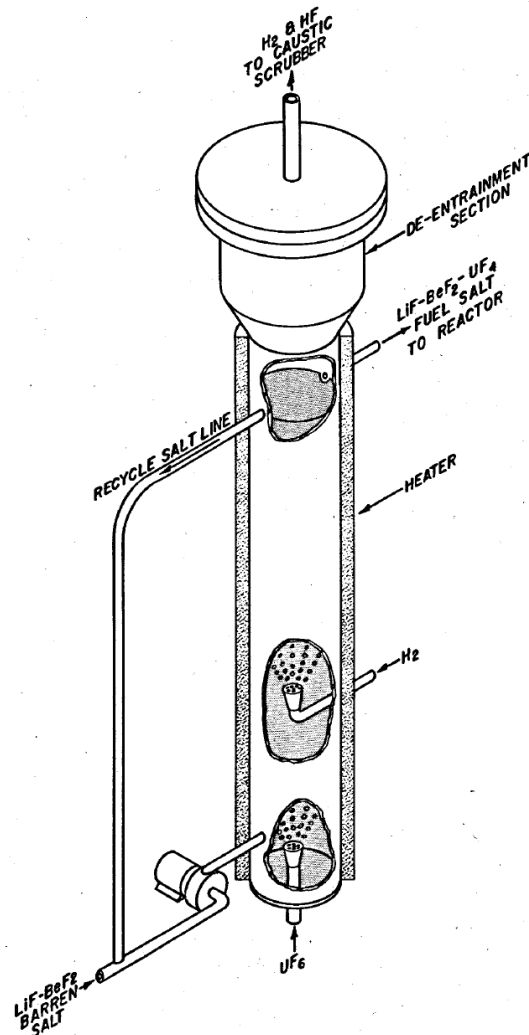


Figure 2-13. Schematic of a continuous  $\text{UF}_6$  reduction column [8].

## 2.11 Vacuum Distillation

Vacuum distillation had a key role in the earlier proposed chemical processing flowsheets applied to the two-fluid MSBR. At that time, the primary purpose of distillation was purification of fuel salt (distillation was not proposed as a means of purifying blanket salt). In this scenario, uranium was removed from the fuel salt by fluorination prior to distillation. Distillation affects separations by exploiting the higher vapor pressures of  $\text{LiF}$  and  $\text{BeF}_2$  relative to many of the fission product fluorides remaining in the salt post-fluorination. Purified  $\text{LiF-BeF}_2$  salt is recovered from the vapor phase, while the fission product fluorides are concentrated in the non-volatilized salt fraction remaining in the distillation bottoms. Distillation is performed under vacuum at  $1,000^\circ\text{C}$ . The solubility limits of fission product fluorides in  $\text{LiF-BeF}_2$  salts at  $1,000^\circ\text{C}$  were sufficiently great to make this process feasible. The fission-product laden salt that accumulates over time ultimately reports to waste.

However, distillation was made obsolete as a key unit operation by the development of reductive extraction and the metal transfer process. In the later proposed chemical processing flowsheets, distillation is relegated to lesser functions such as adjusting the salt composition prior to reductive extraction and the partial recovery of salt from waste streams from a reductive extraction plant. A schematic of a vacuum distillation still is shown in Figure 2-14.

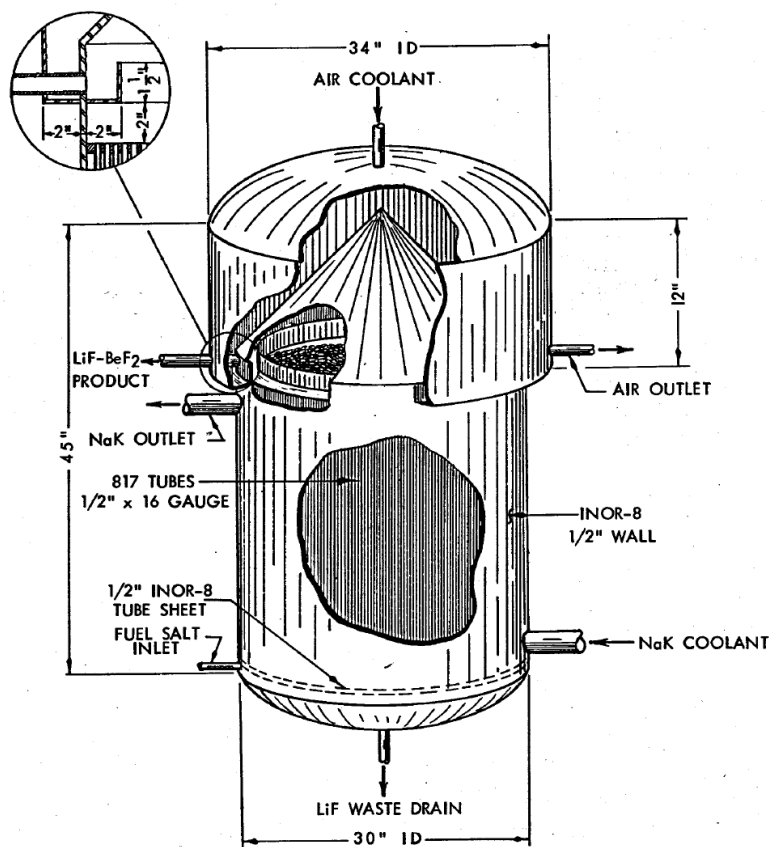
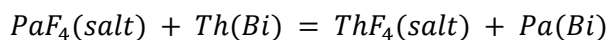
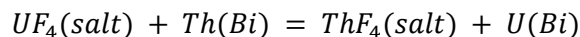


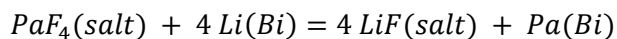
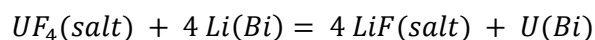
Figure 2-14. Schematic of a vacuum distillation still [8].

## 2.12 Reductive Extraction

Chemical processing strategies based on schemes of combining fluorination and distillation alone were very limited in their abilities to provide efficient separations. However, chemical processing capabilities improved greatly with the development of reductive extraction technologies. Reductive extraction refers to the exchange chemistries that occur between molten fluoride salts and liquid bismuth alloys. Typically, these reactions involve the simultaneous exchange to two or more different metals across the interface between the salt and metal phases. The following reactions represent the exchange between U and Pa cations in the salt with dissolved metallic Th in the liquid bismuth. Here, U and Pa are *reduced* from the salt, while Th is *oxidized* from the bismuth; Th dissolved in the liquid bismuth serves as the *reductant*.



Similarly, the following reactions represent the exchange between U and Pa cations in the salt with dissolved metallic Li in the liquid bismuth. Here, U and Pa are *reduced* from the salt, while Li is *oxidized* from the bismuth; Li dissolved in the liquid bismuth serves as the *reductant*.



These four reactions are thermodynamically favored under all but the most extreme concentration limits. The relative stabilities of fluorides from most-to-least stable are: LiF, ThF<sub>4</sub>, PaF<sub>4</sub>, UF<sub>4</sub>, and BiF<sub>3</sub>;

although the stabilities of  $\text{PaF}_4$  and  $\text{UF}_4$  are very close to each other. These relationships are illustrated graphically in the Ellingham diagram (HSC, Version 9.0) in Figure 2-15. This diagram shows the standard state Gibbs free energies of formation (normalized to 1 mole  $\text{F}_2(\text{g})$ ) of select fluorides as a function of temperature.

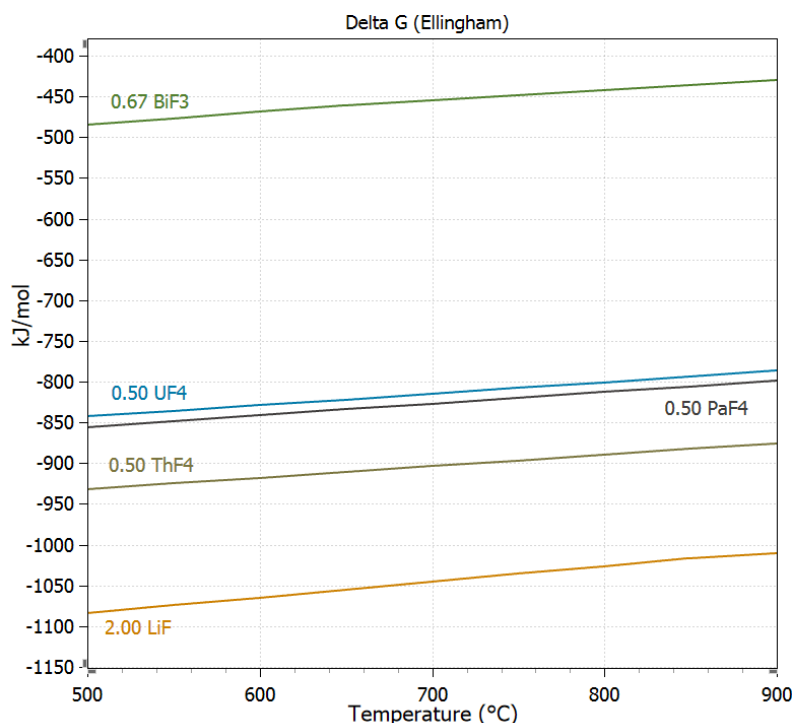
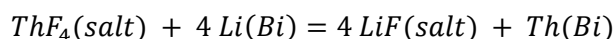
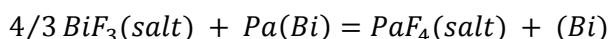
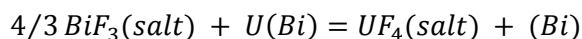


Figure 2-15. Ellingham diagram of select fluorides.

Based on this ranking of fluorides, Li can reduce Th, meaning that Li is a stronger *reductant* than Th.



Conversely, bismuth trifluoride ( $\text{BiF}_3$ ) can oxidize U and Pa from the liquid bismuth. Here, the  $\text{BiF}_3$  in the salt serves as the *oxidant*.



Such exchange reactions, in addition to generally being thermodynamically favored, are kinetically aided by providing an interface between the two phases that is intimately mixed, has a high surface area, and exhibits a high concentration gradients such that all factors work together to aid the completion of the desired reactions. This is precisely the function of the multistage counter-current contactors described next.

Few fission product fluorides are more stable in molten salt than LiF. This implies that Li-metal is a very powerful reductant that is capable of reducing almost any other metal from the molten salt into the liquid bismuth. At the other end of the spectrum lies  $\text{BiF}_3$ . Few fission product fluorides are less stable in molten salt than  $\text{BiF}_3$ . This implies that  $\text{BiF}_3$  is a very powerful oxidant that is capable of oxidizing almost any other metal from the liquid bismuth into the molten salt. Therefore, the chemical control of reductive extraction relies largely on the management of reductants such as Li and Th in the liquid bismuth, and oxidants such as  $\text{BiF}_3$  in the molten salt. In other words, the reactions are largely controlled by the limitations of stoichiometry rather than the limitations of thermodynamics and kinetics.

The metal transfer process is described later. However, the metal transfer process relies on many of the same principles as described for reductive extraction. The most significant difference between the two operations is that the reductive extraction process relies completely on fluoride salts, whereas the metal transfer process introduces chloride salts.

The purpose of reductive extraction is to selectively separate U, Pa, and rare earth fission products between molten salt and liquid bismuth phases. The exact application served by reductive extraction is highly dependent on the specific flowsheet. The purpose of the metal transfer process is to separate and isolate rare earth fission products into a waste stream.

## 2.13 Multistage Contactors

As described earlier, the purpose of multistage contactors is to facilitate the exchange reactions between molten salts and liquid bismuth alloys by providing a high-surface-area intimately-mixed interface between the two phases. Three design concepts were studied.

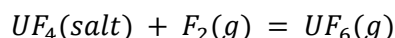
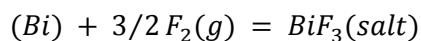
- **Packed Column.** The reaction column is filled with high-surface-area packing media. The liquid bismuth flows downward as the molten salt flows upward. Mixing is provided by the tortuous path around the packing media.
- **Baffled Column.** The reaction column is fitted with perforated distribution plates. The liquid bismuth flows downward as the molten salt flows upward. Mixing is provided by the tortuous path through the distribution plates.
- **Mechanically Agitated.** The reaction column is fitted with mechanically driven impellers. The liquid bismuth and molten salt cascade in opposite directions through a series of reaction columns. Mixing is provided by the forced contact imposed by the impellers.

These systems were studied using mixtures of water and mercury as simulants for molten salt and liquid bismuth, respectively. It was reported that the water/mercury system provided a closer approximation to the behavior of the salt/bismuth system than was possible with the organic/water system commonly used in aqueous separations chemistries.

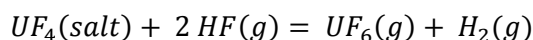
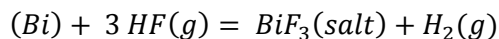
## 2.14 Hydrofluorination

Fluorination was discussed previously as a unit operation applied to process streams of uranium-containing molten salts for the purpose of extracting the uranium to the gas phase as  $UF_6$ . Hydrofluorination serves similar purposes as fluorination, except hydrofluorination applies hydrogen fluoride gas ( $HF(g)$ ) whereas fluorination applies fluorine gas ( $F_2(g)$ ).

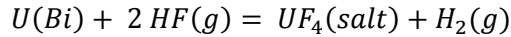
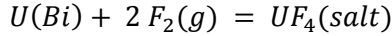
Liquid bismuth and  $UF_4$  are both oxidized by the action of  $F_2(g)$ . These reactions are thermodynamically favorable.



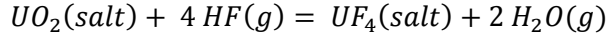
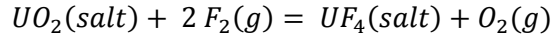
However, liquid bismuth and  $UF_4$  are not oxidized by the action of  $HF(g)$ . These reactions are not thermodynamically favorable.



Therefore,  $F_2(g)$  is capable of oxidizing both Bi and  $UF_4$ , while  $HF(g)$  is not. Furthermore, U, Pa, Th, and Li dissolved in liquid bismuth are oxidized by the actions of both  $F_2(g)$  and  $HF(g)$ . These reactions are thermodynamically favorable. As an example, U is readily oxidized according to the following reactions. Similar reactions can be written for Pa, Th, and Li.



These reactions suggest that liquid bismuth can be purified by the action of HF(g) without concern for the oxidation of bismuth to BiF<sub>3</sub>, which is the primary purpose of hydrofluorination in the chemical processing flowsheets. With regards to salt purification, F<sub>2</sub>(g) and HF(g) are highly effective at removing oxide contaminants from molten fluoride salts. As an example, UO<sub>2</sub> is readily fluorinated according to the following reactions. Similar reactions can be written for PaO<sub>2</sub>, ThO<sub>2</sub>, and Li<sub>2</sub>O.



These relationships are illustrated graphically in the Gibbs free energy diagram [6] in Figure 2-16. This diagram shows the standard state Gibbs free energies (normalized to 1 mole oxide) of select fluorination and hydrofluorination reactions as a function of temperature.

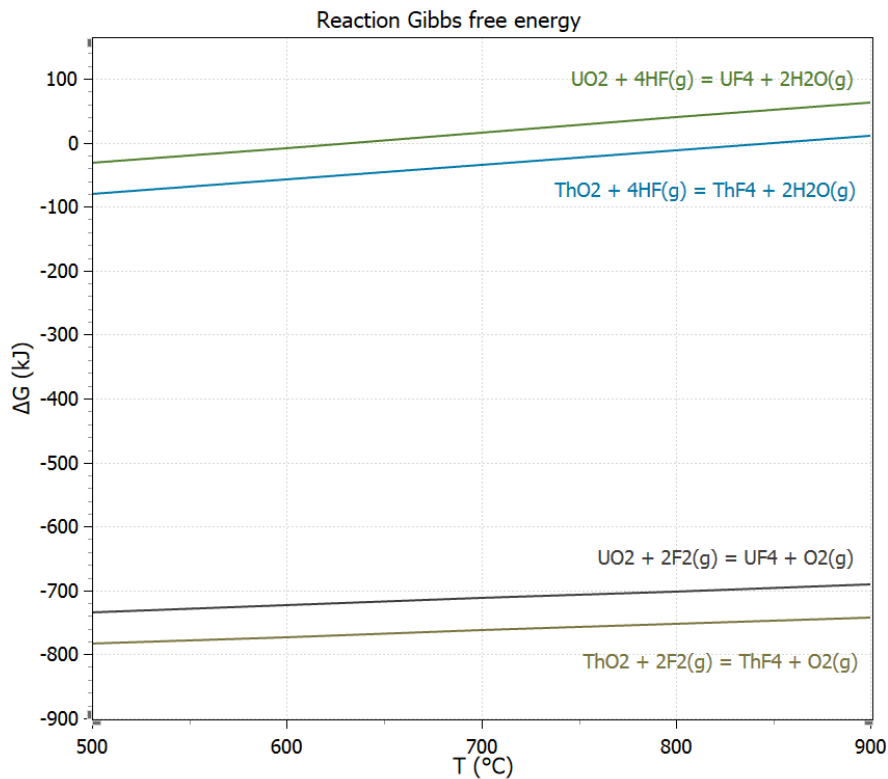


Figure 2-16. Gibbs free energies of select fluorination and hydrofluorination reactions.

## 2.15 Metal Transfer Process

The metal transfer process operates on the same underlying principles as reductive extraction. The primary function of reductive extraction is to separate and isolate protactinium from salt streams; specifically salt streams that have had nearly all of the uranium, and some of the fission products, removed by a preceding fluorination operation. The primary function of the metal transfer process is to separate and isolate fission products from salt streams; specifically salt streams that have had nearly all of the uranium and protactinium, and some of the fission products, removed by preceding fluorination and reductive extraction operations. To frame it in another way, in a sequence of operations, fluorination strips uranium from the salt, reductive extraction then strips protactinium from the salt, and the metal

transfer process then strips the remaining fission-product impurities from the salt. Of course, this description is an oversimplification because the separation efficiencies at each stage are imperfect.

The fission-products remaining in the salt stream entering the metal transfer process tend to be those that form the lowest vapor pressure fluorides (otherwise they would have been stripped along with uranium during fluorination) and the most stable fluorides (otherwise they would have been stripped along with protactinium during reductive extraction). Some of the alkali, alkaline earth, and lanthanide fission products are in this category of stable fluorides.

It was stated earlier in the description of reductive extraction, that the reactions are largely controlled by the limitations of stoichiometry rather than the limitations of thermodynamics and kinetics. This is true, for example, because lithium and thorium metals dissolved in bismuth are powerful reductants for protactinium and uranium in the fluoride salt. This is not the case for the metal transfer process, where lithium and thorium metals are applied to the reduction of some of the most stable metal fluorides and chlorides. A Gibbs free energy diagram [6] of select alkali and alkaline earth reduction reactions for lithium and thorium are shown in Figures 2-17 and 2-18, respectively. Cesium and strontium are selected as representative alkali and alkaline earth metals, respectively. Figure 2-17 shows that lithium is an adequate reductant in each case. However, Figure 2-18 shows that thorium is an adequate reductant for only CsF.

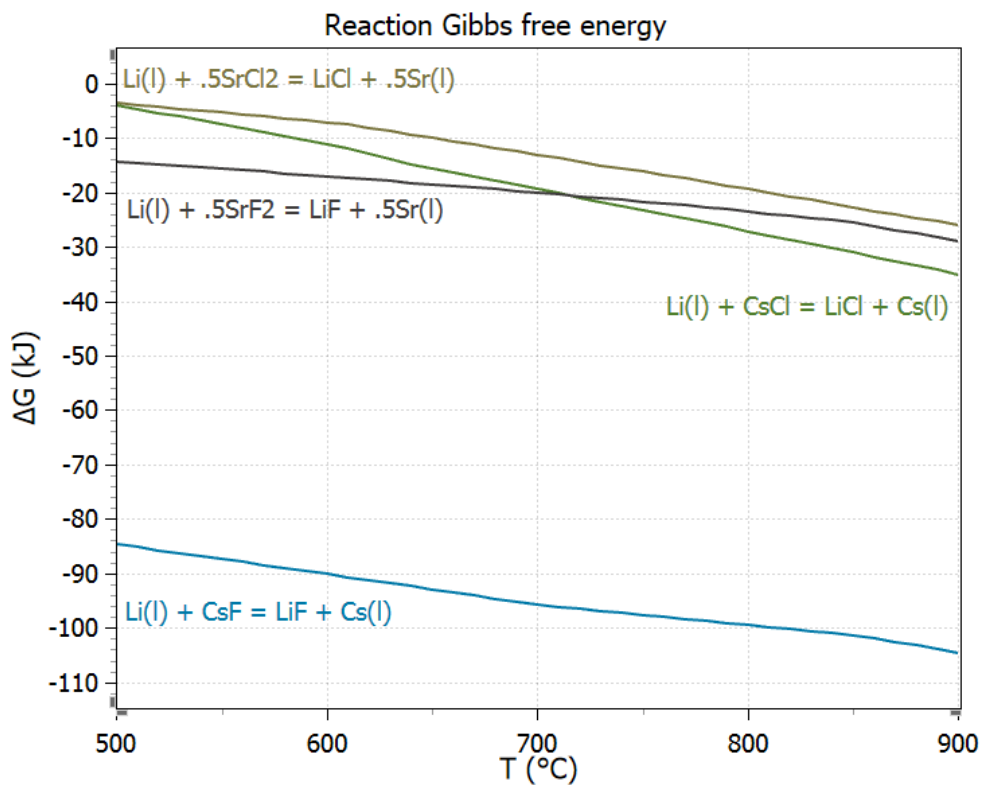


Figure 2-17. Gibbs free energies of select lithium reduction reactions.

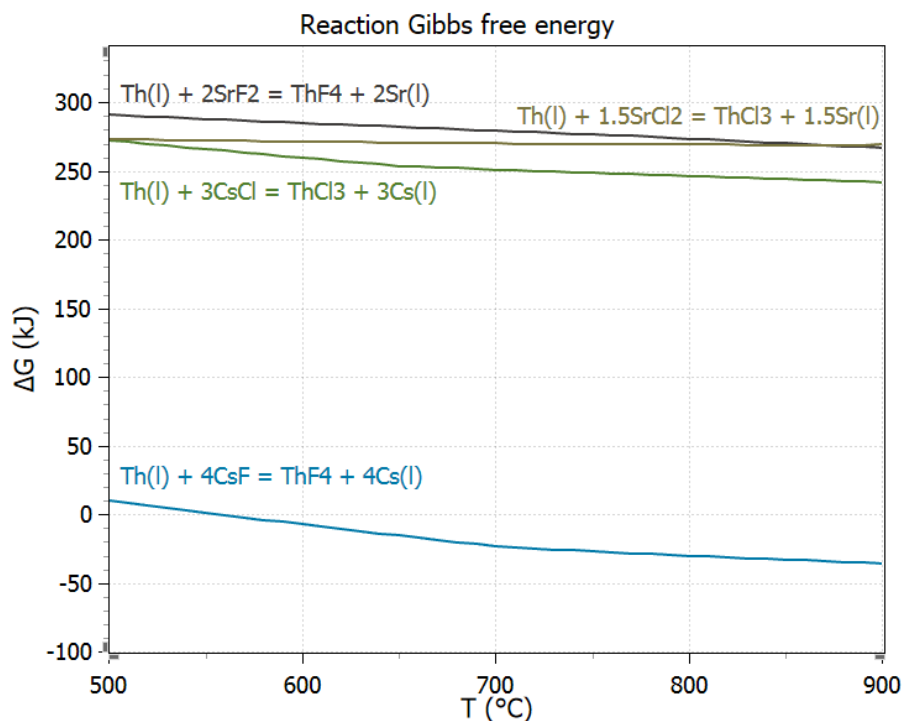


Figure 2-18. Gibbs free energies of select thorium reduction reactions.

A Gibbs free energy diagram [6] of select lanthanide reduction reactions for lithium and thorium are shown in Figures 2-19 and 2-20, respectively. Neodymium and samarium are selected as representative lanthanide metals. Figure 2-19 shows that lithium is an adequate reductant in each case. However, Figure 2-20 shows that thorium is not an adequate reductant for lanthanides.

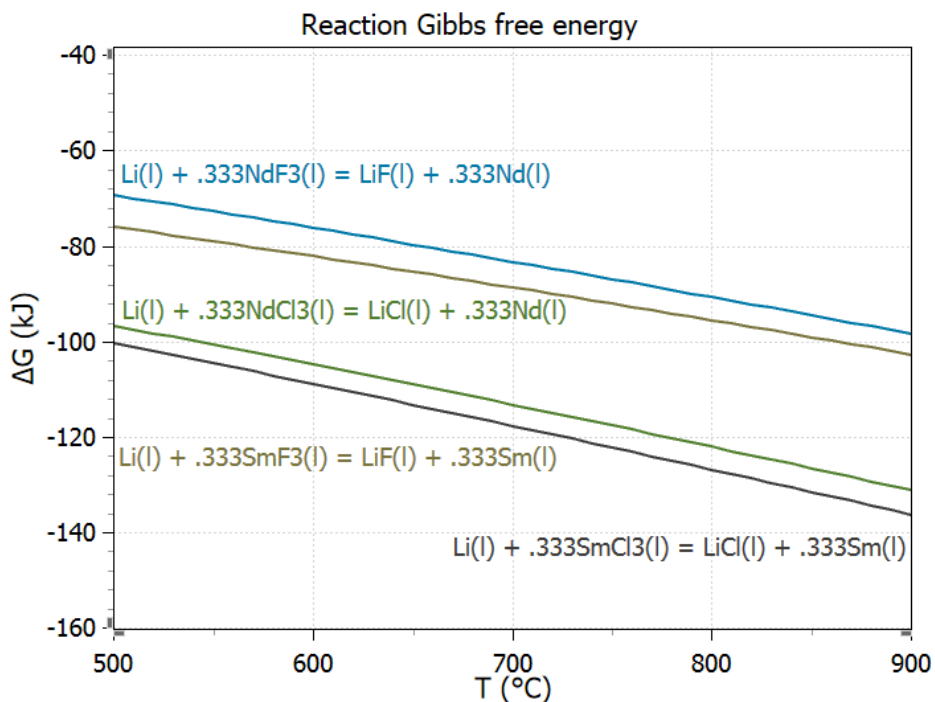


Figure 2-19. Gibbs free energies of select lithium reduction reactions.



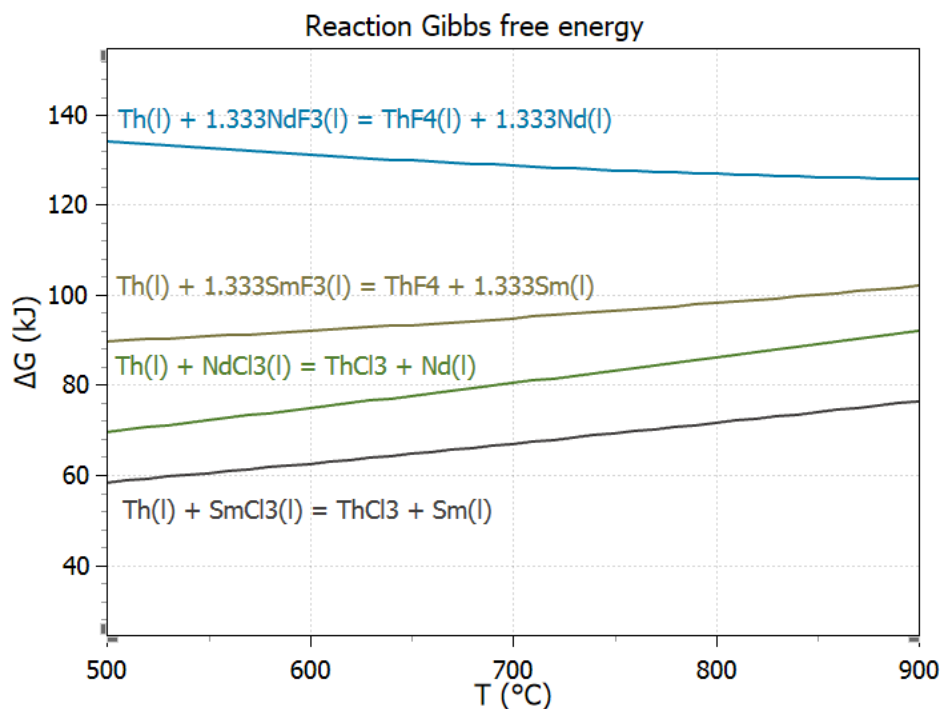


Figure 2-20. Gibbs free energies of select thorium reduction reactions.

The metal transfer process proceeds in four steps as illustrated in Figure 2-21. Generalized reactions involving rare earths (i.e., lanthanides) are shown, but the same reaction mechanisms apply to the alkali and alkaline earth fission products. In Step 1, lithium and thorium in bismuth Alloy #1 are used to reduce a portion of the fission product fluorides that remain in the salt following preceding fluorination and reductive extraction operations. The concentrations of lithium and thorium in bismuth Alloy #1 are relatively low (< 0.2 mol%) in order to minimize its reduction capacity in anticipation of the next step. In Step 2, clean LiCl molten salt is used to extract a portion of the fission product metals from bismuth Alloy #1. Many of the reactions in Step 1 are favored by the thermodynamics presented in Figures 2-17 through 19. The opposite is true in Step 2, where all of the reactions that extract fission products from the bismuth into the LiCl salt have positive Gibbs free energies. Nevertheless, the reactions proceed to some small degree, which is exploited to partition the fission products into the LiCl salt. In Step 3, lithium in bismuth Alloy #2 is used to reduce nearly all of the fission product chlorides present in the salt following Step 2. The concentration of lithium in bismuth Alloy #2 is relatively high ( $\approx 5$  mol%) in order to maximize its reduction capacity. Step 4 is employed when the concentration of fission products is sufficiently high in bismuth Alloy #2. In Step 4, the bismuth alloy is hydrofluorinated to purify the bismuth, while the fission products report to a fluoride salt phase waste product.

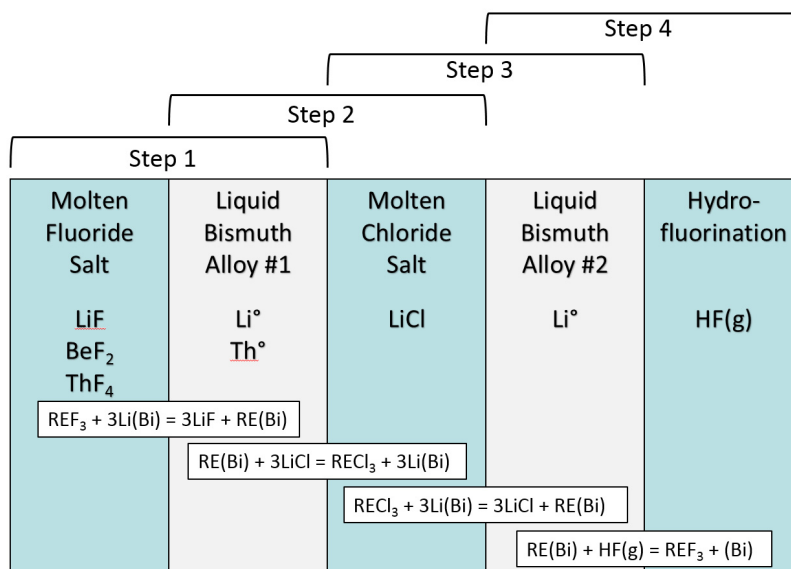


Figure 2-21. Illustration of the metal transfer process.

The intimate mixing of molten salts and liquid bismuth alloys in Steps 1 through 3 are facilitated by the use multistage counter-current contactors for the same purposes as described for reductive extraction. An example of a metal transfer process flowsheet is shown in Figure 2-22.

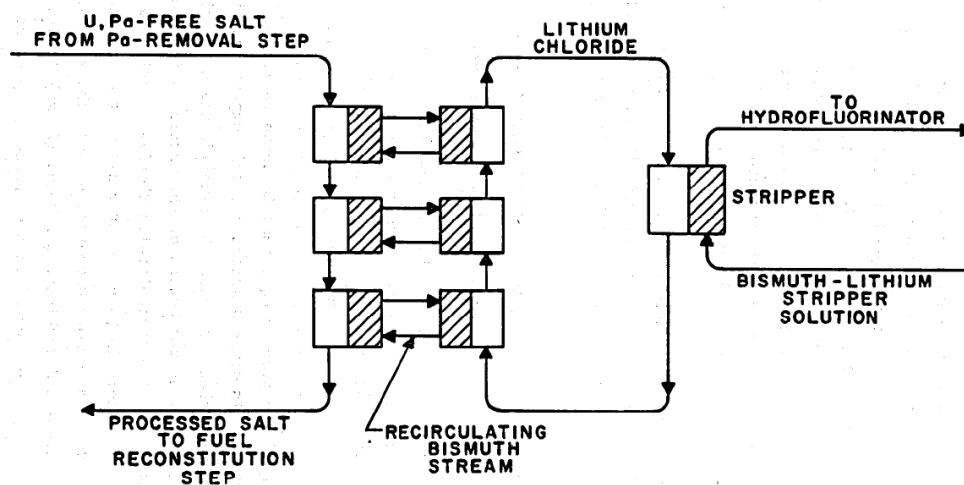


Figure 2-22. Flowsheet for the metal transfer process [9].

## 2.16 Electrolytic Oxidizer/Reducer

Some of the proposed chemical processing flowsheets include electrochemical cells that drive oxidation reactions at a liquid bismuth anode, and reduction reactions at a liquid bismuth cathode, across a flowing stream of molten fluoride salt electrolyte. The purpose of these electrochemical operations is to chemically condition the liquid bismuth alloy, the molten salt, or both. Therefore, the cells are associated with reductive extraction.

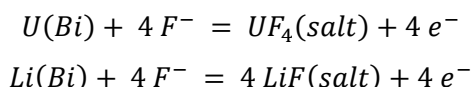
The proposed designs of the electrochemical cells are unique in that they accommodate the continuous flow of molten salt and liquid bismuth through the cell. The cells are not proposed as batch operations. However, in such a design, the bismuth anode and cathode must be electrically isolated from

each other. Electrical isolation is accomplished by using electrically insulating materials of construction to maintain two discrete pools of bismuth serving as electrodes. For example, bismuth flows from the reductive extraction (or metal transfer process) circuit into a pool serving as the anode, from the anode the bismuth flows to the pool serving as the cathode, and from the cathode the bismuth flows back into the reductive extraction (or metal transfer process) circuit. However, the flow paths of bismuth as described above are not contiguous; the paths are interrupted by bismuth dripping from one compartment to the next. (Dripping divides the contiguous flow of bismuth into discrete packets of liquid.) In other words, there is no contiguous path of bismuth through the electrochemical cell, even though the flow of bismuth is continuous through the electrochemical cell.

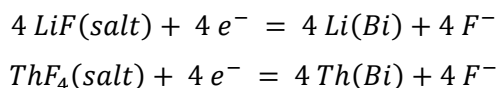
The means of providing electrical isolation of two discrete pools of bismuth serving as the anode and cathode, while bismuth continuously flows through the cell, is described above. However, the materials of construction holding apart from each other these two pools of bismuth must also provide electrical isolation. Two means of providing electrically insulating materials of construction are proposed; by the use of materials that are insulating, or by the use of materials that are not insulating but are insulated by a layer of frozen salt (i.e., “frozen-wall” technology). The electrochemical reactions are driven by an external power supply that provides a voltage potential and a DC current between the electrodes.

The proposed application of the electrochemical cells is to oxidize metals from the bismuth into the salt at the anode, while reducing metals from the salt into the bismuth at the cathode. The exact anode and cathode reactions are flowsheet specific, but one set of reactions include the following reactions.

Anode:



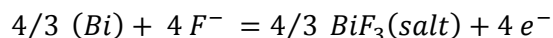
Cathode:



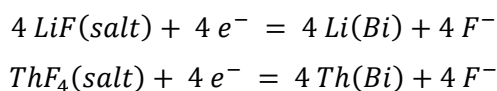
In this scenario, the reduction of uranium at the cathode is prevented by the flow of salt through the cell. Uranium-free salt enters the cell and flows from the cathode toward the anode, while uranium-containing bismuth enters the cell and flows from the anode toward the cathode. The uranium entering the salt at the anode is prevented from reaching the cathode by the flowing salt. The discharge salt contains  $UF_4$  and the discharge bismuth contains lithium and thorium.

The electrochemical cell can also be applied to a stream of clean bismuth.

Anode:



Cathode:



In this scenario, the reduction of bismuth at the cathode is prevented by the flow of salt through the cell. Bismuth-free salt enters the cell and flows from the cathode toward the anode, while clean bismuth enters the cell and flows from the anode toward the cathode. The bismuth entering the salt at the anode is prevented from reaching the cathode by the flowing salt. The discharge salt contains  $BiF_3$  and the discharge bismuth contains lithium and thorium.

The electrochemical cells thus provide reductants to the liquid bismuth and oxidants to the molten salt without increasing the inventories of these process streams. These same effects could be achieved by the

additions of reagent chemicals to the bismuth and salt. However, chemical additions inherently would increase the inventories of these streams and consequently increase the amount of process waste generated.

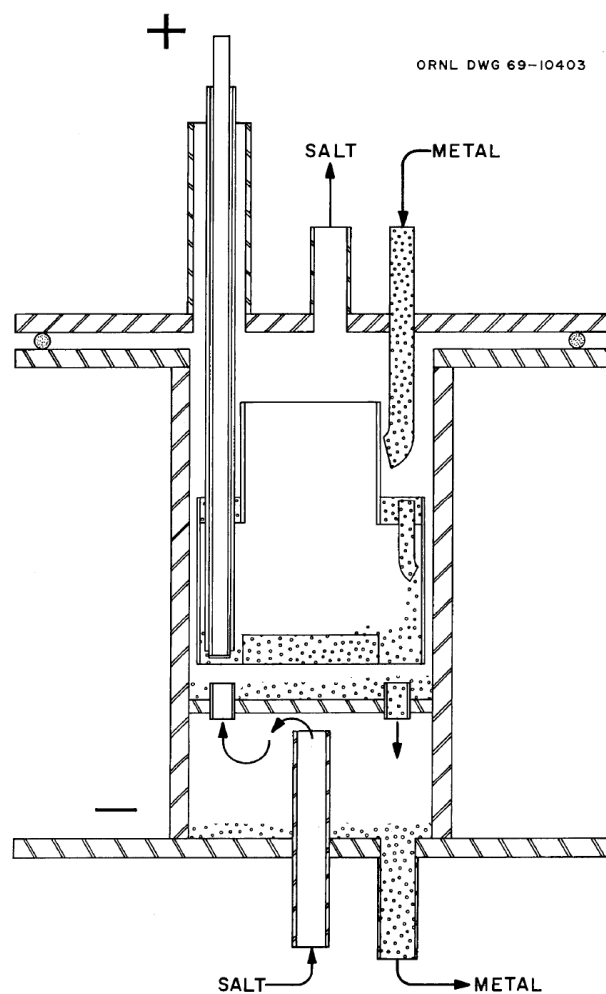


Figure 2-23. Schematic of the electrochemical oxidizer/reducer [10].

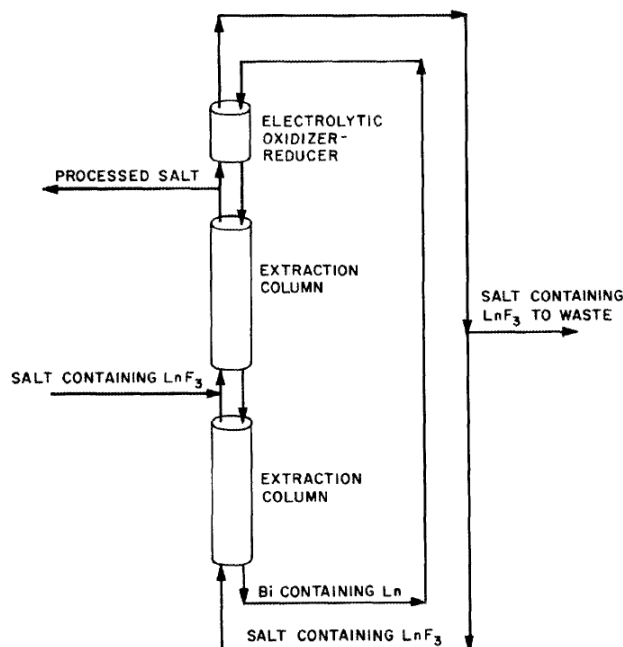
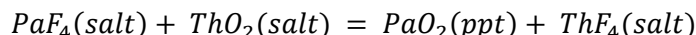


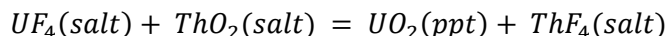
Figure 2-24. Flowsheet including an electrolytic cell in a reductive extraction circuit [11].

## 2.17 Oxide Precipitation

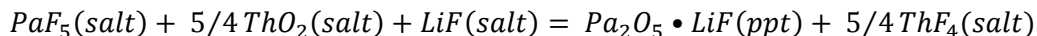
Oxide precipitation exploits differences between the relative stabilities of oxides and the relative saturation limits of oxides to affect chemical separations in molten salts. For example, in the absence of uranium in the salt, the following exchange reaction will separate protactinium from the salt as an oxide precipitate.



However, when uranium is present in the salt, the following exchange reaction is more favorable.



Therefore, if oxide precipitation is to separate protactinium from a uranium-containing fuel salt, the temperature and redox potential of the salt must favor the formation of complex species, which is postulated to be  $Pa_2O_5 \cdot LiF$ .



## 2.18 Selective Crystallization

Selective crystallization is proposed in some chemical processing flowsheets as a means of selectively removing thorium from bismuth alloys of thorium and rare earths. For example, the bismuth leaving the metal transfer process will contain appreciable concentrations of thorium and rare earths. The solubility of thorium in bismuth is significantly less than the solubilities of rare earths in bismuth. This property is exploited to precipitate thorium bismuthide ( $ThBi_2$ ) from liquid bismuth alloys as a means of separating thorium from rare earths.

## 2.19 Process Gas Purification

The chemical processing flowsheets use significant quantities of argon, hydrogen, and anhydrous hydrogen fluoride gases. Proposed methods of purifying these gases are as follows.

- Argon: flow through a bed of molecular sieve to remove impurities including moisture, and then over heated uranium turnings to remove oxygen.
- Hydrogen: utilize commercially available purification equipment that employs selective diffusion of hydrogen across a palladium alloy barrier.
- Anhydrous Hydrogen Fluoride: no additional purification was proposed.

## 2.20 Fates of Fission Products

The fates of fission products are not determined solely by the separations performance of the chemical processing plant. Certain fission products (or some portion of certain fission products) will react with the materials of construction of the reactor system before reaching the chemical processing plant. And likewise, certain gaseous fission products are separated and captured directly from the molten salt circulating through the reactor system at much shorter cycle times that could ever be achieved by the chemical processing plant. Such considerations make it a challenge to determine the exact fate of any individual fission product.

## 2.21 Chemical Processing Plant Flowsheets

Several variations of chemical processing plant flowsheets were proposed by ORNL to accommodate changes in reactor technologies and separations technologies. A few of these variations are discussed here. The earlier flowsheets were designed to support the two-fluid MSBR, which uses separate and distinct blanket and fuel salts. With regards to blanket salt, the basic functions of chemical processing are to strip uranium from the salt as  $\text{UF}_6$  (fluorination), purify the  $\text{UF}_6$  from associated fission product (absorption), reduce the purified  $\text{UF}_6$  to  $\text{UF}_4$  (reduction), and return the  $\text{UF}_4$  to the fuel salt (recombination). With regards to the fuel salt, the basic function of chemical processing are to strip the uranium from the salt as  $\text{UF}_6$  (fluorination), separate the  $\text{LiF}$  and  $\text{BeF}_2$  from the uranium-barren salt (distillation) to concentrate the fission product in the distillate bottoms, purify the  $\text{UF}_6$  from associated fission product (absorption), reduce the purified  $\text{UF}_6$  to  $\text{UF}_4$  (reduction), and return the  $\text{UF}_4$  to the fuel salt (recombination). These features are seen in the flowsheets shown in Figures 2-25 through 2-27. The flowsheet in Figure 2-25 uses caustic scrubbers to capture volatile fission products from gas streams prior to atmospheric discharge through a stack. The flowsheet in Figure 2-26 uses a combination of  $\text{NaF}$  and  $\text{MgF}_2$  to capture volatile fission products from fluorination. Otherwise, fission products are removed via the distillate bottoms. The flowsheet in Figure 2-27 includes protactinium stripping from the blanket salt (reductive extraction) prior to fluorination, which significantly reduces the blanket salt inventory (and consequently the thorium inventory) needed to support the reactor. The recovered protactinium is allowed to decay to uranium in a reservoir salt.

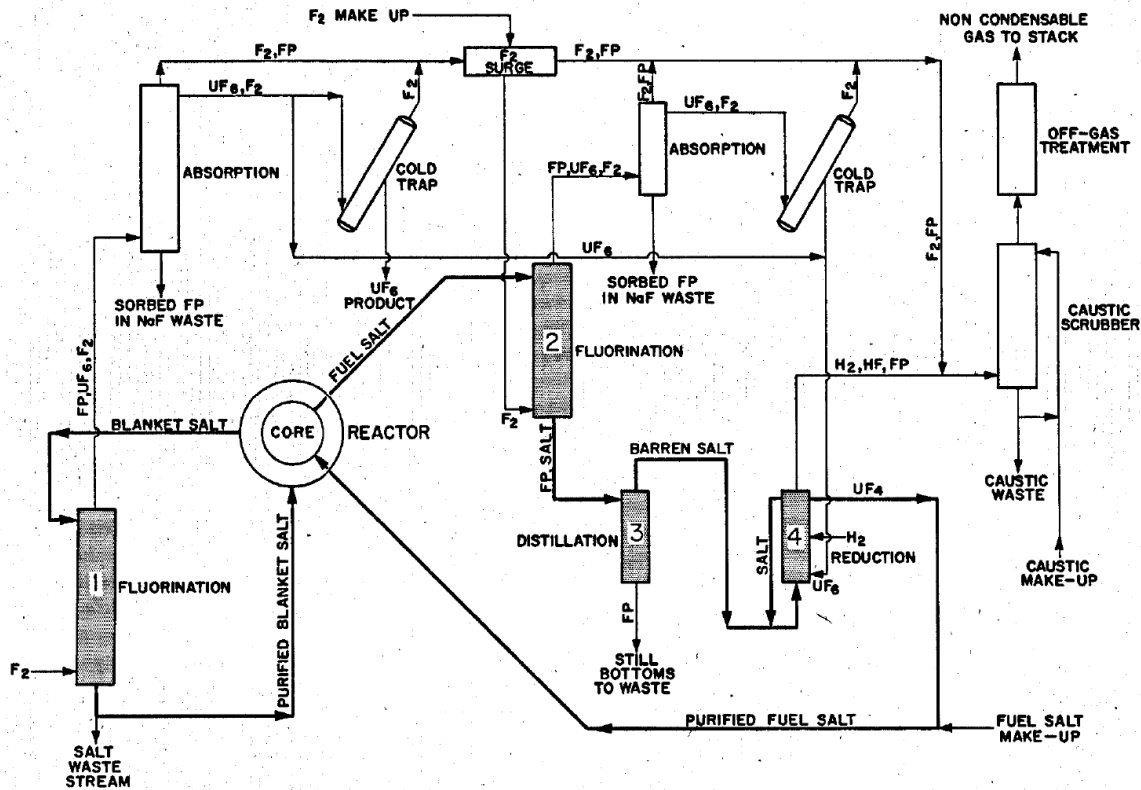


Figure 2-25. Flowsheet of chemical processing plant supporting a two-fluid MSBR caustic scrubber [12].

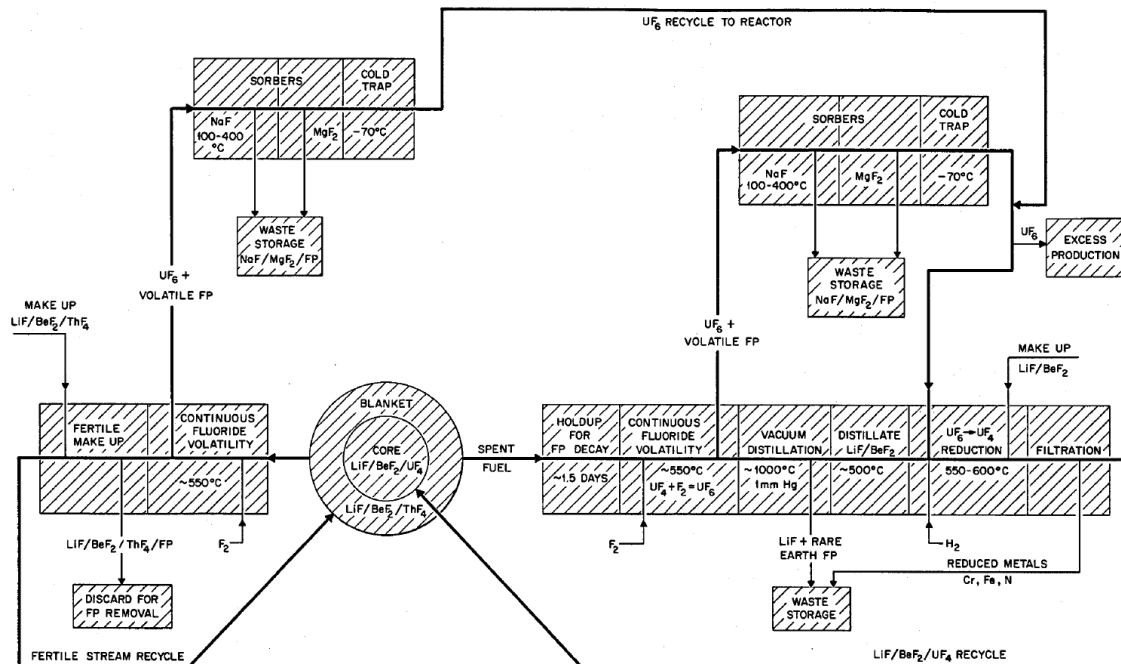


Figure 2-26. Flowsheet of chemical processing plant supporting a two-fluid MSBR NaF and MgF<sub>2</sub> [13].





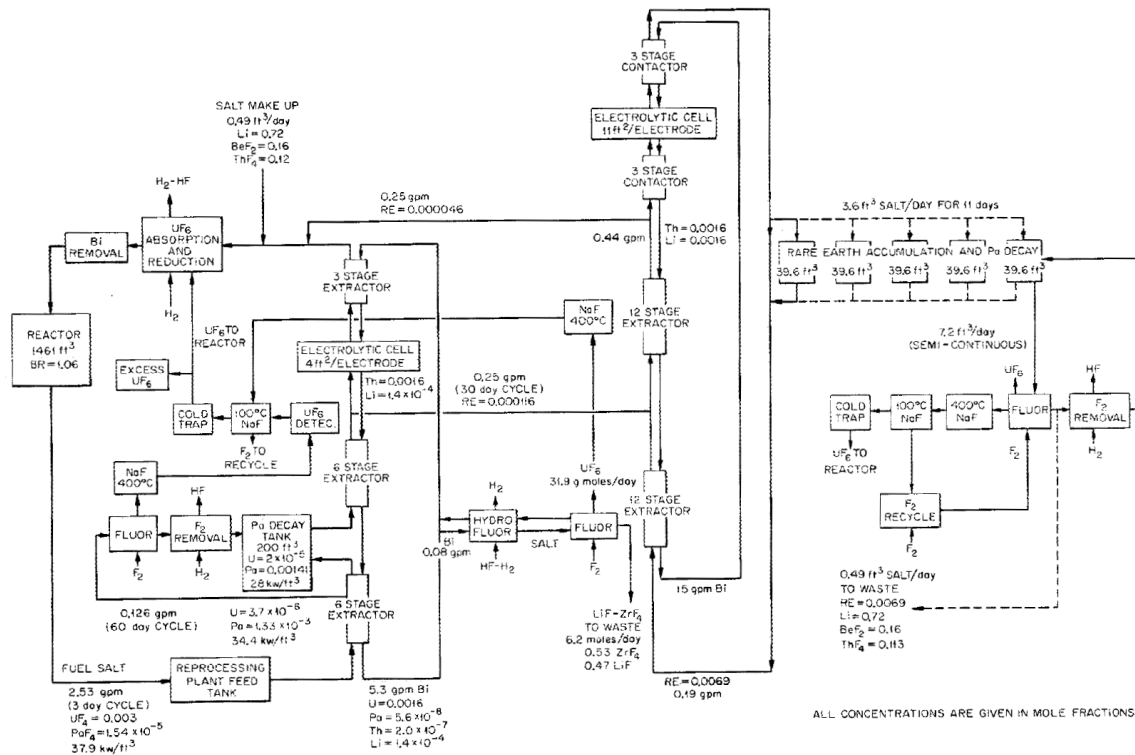


Figure 2-28. Flowsheet of chemical processing plant supporting a single-fluid MSBR no metal transfer [14].

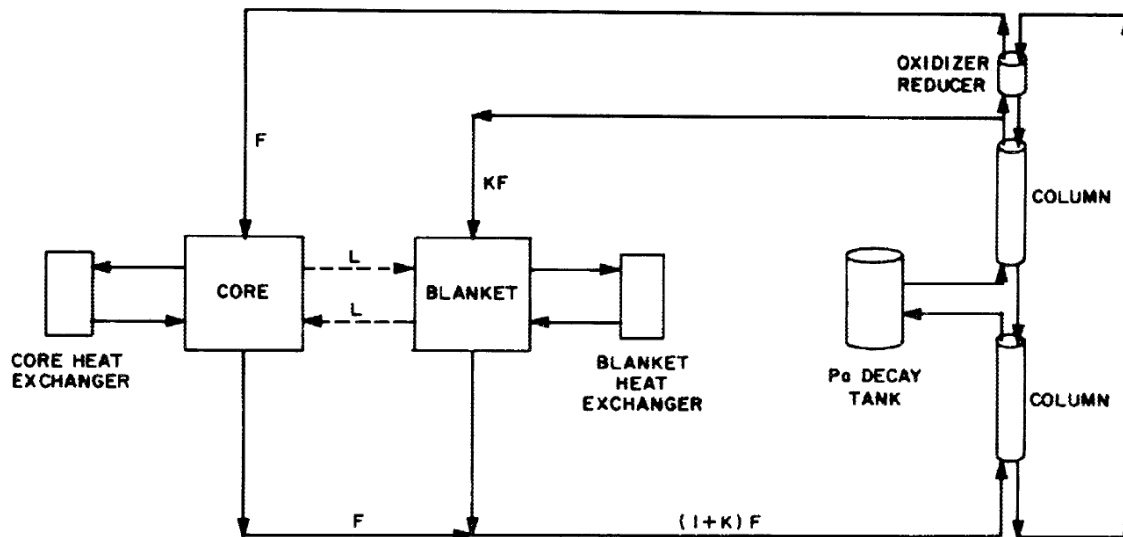


Figure 2-29. Flowsheet of chemical processing plant supporting a single-fluid MSBR fuel salt and salt blanket [14].

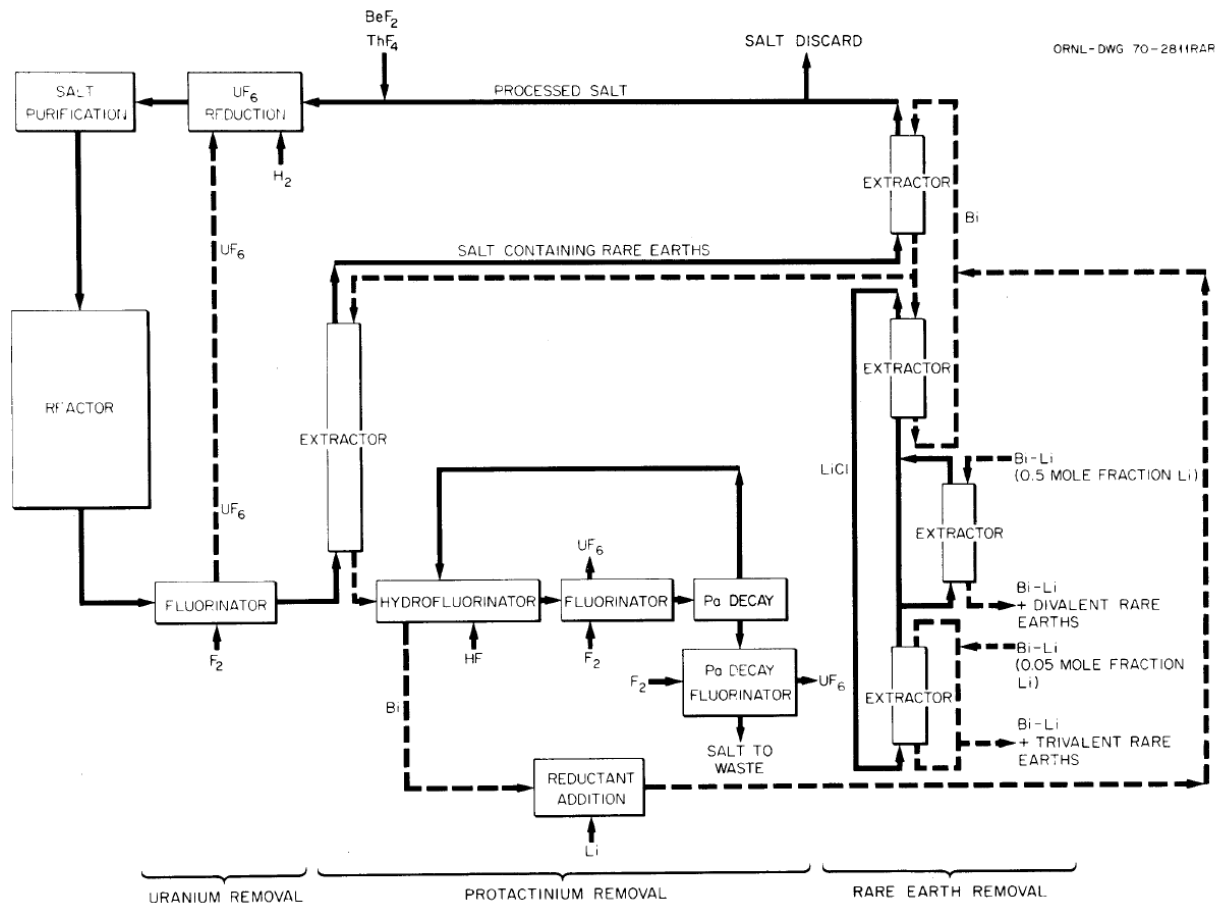


Figure 2-30. Flowsheet of chemical processing plant supporting a single-fluid MSBR with metal transfer process [16].

The final two flowsheets in Figures 2-31 and 2-32 are variations utilizing oxide precipitation to separate and isolate protactinium from the fuel salt. These flowsheets also utilize fluorination, hydrofluorination, reductive extraction, and the metal transfer process.

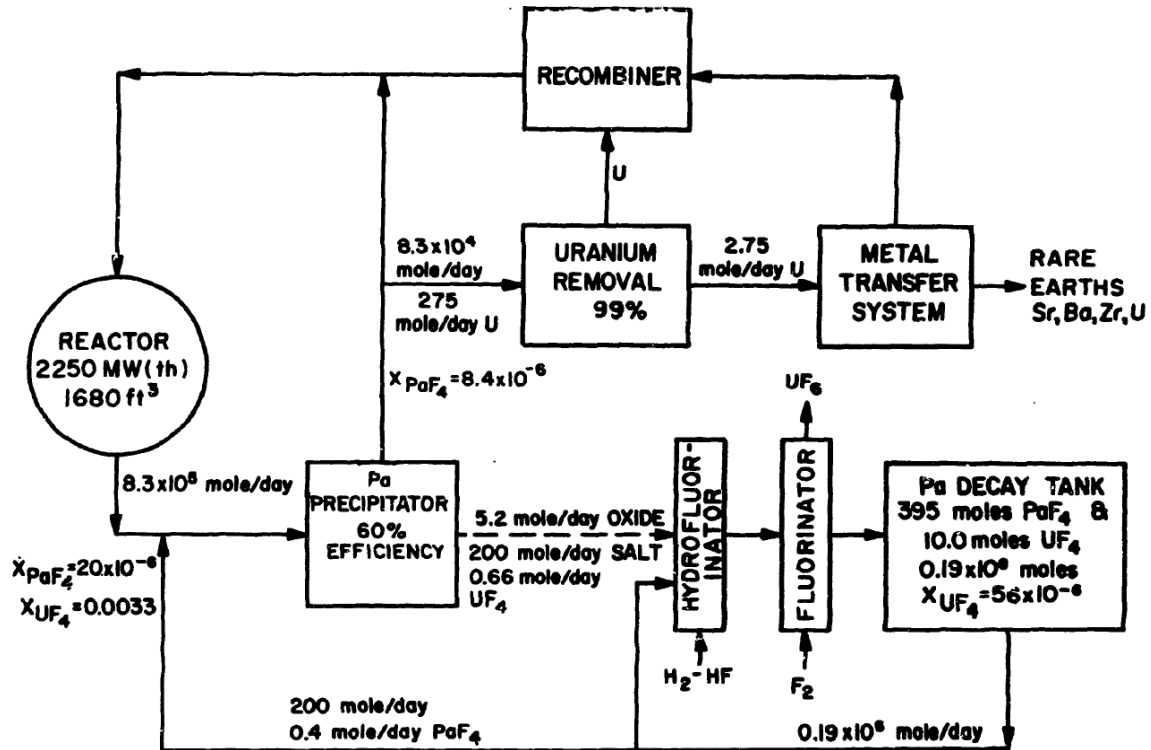


Figure 2-31. Flowsheet of chemical processing plant supporting a single-fluid MSBR, Variation 1 [17].

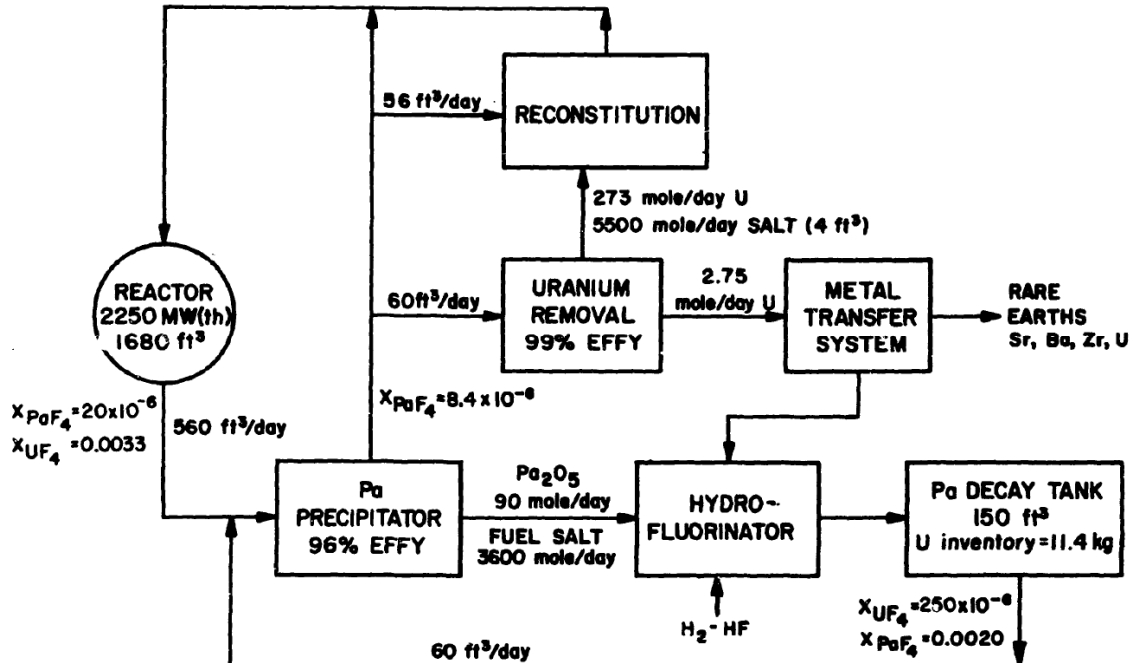


Figure 2-32. Flowsheet of chemical processing plant supporting a single-fluid MSBR, Variation 2 [17].

### 3. HEAD-END PROCESSES

*Guoping Cao*

The primary goal of the head end processes is to prepare the clean fuel salts—free from impurities such as oxides, water moisture, and other oxidants—for MSRs. The salt purification process can be performed to remove the impurities before the fuel salts are added into the reactor vessel. In this report, the head-end process applies to both molten salt breeder reactor and molten salt fast reactors (like the fast reactors under development at TerraPower, Moltex Energy, and Elysium) that are actively considered. In the breeder reactor, fluoride salt was usually used. In a reference MSBR designed by ORNL, the fuel carrier salt is FLiBe (a mixture of LiF-BeF<sub>2</sub>). In molten chloride fast reactors, NaCl, UCl<sub>3</sub>, PuCl<sub>3</sub>, etc. are being actively considered as the fuel salt. Both FLiBe and NaCl salts are common chemicals [14]. However, to improve the neutronics in the reactors, the LiF for MSR has to be highly enriched <sup>7</sup>Li to avoid excessive tritium formation, and the Cl for making the chloride salt has to be enriched <sup>37</sup>Cl. The enrichment of <sup>7</sup>Li and <sup>37</sup>Cl can be found in [15] or elsewhere and is not included in this discussion.

A big advantage of the MSBR using the Th-U cycle and the chloride fast reactors is that they can use the removed uranium elements in fluoride or chloride form, from the spent nuclear fuels including oxide, metal, etc., for the reactors. The management of spent nuclear fuel is a significant issue. It is highly desired to use the recovered fuel elements from the spent fuels. Thus, this section focuses on head end processes (fluorination and chlorination) for preparing fluoride salts by fluorination for MSBR and for preparing chloride salts by chlorination for fast reactors. (The purification of the fluoride and chloride salts for removing the impurities is discussed in the molten salt chemistry managements section.)

#### 3.1 Fluorination

The processing of pure UF<sub>4</sub> and ThF<sub>4</sub> is a widely known in nuclear industry. The pure UF<sub>4</sub> and ThF<sub>4</sub> can be produced from the high temperature fluorination of pure uranium oxide and thorium oxide by employing anhydrous hydrogen fluoride (HF) gas through the following reactions:  $\text{UO}_2 + 4\text{HF} = \text{UF}_4 + 2\text{H}_2\text{O}$ , and  $\text{ThO}_2 + 4\text{HF} = \text{ThF}_4 + 2\text{H}_2\text{O}$ . P. Soucek et al. reviewed the synthesis of UF<sub>4</sub> and ThF<sub>4</sub> [16].

There are different gases that can be used for the fluorination process: pure fluorine gas (F<sub>2</sub>), HF, ClF<sub>3</sub>, and ClF<sub>5</sub>. Almost all forms of uranium compounds in the different spent fuels (oxide, nitride, metal fuels) can be processed by the fluorination process. Most of the light water reactors use oxide fuels and there have been a lot of studies on the fluorination of spent oxide fuels [17, 18, 19]. Jan Uhler and coworkers investigated extensively the fluorination of spent oxide fuel [20, 21, 22, 23]. When fluorine gas is used, the main fluorination reactions for uranium oxide in the spent fuels are  $\text{UO}_2(\text{s}) + 3\text{F}_2(\text{g}) = \text{UF}_6(\text{g}) + \text{O}_2(\text{g})$  and  $\text{U}_3\text{O}_8(\text{s}) + 9\text{F}_2(\text{g}) = 3\text{UF}_6(\text{g}) + 4\text{O}_2(\text{g})$ . The plutonium oxide in the spent fuels is also converted to the plutonium fluorides during the fluorination process by the following reactions:  $\text{PuO}_2(\text{s}) + 2\text{F}_2(\text{g}) = \text{PuF}_4(\text{s}) + \text{O}_2(\text{g})$ ,  $\text{PuO}_2(\text{s}) + 3\text{F}_2(\text{g}) = \text{PuF}_6(\text{g}) + \text{O}_2(\text{g})$ , and  $\text{PuF}_4(\text{s}) + \text{F}_2(\text{g}) = \text{PuF}_6(\text{g})$ .

Before the fluorination process, the spent fuels would be decladded and then converted to the powdered forms by grinding and voloxidation, to enhance the fluorination reaction rate because fluorination process is a gas solid reaction. The fluorination process is usually in a fluidized bed or flame reactor [24, 25].

The recovery of uranium and plutonium from spent fuel by fluorination is based on the inherent volatility of the uranium hexafluoride and plutonium hexafluoride. Table 3-1 shows boiling points the volatile and non-volatile fluorides from the fluorination of spent fuels.

Table 3-1. Boiling points of typical volatile, semi-volatile, and non-volatile fluorides during the fluorination of spent fuels [25].

Highly volatile species		Volatile species		Semi-volatile species		Non-volatile species	
Species	Boiling point	Species	Boiling point	Species	Boiling point	Species	Boiling point
Kr	-153.4	IF <sub>7</sub>	4	AmF <sub>4</sub>	51	AmF <sub>3</sub>	2,067
CF <sub>4</sub>	-129	MOF <sub>6</sub>	33.88	RhF <sub>3</sub>	600	YF <sub>3</sub>	2,230
Xe	-108.1	RUF <sub>6</sub>	45.9	SnF <sub>4</sub>	705	BaF <sub>2</sub>	2,260
TeF <sub>6</sub>	-38.6	NpF <sub>6</sub>	55.18	ZrF <sub>4</sub>	918	EuF <sub>3</sub>	2,280
SeF <sub>6</sub>	-34.5	TcF <sub>6</sub>	55.2	PuF <sub>4</sub>	927	GeF <sub>3</sub>	2,327
		UF <sub>6</sub>	56.5	CsF	1,231	LaF <sub>3</sub>	2,327
		PuF <sub>6</sub>	62.2	RbF	1,410	NdF <sub>3</sub>	2,327
		IF <sub>5</sub>	98	UF <sub>4</sub>	1,450	CeF <sub>3</sub>	2,330
		SbF <sub>5</sub>	142.7			PmF <sub>3</sub>	2,330
		NbF <sub>5</sub>	235			SmF <sub>3</sub>	2,330
		RuF <sub>5</sub>	280			SrF <sub>2</sub>	2,460
		RhF <sub>5</sub>	95.5				
		RhF <sub>6</sub>	73.5				

The products of the fluorination process were then separated and purified by sorption and desorption process. NaF is commonly used for absorbing UF<sub>6</sub>, and other fluorides such as MgF<sub>2</sub> have been used for sorbing NpF<sub>6</sub> and TcF<sub>6</sub> from the UF<sub>6</sub> gas.

All the UF<sub>6</sub>, PuF<sub>6</sub> and NpF<sub>6</sub> are absorbed by the NaF trappings at 100°C, but at 400°C, the UF<sub>6</sub> and NpF<sub>6</sub> can be desorbed by F<sub>2</sub> gas. The thermal instability of the PuF<sub>6</sub> is used to separate the plutonium from uranium at 100°C. Desorption of PuF<sub>6</sub> is not possible because of the formation of the PuF<sub>4</sub>·3NaF, which is thermally stable even in fluorine atmosphere. The final purification of UF<sub>6</sub> from MoF<sub>6</sub>, TcF<sub>6</sub>, IF<sub>5</sub> and SbF<sub>5</sub> can be achieved by distillation at 75–90°C and 200–300 kPa. Under these conditions, the UF<sub>6</sub> becomes liquid. For preparing the needed UF<sub>4</sub> for MSBR, the UF<sub>6</sub> can be readily reduced to UF<sub>4</sub> by hydrogen gas (in H<sub>2</sub>/HF gas mixture) through UF<sub>6</sub>+H<sub>2</sub>=UF<sub>4</sub>+HF.

Figure 3-1 shows a typical flow-sheet used by Jan Uhlir for spent fuel processing by the fluorination process. A separation efficiency of 95–99.5% for U, 98–99.5% for Pu, 60–70% for Nb, Ru, and 95–99% for Nb and Ru was reported [23].

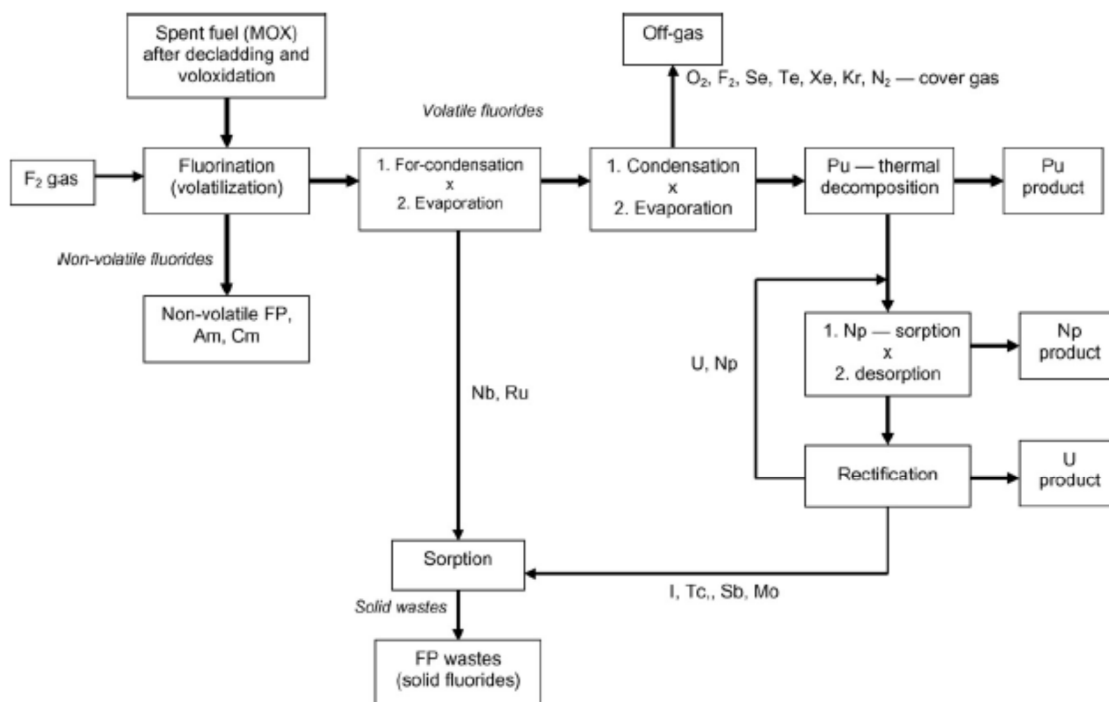
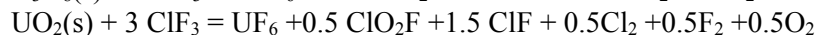
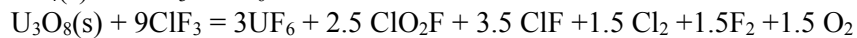
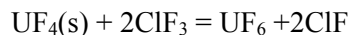


Figure 3-1. A typical process flow-sheet of the spent fuel processing by fluorination [23].

UF<sub>6</sub> can be produced from virtually any uranium compound with fluorine gas at elevated temperatures. For example, uranium metal fuel, and uranium nitride fuels, can also process the fluorination process by the following reactions:  $U + 3F_2 = UF_6$  and  $2UN + 9F_2 = 2UF_6 + 2NF_3$ .

In addition to the HF and F<sub>2</sub> gases mentioned above, other gases (such as ClF<sub>3</sub>, BrF<sub>3</sub>, BrF<sub>5</sub>, 2NH<sub>4</sub>HF<sub>2</sub>, NF<sub>3</sub>, etc.) were also reported as the fluorinating reagents [26, 27, 28, 29]. For example, ClF<sub>3</sub> can convert uranium of various chemical forms into UF<sub>6</sub> by the following reactions, and it was reported ClF<sub>3</sub> has a strong fluorination ability under low temperature (for U<sub>3</sub>O<sub>8</sub>, the fluorination started at room temperature) [26]. The fluorination strength of ClF<sub>3</sub> was higher than BrF<sub>5</sub> and BrF<sub>3</sub>.



Iwasaki and Sakurai [17] studied the fluorination of UO<sub>2</sub> and U<sub>3</sub>O<sub>8</sub> pellets by BrF<sub>3</sub> gas. The reactivity of BrF<sub>3</sub> appeared similar to that of ClF<sub>3</sub>. The U<sub>3</sub>O<sub>8</sub> oxides were found to be fluorinated by BrF<sub>3</sub> gas below 200°C at a controllable rate, but liquid BrF<sub>3</sub> can explosively react with U<sub>3</sub>O<sub>8</sub> powder. The products of the fluorination by BrF<sub>3</sub> are UF<sub>6</sub>, Br<sub>2</sub>, and O<sub>2</sub>. Based on the gravimetric measurements during the fluorination process at a temperature range of 100–250°C, the activation energy and the kinetics (in  $\frac{g}{cm^2h}$ ) of the fluorination reactions were determined: for UO<sub>2</sub>, 3.9 kcal/mol,  $k = 0.346 \exp(-\frac{3900}{RT})$  p; for U<sub>3</sub>O<sub>8</sub>, 0.95 kcal/mol,  $k = 0.346 \exp(-\frac{950}{RT})$  p. In comparison with using F<sub>2</sub> as a fluorination reagent, the fluorination by BrF<sub>3</sub> proceeded at much lower temperatures and lower gas pressures. Figure 3-2 shows the comparison of the rate of fluorination of uranium oxides with BrF<sub>3</sub> and fluorine gas.

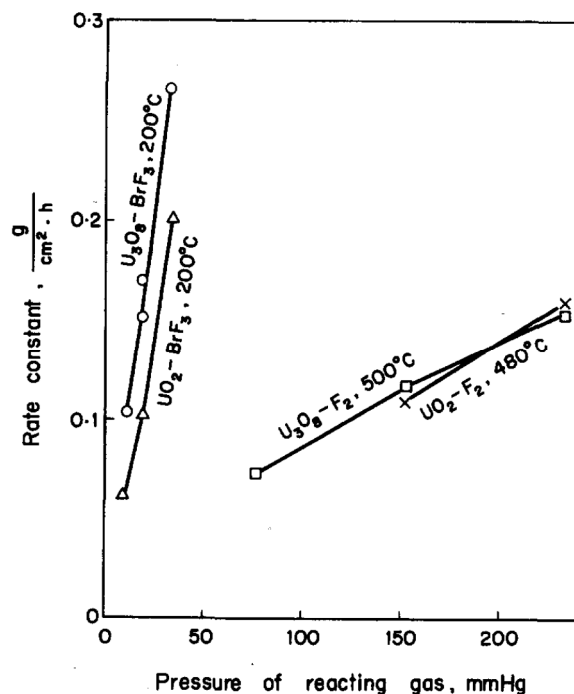


Figure 3-2. Relationships between rate of fluorination of uranium oxides with  $\text{BrF}_3$  or fluorine [17].

It was reported [30] that  $\text{U}_3\text{O}_8$  fines can be converted by  $\text{BrF}_5$  to  $\text{UF}_6$  at 225–300°C and no external heat was needed during the fluorination. The reaction of the fluorination process is  $\text{U}_3\text{O}_8 + 3.6\text{BrF}_5 = 3\text{UF}_6 + 1.8\text{Br}_2 + 4\text{O}_2$ .  $\text{PuO}_2$  in the fines were converted to  $\text{PuF}_4$  (solid), which can be further fluorinated by fluorine gas to be converted to volatile  $\text{PuF}_6$ , at 250–550°C.

Scheele et al. [31] reported that  $\text{NF}_3$  can be used as an effective fluorinating reagent for oxides including  $\text{UO}_2$ ,  $\text{U}_3\text{O}_8$ ,  $\text{CoO}$ ,  $\text{Y}_2\text{O}_3$ ,  $\text{ZrO}_2$ , and oxides of lanthanides below Ho. The fluorination reaction by  $\text{NF}_3$  with oxides is thermally sensitive with reaction temperature and the reaction rate is dependent on the compound to be fluorinated. For example, the onset temperature of fluorination for  $\text{UO}_2$ ,  $\text{U}_3\text{O}_8$ , and  $\text{PuO}_2$  is 360, 530, and 450°C respectively. The thermally-based  $\text{NF}_3$ -fluorination process may be used for separation purposes based on the different fluoride volatilities.  $\text{NF}_3$  appears promising as a substitute for other more chemically hazardous and corrosive fluorinating agents. Table 3-2 shows the calculated reactions enthalpies and free energies for fluorination by  $\text{NF}_3$  of uranium oxides and plutonium oxide at 300°C.

Table 3-2. Calculated reactions enthalpies and free energies for fluorination by  $\text{NF}_3$  of uranium oxides and plutonium oxide at 300°C [31].

Reaction	$\Delta H$ (kJ/mol metal)	$\Delta G$ (kJ/mol metal)
$\text{UO}_2 + 2\text{NF}_{3(\text{g})} = \text{UF}_{6(\text{g})} + \text{N}_{2(\text{g})} + \text{O}_{2(\text{g})}$	-799	-901
$\text{UO}_2 + 2\text{NF}_{3(\text{g})} = \text{UF}_{6(\text{g})} + \text{N}_{2(\text{g})} + \text{O}_{2(\text{g})}$	-799	-901
$\text{UO}_2 + 1.33\text{NF}_{3(\text{g})} = \text{UF}_4 + 0.666\text{N}_{2(\text{g})} + \text{O}_{2(\text{g})}$	-983	-1044
$\text{UO}_2 + 1.333\text{NF}_{3(\text{g})} = \text{UO}_2\text{F}_2 + 0.666\text{N}_{2(\text{g})} + \text{F}_{2(\text{g})}$	-391	-417
$\text{U}_3\text{O}_8 + 6\text{NF}_{3(\text{g})} = 3\text{UF}_6 + 3\text{N}_{2(\text{g})} + 4\text{O}_{2(\text{g})}$	-708	-806
$\text{U}_3\text{O}_8 + 4\text{NF}_{3(\text{g})} = 3\text{UF}_4 + 2\text{N}_{2(\text{g})} + 4\text{O}_{2(\text{g})}$	-551	-618

Reaction	$\Delta H$ (kJ/mol metal)	$\Delta G$ (kJ/mol metal)
$U_3O_8 + 2NF_{3(g)} = 3UO_2F_2 + N_{2(g)} + O_{2(g)}$	-374	-374
$PuO_2 + 2NF_{3(g)} = PuF_{6(g)} + N_{2(g)} + O_{2(g)}$	-450	-516
$PuO_2 + 1.33NF_{3(g)} = PuF_4 + 0.666N_{2(g)} + O_{2(g)}$	-815	-880

B. Claux, et al. [32] reported that in a closed system, using ammonium hydrogen fluoride,  $NH_4HF_2$ , the  $PuO_2$  can be converted to  $PuF_3$  at  $350^\circ C$ , through the reaction  $2NH_4HF_2 + PuO_2 = N_2 + H_2 + PuF_3 + HF + 2H_2O$ . The Gibbs free energy of the reaction is -107 kJ/mol at  $350^\circ C$ . At  $350^\circ C$ , the products of the fluorination process are a mixture of 92 wt% purity  $PuF_3$  and minor  $(NH_4)_2PuF_6$ . Further evaporation was considered necessary to improve the product purity.  $NH_4HF_2$  will decompose to  $NH_3$  and  $HF$  at above  $200^\circ C$  [33], and to  $N_2$ ,  $H_2$ , and  $HF$  when temperature is higher than  $400^\circ C$  [34]. Because of the presence of reducing  $H_2$ , only  $PuF_3$  was formed even at higher temperature.

In all the fluorinating reagents,  $F_2$  is the most widely reported for spent fuel processing and  $HF$  is widely used gas for processing pure  $UF_4$  and  $ThF_4$  from pure uranium oxides and thorium oxides.  $F_2$  and  $HF$  gases are very corrosive at high temperatures and corrosion resistant container materials are needed.

Fluorination processes require specially designed reactors to address the corrosive gases and volatile products. Small laboratory scale fluorination vessel, flame reactor, and fluidized bed were unusually used in literature. Some typical fluorination reactors reported in literature are listed here. Figure 3-3 shows a fluorination reactor inserted in a horizontal tube for fluorination by  $HF$ , used by Souček [16]. The reactor was used for solid gas reaction and powder starting material was inserted in the center of the heating zone. A  $50 \times 50 \times 10$  mm Inconel boat for powder can be used for fluorinating about 10g powders. All materials in contact with  $HF$  was heat resistant and corrosion resistant stainless steel.

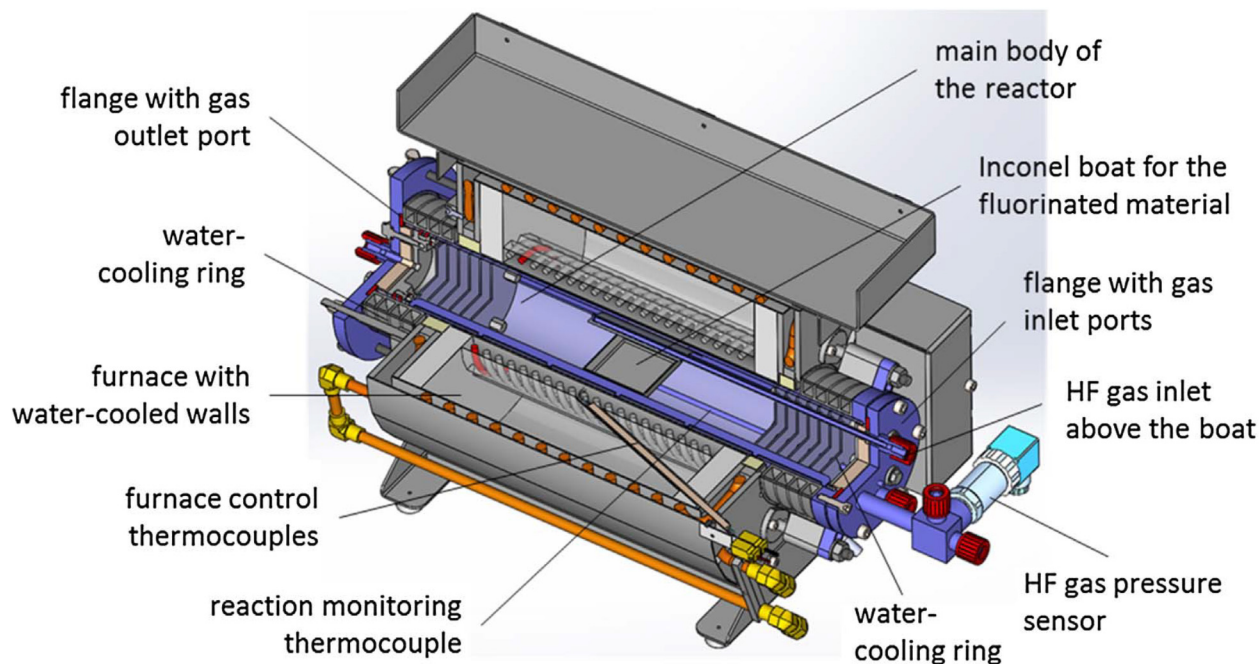


Figure 3-3. Scheme of a fluorination reactor inserted in a horizontal tube furnace [16].



Figure 3-4 shows a flame reactor for fluorination of spent nuclear fuel using fluorine gas, used by D. Watanabe et al. [25]. The flame reactor material is nickel with an operating temperature of 300°C. The residue recovery tank and the filter (0.01 mm diameter pore) were also made of nickel, and with a 150°C operating temperature.

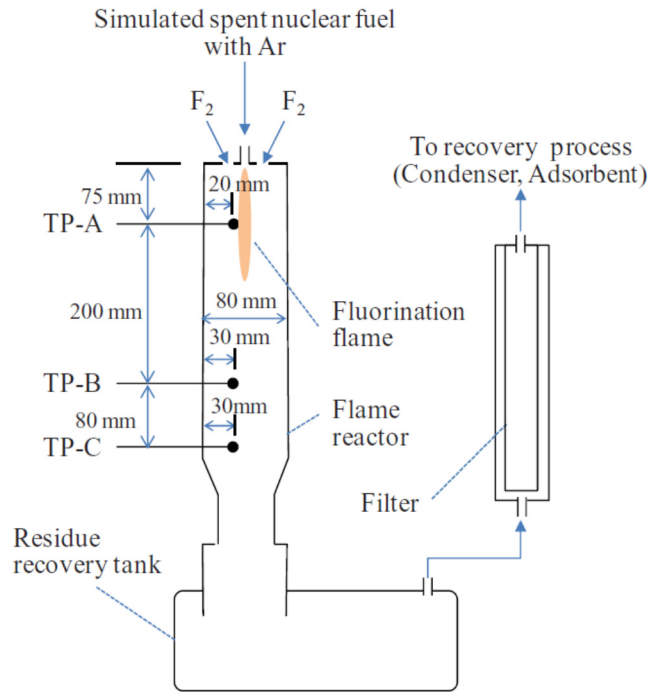


Figure 3-4. A schematic of the flame fluorination reactor used by D. Watanabe et al. [25].

Figure 3-5 shows the diagram of the engineering fluorination facility by  $\text{BrF}_5$ , reported by J. T. Holmes et al. [30]. The reaction section is a 3-inch diameter and 72-inch-long nickel pipe, which contains the fluidized bed and fuel charge. The  $\text{NaF}$  traps were used for sorption of  $\text{UF}_6$ . The off gases after the  $\text{NaF}$  traps were routed to caustic scrubber system.

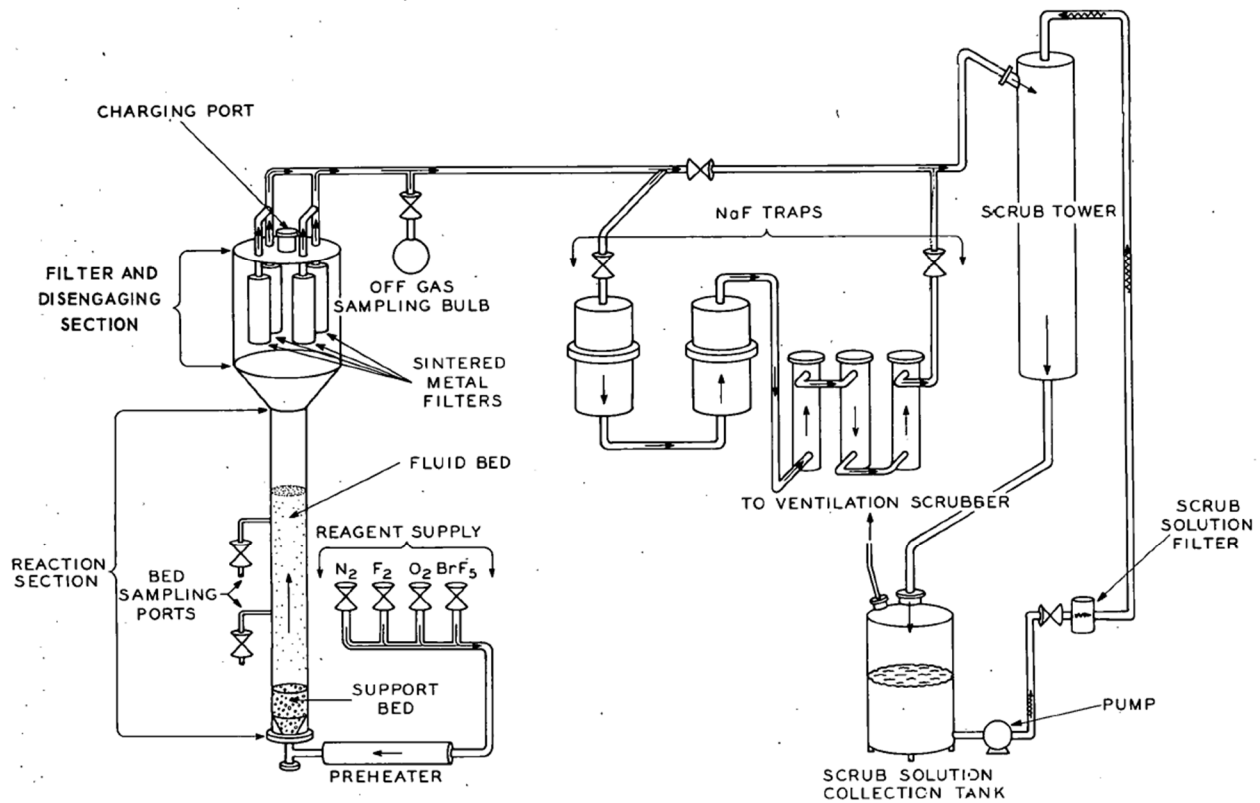


Figure 3-5. Schematic Fluorination Facility by  $\text{BrF}_5$  [30].

### 3.2 Key Findings and Future Research and Development Needs for Fluorination

Almost all the different spent fuels (including the widely used oxide fuel, uranium nitride fuel, uranium carbide, and metal fuels) can be fluorinated by using  $\text{F}_2$  and other fluorinating reagents.

The main mechanism for the fluorination process is that the volatile  $\text{UF}_6$  can be separated easily by chemical reaction between spent fuel and fluorination reagent, followed by sorption and then desorption.  $\text{UF}_6$  can be further reduced to  $\text{UF}_4$  and the  $\text{UF}_4$  can also easily converted to  $\text{UF}_6$  by  $\text{F}_2$  gas. This is the also the main mechanism for on-line salt processing to remove the  $\text{UF}_4$  from the MSBR.

A large quantity of  $\text{F}_2$  or  $\text{HF}$ , which are corrosive, may be needed for the fluorination process and thus the fluorination process may be costly and corrosion resistant container materials are needed. Most of the reported literature on fluorination are about the fluorination of spent oxide fuels, and research on other fuels is needed.

Since most published literature are lab-scale results; large scale fluorination processes, in particular, the fluorination reactor and corrosion protection during fluorination, need to be studied and demonstrated. Fluorination and efficiency of irradiated fuels needs to be studied and demonstrated.

### 3.3 Chlorination

To produce pure  $\text{UCl}_3$  salt, the pure uranium metal can be chlorinated by using chlorine gas  $\text{Cl}_2$  or  $\text{HCl}$ . Similar to the fluorination process, the chlorination reaction is also a solid gas reaction. To enhance the chlorination rate, uranium metal is usually subject to hydride and then de-hydride to make the uranium powders so that the surface areas for the chlorination reaction are increased. The  $\text{UCl}_3$  can be further chlorinated by  $\text{Cl}_2$  gas to produce the needed  $\text{UCl}_4$ . The pure  $\text{PuCl}_3$  can be made by chlorination of pure plutonium metal. Because of the inherent solid gas reaction, the chlorination reaction rate is usually slow, and also this process is also costly. Friedman made a review on the preparation, purification, and properties of uranium chlorides [35].

The spent fuels can also be chlorinated to produce the chloride salt for molten fast reactors. Considering the importance of the management of the spent fuels from existing nuclear reactors, this section mainly focus on the chlorination of spent oxide fuels from light water reactors and from uranium metal fuels, to convert the uranium and plutonium component in oxide form or metal form to uranium chloride and plutonium chloride, which can be used as fuel for MSFRs.

Unlike the fluorination of spent oxide fuels by using  $\text{F}_2$ , due to thermodynamic stability of  $\text{UO}_2$ , the chlorination reaction of  $\text{UO}_2$  by using chlorine gas is not favorable. Some other reducing reagents employed to enhance the chlorination reaction were  $\text{CCl}_4$ ,  $\text{COCl}_2$ ,  $\text{Cl}_2\text{-CCl}_4$ ,  $\text{NH}_4\text{Cl}$ , or  $\text{Cl}_2$  gas with carbon presence. P. Hass made a detailed review on the information applicable to reaction of uranium oxides with chlorine to prepare the uranium tetrachloride [36]. This review showed that (1) there were no significant reports on the chlorination of uranium by  $\text{Cl}_2$ , C, or CO, but  $\text{CCl}_4$  was widely used as a chlorination reagent, (2) when chlorine was used as an chlorination reagent, carbon was usually used an reactant, with  $\text{CO}_2$  or CO as products, and (3) phosgene  $\text{COCl}_2$  was an effective reagent when the chlorination temperature was  $450^\circ\text{C}$  or higher.

Similar to uranium fluorides, uranium chlorides of different valence had different vapor pressure, and these volatility can be used for separating uranium chloride during chlorination process. Figure 3-6 shows the vapor pressures of several uranium chlorides,  $\text{UCl}_3$ ,  $\text{UCl}_4$ ,  $\text{UCl}_5$ , and  $\text{UCl}_6$ . All are possible during the chlorination process and  $\text{UCl}_5$  and  $\text{UCl}_6$  are not stable unless excess  $\text{Cl}_2$  gas is present and may decompose to  $\text{UCl}_4$  and  $\text{Cl}_2$  gas [36].

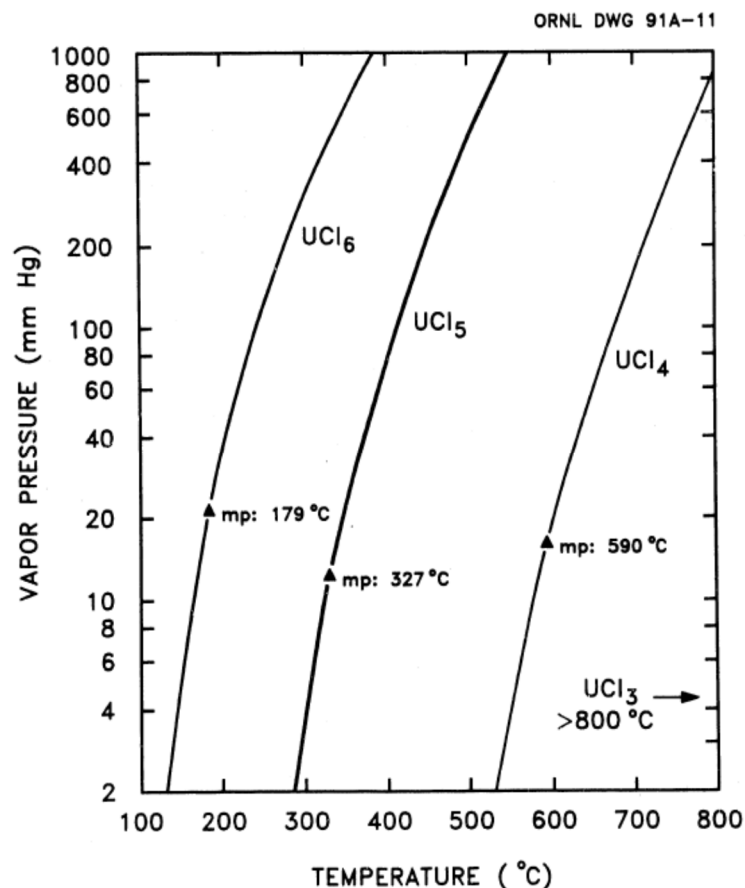


Figure 3-6. Vapor pressures of chlorides versus temperature [36].

$\text{CCl}_4$  was commonly used as a chlorination reagent. It was reported that chlorinating the  $\text{UO}_2$  using  $\text{CCl}_4$  gas at  $580^\circ\text{C}$  can effectively produce  $\text{UCl}_4$ ,  $\text{UCl}_5$ , and  $\text{UCl}_6$ . The chlorination temperature can increase the percentage  $\text{UCl}_5$  and  $\text{UCl}_6$ , both of which are unstable and will decompose to  $\text{UCl}_4$  and  $\text{Cl}_2$  when cooled down.

A low temperature chlorination method, with involvement of the mechanical ball milling—or called a mechanochemical process, for uranium oxides ( $\text{UO}_2$  and  $\text{U}_3\text{O}_8$ ) was investigated [37]. It was found that the mechanochemical chlorination of  $\text{U}_3\text{O}_8$  with  $\text{CCl}_4$  to  $\text{UOCl}_2$ ,  $\text{UCl}_4$ , and  $\text{U}_2\text{O}_2\text{Cl}_5$  proceeded— even at room temperatures, but the chlorination of  $\text{UO}_2$  at low temperature was unlikely.

By using a mixture of 85%  $\text{Cl}_2$ -15% $\text{CCl}_4$ ,  $\text{U}_3\text{O}_8$  oxides (which was converted from  $\text{UO}_2$  in oxygen atmosphere at  $500$ – $800^\circ\text{C}$ ) can be chlorinated and volatized as  $\text{UCl}_5$  and  $\text{UCl}_6$ . By distillation and sublimation, 90–98% uranium was recovered.

Using  $\text{Cl}_2$  with carbon presence, chlorination of  $\text{U}_3\text{O}_8$  was also confirmed. Different chloride compounds such as  $\text{UCl}_3$ ,  $\text{UCl}_4$ ,  $\text{UCl}_5$ , and  $\text{UCl}_6$  were produced and the proper chlorination in the  $\text{U}_3\text{O}_8$ - $\text{Cl}_2$ -C system was found in the range of 863 to 953 K.

A systematic study on the chlorination of  $\text{PuO}_2$  by using  $\text{COCl}_2$  and  $\text{Cl}_2$ - $\text{CCl}_4$  mixture was investigated by Los Alamos National Laboratory researchers [38]. Both phosgene ( $\text{COCl}_2$ ) and chlorine-carbon tetrachloride ( $\text{Cl}_2$ - $\text{CCl}_4$ ) were found to be effective reagents to produce  $\text{PuCl}_3$ , as shown in Table 3-3. A 500g-scale  $\text{PuCl}_3$  was successfully synthesized at  $500^\circ\text{C}$  in a pyrex reactor vessel. The

reaction of  $\text{COCl}_2$  and  $\text{CCl}_4$  with  $\text{PuO}_2$  was  $\text{PuO}_2 + 2\text{COCl}_2 = \text{PuCl}_3 + 1/2 \text{Cl}_2 + 2\text{CO}_2$ . Since the chlorination reaction is a solid gas reaction, the reaction kinetics slows down over time and it was suggested that stirring can help enhance the chlorination rate.

Table 3-3. Comparison between  $\text{COCl}_2$  and  $\text{Cl}_2\text{-CCl}_4$  as chlorinating agents for  $\text{PuO}_2$  [38].

Chlorinating agent	Plutonium weight percent	Chloride weight percent	Number of runs
$\text{COCl}_2$	$69.32 \pm 0.38$	$29.9 \pm 0.6$	112
$\text{Cl}_2\text{-CCl}_4$	$69.59 \pm 0.27$	$29.7 \pm 0.4$	16
An uncertainty of one standard deviation is noted.			

$\text{NH}_4\text{Cl}$  was also reported to be used as a chlorination reagent for uranium metal fuels [39]. By using  $\text{NH}_4\text{Cl}$ ,  $\text{UCl}_3$ , and  $\text{UCl}_4$  particles can be obtained. The reaction is  $\text{U} + 3\text{NH}_4\text{Cl} = \text{UCl}_3 + 3\text{NH}_3 + 1.5\text{H}_2$ . As an example of the chlorination process, Figure 3-3 shows the products after the chlorination at  $300^\circ\text{C}$  using  $\text{NH}_4\text{Cl}$ . Using  $\text{NH}_4\text{Cl}$  was considered an easy and simple process to produce the uranium chloride. But due to the solid gas reaction, some unreacted uranium metal still remained in the center of the fuel pellet, which requires further studies.

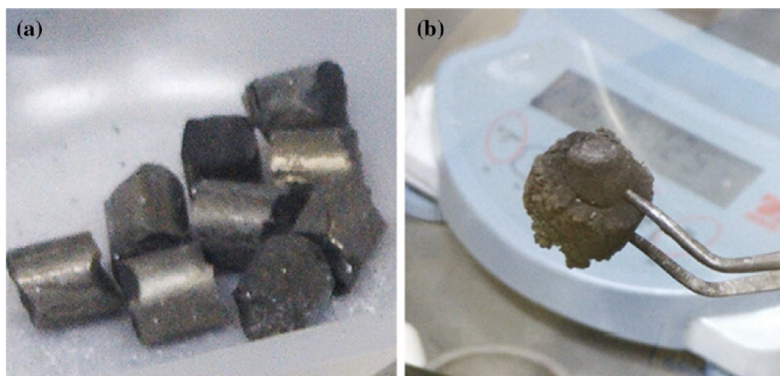


Figure 3-7. Photos of uranium metal fuels and chlorination product: uranium metal pellet (left) and chlorination product (right) [39].

$\text{NH}_4\text{Cl}$  was also investigated, recently, by H.C. Eun et al [40] to chlorinate uranium oxide. By adding Zr as a reactant, the  $\text{UO}_2$  can be chlorinated to  $\text{UCl}_3$  by  $\text{NH}_4\text{Cl}$  at  $320^\circ\text{C}$ . The chlorination reaction is  $\text{UO}_2 + 3\text{NH}_4\text{Cl} + \text{Zr} = \text{UCl}_3 + 1.5\text{N}_2(\text{g}) + \text{ZrO}_2 + 6\text{H}_2(\text{g})$ . This chlorination reaction is a solid–solid reaction, below the melting point of  $\text{NH}_4\text{Cl}$  ( $337^\circ\text{C}$ ). Some  $\text{UO}_2$  remained unchlorinated and  $\text{ZrO}_2$ ,  $\text{Zr}_2\text{O}_3$ , and  $\text{ZrCl}_2$  were byproducts.

By sparging a  $\text{Cl}_2$  and  $\text{CO}$  gas mixture into a molten halide media, the uranium oxides could be chlorinated [41]. In this chlorination process, the suspended oxides were dissolved in the halide media and fission products could also be removed, the rate of which were dependent on the composition of used halide media. The following reactions have been proposed:

- $\text{UO}_2 + \text{Cl}_2 = \text{UO}_2\text{Cl}_2$  (in  $\text{NaCl-KCl}$ , at higher than  $660^\circ\text{C}$ )
- $\text{U}_3\text{O}_8 + 3\text{Cl}_2 = 2\text{UO}_2\text{Cl}_2 + \text{O}_2$  (in  $\text{NaCl-KCl}$ , at higher than  $660^\circ\text{C}$ )
- $\text{UO}_3 + \text{Cl}_2 = \text{UO}_2\text{Cl}_2 + 1/2\text{O}_2$  (in  $\text{NaCl-KCl}$ , at higher than  $660^\circ\text{C}$ )

- $2\text{UO}_2 + 3\text{Cl}_2 = 2\text{UCl}_3 + 2\text{O}_2$  (in NaCl-KCl, at  $820^\circ\text{C}$ ).

It was considered that, based on the effect of salt composition on the chlorination of uranium oxides, the salt not only acts as media for chlorination, but also actively enters the chlorination mechanism. Addition of iron or zinc chlorides can increase the oxide dissolution rate. Figure 3-6 shows an example of the chlorinated uranium versus the time during the chlorination process using different salts. (20g reconstituted uranium oxide and 200g salt were used; temperature was  $800\text{--}850^\circ\text{C}$ , the salt was stirred at 640 rpm by a quartz stirrer)

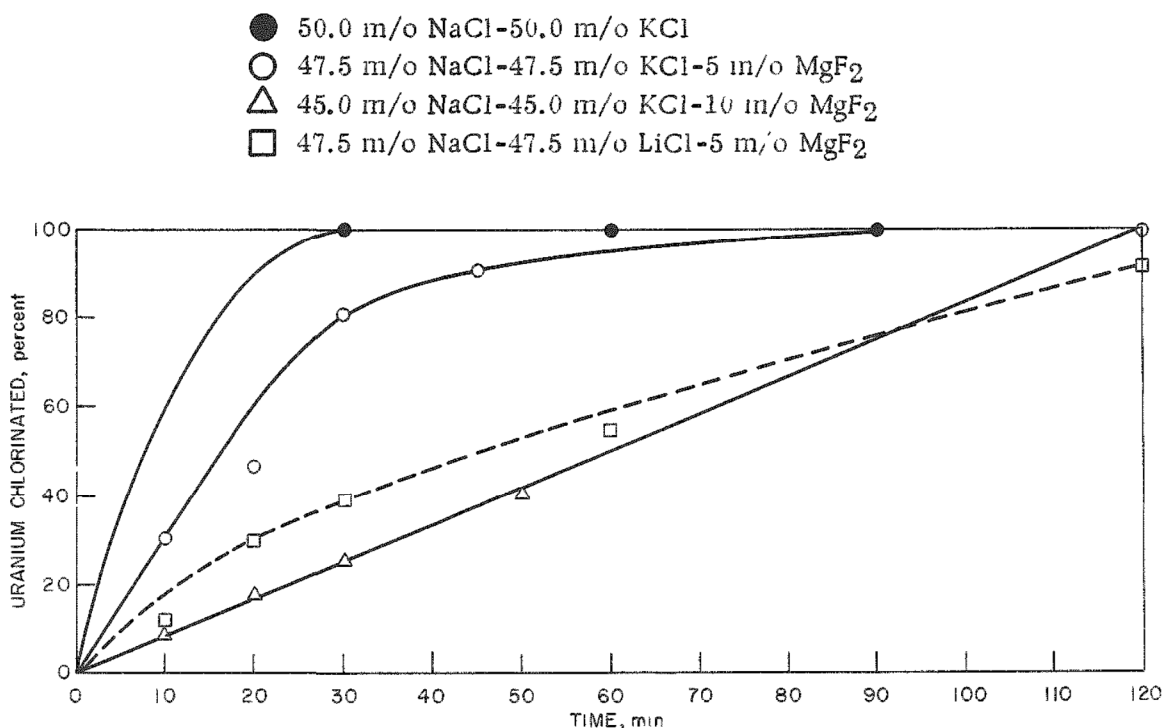


Figure 3-8. Uranium chlorinated versus time using different salt media [41].

By using LiCl-KCl media, chlorination of  $\text{UO}_3$  (which was converted from  $\text{UO}_2[\text{NO}_3]_3$  by a denitration process) by chlorine gas and carbon was also reported by K. Uozumi et al. [42]. The chlorination reaction is  $\text{UO}_3 + 1.5\text{Cl}_2 + 3\text{C} = \text{UCl}_3 \text{ (in LiCl-KCl)} + 3\text{CO}$ . Almost all the actinide elements remained in the chlorination product. The experimental conditions ( $650^\circ\text{C}$ , introduction of  $\text{Cl}_2$  in a  $\text{Cl}_2/\text{Ar}$  gas mixture) was believed to avoid the evaporation of U and Tc. Figure 3-7 shows the chlorination process.

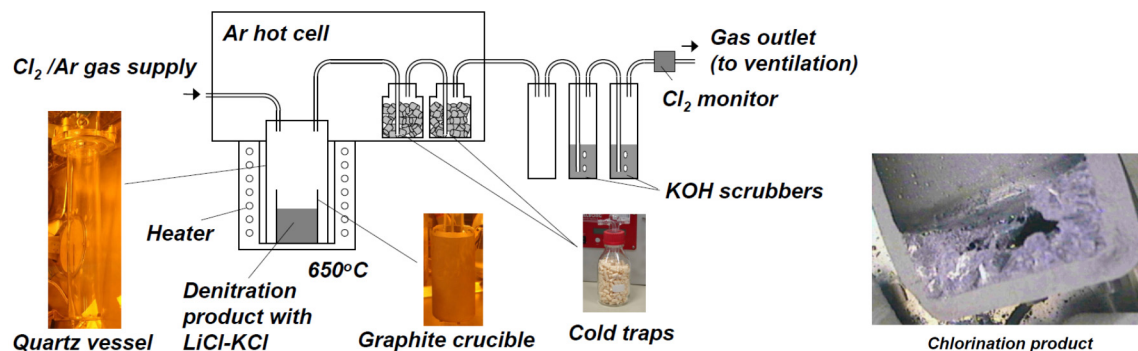


Figure 3-9. Chlorination process by using Cl<sub>2</sub>, carbon and LiCl-KCl salt media [42].

In recent years, ZrCl<sub>4</sub> and MoCl<sub>5</sub> were reported to be used as effective chlorination reagents for chlorinating spent oxide fuels [43, 44]. Sakamura et al. [44] used ZrCl<sub>4</sub> to chlorinate the UO<sub>2</sub> and PuO<sub>2</sub> in a liquid phase of LiCl-KCl at 500°C, and found that when zirconium was also added, the oxides were effectively chlorinated, in particular, when the oxides were in powder form. Because the ZrCl<sub>4</sub> is non-corrosive, it was considered a simple and promising chlorinating reagent for UO<sub>2</sub> and PuO<sub>2</sub>. The reactions were shown in Table 3-4.

Table 3-4. Chlorination reactions of UO<sub>2</sub> and PuO<sub>2</sub> when ZrCl<sub>4</sub> is used as a chlorination reagent. ΔG° for reactions of UO<sub>2</sub> and PuO<sub>2</sub> with ZrCl<sub>4</sub> at 773K (retyped from [43])

Reaction	ΔG° (kcal /mol-O)
$\text{UO}_2 + 3/4\text{ZrCl}_4 + 1/4\text{Zr} = \text{UCl}_3 + \text{ZrO}_2$	-13.5
$\text{UO}_2 + \text{ZrCl}_4 = \text{UCl}_4 + \text{ZrO}_2$	-1.9
$\text{UO}_2 + 1/2\text{ZrCl}_4 = \text{UOCl}_2 + 1/2\text{ZrO}_2$	-2.9
$\text{UOCl} + 1/2\text{ZrCl}_4 = \text{UCl}_3 + 1/2\text{ZrO}_2$	-16.7
$\text{PuO}_2 + 3/4\text{ZrCl}_4 + 1/4\text{Zr} = \text{PuCl}_3 + \text{ZrO}_2$	-29.4
$\text{PuOCl} + 1/2\text{ZrCl}_4 = \text{PuCl}_3 + 1/2\text{ZrO}_2$	-16.2
$\text{Pu}_2\text{O}_3 + 3/2\text{ZrCl}_4 = \text{PuCl}_3 + 3/2\text{ZrO}_2$	-29.5

This technology (by using ZrCl<sub>4</sub> as a chlorination reagent and a molten salt for preparing the fuel needed for the fast reactors) has been considered to be used in the Elysium Industries, as shown in the flow sheet (Figure 3-8) [45].

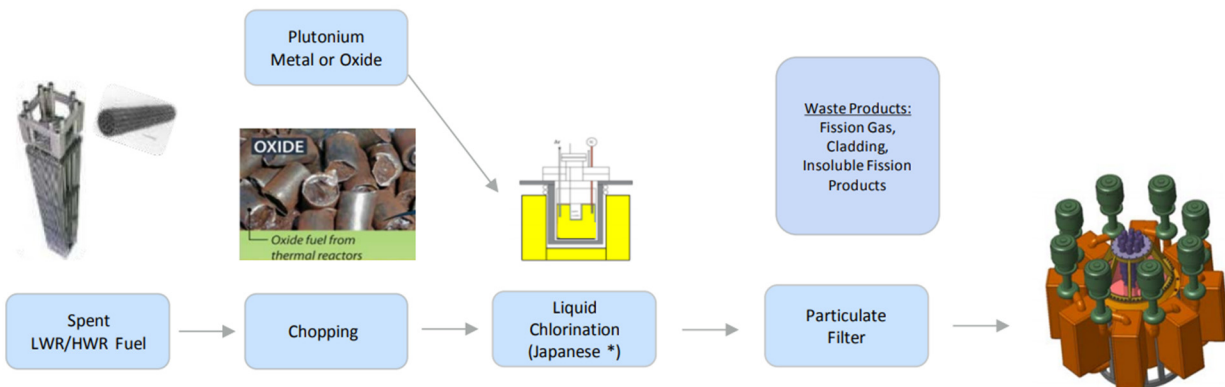


Figure 3-10. A flow sheet proposed by Elysium on utilizing the recovered fuels from chlorination of spent fuels for their fast reactors [45]. The liquid chlorination in the flowsheet is shown in [44].

By using  $\text{MoCl}_5$  as a chlorination reagent, through the following reaction:  $2(\text{U}_{0.5}\text{Zr}_{0.5})\text{O}_2 + 4\text{MoCl}_5 = \text{UCl}_4 + \text{ZrCl}_4 + 4\text{MoOCl}_3$ , chlorination of  $(\text{U}_{0.5}\text{Zr}_{0.5})\text{O}_2$  powders was reported to be successfully achieved at 573 and 773 K [43].  $\text{MoCl}_5$ ,  $\text{ZrCl}_4$ , and  $\text{MoOCl}_3$  were separated from  $\text{UCl}_4$  by volatilization under a temperature gradient. This shows the feasibility of using  $\text{MoCl}_5$  as the chlorination reagent. As expected, higher temperature is desired for chlorination of dense  $(\text{U}_{0.5}\text{Zr}_{0.5})\text{O}_2$  solid solution.

Uranium metal fuels, as expected, can be chlorinated by using chlorine and HCl gas. It was reported [46] the U-Al metal fuels was successfully chlorinated by using  $\text{Cl}_2$  and HCl gas. The Gibbs free energy of the chlorination reactions, with HCl as chlorination reagent, are all negative at 300°C, as shown in Table 3-5. Chlorination experiments at 300 to 400°C showed the chlorination with an HCl/U-Al ratio of 25 was effective and  $\text{UCl}_4$  was achieved, even without the need for sublimation of  $\text{AlCl}_3$ .

Table 3-5. Gibbs free energy of the chlorination reactions when HCl is used as chlorination reagent [46].

Reaction	$\Delta G$ (kJ) at 573.15K
$1/13\text{UAl}_3 + \text{HCl} = 1/13\text{UCl}_4 + 3/13\text{AlCl}_3 + 1/2\text{H}_2$	-87
$1/10\text{UAl}_2 + \text{HCl} = 1/10\text{UCl}_4 + 3/10\text{AlCl}_3 + 1/2\text{H}_2$	-89
$\text{UCl}_3 + \text{HCl} = \text{UCl}_4 + 1/2\text{H}_2$	-16
$\text{UCl}_4 + \text{HCl} = \text{UCl}_5 + 1/2\text{H}_2$	114
$1/3\text{U} + \text{HCl} = \text{UCl}_6 = 1/2\text{H}_2$	105
$1/3\text{U} + \text{HCl} = 1/3\text{UCl}_3 + 1/2\text{H}_2$	-221
$1/4\text{U} + \text{HCl} = 1/4\text{UCl}_4 + 1/2\text{H}_2$	-115
$1/3\text{Al} + \text{HCl} = 1/3\text{AlCl}_3 + 1/2\text{H}_2$	-88
$1/3\text{Al} + \text{HCl} = 1/3\text{AlCl}_3 + 1/2\text{H}_2$	-92
$1/3\text{Al} + \text{HCl} = 1/6\text{Al}_2\text{Cl}_6 + 1/2\text{H}_2$	-189

Lebedev et al. [47, 48] studied the chlorination of U-Al fuels (with 39.5%U) at 350°C and found that the chlorination is effective, though some of the chlorinated uranium produces were removed into the sublimates.

$\text{UAl}_2$ ,  $\text{UAl}_3$ ,  $\text{NpAl}_2$ , and  $\text{PuAl}_2$  were chlorinated with  $\text{HCl(g)}$  at 300-400°C and  $\text{UCl}_4$ ,  $\text{NpCl}_4$ , or  $\text{PuCl}_3$  formed and a high chlorination efficiency was achieved. Higher temperature was found to be able to enhance the fluorination reaction rate and efficiency, but when the chlorination was carried out at lower temperature, the formation of  $\text{UCl}_5(\text{g})$  or  $\text{UCl}_6(\text{g})$  was avoided.



Somewhat similar to the chlorination by employing  $\text{ZrCl}_4$  and molten salt to chlorinate spent oxide fuels, chlorination of metal fuels by employing the molten salt and chlorine gas was also reported. By chlorinating the U-Al metal fuels in LiCl-KCl using  $\text{Cl}_2$  gas, it was found that complete chlorination was achieved, even without the formation of the volatile  $\text{UCl}_5$  and  $\text{UCl}_6$ .

### **3.4 Key Findings and Future Research and Development Needs for Chlorination**

The spent oxide fuels can be reasonably effectively chlorinated by using different chlorination reagents including  $\text{CCl}_4$ ,  $\text{COCl}_2$ ,  $\text{Cl}_2\text{-CCl}_4$ ,  $\text{NH}_4\text{Cl}$ , or  $\text{Cl}_2$  gas with carbon presence. Due to the inherent characteristics of solid gas chlorination reactions, the chlorination rate may decrease over time and the center of the oxide may be difficult to be chlorinated and result in incomplete chlorination. High temperature may enhance the chlorination rate, and uranium oxide in powder form is desired for improved kinetics and efficiency.  $\text{U}_3\text{O}_8$  is found to be easier to be chlorinated than  $\text{UO}_2$  and therefore the conversion of  $\text{UO}_2$  to  $\text{U}_3\text{O}_8$  before chlorination (if the conversion process does not significantly complicate the process sheet and increase the processing cost) may be considered for engineering application of chlorination.

The chlorination of metal fuels are relatively easier than of oxide fuel, and good chlorination efficiency can be achieved.

All the reported chlorination processes using different chlorination reagents are at lab scale. And the suitability of these chlorination processes on a larger scale needs to be investigated and demonstrated for MSFR applications.

## 4. MOLTEN SALT CHEMISTRY MANAGEMENT

*Guoping Cao*

### 4.1 Fluoride Salt Purification

The goal of the salt purification is remove the salt impurities (such as H<sub>2</sub>O, oxides, oxyfluoride, sulfur impurity, etc.) to minimize the corrosion of materials. Oxides are important impurities in the fluoride salts. It was found that BeO is fairly insoluble in the FLiBe, and the ThO<sub>2</sub>, PaO<sub>2</sub>, UO<sub>2</sub> and PuO<sub>2</sub> are increasingly insoluble in the FLiBe salt [49].

The MSRE operation has gained a lot of experience on the purification of fluoride salt and has been well documented [50]. In MSRE, HF was used to remove the oxides and other impurities in the fluoride salts. The reactions of the HF with typical impurities (oxygen ion, sulfide, and iodide) in the fluorides are  $2\text{HF}(\text{g}) + \text{O}^{2-} = 2\text{F}^- + \text{H}_2\text{O}(\text{g})$ ,  $2\text{HF}(\text{g}) + \text{S}^{2-} = 2\text{F}^- + \text{H}_2\text{S}(\text{g})$ , and  $\text{HF}(\text{g}) + \text{I}^- = \text{F}^- + \text{HI}(\text{g})$ .

During the MSRE program, the purification of the FLiBe salt was achieved by sparging H<sub>2</sub>/HF gas in the molten salt. The H<sub>2</sub>/HF ratio was usually controlled at around 10 to achieve purification efficiency and also avoid the corrosion of the container materials [51], and most of the impurities including moisture, oxide, and halide contaminate such as chlorine and sulfur can be removed effectively. After the H<sub>2</sub>/HF sparging processing, hydrogen gas was used to precipitate the metal fluorides formed from the H<sub>2</sub>/HF sparging, and reducing metal Be or Zr was also added. The purified salt was then filtered and transferred to storage container.

Some other chemical reagents were also reported for the purification of the fluoride salts such as NH<sub>4</sub>HF<sub>2</sub> (a solid ammonium hydrogen fluoride) and NF<sub>3</sub> gases. NH<sub>4</sub>HF<sub>2</sub> was reported to be able to remove impurity oxide from the fluoride salt, through the reaction  $\text{MeO}_2 + 4\text{NH}_4\text{HF}_2 = \text{MeF}_4 + 4\text{NH}_4\text{F}(\text{g}) + 2\text{H}_2\text{O}(\text{g})$  [52]. A study by R. D. Scheele et al. on the purification of fluoride salt by NF<sub>3</sub> shows that the nitrogen trifluoride is a viable for purifying the fluoride salts and it is safer than the HF + H<sub>2</sub> mixture during purification process [53]. Because the HF is corrosive, the use of NH<sub>4</sub>HF<sub>2</sub> and NF<sub>3</sub> gas may be significant for the fluoride salt purification processes.

### 4.2 Corrosion in Fluoride Salt

In the fluoride salt system, there are several different corrosion mechanisms[54, 55]: (1) intrinsic corrosion, (2) impurity driven corrosion, (3) thermally driven or temperature gradient driven corrosion, (4) dissimilar metal driven corrosion or galvanic corrosion, (5) stress corrosion cracking.

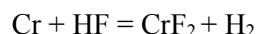
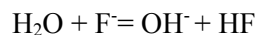
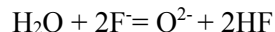
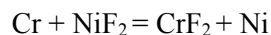
#### 4.2.1 Intrinsic Corrosion

The intrinsic corrosion is referred to the corrosion by the salt itself. When the salt is clean and free from any impurities and the metal surface is free from any oxide layers (in the fluoride salts, the oxide layer does not provide passive protection as in other oxidizing environments such as helium for very high temperature reactors), the corrosion is, theoretically, from the reaction of the alloy elements and the fluoride salt. Due to the negative Gibbs free energy of the fluoride salts such as LiF, BeF<sub>2</sub> for the reference MSBR under development, the reaction of the alloy elements with salts were thermodynamically unfavorable.

#### 4.2.2 Impurity Driven Corrosion

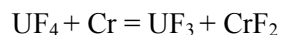
Ideally the impurities should be removed by the salt purification process. But impurities in the fluoride salt can come from different sources during salt handling because of the hygroscopic characteristic of the fluoride salt. Moisture, oxide, and other oxidants can be introduced into the salts. One characteristic of the impurities is they will react with salt and form corrosive agents in the fluorides salt, and then attack the surface of the structural materials. Although the reaction between the impurity and

structural is very aggressive, the corrosion due to impurity trappings during salt handling will be completed in a reasonable short time; that is, all the impurities will be consumed. The following reactions, using Cr as an example since Cr is the easiest alloying element in most structural alloys, are typical corruptions due to impurities.



During the operation of the MSBR operation, some excess fluorine gas will be formed and the  $\text{F}_2$  gas can also react with the tritium formed during neutron irradiation to form tritium fluoride (TF). These excessive fluorine gas and TF can react with the structural material if the effects from  $\text{F}_2$  and TF are not mitigated. The effects can be well controlled by maintaining the salt at a slightly reducing condition, and during the MSRE operation, the salt was maintained with a  $\text{UF}_4/\text{UF}_3$  ratio of about 100 to control the salt at a condition that is not corrosive to the structural materials. It should be noted that in molten fluoride salt solution, it was found that the  $\text{UF}_3$  is not stable unless when a lot of  $\text{UF}_4$  is present. The MSRE operation experience shows that the  $\text{UF}_4/\text{UF}_3$  can provide a good buffer for controlling the corrosion of materials.

The mechanism for using  $\text{UF}_4/\text{UF}_3$  ratio as a redox buffer is shown below:



The operation of the MSBR will tend to increase the  $\text{UF}_4/\text{UF}_3$  ratio and make the salt more and more corrosive over time. But by adding another reactive reducing reagent such as Be used in MSBR can effective adjust back the  $\text{UF}_4/\text{UF}_3$  ratio to the desired level, by the reaction  $\text{Be} + 2\text{UF}_4 = 2\text{UF}_3 + \text{BeF}_2$ . Figure 4-1 shows the recorded history of the ratio of  $\text{UF}_4$  and  $\text{UF}_3$  versus time during the MSRE operation.

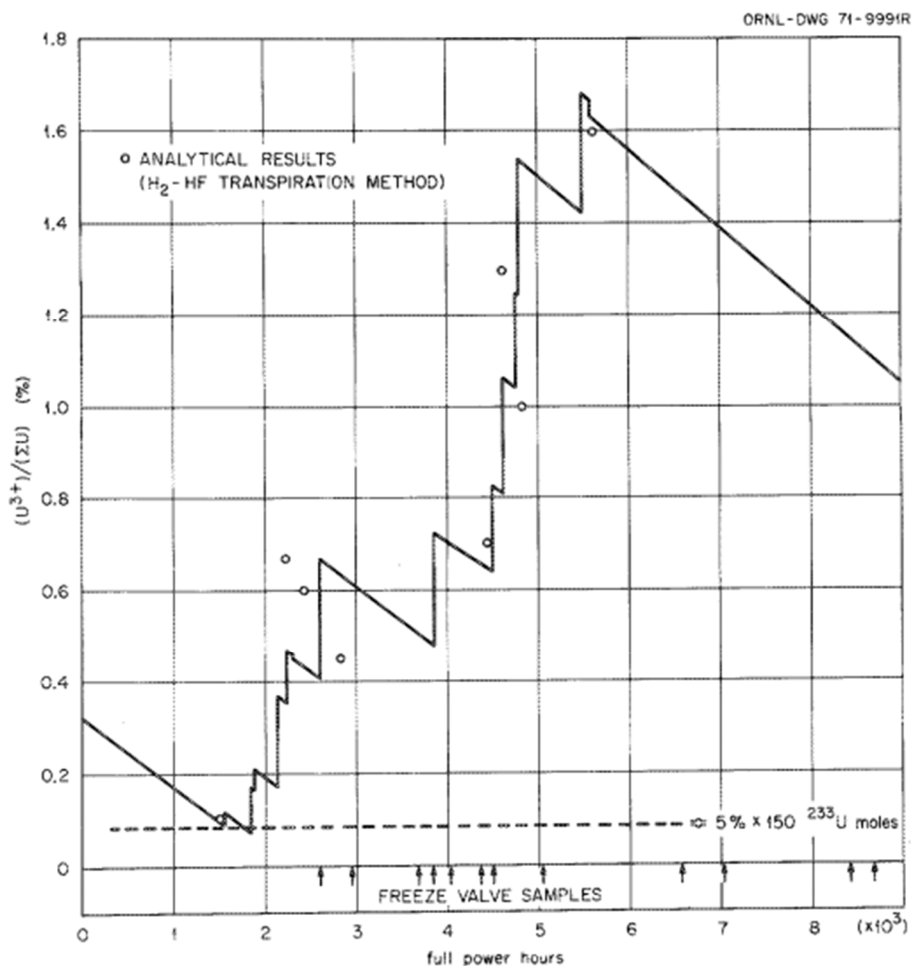


Figure 4-1.  $U^{3+}/U^{4+}$  in the MSRE fuel salt runs 5-14 [57].

In MSRE, the desired  $UF_4/UF_3$  ratio is around 100. The salt is called oxidizing if significantly above 100, and it is reducing if the ratio is lower than 100. Figure 4-2 shows the effects of different  $UF_4/UF_3$  ratios on the corrosion of fluoride salt on a nickel based alloy [56].



Figure 4-2. Nickel base alloys after immersion in  $LiF-ThF_4-UF_4-UF_3$  molten salt at  $800^\circ C$  for two compositions of  $UF_4/UF_3$  ratios: left  $UF_4/UF_3 = 80-100$ , and right  $UF_4/UF_3 = 500$  [56].

The above  $\text{UF}_4 + \text{Cr} = \text{UF}_3 + \text{CrF}_2$  is also called a disproportionation reaction. This reaction is significant because it provides the redox buffer to the fuel salt. It was found that the equilibrium constant at 900 K is  $K = N_{\text{UF}_4}^3 \cdot a_{\text{U}} / N_{\text{UF}_3}^4 = 6.3 \times 10^{-7}$ , where  $N$  is the molar fraction. In MSBR,  $n_{\text{UF}_4} = 3 \times 10^{-3}$  and  $N_{\text{UF}_3}$  is about  $3 \times 10^{-5}$ , and the uranium activity at equilibrium at 900 K is  $2 \times 10^{-17}$ , which is very low. Even at 5%  $\text{UF}_3$ , the uranium activity is still below  $10^{-14}$  [57]. If the  $\text{UF}_3$  is much greater than 5%, the uranium metal may be formed, and it will plate with the structural materials and may form uranium carbide when graphite is present, possibly by  $\text{UF}_3 + \text{C} + \text{Cr} = \text{UF}_4 + \text{CrC}$ .

It should be noted that different fluoride salts have different corrosivities. For example, in FLiBe, the corrosion products of Cr are largely  $\text{Cr}^{2+}$ , as shown from the MSRE experience. In FLiNaK, the Cr dissolved in the salt is mainly  $\text{Cr}^{3+}$ , which indicates that FLiNaK is more corrosive than FLiBe.

### 4.2.3 Temperature Gradient Driven Corrosion

The equilibrium constant for the disproportionation reaction  $\text{UF}_4 + \text{Cr} = \text{UF}_3 + \text{CrF}_2$  is temperature dependent: at high temperature, the equilibrium constant is higher which means higher corrosion rate, and at lower temperature, the equilibrium constant is lower and the corrosion rate is lower. At some coldest point, the Cr can be deposited on the surface of the structural materials. This temperature gradient driven corrosion can be seen in the thermal convection loop operation. It was found that higher corrosion rate occurred in the hot areas but some Cr was deposited in the coldest area, as shown in Figure 4-3 [58]. These deposits may block the salt flow and some filtering may be needed to remove the deposits. This temperature gradient driven corrosion mechanism is considered to be the sustained corrosion mechanism for the continued corrosion in MSBRs.

In addition to the temperature dependence of the equilibrium constant, the saturation solubility of the corrosion products in the molten fluorides is also a strong function of temperature, which can accelerate the corrosion of materials in the convection loop. Greater solubility difference at hot and cold legs in the convection loop may suggest more severe corrosion. This may partly explain the higher corrosivity in FLiNaK (relatively higher solubility difference) than in FLiBe (relatively lower solubility difference) [59, 60]. Table 4-1 shows the equilibrium level of dissolved metals for pure elements in contact with FLiNaK and FLiBe salts [59].

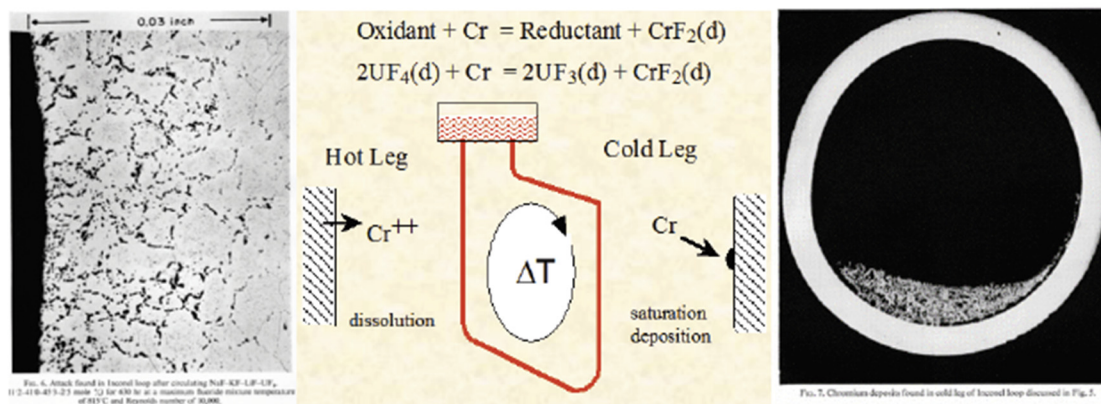


Figure 4-3. Temperature gradient driven corrosion in MSRE: left high corrosion in hot leg and Cr was dissolved into the molten salt persistently, and right, the Cr was deposited on the surface of the coldest area [58].

Table 4-1 Equilibrium level of dissolved metals for pure elements in contact with FLiNaK and FLiBe salts [59].

Molten salt	Mol%, BeF <sub>2</sub>	Mol%, UF <sub>4</sub>	Cr content at 600°C, ppm	Cr content at 800°C, ppm
FLiNaK	0	2.5	1,100	2,700
LiF-BeF <sub>2</sub>	48	1.5	1,470	2,260

#### 4.2.4 Dissimilar Materials Effects

When dissimilar materials were present in the molten salt, the corrosion rate can be accelerated. The dissimilar materials do not have to be electrically contacted each other, particularly when one of the materials has a chemical affinity for the corroded species in the salt and forms a compound. For example, when Co from Alloy 25 (53% Co) was found to be deposited onto Hastelloy N (0.1% Co) [55, 61]. Another effect from the presence of dissimilar materials is that the corrosion of the materials may be accelerated due to the galvanic corrosion effects (when the two dissimilar materials are electrically contacted). For example, the Alloy 800H tested in graphite crucible was found to have much higher corrosion rate than tested in Alloy 800H crucible (same crucible material as the test material). To avoid the galvanic corrosion, it has been recommended that the same material should be used for the structures that contact the salts [62]. It should be noted that sometimes during welding, the composition of the welded zone may be different from other matrix area and this can introduce micro-dissimilar material effect corrosion, in contrast to the general macro-dissimilar material effect [60].

#### 4.2.5 Stress Corrosion Cracking

In MSRE, it was found that tellurium-assisted stress corrosion cracking occurred in Hastelloy N in FLiBe. Tellurium was found to be diffused into the Hastelloy N and brittle intergranular precipitates were formed [55]. Tellurium-assisted stress corrosion cracking can be avoided by the following two options: (1) using a 95:5 ratio for UF<sub>4</sub>/UF<sub>3</sub> (a more reducing environment than a UF<sub>4</sub>/UF<sub>3</sub> ratio of 100 for the molten salt), or (2) using another modified Hastelloy N with extra Ti or Nb additions can also prevent the stress corrosion cracking in the operation of MSR.

#### 4.2.6 Corrosion Data in FLiBe Salt

In the purified FLiBe salt, the corrosion rate is usually very low. For example, in corrosion tests in purified FLiBe salt at 600°C, the corrosion rate of JLF-1, Inconel, Inconel 600, Hastelloy C-276, 316SS, 304SS, with 9 to 18 wt% Cr range, have a very low corrosion rate: between 0.0056 to 0.01 mm/year. In the loop corrosion tests at 650°C, the corrosion rate of Hastelloy N and 316SS is less than 0.025 and 0.008 mm/year. However, in as received FLiBe (with higher impurity) loop test at 650 °C, the corrosion rate of the 316SS is very high [60]. S. Guo et al. [63] summarized the corrosion data of Inconel and Hastelloy N tested in forced-circulation loops operated at a 704°C maximum temperature with LiF-BeF<sub>2</sub> salts at ORNL, as shown in Table 4-2.

Table 4-2. Summary of corrosion data of Inconel and Hastelloy N tested in forced-circulation loops operated at maximum temperature 704°C with LiF-BeF<sub>2</sub> salts at ORNL forced-circulation loop tests operated with LiF-BeF<sub>2</sub> salts at ORNL [63].

Material	Salt composition (mol%)	Duration (hours)	Corrosion attack at hot sections
Inconel	53LiF-46BeF <sub>2</sub> -1UF <sub>4</sub>	3,390	Intergranular voids to a depth of 178 μm
Inconel	62LiF-37BeF <sub>2</sub> -1UF <sub>4</sub>	3,046	Intergranular voids to a depth of 203 μm
Inconel	60LiF-36BeF <sub>2</sub> -4UF <sub>4</sub>	8,746	Intergranular voids to a depth of 356 μm
Inconel	62LiF-37BeF <sub>2</sub> -1UF <sub>4</sub>	9,574	Intergranular voids to a depth of 381 μm

Material	Salt composition (mol%)	Duration (hours)	Corrosion attack at hot sections
Inconel	71LiF-16BeF <sub>2</sub> -13ThF <sub>4</sub>	13,155	Intergranular voids to a depth of 330 $\mu\text{m}$
Inconel	62LiF-36.5BeF <sub>2</sub> -1ThF <sub>4</sub> -0.5UF <sub>4</sub>	15,038	Intergranular voids to a depth of 610 $\mu\text{m}$
Hastelloy N	53LiF-46BeF <sub>2</sub> -1UF <sub>4</sub>	14,563	Heavy surface roughening and pitting
Hastelloy N	62LiF-37BeF <sub>2</sub> -1UF <sub>4</sub>	15,140	Light surface roughening and pitting
Hastelloy N	62LiF-37BeF <sub>2</sub> -1UF <sub>4</sub>	14,503	No observable attack
Hastelloy N	70LiF-10BeF <sub>2</sub> -20UF <sub>4</sub>	14,498	No observable attack
Hastelloy N	71LiF-16BeF <sub>2</sub> -13ThF <sub>4</sub>	20,000	Pitted surface layer to 25 $\mu\text{m}$
Hastelloy N	62LiF-36.5BeF <sub>2</sub> -1ThF <sub>4</sub> -0.5UF <sub>4</sub>	14,498	No observable attack
Hastelloy N	62LiF-36.5BeF <sub>2</sub> -1ThF <sub>4</sub> -0.5UF <sub>4</sub>	20,000	Pitted surface layer to 51 $\mu\text{m}$
Hastelloy N	62LiF-36.5BeF <sub>2</sub> -1ThF <sub>4</sub> -0.5UF <sub>4</sub>	9,687	No observable attack

Some corrosion tests conducted in recent years in purified MSRE FLiBe salts also confirmed that when the salt is purified, the corrosion rate is very low. Figure 4-4 shows that corrosion of 316SS materials that were tested in purified FLiBe salt at 700°C for 1,000, 2,000, and 3,000 hours, in stainless steel and graphite crucibles [64]. The extrapolated Cr depletion depth is very low: 17.1  $\mu\text{m}/\text{year}$  for in stainless steel crucible and 31.2  $\mu\text{m}/\text{year}$  for in graphite crucible.

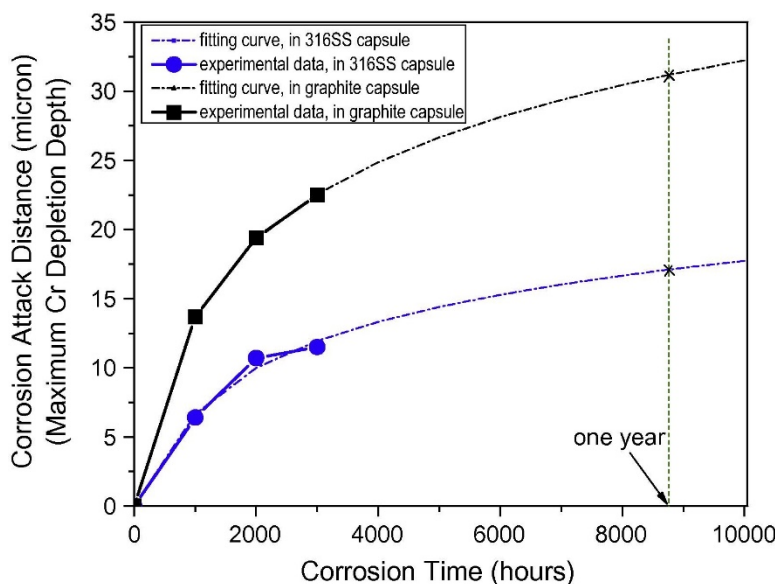


Figure 4-4. Depth of corrosion attack, in terms of maximum Cr depletion depth, as a function of corrosion time [64].

To minimize the corrosion of structural materials and ensure the long term service in fluoride salt such as FLiBe, usually nickel alloys with low Cr content such as Hastelloy N are considered. If the redox potential of the FLiBe salt is controlled, 316SS also performs satisfactorily and can be considered as loop structural materials.

It should be noted that because the graphite and structural materials are both present in the molten salt in MSBR, carbides may be formed in some structural materials. Carbides were formed in Hastelloy N that was tested in FLiBe at 700°C in graphite crucible [65]. The carbide formation was also confirmed by Chan et al. [66] in tests in FLiNaK at 700°C, using pure metallic elements. The carbides presence in the

structural materials appear to be able to inhibit the corrosion of the materials from the molten salt, though it will affect the mechanical properties.

### 4.3 Chloride Salt Purification

The purification of the chloride salt system is somewhat similar to the purification of fluoride salt system. Purification of the chloride salt is usually achieved by chlorination, by  $\text{CCl}_4$ ,  $\text{HCl}$ , or other chlorination chemicals [67, 68] or by reduction of the salt using reactive metals such as  $\text{Mg}$  [69]. Some physical processes may be also used before chlorination such as heating under vacuum, inert gas (such as argon) sparging. The reactions of  $\text{CCl}_4$  with the oxide ion impurity were:  $\text{CCl}_4 + 2\text{O}^{2-} = \text{CO}_2 + 4\text{Cl}^-$  and  $\text{CCl}_4 + \text{O}^{2-} = \text{COCl}_2 + 2\text{Cl}^-$ . The oxide ion was converted to carbon dioxide gas or a phosgene gas—which may further change to  $\text{CO}$  and  $\text{Cl}_2$ . By bubbling  $\text{CCl}_4$  gas in  $\text{KCl-LiCl}$  salt at  $800^\circ\text{C}$  for 4 hours, the oxygen concentration in the salt can be decreased to about 3ppm [68].

Because the chloride salts are more sensitive to moisture than fluoride salt, for example the  $\text{KCl-MgCl}_2$  may contain up to 30% water. The purification of chloride salt is found more difficult. The removal of oxygen in chloride salt is also more difficult to be removed by  $\text{HCl}$  sparging, particularly for removing the last portion of bound oxygen from the salt [67]. It was found [68] that  $\text{CCl}_4$  is much more effective than  $\text{HCl}$  sparging. The difficulty in the purification of chloride salts may partly contribute to the inconsistency in the corrosion results of alloys in chloride salt conducted across different institutions—different impurities in the chloride salts may significantly result in different, unpredictable corrosion rates.

### 4.4 Corrosion in Chloride Salt

In comparison with corrosion of materials in fluoride salts, a lot of corrosion data of different materials and in particular salt behavior during reactor operation are available, there are fewer corrosion data in chloride salt systems that may apply to the molten chloride reactor systems. Some chloride salts were being studied for the concentrated solar power system and the corrosion data in the salts for concentrated solar power can also help understand the corrosion in nuclear chloride salt systems.

Generally, most of the corrosion mechanisms (intrinsic corrosion, impurity driven corrosion, temperature gradient driven corrosion, and dissimilar metal corrosion) should also apply to the corrosion of materials in chloride salt system, but there are some differences between the corrosion in chloride and fluoride salts [67]. For example, the Gibbs free energies of chloride salt is less negative than the fluoride salt, for example  $-87.4$  kcal/mol for  $\text{KCl}$  is more positive than  $-109$  kcal/mol for  $\text{KF}$ , which may indicate somewhat less thermodynamic stability of structural materials in chloride salts [60]. The corrosion products chromium chlorides have higher solubility in molten chloride salt than the chromium fluoride corrosion products in molten fluoride salt, which indicate favoring corrosion in chloride salts. Nonetheless, because the free energies of formation of  $\text{NaCl}$  and  $\text{MgCl}_2$  is much more negative than for  $\text{CrCl}_2$ ,  $\text{FeCl}_2$ , and  $\text{NiCl}_2$ , the corrosion of structural materials by chlorides salt (free from any impurities) itself is thermodynamically unfavorable [60].

In comparison with uranium fluoride salt, fluorine is the most electronegative element and it has a single oxidation number (+1), chlorine has several different oxidation numbers (+1, +3, +5, and +7); this may make the corrosion of materials in chloride salt system more complicated [70]. Available data on corrosion of materials in chloride salts appear not consistent. Jackson et al. [72] found that the corrosion in  $\text{Fe-Cr-Ni}$  alloys is accelerated when the  $\text{Cr}$  and  $\text{C}$  contents are increased, but Vignarooban et al [72] found some results that are somewhat contrary to that of Jackson: the C276 alloy with higher  $\text{Cr}$  content is corroded much slower than the Hastelloy N in  $\text{NaCl-KCl-ZnCl}_2$  salt ( $50 \mu\text{m/year}$  versus  $150 \mu\text{m/year}$  at  $500^\circ\text{C}$ ).



D. Williams summarized some salts corrosion results in chloride salt loop tests, as shown in Table 4-3 [67]. It was also found, from the salt loop tests, that the corrosion in chloride salt is not predictable. As shown in the table, the content of chromium appears not a significant factor for corrosion in structural materials, and the temperature effect on corrosion in chloride salts is also unknown. It was indicated that the corrosion of some materials tested at lower temperature shows high corrosion rates.

Table 4-3. Corrosion rates of several high chromium steels in chloride salts in ORNL loop tests [67].

<b>Alloy</b>	<b>Composition (%) Cr-Ni-Mo</b>	<b>Test Duration (hours)</b>	<b>Maximum Temperature (°C)</b>	<b>Corrosion Rate (mil/year)</b>
<b>LiCl-KCl</b>				
347SS	17.5-1.4-0.2	5,500	575	0.5
410SS	12.4-0.2-0.1	2,200	570	2.1
2.25Cr-1Mo	2.25-0-1	697	550	high
<b>NaCl-KCl-MgCl<sub>2</sub></b>				
347SS	17.5-1.4-0.2	2,467	500	3.9
410SS	12.4-0.2-0.1	3,971	494	3.3
347SS	17.5-1.4-0.2	1,034	520	1.3
347SS toughened	17.5-1.4-0.2	656	515	10.7

Sridharan and coworkers [55, 73] studied the corrosion of high nickel alloys in KCl-MgCl<sub>2</sub> salt at 850°C for 100 hours using quartz and graphite crucible. And the corrosion data were summarized in Table 4-4 by Sohal et al. [60].

Table 4-4. Corrosion of several alloys in KCl-MgCl<sub>2</sub> at 850°C for 100 hours in quartz crucible and graphite crucible [60, 73, 74].

<b>Alloy</b>	<b>Crucible</b>	<b>Corrosion Rate (mm/y)</b>	<b>Comments</b>
Haynes 230	quartz	0.67	Good corrosion to intergranular attack
316SS	quartz	1.0	Deepest intergranular attack, worst Cr depletion
Hastelloy X	quartz	1.1	
Hastelloy N	quartz	1.1	Least intergranular attack
Inconel 718	quartz	1.2	
Inconel 617	quartz	1.3	
Incoloy 800H	quartz	1.4	
Incoloy 800H -GBE	quartz	0.89	Good corrosion to intergranular attack
Incoloy 800H	graphite	0.24	
Ni-210	quartz	1.3	Least intergranular attack
Inconel 625	quartz	1.5	
Inconel 600	quartz	1.5	

When comparing different corrosion test results, it was generally found that Co, Mo, W, and Ta elements in nickel based alloy can improve the corrosion of materials in chloride salt. The reason is most likely because these refractory elements such as Co, Mo, W, and Ta in the nickel based alloys may inhibit the outward diffusion of Cr in nickel based alloys to the surface contacting the chloride salt [68]. A recent study by H. Sun et al. [75] of testing different materials (Ni-Fe-Cr, Ni-W-Cr, and Ni-Mo-Cr alloys) in NaCl-KCl-MgCl<sub>2</sub> at 700°C under a N<sub>2</sub> atmosphere showed that the corrosion resistance of nickel-based alloys is in the order of Ni-Fe-Cr < Ni-W-Cr < Ni-Mo-Cr, and the alloying elements of Mo and W (by slowing the diffusion of Cr) may contribute to the better corrosion performance, as shown in Table 4-5.

Table 4-5 Weight changes for the alloys exposed in molten NaCl-KCl-MgCl<sub>2</sub> (33–21.6–45.4 mol%) under N<sub>2</sub> atmosphere at 700°C for 100 h. [75]

Alloy	Main components	Weight changes (mg/cm <sup>2</sup> )
316SS	64.5Fe-17Cr-13Ni	2.38 ± 0.20
617	53.3Ni-22.5Cr-9.8Mo-11.4Co	0.85 ± 0.07
242	65.5Ni-8Cr-24.9Mo	0.62 ± 0.04
C276	58Ni-16.2Cr-15.6Mo-3.2W	1.05 ± 0.10
C22	57.9Ni-21.6Cr-13.1Mo-2.9W	0.74 ± 0.07
600	73.4Ni-16.4Cr-9.2Fe	2.16 ± 0.02
625	62Ni-21.5Cr-9Mo-3.6Nb	0.67 ± 0.09
230	61Ni-21.6Cr-13.4W-1.2Mo	0.82 ± 0.05

The presence of graphite and SiO<sub>2</sub> can accelerate the corrosion in chloride salts [76]. From Sridharan et al.'s corrosion tests of 800H in KCl-MgCl<sub>2</sub> at 850°C for 100 hours, as shown in the Table 4-4, the quartz appears to have greater effects in accelerating the corrosion of alloys in chloride than the graphite. This shows that the contact of graphite with structural materials should be avoided, and the presence of SiO<sub>2</sub> in the chloride salt should also be avoided.

Recently, Mehrabadi et al. [77] studied the corrosion of Haynes -230, 163 and Incoloy 800H in KCl-MgCl<sub>2</sub> salt at 850°C for 100 hours in a nickel crucible, and also studied the effects of cathodic protection effects (by contacting a more active Mg metal piece with the test samples) on the mitigation of corrosion. Haynes 230 shows lowest corrosion rate without Mg cathodic protection. When the samples are cathodically protected by even a small amount of Mg, the corrosion rate of the samples was decreased tremendously (35 times lower when 1.15 mol% Mg was added than when no Mg was present to provide cathodic protection). It is considered that the  $\text{Cr}^{2+} = \text{Cr}^{3+} + \text{Cr}$  reaction may contribute to the acceleration of the corrosion of the structural materials in the KCl-MgCl<sub>2</sub> salts contained in nickel crucible at higher temperature. The reaction was explained as follows: the active element Cr in the structural alloys is dissolved into a low oxidation state (CrCl<sub>2</sub>). At higher temperatures, the CrCl<sub>2</sub> can disproportionate to CrCl<sub>3</sub> and Cr through  $3\text{CrCl}_2 = 2\text{CrCl}_3 + \text{Cr}$ . In coupling with the galvanic corrosion effect (the structural alloy and nickel crucible are dissimilar materials), the CrCl<sub>3</sub> will further contribute to the corrosion of alloys and also alloying of the Cr with Ni crucible, that is  $\text{Ni} + 3\text{CrCl}_2 = 2\text{CrCl}_3 + \text{NiCr}$ . This disproportionation reaction of  $3\text{CrCl}_2 = 2\text{CrCl}_3 + \text{Cr}$  has also been studied in other corrosion studies by B. Mehrabadi et al. [78, 79] and H. Cho et al. [80].

It is expected that the disproportionation reaction at high temperature may make the corrosion and its control in fast reactor more complicated. The typical operation temperature in a chloride fast reactor is much lower than the test temperature of 850°C used by Mehrabadi et al. It is unknown how the disproportionation reaction equilibrium is at the temperature ranges of the fast reactor operation and there is little available data in this area.

Because of the different testing conditions including crucible materials, cover gas composition, and unknown impurity control in the chloride salt, which may significantly affect the corrosion if impurities were not well controlled, the corrosion results of materials in chloride salt are inconsistent and more study is needed for selecting a structural material that is compatible with the chloride salt and last for a long term during the reactor service life.

For the redox control in chloride salt, it is considered that similar to redox control in fluoride by controlling the  $\text{UF}_4/\text{UF}_3$  ratio,  $\text{UCl}_4/\text{UCl}_3$  ratios of roughly 0.003 to 5% can be used to mitigate the corrosion of structural nickel-based structural alloys. This small amount of  $\text{UCl}_4$  can help inhibit the disproportionation reaction of  $\text{UCl}_3$ , which is  $3\text{UCl}_3 = 3\text{UCl}_4 + \text{U}$  [81]. Some industries such as Moltex [82], consider using the option of adding reactive Zr into the fuel salt.  $\text{UCl}_3$  is substantially more stable in chloride salts than the  $\text{UF}_3$  in the fluoride salt system. Therefore, the small amount of  $\text{UCl}_4$  is not needed and the chloride fuel salt can be operating at a very reducing environment by adding Zr in the salt.

Moltex technology reported [34] that by adding a reducing agent Zr to the chloride salt, the corrosion of Hastelloy N was tremendously reduced, and they concluded that one other high chromium content 316SS alloy also can be used in the chloride salt with Zr additions, as shown in Figure 4-5. In the coolant salt, when  $\text{ZrF}_2$  was added into the salt system, the corrosion of the materials was significantly mitigated, as shown in Figure 4-6.

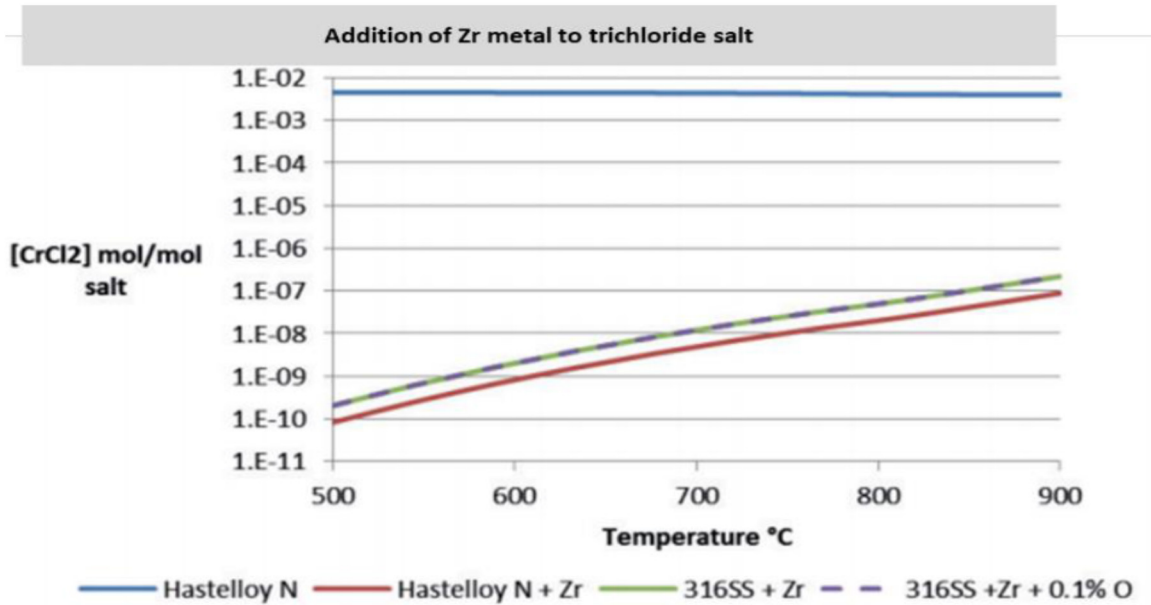


Figure 4-5. Chromium concentration in the fuel salt with and without Zr redox stabilization. Higher Cr concentration means higher corrosion rate [34].

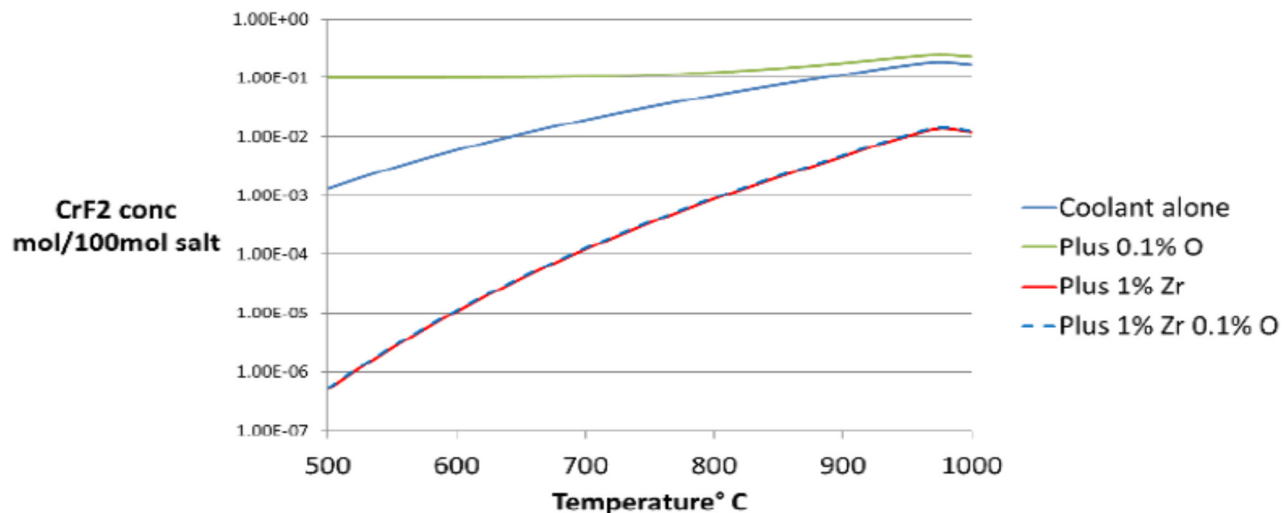


Figure 4-6. Chromium concentration in the coolant salt with and without 2%  $\text{ZrF}_2$  redox stabilization. Higher Cr concentration means higher corrosion rate [34].

## 4.5 Key Findings and Future Research and Development Needs

Current materials corrosion data in chloride salts are very limited and inconsistent.

The redox potential control methodology—for example by controlling  $\text{UCl}_4/\text{UCl}_3$  ratio or by adding Zr metal (for chloride fuel salt systems needs to be identified for specific reactor salt systems), and which is the best salt option—slightly reducing by controlling  $\text{UCl}_4/\text{UCl}_3$  ratio or reducing as the salt in Moltex salt system by adding Zr (for controlling the corrosion in chloride salt system should be identified in the context of reactor operation conditions). The following needs should be considered for research and development.

- Purification of the chloride salts need to be studied to make high quality, impurity free chloride salts.
- The materials for some chloride salt systems has yet to be identified.
- It is unknown whether the materials will be susceptible to stress corrosion cracking in chloride salt system, and this should be investigated and demonstrated for reliable long term reactor operation.
- Irradiation effects of materials on the mechanical properties and corrosion performance in aggressive salt reactor operating conditions need to be studied.

## **5. LITERATURE REVIEW ON THERMO-PHYSICAL PROPERTIES AND PHASE DIAGRAM OF MOLTEN SALTS FOR MSR APPLICATIONS**

*Ruchi Gakhar*

### **5.1 Introduction**

With a renewed interest in MSR technologies, comprehensive knowledge of the fuel salt and coolant salt properties (with uncertainties) is crucial for better assessment of reactor designs and technologies. For example, properties of water as a heat transfer fluid are well-known and extensive literature on steam tables is available. A similar knowledge database for molten salts is needed to define technical readiness level of various design concepts. Hence, it is essential to summarize the properties of proposed fuel and coolant salts known to date, to present a comprehensive picture of research on the systems. The data are summarized here with the aim of giving researchers a path forward with the property estimation of a particular salt system, using experimental or computational techniques.

This chapter is a consolidation of the thermo-physical properties and respective correlations for various salt systems proposed and/or considered over the years for MSR concepts. The salt systems are divided into two subclasses: (1) fuel salts (fuel and heat transfer fluids) and (2) coolant salts (heat transfer fluids only). For each system various properties such as density, viscosity, surface tension, thermal conductivity, heat capacity, vapor pressure, have been summarized. Phase diagrams are included for most of the systems, however no general discussion of the principles of heterogeneous phase equilibrium has been included since excellent discussions are available in many well-known publications. Please refer to the cited works for detailed discussions. The two reports published in 2006 by D. F. Williams (ORNL) have more details on measurement of various coolant salt-mixtures [83, 84].

Thermal conductivity is most difficult fluid property to measure for molten salts, therefore considerable scatter can be observed in the reported values.

### **5.2 Fuel Salts**

The fuel salts have been categorized in terms of MSR development at ORNL in chronological order. For each design the fuel, blanket, and coolant salts are mentioned and their properties are reported from literature. In a few cases, data for exact salt compositions were not available. Therefore, the properties of the composition closest to it are considered.

#### **5.2.1 Fluoride Salts**

The following tables present the phase diagrams and thermo-physical properties for fluoride salt mixtures proposed for various nuclear reactor designs proposed by ORNL over the period 1949–1980.

### Aircraft Nuclear Propulsion Program (1949–1961)

Table 5-1. Aircraft Reactor Experiment, 2.5 MWt operated.

<b>Fuel salt:</b>	NaF-ZrF <sub>4</sub> -UF <sub>4</sub> (53.09-40.73-6.18 mol%) NaF-ZrF <sub>4</sub> -UF <sub>4</sub> (53.5-40.0-6.5 mol%) – closest composition			
<b>Melting point:</b>	813 K			
<b>Heat of fusion:</b>	63 cal/g			
<b>Enthalpy (H<sub>t</sub>–H<sub>0</sub> °C):</b>	34.5+0.235T cal/g			
<b>Electrical conductivity (Ohm-cm)<sup>-1</sup>:</b>	0.66 (at 866 K), 0.97 (at 977 K), 1.27 (at 1088 K)			
<b>Volume expansion:</b>	3.36 (1/°C × 10 <sup>4</sup> )			
<b>Prandtl number:</b>	2.7 (at 977 K)			
<b>Phase diagram:</b>	The three-component fuel system (shown in Figure 5-1) has been discussed in detail by Grimes and Cuneo [85].			
	Density (g/cm <sup>3</sup> )	Heat capacity (cal/g°C)	Viscosity (cP)	Thermal conductivity (BTU/hr ft °F)
<b>Value</b>	4.19 (at RT)	0.19 (at 573 K)	5.7 (at 973 K)*	1.2(liquid)
<b>Correlation</b>	4.04–0.0011×T	0.3969–16.1×10 <sup>-5</sup> T	0.194 exp(3302/T, K)	–
<b>Error (if applicable)</b>	±5%	±10%	±10%	±25%
<b>Temperature range for correlation</b>	813–1273 K	–	–	–
References:[86, 87]				
*Data also available for 873 K, 1073 K, and 1123 K.				

Table 5-2. Aircraft Reactor Test, 60 MWt proposed.

<b>Fuel salt:</b>	NaF-ZrF <sub>4</sub> -UF <sub>4</sub> (50-46-4 mol%)			
<b>Melting point:</b>	793 K			
<b>Heat of fusion:</b>	57 cal/g			
<b>Enthalpy (H<sub>t</sub>-H<sub>o</sub> °C):</b>	2.1+0.3178T-4.28 × 10 <sup>-5</sup> T <sup>2</sup> cal/g			
<b>Electrical conductivity (Ohm-cm)<sup>-1</sup>:</b>	0.87 (at 866 K), 1.16 (at 977 K), 1.45 (at 1088 K) Electrical conductivity correlation, k <sub>e</sub> = -0.68+2.62×10 <sup>-3</sup> T, 550°C≤T≤850°C (Ohm-cm) <sup>-1</sup>			
<b>Volume expansion:</b>	2.84 (1/°C × 10 <sup>4</sup> )			
<b>Prandtl number:</b>	2.5 (at 977 K)			
<b>Surface tension:</b>	132 (at 903 K), 157 (at 803 K), 115 (at 1003 K) dynes/cm			
<b>Phase diagram:</b>	The three-component fuel system (shown in Figure 5-2) has been discussed in detail by Grimes and Cuneo [85].			
	Density (g/cm <sup>3</sup> )	Heat capacity (cal/g°C)	Viscosity (cP)	Thermal conductivity (BTU/hr ft °F)
<b>Value</b>	4.09 (at RT)	0.278 (at 973 K)	5.4 (at 973 K)*	1.3 (liquid)
<b>Correlation</b>	3.93-0.00093×T	0.3178- 8.56×10 <sup>-5</sup> T	0.0981 exp(3895/T, K)	—
<b>Error (if applicable)</b>	±5%	±10%	±10%	±25%
<b>Temperature range for correlation</b>	793-1273 K	—	—	—
References: [86, 87]				
*Data also available for 873 K, 1073 K, and 1123 K.				

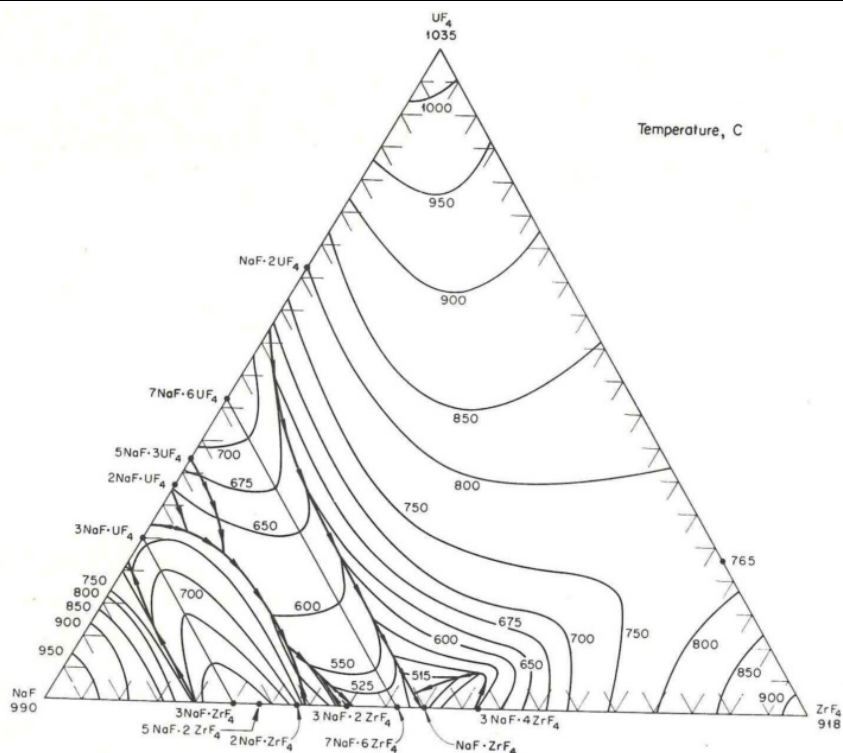


Figure 5-1. NaF-ZrF<sub>4</sub>-UF<sub>4</sub> system.

## Two-Fluid Molten Salt Breeder Reactor (1961–1970)

Table 5-3. MSBR 1,000 MWe design for fuel salt.

<b>Fuel salt:</b>	Carrier salt for the fissile isotope U-233 with the nominal composition LiF-BeF <sub>2</sub> -UF <sub>4</sub> (68.5-31.3-0.2, mol%)			
<b>Melting point:</b>	723 K			
<b>Vapor pressure:</b>	< 0.1 mm Hg (at 894K)			
<b>Phase diagram:</b>	Phase diagram for the fuel salt part of the two ternary systems is shown in Figure 5-3 [88].			
	Density (g/cm <sup>3</sup> )	Specific Heat (BTU/lb-°F)	Viscosity (cP)	Thermal conductivity (BTU/hr ft °F)
Value	2.034	0.55	11.161	0.8
Correlation	—	—	—	—
Error (if applicable)	0.096	0.14	1.24	—
Reference: [88]				

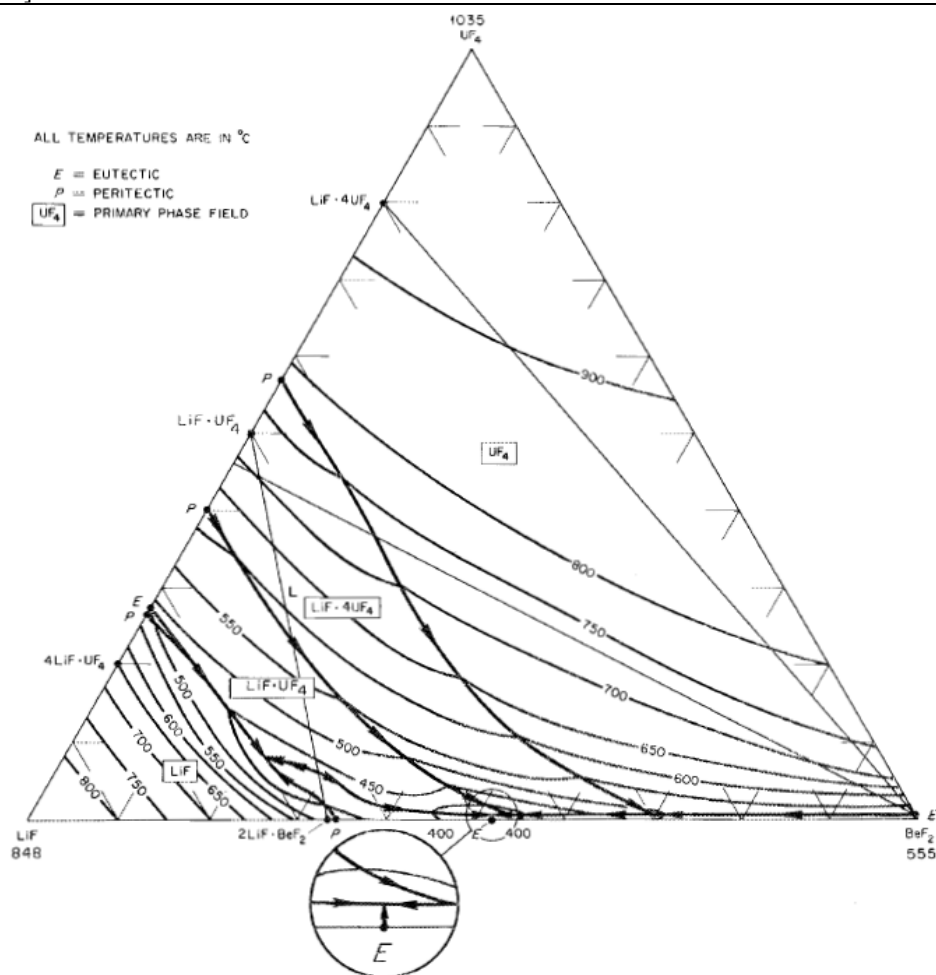


Figure 5-2. Two-fluid MSBR fuel salt – LiF-BeF<sub>2</sub>-UF<sub>4</sub> system.



Table 5-4. MSBR 1,000 MWe design for blanket salt.

<b>Blanket salt:</b>	Carrier salt for the fertile isotope Th-232 with the nominal composition LiF-BeF <sub>2</sub> -ThF <sub>4</sub> (71-27-2, mol%)			
<b>Melting point:</b>	833 K			
<b>Vapor pressure:</b>	< 0.1 mm Hg (at 894K)			
<b>Phase diagram:</b>	Phase diagram for the blanket salt part of the two ternary systems is shown in Figure 5-3 [88].			
	Density (g/cm <sup>3</sup> )	Specific Heat (BTU/lb-°F)	Viscosity (cP)	Thermal conductivity (BTU/hr ft °F)
Value	4.437	0.22	15.708	0.6
Correlation	—	—	—	—
Error (if applicable)	0.224	0.06	7.854	—
Reference: [88]				

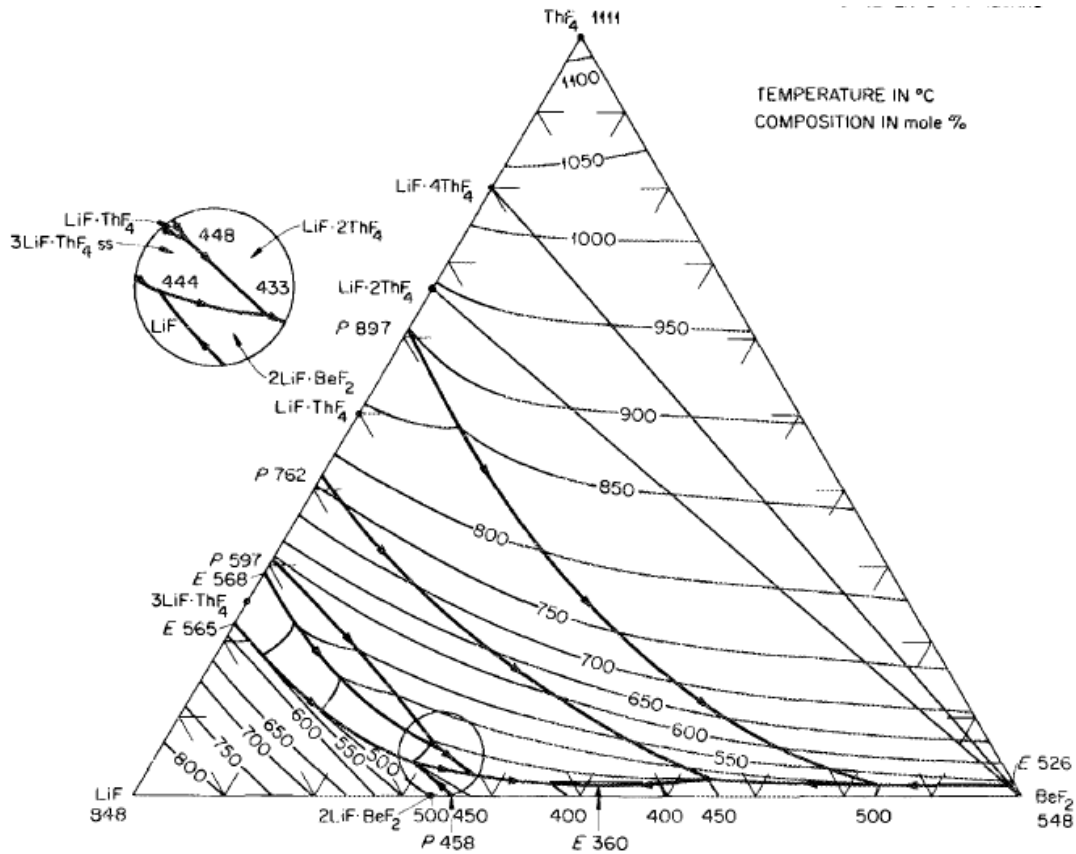


Figure 5-3. Two-fluid MSBR blanket salt – LiF-BeF<sub>2</sub>-ThF<sub>4</sub> system.

## Molten Salt Reactor Experiment (1960–1975)

Table 5-5. MSRE 8 MWt operated.

<b>Fuel salt:</b>	LiF-BeF <sub>2</sub> -UF <sub>4</sub> -ZrF <sub>4</sub> (65-29.2-0.8-5 mol%)			
<b>Vapor pressure:</b>	$\log P$ (torrs) = $8.0-10^4/T(K)$ , precision factor 50 from 500–700°C			
<b>Prandtl number:</b>	13 (at 973 K)			
<b>Surface Tension:</b>	$260-0.12T$ (°C) dynes/cm, +30%, -10%			
<b>Phase diagram:</b>	Recently, van der Meer et al. [89] assessed the thermodynamic properties of the LiF-BeF <sub>2</sub> -ThF <sub>4</sub> -UF <sub>4</sub> system based on the quasi-chemical model applied to the binary and ternary liquid phases. The combined resultant boundaries of the quaternary system is shown in Figure 5-4.			
	Density (g/cm <sup>3</sup> )	Heat capacity (cal/g°C)	Viscosity (cP)	Thermal conductivity (W/cm-°C)
Value	2.2409 (at 923 K)	0.57 (liquid)	—	0.010
Correlation	$2.575-0.000513 \times T$	$0.31-3.61 \times 10^{-4} T$ (solid)	$0.116 \exp(3755/T, K)$	—
Error (if applicable)	±1%	±3%	±7%	±10%
Temperature range for correlation	793–1273 K	—	—	—
References: [86, 87]				
*Data also available for 873 K, 1073 K, and 1123 K.				

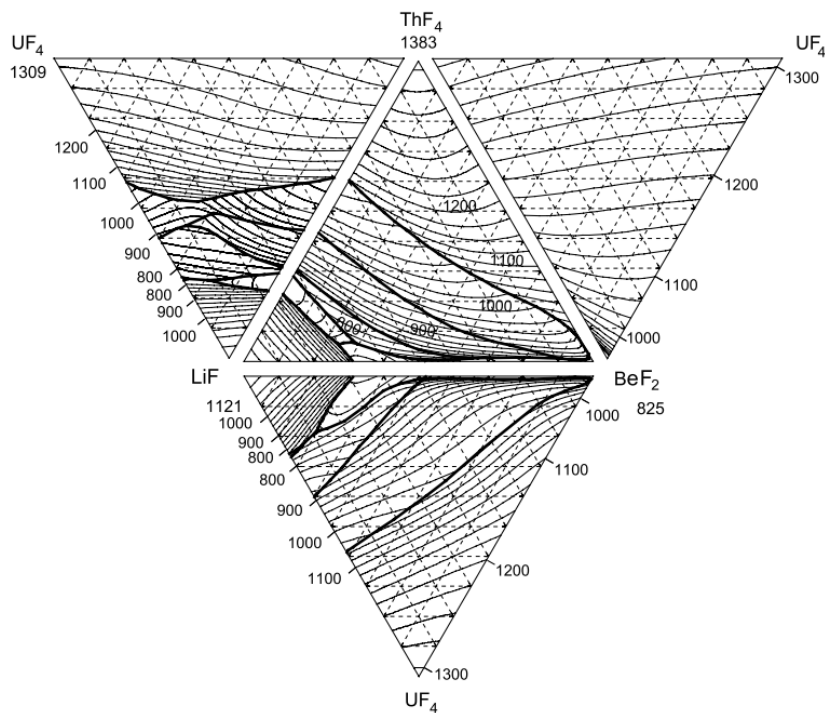


Figure 5-4. Calculated liquid surface of LiF-BeF<sub>2</sub>-ThF<sub>4</sub>, LiF-BeF<sub>2</sub>-UF<sub>4</sub>, LiF-ThF<sub>4</sub>-UF<sub>4</sub> and BeF<sub>2</sub>-ThF<sub>4</sub>-UF<sub>4</sub>, combined to a quaternary system. Melting temperatures are labeled in K and isotherms with an interval of 25 K are shown [89].

## Molten Salt Converter Reactor (1961–1965)

Table 5-6. 1,000 MWe design.

<b>Fuel salt:</b>	LiF-BeF <sub>2</sub> -ThF <sub>4</sub> -UF <sub>4</sub> (68-22-9-1 mol%) LiF-BeF <sub>2</sub> -ThF <sub>4</sub> (68-23-9 mol%)*			
<b>Melting point:</b>	748 K			
<b>Salt properties:</b>	922 K			
<b>Phase diagram:</b>	A diagram of the LiF-BeF <sub>4</sub> -ThF <sub>4</sub> ternary system, based solely on thermal data, is shown in Figure 5-5 [85].			
	Density (lb/ft <sup>3</sup> )	Specific heat (BTU lb <sup>-1</sup> °F <sup>-1</sup> )	Viscosity (lb hr <sup>-1</sup> ft <sup>-1</sup> )	Thermal conductivity (BTU hr <sup>-1</sup> ft <sup>-1</sup> °F <sup>-1</sup> )
Value	—	0.32 (at 922 K)	—	0.75 (at 922 K)
Correlation	236.3–0.0233×T (°F)	—	0.2637 exp (7362/459.7+T, °F)	—
Error (if applicable)	—	—	—	—
Reference:[90]				
*Similar data for compositions LiF-BeF <sub>2</sub> -ThF <sub>4</sub> (71-16-13 mol%) and LiF-BeF <sub>2</sub> -ThF <sub>4</sub> (66-29-5 mol%) has been provided in [90].				

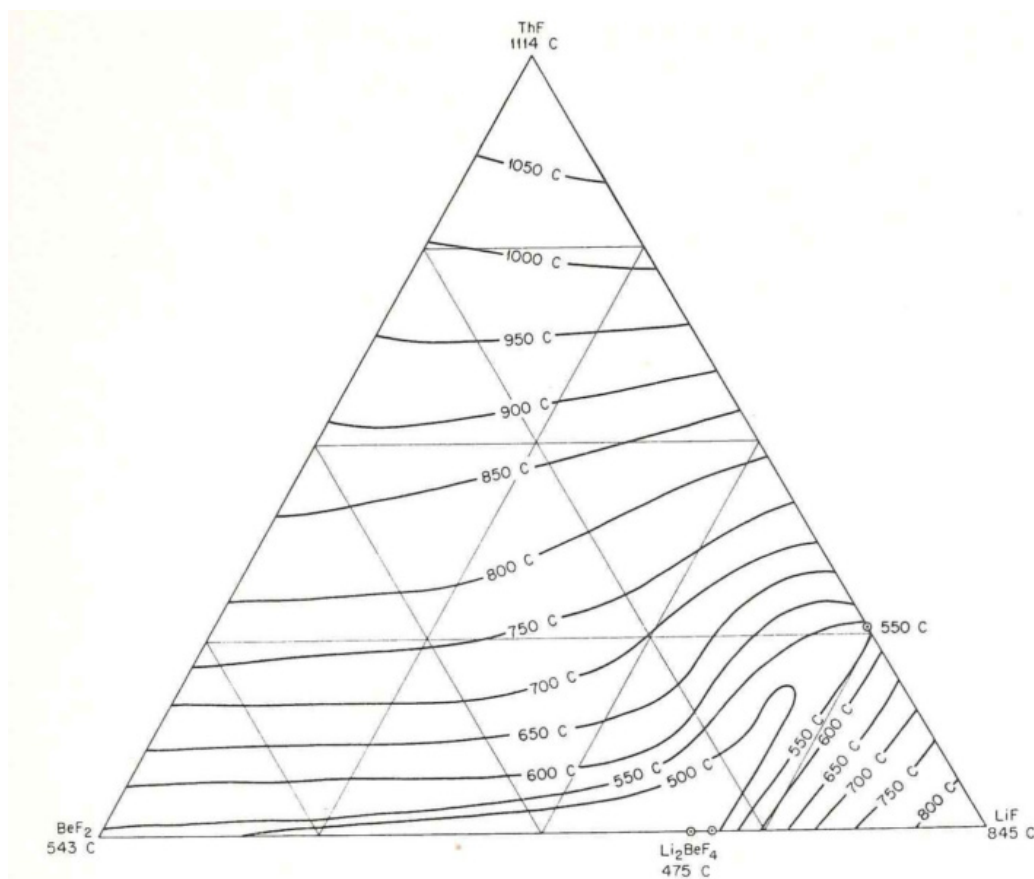


Figure 5-5. LiF-BeF<sub>2</sub>-ThF<sub>4</sub> system.

### ***Molten Salt Breeder Experiment (1969–1970)***

Table 5-7. 150 MWt proposed.

<b>Fuel salt:</b> LiF-BeF <sub>2</sub> -ThF <sub>4</sub> -UF <sub>4</sub> (71.5-16-12-0.5 mol%)				
<b>Phase diagram:</b> See Figure 5-4.				
	Density (lb/ft <sup>3</sup> )	Heat capacity (BTU lb <sup>-1</sup> °F <sup>-1</sup> )	Viscosity (lb hr <sup>-1</sup> ft <sup>-1</sup> )	Thermal conductivity (BTU hr <sup>-1</sup> ft <sup>-1</sup> °F <sup>-1</sup> )
Value	–	0.32	–	0.75
Correlation	236.3– 0.0233×T	–	0.2637 exp(7362/459.7+T, °F)	–
Error (if applicable)	–	–	–	–
<b>Coolant salt:</b> KNO <sub>3</sub> -NaNO <sub>2</sub> -NaNO <sub>3</sub> (44-49-7 mol%)				
	Density (lb/ft <sup>3</sup> )	Specific heat (BTU lb <sup>-1</sup> °F <sup>-1</sup> )	Viscosity (lb hr <sup>-1</sup> ft <sup>-1</sup> )	Thermal conductivity (BTU hr <sup>-1</sup> ft <sup>-1</sup> °F <sup>-1</sup> )
Value	–	0.37	–	0.33
Correlation	130.6– 0.0254×T (°F)	–	0.1942 exp (3821.6/459.7+T, °F)	–
Error (if applicable)	–	–	–	–
Reference: [91]				

### ***Molten Salt Reactor Demonstration (1972)***

#### **350 MWe Proposed**

Fuel salt: LiF-BeF<sub>2</sub>-ThF<sub>4</sub>-UF<sub>4</sub> (71.5-16-12-0.5 mol%), which is the same as MSBE (see Table 5-7).

#### ***Single-Fluid Molten Salt Breeder Reactor (1969–1978)***

Table 5-8. 1,000 MWe design for fuel salt.

<b>Fuel salt:</b> LiF-BeF <sub>2</sub> -ThF <sub>4</sub> -UF <sub>4</sub> (71.7-16.0-12.0-0.3 mol%)				
<b>Melting point:</b> 772 K				
<b>Vapor pressure:</b> <0.1 mm Hg (at 894 K)				
<b>Vapor pressure correlation:</b> log P (mm Hg) = 9.024 – 5920/T (K)				
<b>Phase diagram:</b> See Figure 5-4 [89].				
	Density (g/cm <sup>3</sup> )	Specific heat (J/g·K)	Viscosity (cP)	Thermal conductivity (W/m·K)
Value (at 978 K)*	3.2839	1.357	7.1515	1.19
Correlation	3.752–0.000668×T	–	0.109 exp(4090/T, K)	–
Error (if applicable)	–	±4%	–	–
Reference: [92]				
*Data also available for 908 K and 839 K.				

Table 5-9. 1,000 MWe design for coolant salt.

<b>Coolant salt:</b>	NaBF <sub>4</sub> -NaF (92-8 mol%)			
<b>Melting point:</b>	658 K			
<b>Vapor pressure:</b>	252 mm Hg (at 894 K)			
<b>Vapor pressure correlation:</b>	$\log P \text{ (mm Hg)} = 9.024 - 5920/T \text{ (K)}$			
	Density (g/cm <sup>3</sup> )	Heat capacity (J/g-K)	Viscosity (cP)	Thermal conductivity (W/m-K)
Value (at 894 K)*	1.811	1.507	1.075	0.398
Correlation	$2.252 - 0.000711 \times T$	—	$0.0877 \exp(2240/T, \text{K})$	—
Error (if applicable)	—	±2%	—	—
Reference: [92]				
*Data also available for 811 K and 727 K.				

### Denatured Molten Salt Reactor (1977–1980)

#### 1,000 MWe Design

Fuel salt composition (initial): Similar to single-fluid MSBR (See Table 5-8).

#### 5.2.2 Chloride Salts

Experimental studies of chloride salt systems for use as reactor fuels have, apparently, been much less extensive than those with fluoride salt systems, presumably because of the much lower cross section of F<sup>-</sup> for thermal neutrons. However, since F<sup>-</sup> acts as a moderator for neutrons, Cl<sup>-</sup> must be preferred to F<sup>-</sup> for fast reactor cycles. The properties and phase diagram for molten chloride fast breeder reactor has been summarized below.

Table 5-10. Molten chloride fast breeder reactor (2,000 MWth).

<b>Fuel salt:</b>	PuCl <sub>3</sub> -NaCl (15-85 mol%)			
<b>Coolant/blanket salt:</b>	UCl <sub>3</sub> -NaCl (65-35 mol%) Note for depleted U-238: it also forms the fertile material along with the blanket.			
<b>Phase diagrams:</b>	A combined phase diagram for the two binary systems PuCl <sub>3</sub> -NaCl and UCl <sub>3</sub> -NaCl, is shown in Figure 5-6 [13].			
<b>Melting point:</b>	958 K			
<b>Boiling point:</b>	1973 K			
	Density (g/cm <sup>3</sup> )	Heat Capacity (kJ/kg – °C)	Viscosity (g/cm-s)	Thermal conductivity (BTU/hr ft °F)
Value (at 1257 K)	2.340	0.95	0.0217	0.8
Correlation	—	—	—	—
Error (if applicable)	—	—	—	—
Reference: [13]				

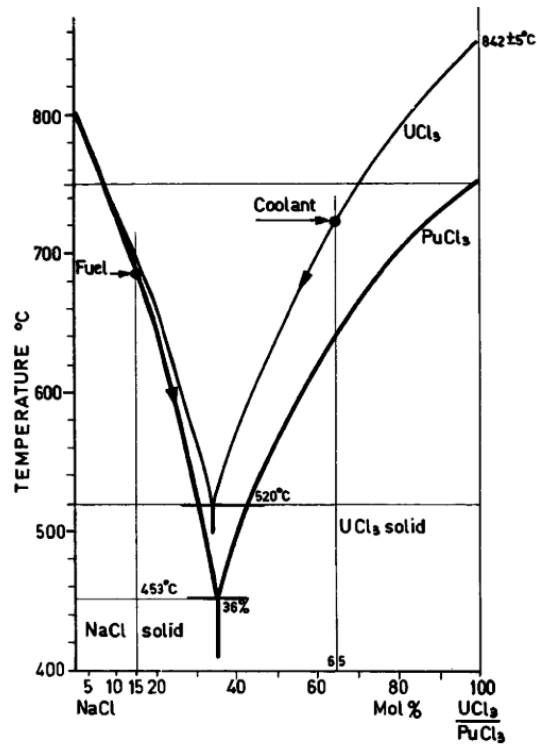


Figure 5-6. Phase diagram for  $\text{PuCl}_3\text{-NaCl}$  and  $\text{UCl}_3\text{-NaCl}$  systems.

Apart from this design, literature available on chloride fuel salts is scarce. Phase diagrams of few potential binary systems ( $\text{KCl-UCl}_4$ ,  $\text{LiCl-UCl}_4$ ,  $\text{NaCl-UCl}_4$ ,  $\text{KCl-UCl}_3$ ,  $\text{LiCl-UCl}_3$ ,  $\text{NaCl-UCl}_3$ ) of interest have been included in this section (Figures 5-7 through 5-12, [85]). Property correlations for density, electrical conductivity, and surface tension, for these salt-mixtures can be found in Janz [93]. However, the data provided covers a broad and varied composition range. Since it is unclear which composition might be applicable for reactor design, the data were included in this report.

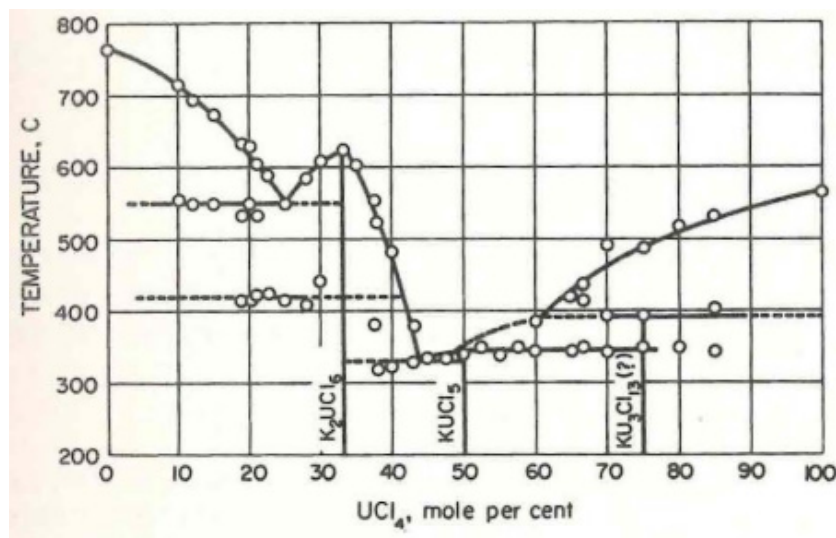


Figure 5-7. Phase diagram for  $\text{KCl-UCl}_4$  system.

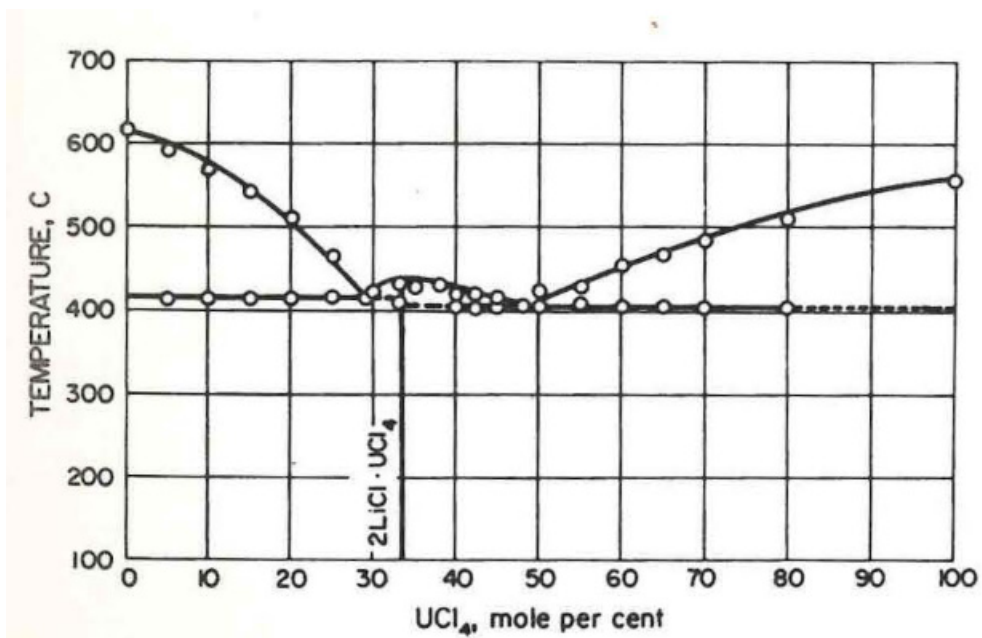


Figure 5-8. Phase diagram for LiCl-UCl<sub>4</sub> system.

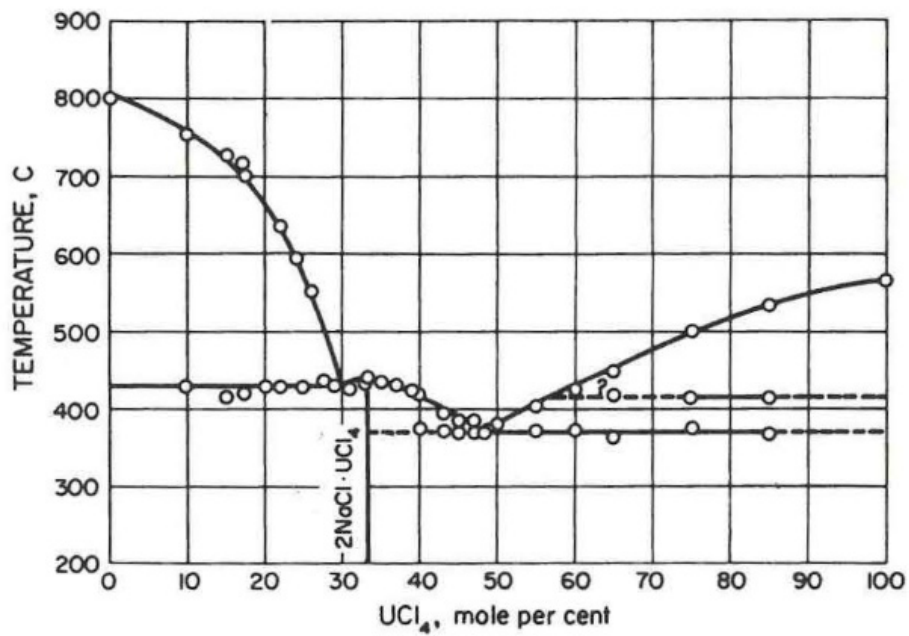


Figure 5-9. Phase diagram for NaCl-UCl<sub>4</sub> system.

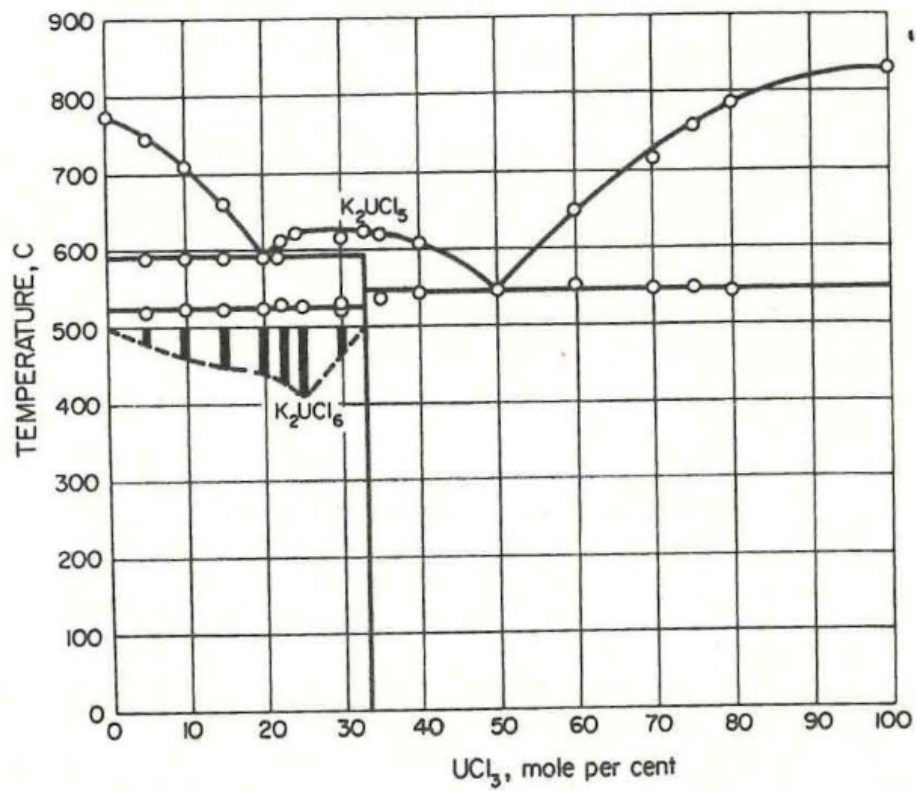


Figure 5-10. Phase diagram for KCl-UCl<sub>3</sub> system.

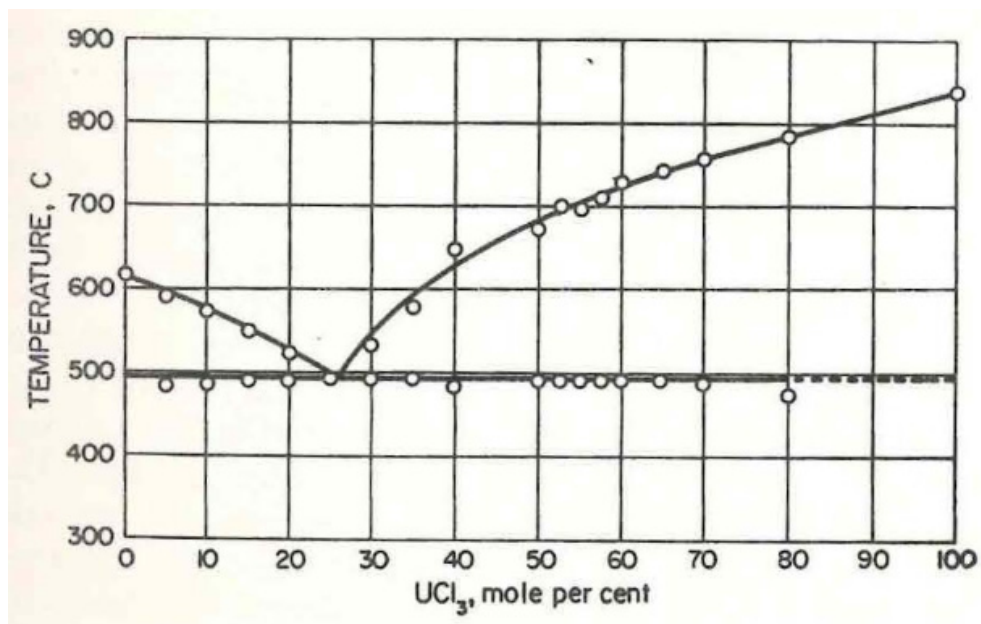


Figure 5-11. Phase diagram for LiCl-UCl<sub>3</sub> system.



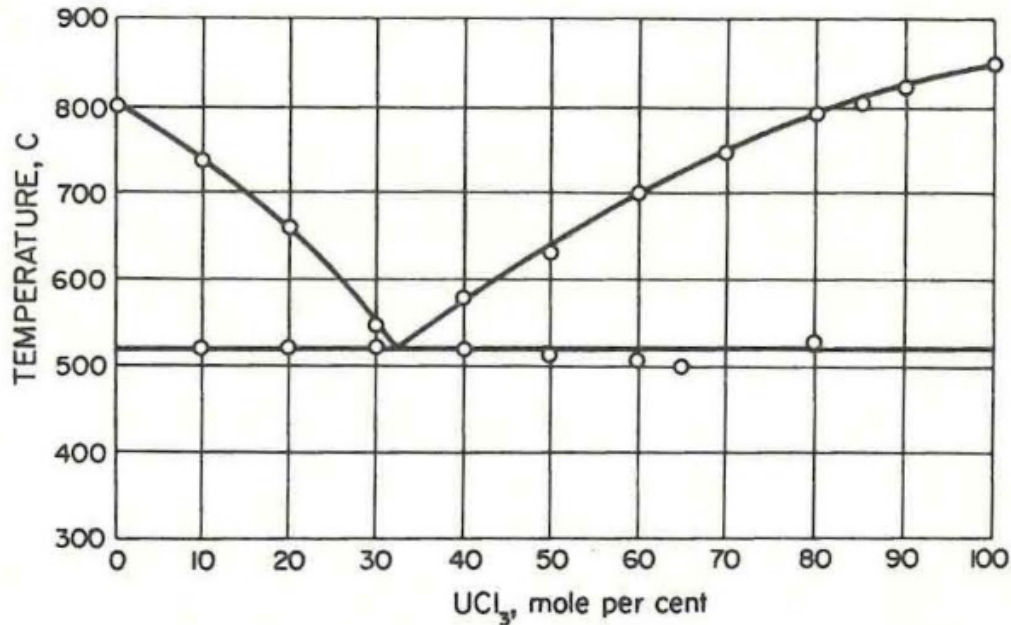


Figure 5-12. Phase diagram for NaCl-UCl<sub>3</sub> system.

### 5.3 Coolant Salts

Several salt-mixtures (binary and ternary) have been identified in literature for application as coolant salts for MSR, AHTR, and other advanced reactor designs [83, 84, 94]. For the sake of simplicity, these salt-mixtures have been categorized into following subclasses (1-5). Among these systems, FLiBe and FLiNaK have been investigated in more detail and therefore data available for the two mixtures is more prolific.

1. Alkali fluorides: LiF-KF (50-50 mol%), LiF-RbF (44-56 mol%), LiF-NaF-KF (46.5-11.5-42 mol%), LiF-NaF-RbF (42-6-52 mol%)
2. ZrF<sub>4</sub> containing salts: LiF-ZrF<sub>4</sub> (51-49 mol%), NaF-ZrF<sub>4</sub> (59.5-40.5 mol%), LiF-NaF-ZrF<sub>4</sub> (26-37-37 mol%), RbF-ZrF<sub>4</sub> (58-42 mol% and 52-48 mol%), KF-ZrF<sub>4</sub> (58-42 mol%)
3. BeF<sub>2</sub> containing salts: LiF-BeF<sub>2</sub> (66-34 mol%), NaF-BeF<sub>2</sub> (57-43 mol%), LiF-NaF-BeF<sub>2</sub> (31-31-38 mol%)
4. Chloride salts: LiCl-KCl (59.5-40.5 mol%), LiCl-RbCl (58-42 mol%), NaCl-MgCl<sub>2</sub> (58-42 mol%), KCl-MgCl<sub>2</sub> (68-32 mol%)
5. Fluoroborate salts: NaF-NaBF<sub>4</sub> (8-92 mol%), KF-KBF<sub>4</sub> (25-75 mol%), RbF-RbBF<sub>4</sub> (31-69 mol%)

### 5.3.1 Alkali Fluorides

#### *LiF-KF System*

Table 5-11. LiF-KF (50-50 mol%).

<b>Melting point:</b>	765 K			
<b>Heat of fusion:</b>	93 cal/g			
<b>Volume expansivity, <math>\beta</math>:</b>	3.40E-04 (1/°C)			
<b>Enthalpy:</b>	$-23.8+0.5839T-10.28 \times 10^{-5}T^2$ cal/g (T: 805-1166 K)			
<b>Surface tension:</b>	$\gamma = 253.29-0.08601 \times T$ , T range: 1073-1173K [93]			
<b>Phase diagram:</b>	See Figure 5-13 [83].			
	Density (g/cm <sup>3</sup> )	Heat capacity (cal/g°C)	Viscosity (cP)	Thermal conductivity (BTU/hr ft °F)
Value	2.43 (at RT)	0.440 (at 973 K)	2.9 (at 973 K)	—
Correlation	$2.46-0.00068 \times T$	$0.5839-20.56 \times 10^{-5}T$	—	—
Error (if applicable)	±5%	±10%	±20%	—
Temperature range for correlation	765–1273 K	805-1166 K	—	—
References: [86, 87]				

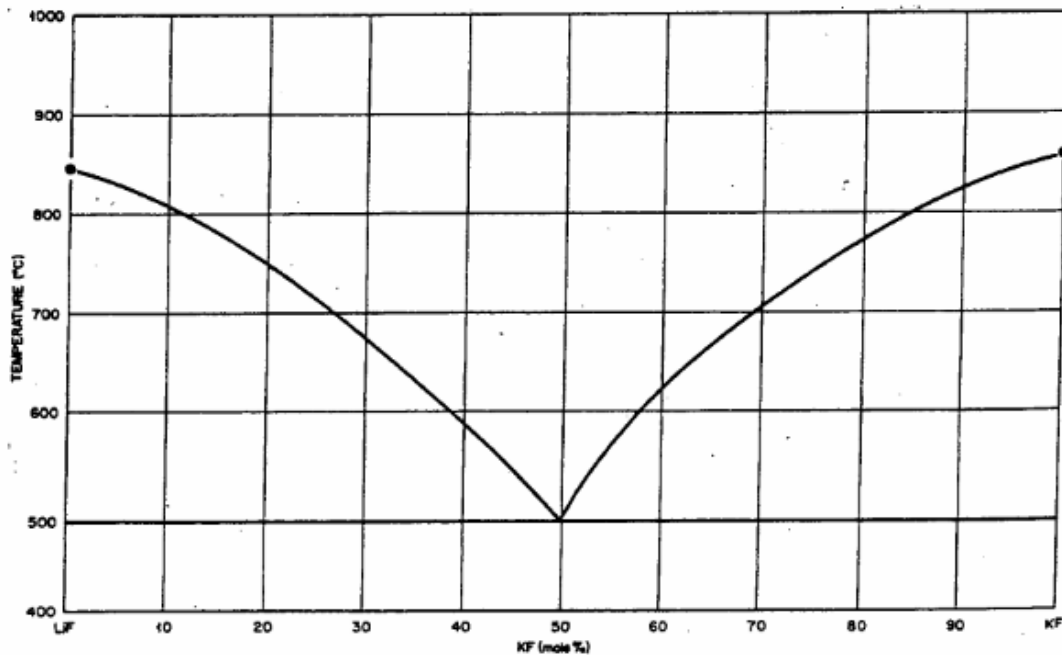


Figure 5-13. LiF-KF phase diagram.

## LiF-RbF System

Table 5-12. LiF-RbF (43-57 mol%).

<b>Melting point:</b>	748K			
<b>Heat of fusion:</b>	55 cal/g			
<b>Volume expansivity, <math>\beta</math> (at 973K):</b>	$3.65\text{E-}04$ (1/°C)			
<b>Enthalpy:</b>	$-22.9+0.3969T-8.1 \times 10^{-5}T^2$ cal/g (T: 770-1151 K)			
<b>Prandtl number (at 866 K):</b>	$2.9 C_p^* \mu/k$			
<b>Phase diagram:</b>	See Figure 5-14 [83].			
	Density (g/cm <sup>3</sup> )	Heat capacity (cal/g°C)	Viscosity (cP)	Thermal conductivity (BTU/hr ft °F)
Value	3.27 (at RT)	0.284 (at 973 K)	3.4 (at 923 K)	1.2 (liquid)
Correlation	$3.30-0.00096 \times T$	$0.3969-16.1 \times 10^{-5}T$	$0.0212 \exp(4678/T, K)$	—
Error (if applicable)	±5%	±10%	±10%	±25%
Temperature range for correlation	748–1273 K	770–1151 K	—	—
References: [86, 87]				

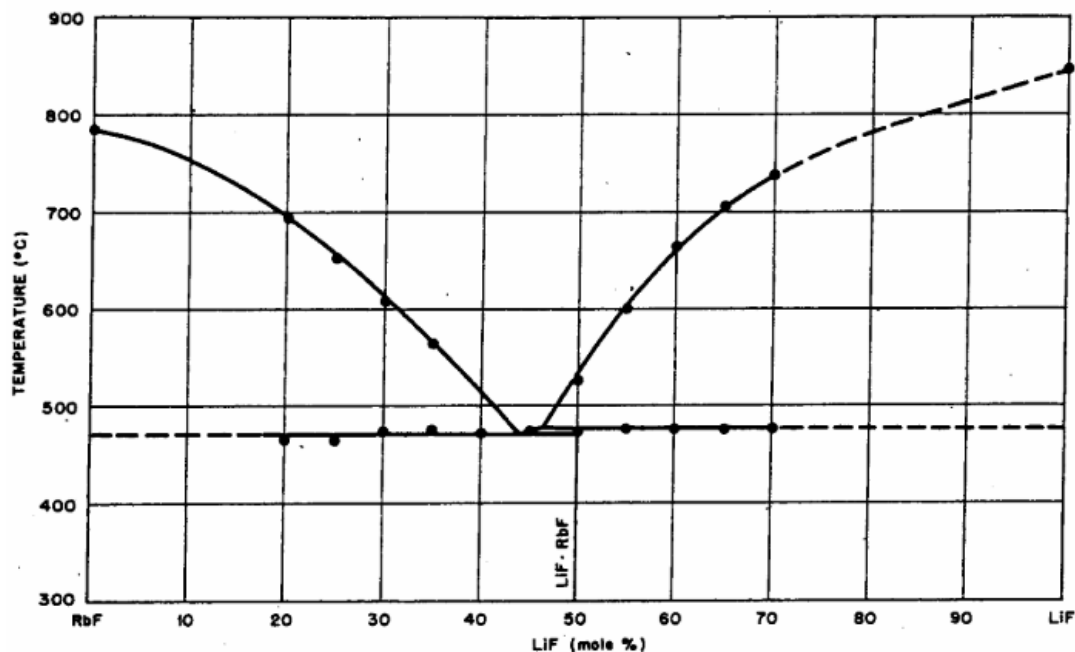


Figure 5-14. LiF-RbF system.

## LiF-NaF-KF System

Table 5-13. LiF-NaF-KF (46.5-11.5-42.0 mol%), FLiNaK.

Vapor Pressure: 0.7 mm Hg (at 1173 K) [84]

	Density (kg/m <sup>3</sup> )	Heat capacity (cal/cm <sup>3</sup> -°C)	Viscosity (Pa*s)	Thermal conductivity (W/m-K)
Value	2.02 (at 973 K)	0.91	0.0029	0.60 (measured value at 773 K)
Correlation	$2579.3-0.624\times T$	—	$2.487\times 10^{-5} \exp(4478.62/T)$	$0.36+5.6\times 10^{-4}T$
Error (if applicable)	±2%	-	±2%	±0.012
Temperature	940–1170 K	973 K	770–970 K	790–1080 K
References: [84, 95, 96]				

Phase diagram: See Figure 5-15 [97].

Melting point (°C)	References
454.0	[98, 99, 100]
454.3	[101]
464.2	[102]

### Density

Correlation	Error	Temperature range	References
$2729.29-0.73\times T$	±5%	940–1170 K	[103, 104]
$2579.3-0.624\times T$	±2%	940–1170 K	[95, 105, 106]
$2530-0.73\times T$ (additive molar volume method)	-	-	[83]
$2603-0.669\times T$	—	—	[107, 108]
$2655.64-0.68\times T$	—	—	[107]
$2485.8-0.69451\times T^*$	±2.7%	740.45–980.35 K	[109]

\*Composition: 41.98-11.77-46.23 mol% LiF-NaF-KF (±0.43%)

### Viscosity (Pa\*S)

Correlation	Error	Temperature range	References
$4.0\times 10^{-5} \exp(4170/T)$	±10%	773–1073 K	[86, 87, 109, 110]
$2.487\times 10^{-5} \exp(4478.62/T)$	±2%	773–1073 K	[93, 95, 109]

### Thermal conductivity (W/m\*K)

Correlation	Error	Temperature range	References
$0.43482 + 5.0 \times 10^{-4}T$	–	–	[109, 111, 112]
$0.36 + 5.6 \times 10^{-4}T$	$\pm 0.012$	790–1080 K	[96, 109]

### Specific heat capacity (cal/g-°C)

Correlation	Error	Temperature range	References
0.45	–	973 K	[84, 113]
$0.27 + 19.6 \times 10^{-5}T$ (K)	–	333–727 K	[87]
$0.2333 + 2.54 \times 10^{-4}T$ (K)	–	–	[84, 114]
0.33	10%	–	[87]

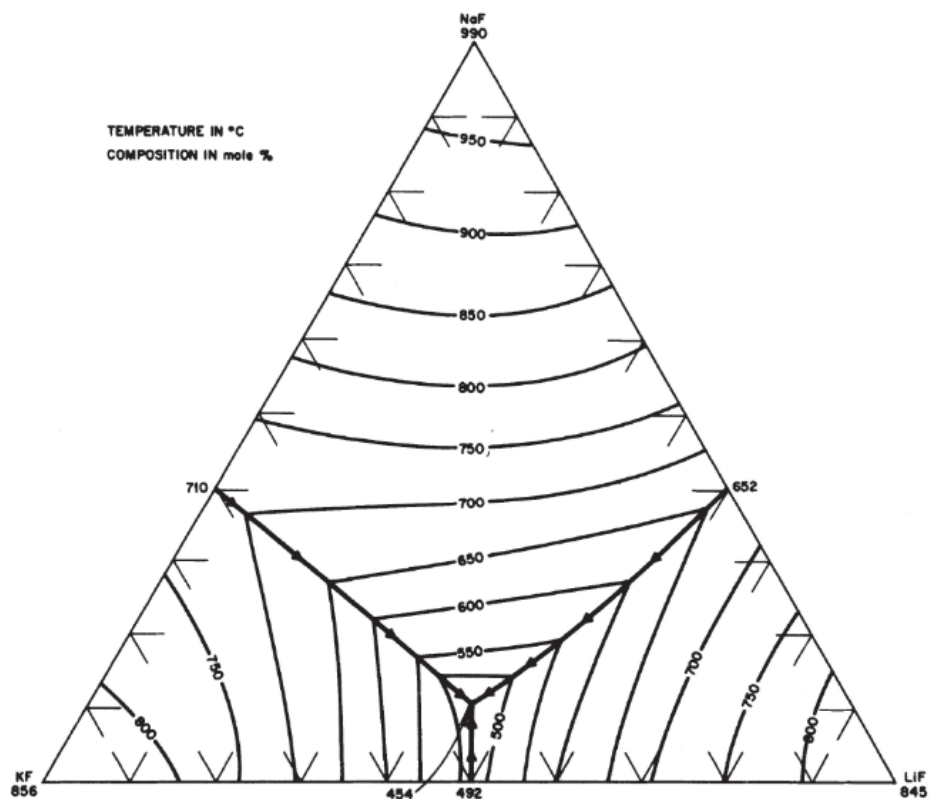


Figure 5-15. LiF-NaF-KF ternary system phase diagram

## LiF-NaF-RbF System

Table 5-14. LiF-NaF-RbF (42-6-52 mol%).

<b>Melting point:</b> 708 K <b>Vapor pressure (at 1173 K):</b> ~0.8mm Hg <b>Volume expansivity, <math>\beta</math> (at 973K):</b> 3.01E-04 (1/°C) <b>Prandtl number (at 973 K):</b> 4.413 $C_p^* \mu/k$				
	Density (g/cm <sup>3</sup> )	Heat capacity (cal/cm <sup>3</sup> -°C)	Viscosity (cP)	Thermal conductivity (W/m-K)
Value (at 973 K)	2.69	0.63	2.6	0.62
Correlation	3.261–0.000811×T (additive molar volume method)	—	—	—
Error (if applicable)	—	—	—	—
Reference: [84]				

## 5.3.2 ZrF<sub>4</sub> Containing Salts

### LiF-ZrF<sub>4</sub> System

Table 5-15. LiF- ZrF<sub>4</sub> (51-49 mol%).

<b>Melting point:</b> 782 K <b>Vapor pressure (at 1173 K):</b> 77 mm Hg <b>Volume expansivity, <math>\beta</math> (at 973K):</b> 2.99E-04 (1/°C) <b>Prandtl number (at 973 K):</b> >13.241 $C_p^* \mu/k$ <b>Phase diagram:</b> See Figure 5-16 [83].				
	Density (g/cm <sup>3</sup> )	Heat capacity (cal/cm <sup>3</sup> -°C)	Viscosity (cP)	Thermal conductivity (W/m-K)
Value (at 973 K)	3.09	0.90	> 5.1	0.48
Correlation	3.739–0.000924×T (additive molar volume method)	—	—	—
Error (if applicable)	—	—	—	—
Reference: [84]				

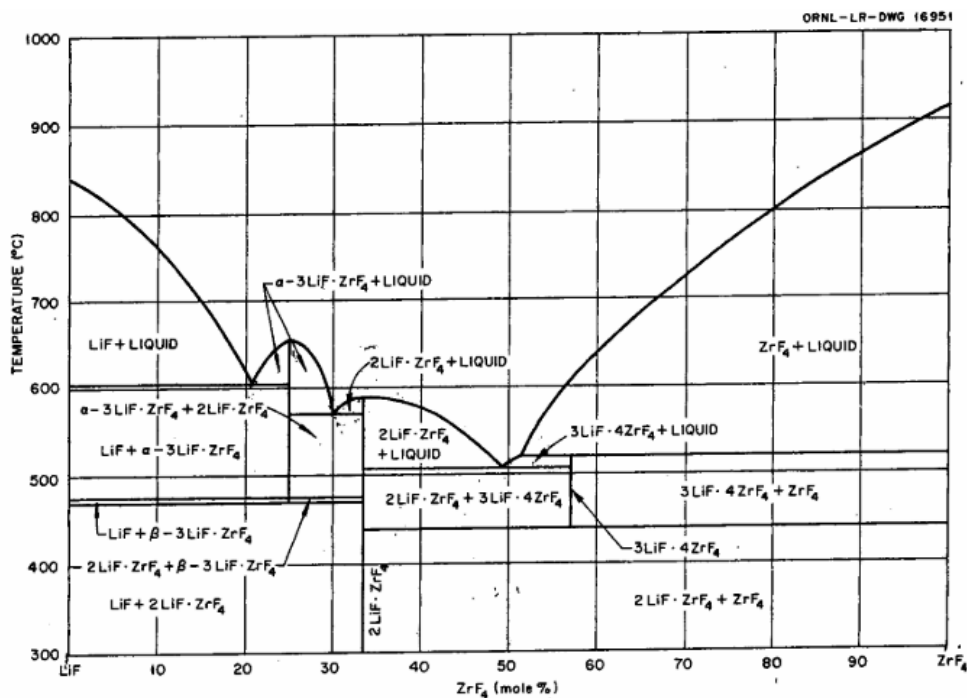


Figure 5-16. LiF-ZrF<sub>4</sub> system.

### NaF-ZrF<sub>4</sub> System

Table 5-16. NaF-ZrF<sub>4</sub> (59.5-40.5 mol%).

<b>Melting point:</b> 773 K				
<b>Vapor pressure (at 1173 K):</b> 5 mm Hg				
<b>Phase diagram:</b> See Figure 5-17 [84].				
	Density (g/cm <sup>3</sup> )	Heat capacity (cal/cm <sup>3</sup> ·°C)	Viscosity (cP)	Thermal conductivity (W/m·K)
Value (at 973 K)	3.14	0.88	5.1	0.36 (Rao-Turnball prediction)
Correlation	3.584-0.000889×T (additive molar volume method)	—	—	—
Error (if applicable)	—	—	—	—
References: [83, 84]				

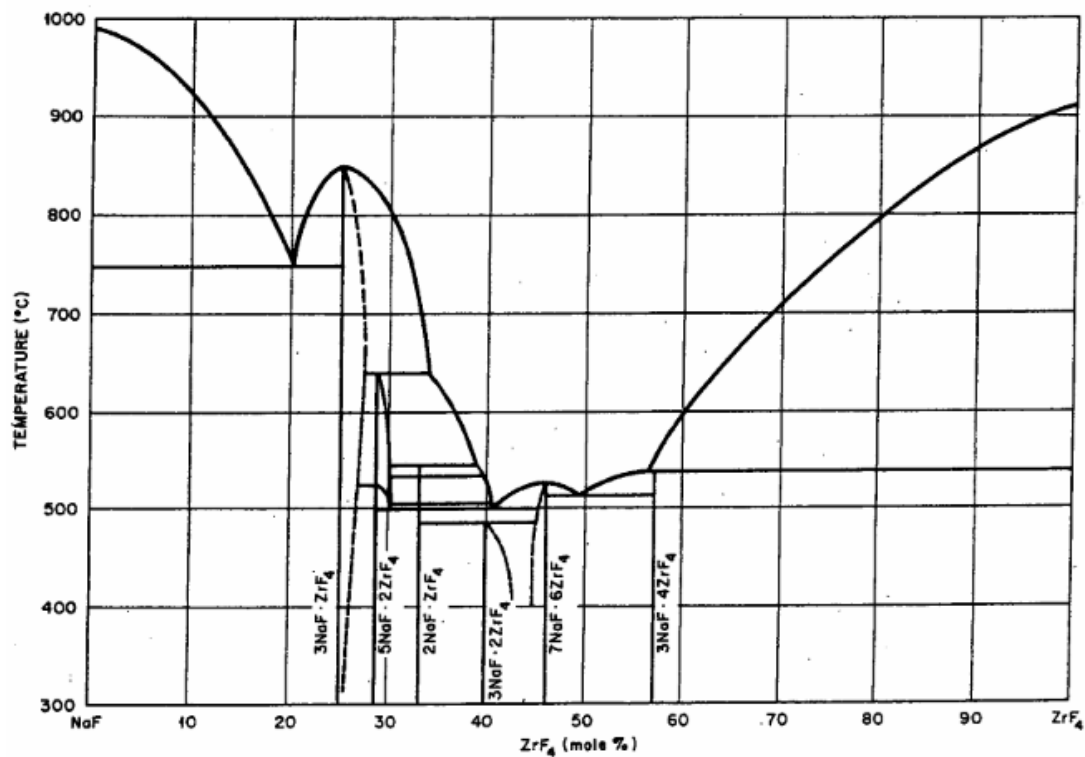


Figure 5-17. NaF-ZrF<sub>4</sub> system.

### LiF-NaF-ZrF<sub>4</sub> System

Table 5-17. LiF-NaF-ZrF<sub>4</sub> (26-37-37 mol%).

<b>Melting point:</b> 709 K				
<b>Vapor pressure (at 1173 K):</b> 5 mm Hg				
<b>Volume expansivity, <math>\beta</math> (at 973K):</b> 3.12E-04 (1/°C)				
<b>Prandtl number (at 973 K):</b> 19.073 $C_p \cdot \mu / k$				
<b>Phase diagram:</b> See Figure 5-18 [84].				
	Density (g/cm <sup>3</sup> )	Heat capacity (cal/cm <sup>3</sup> ·°C)	Viscosity (cP)	Thermal conductivity (W/m·K)
Value (at 973 K)	2.79*	0.84	6.9	0.53
Correlation (if any)	3.533-0.000870×T (additive molar volume method)	—	—	—
Error (if applicable)	—	—	—	—
References: [84]				
*2.92 g.cm <sup>3</sup> at 973 K [83]				



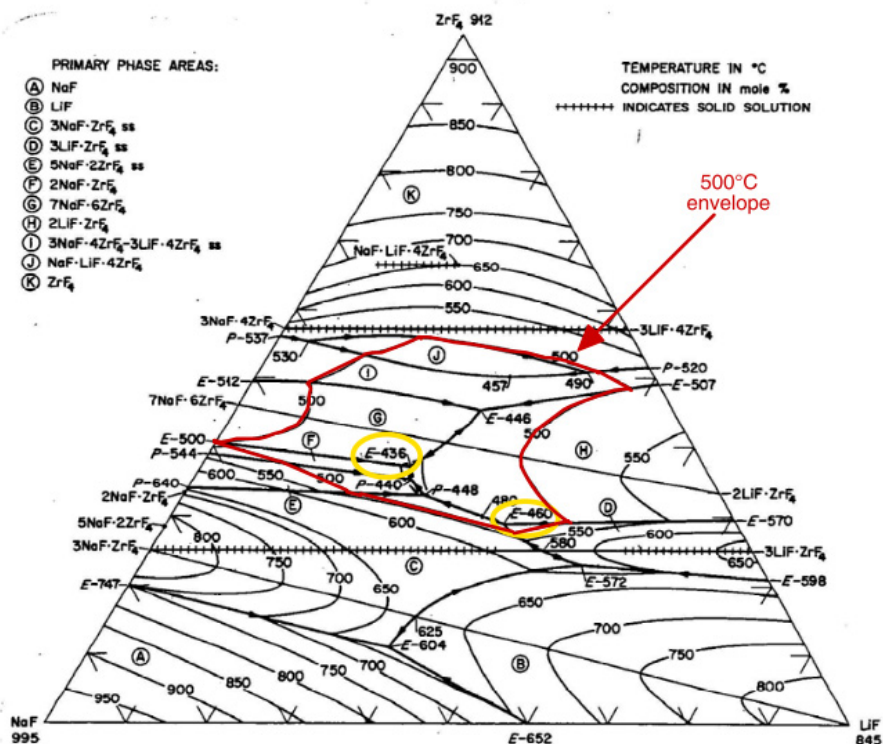


Figure 5-18. NaF-LiF-ZrF<sub>4</sub> system.

## RbF-ZrF<sub>4</sub> System

Table 5-18. RbF-ZrF<sub>4</sub> (58-42 mol%).

<b>Melting point:</b>		683 K		
<b>Vapor pressure (at 1173 K):</b>		1.3 mm Hg		
<b>Volume expansivity, <math>\beta</math> (at 973K):</b>		3.11E-04 (1/°C)		
<b>Prandtl number (at 973 K):</b>		10.948		
<b>Phase diagram:</b>		See Figure 5-19 [84].		
	Density (g/cm <sup>3</sup> )	Heat capacity (cal/cm <sup>3</sup> ·°C)	Viscosity (cP)	Thermal conductivity (W/m·K)
Value (at 973 K)	3.22	0.64	5.1	0.39
Correlation	3.923-0.00100×T (additive molar volume method)	—	—	—
Error (if applicable)	—	—	—	—
References: [83, 84, 87]				

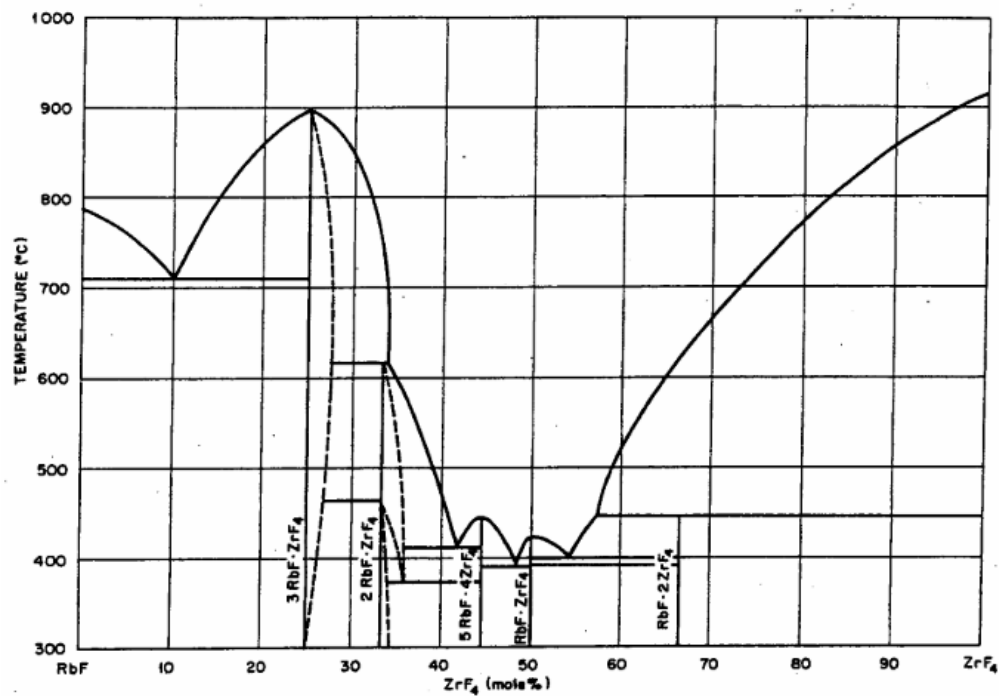


Figure 5-19. RbF-ZrF<sub>4</sub> system.

### KF-ZrF<sub>4</sub> System

Table 5-19. KF-ZrF<sub>4</sub> (58-42 mol%).

<b>Melting point:</b>		663 K [83, 98] 693.45 K (for 41.4 mol% ZrF <sub>4</sub> ) [115]		
<b>Vapor pressure (at 1173 K):</b>		1.2 mm Hg		
<b>Volume expansivity, <math>\beta</math> (at 973K):</b>		3.17E-04 (1/°C)		
<b>Prandtl number (at 973 K):</b>		<11.907		
<b>Phase diagram:</b>		See Figure 5-20 [84, 98].		
	Density (g/cm <sup>3</sup> )	Heat capacity (cal/cm <sup>3</sup> ·°C)	Viscosity (cP)	Thermal conductivity (W/m·K)
Value (at 973 K)	2.80	0.70	<5.1	0.45
Correlation	3.416-0.000887×T (additive molar volume method)	—	—	—
Error (if applicable)	—	±10%	—	—
References: [83]				

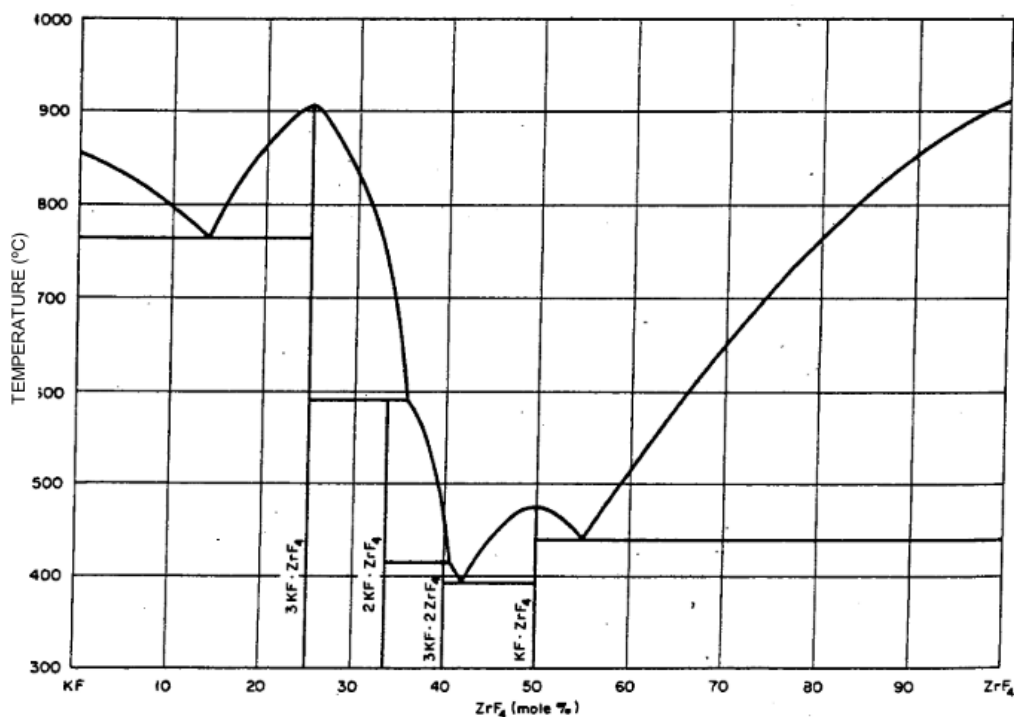


Figure 5-20. KF-ZrF<sub>4</sub> system.

### 5.3.3 BeF<sub>2</sub> Containing Salts

#### *LiF-BeF<sub>2</sub> System*

Table 5-20. LiF-BeF<sub>2</sub> (67-33 mol%), FLiBe.

	Vapor Pressure (mm Hg)	Density (g/cm <sup>3</sup> )	Volumetric heat capacity (cal/cm <sup>3</sup> -°C)	Viscosity (cP)	Thermal conductivity (W/m-K)	Surface tension (dynes/cm)
Value	1.2	1.94	1.12	5.6	1.0	250
Temperature	1173 K	973 K	973 K	973 K	973 K	731 K
References: [84, 100, 116]						

Phase diagram: See Figure 5-21 [84, 116].

There are several consolidated reports in the literature on the thermo-physical properties of FLiNaK and FLiBe [107, 117, 118]. LiF-BeF<sub>2</sub> in 2:1 ratio (67-33 mol%) is considered most suitable for nuclear applications (principally due to its more favorable properties).

Melting point (°C)	References
454	[98, 116]
456	[99]
458	[100]
459	[111]
460	[84]

For a broader range of compositions (47 to 67 mol% LiF), Gierszewski et al. reported the following equation [119]:

$$T = 1940x - 1260x^2 - 1$$

x: mol fraction of LiF

### Density

Density and surface tension are functions of the melt temperature. Compared to other properties, literature available on density (data and empirical correlations) for FLiBe is widespread, covering a broad range of compositions; for example, Blanke et al. measured the density for 0 to 55 mol% BeF<sub>2</sub> [120] and Cantor et al. investigated 50.2, 74.9 and 89.2 mol% BeF<sub>2</sub> [121]. Considering the scope of this work, only the composition applicable for reactor coolants - 33 mol% BeF<sub>2</sub> is considered here.

Several correlations proposed for the density of Flibe are included in the following table (for 67-33 mol% LiF-BeF<sub>2</sub>). Initial literature on density of Flibe and other fluoride salt-mixtures was published by ORNL [93, 99, 116, 122] and Zaghloul et al. [123].

Experimental data points (tabular and graphic) [99, 109, 121].

Correlation (kg/m <sup>3</sup> )	Error (%)	Temperature Range	References
2214-0.42×T	—	-	[116]
2280-0.488×T*	-	787.65-1093.45 K	[122]
2413-0.488×T	—	800-1080 K	[93, 99]
2330-0.42×T	±4	600-1200 K	[119]
2415.6-0.49072×T	—	732.2-4498.8 K	[123]
2241.6-0.42938×T**	±0.22	734.55-973.35 K	[109]

\*For 66-34 mol% composition

\*\*For 67.43-32.57 mol% composition (±1.50%)

### Viscosity (Pa\*s)

Williams et al. [2006] have given the following correlation for viscosity, which is applicable in the temperature range of 873-1073 K. Experimental data points (tabular and graphic) provided by Cantor et al. [124].

Correlation (cP), T in K	Error (%)	Temperature Range	References
0.116 exp (3755/T)*	±15-20%	873-1073 K	[84, 100, 107, 118]
0.118 exp (3624/T)	±10-20%	773-1073 K	[87, 107, 125]
0.116 exp (3760/T)*	—	600-1200 K	[107, 119]
0.059 exp (4605/T)**	4%	740-860 K	[93, 99, 107, 124]

\*For 66-34 mol% composition

\*\* For 64-36 mol% composition

### Thermal conductivity (W/m\*K)

Value	Error (%)	Temperature Range	References
1.0	±10%	—	[84, 100, 109, 118]

1.1	$\pm 10\%$	459-610 K	[109, 111, 118]
1.07	—	Liquid	[116]

**Specific heat capacity (J/kg\*K)**

Value	Error (%)	Temperature Range	References
2415.78	—	973 K	[84, 109]
2386	$\pm 3\%$	—	[100, 109]

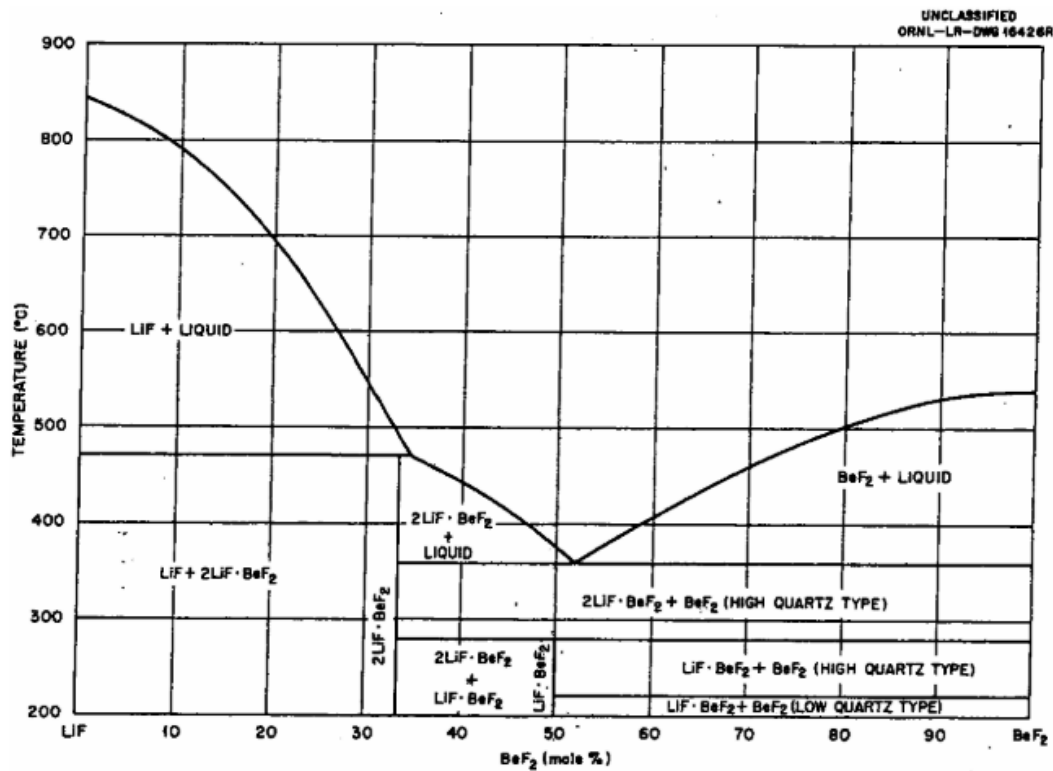


Figure 5-21. LiF-BeF<sub>2</sub> system.

## NaF-BeF<sub>2</sub> System

Table 5-21. NaF-BeF<sub>2</sub> (57-43 mol%).

<b>Melting point:</b>	613 K*			
<b>Vapor pressure (at 1173 K):</b>	1.4 mm Hg			
<b>Volume expansivity, <math>\beta</math> (at 973K):</b>	1.84E-04 (1/°C)			
<b>Prandtl number (at 973 K):</b>	17.513 C <sub>p</sub> *μ/k			
<b>Phase diagram:</b>	See Figure 5-22 [83].			
	Density (g/cm <sup>3</sup> )	Heat capacity (cal/g-°C)	Viscosity (cP)	Thermal conductivity (W/m-K)
Value (at 973 K)	2.01	0.52	7.0	0.87***
Correlation	2.2971-0.000507×T**	—	0.0346 exp(5164/T ,K)	—
Error (if applicable)	—	±10%	±10%	—
References: [84, 87]				
*633 K [87]				
**2.27-0.00037T (°C) g/cm <sup>3</sup> , T: 633-1273 K [87]				
***4.154 W/m-K (for liquid) [87], Error: ±25%				

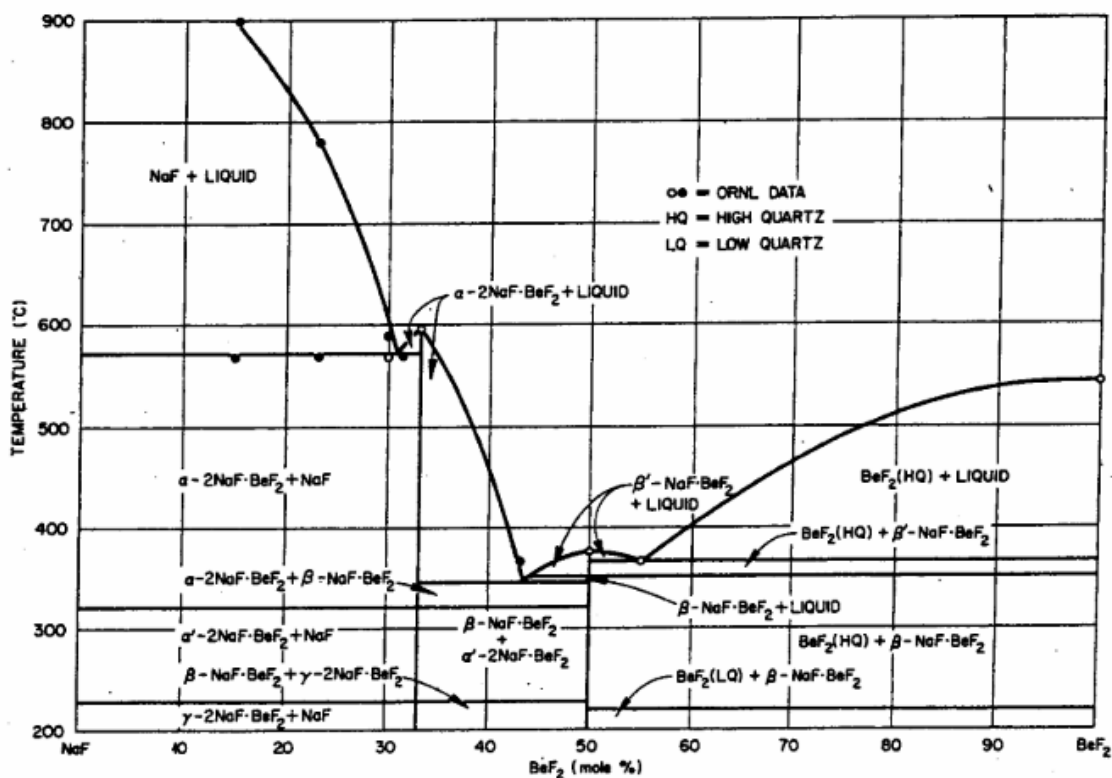


Figure 5-22. NaF-BeF<sub>2</sub> system.

## LiF-NaF-BeF<sub>2</sub> System

Table 5-22. LiF-NaF-BeF<sub>2</sub> (31-31-38 mol%).

<b>Melting point:</b>	588 K			
<b>Vapor Pressure (at 1173 K):</b>	1.7 mm Hg			
<b>Volume expansivity, <math>\beta</math> (at 973K):</b>	2.25E-04 (1/°C)			
<b>Prandtl number (at 973 K):</b>	10.551 $C_p \mu/k$			
<b>Phase diagram:</b>	See Figure 5-23 [97].			
	Density (g/cm <sup>3</sup> )	Heat capacity (cal/g-°C)	Viscosity (cP)	Thermal conductivity (W/m-K)
Value (at 973 K)	2.00	0.489	5.0	0.97
Correlation	2.313-0.000450×T (additive molar volume method)	—	—	—
Error (if applicable)	—	—	—	—
Reference: [84]				

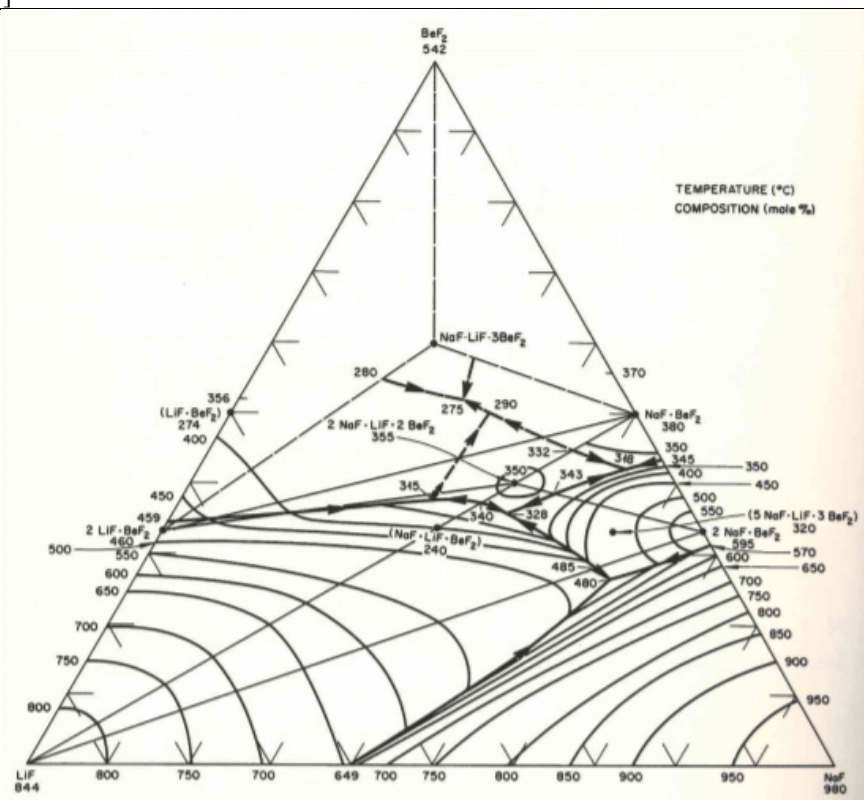


Figure 5-23. LiF-NaF-BeF<sub>2</sub> system.

### 5.3.4 Chloride Salts

#### *LiCl-KCl System*

Table 5-23. LiCl-KCl (59.5-40.5 mol%).

<b>Melting point:</b> 628 K				
<b>Vapor Pressure (at 1173 K):</b> 5.8 mm Hg				
<b>Volume expansivity, <math>\beta</math> (at 973K):</b> $g=189.4704-0.084525T$ , T range: 880–1020K [93]				
<b>Phase diagram:</b> See Figure 5-24 [83].				
	Density (g/cm <sup>3</sup> )	Heat capacity (cal/g-°C)	Viscosity (cP)	Thermal conductivity (W/m-K)
Value (at 973 K)	1.515	0.287	1.15	0.38 (measured value)
Correlation	$1.8772-0.00087 \times T^*$ (additive molar volume method)	—	—	—
Error (if applicable)	—	—	—	—
Reference: [83]				
*For 59–41 mol% composition.				



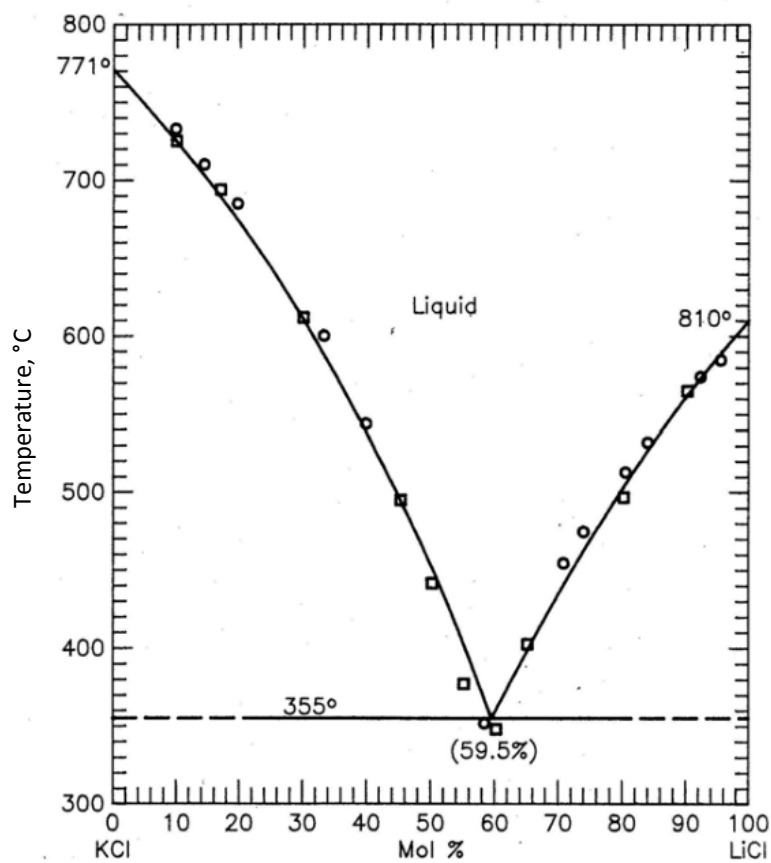


Figure 5-24. LiCl-KCl system.

### ***LiCl-RbCl System***

Table 5-24. LiCl-RbCl (58-42 mol%).

<b>Melting point:</b>		586 K		
<b>Phase diagram:</b>		See Figure 5-25 [83].		
	Density (g/cm <sup>3</sup> )	Heat capacity (cal/g-°C)	Viscosity (cP)	Thermal conductivity (W/m-K)
Value (at 973 K)	1.883	0.213	1.30	0.36
Correlation	2.7416-0.000689×T (additive molar volume method)	—	—	—
Error (if applicable)	—	—	—	—
Reference: [83]				

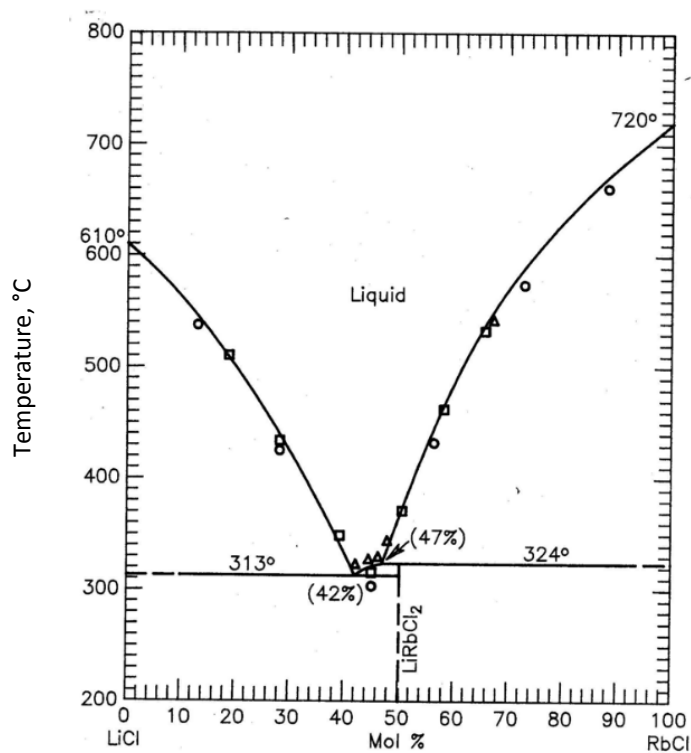


Figure 5-25. LiCl-RbCl system.

### ***NaCl-MgCl<sub>2</sub> System***

Table 5-25. NaCl-MgCl<sub>2</sub> (58-42 mol%).

<b>Melting point:</b> 718 K <b>Vapor pressure (at 1173 K):</b> <2.5 mm Hg <b>Phase diagram:</b> See Figure 5-26 [83].				
	Density (g/cm <sup>3</sup> )	Heat capacity (cal/g-°C)	Viscosity (cP)	Thermal conductivity (W/m-K)
Value (at 973 K)	1.68	0.258	1.36	0.50
Correlation	2.2971-0.000507×T (additive molar volume method)	—	—	—
Error (if applicable)	—	—	—	—
Reference: [83]				

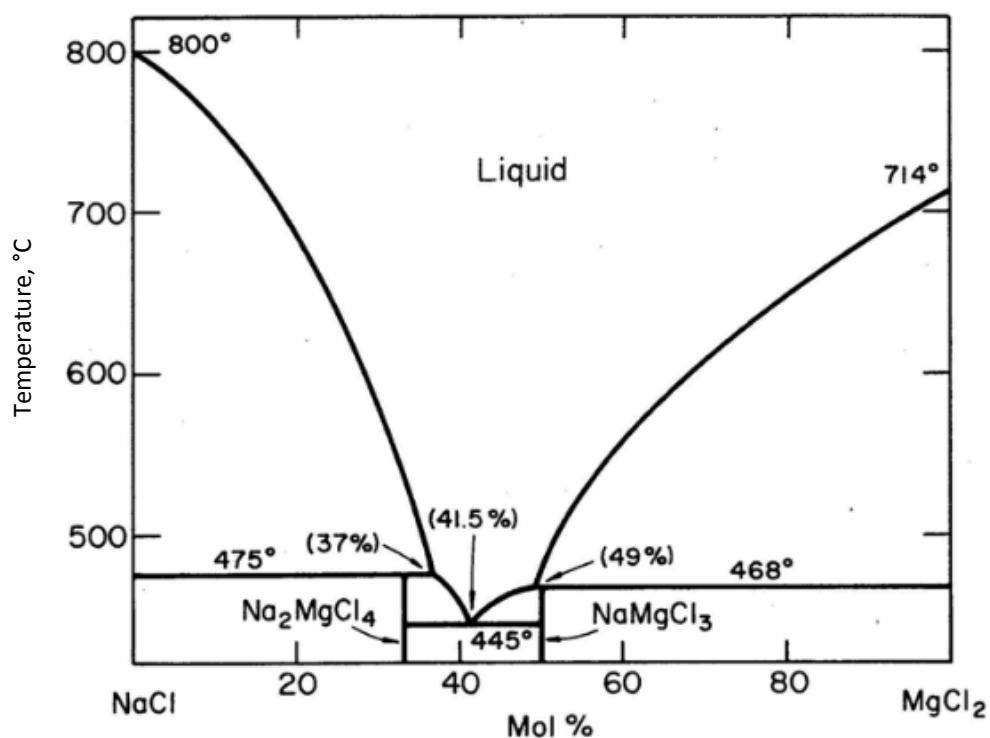


Figure 5-26. NaCl-MgCl<sub>2</sub> system.

### KCl-MgCl<sub>2</sub> System

Table 5-26. KCl-MgCl<sub>2</sub> (68-32 mol%).

<b>Melting point:</b>		699 K		
<b>Vapor pressure (at 1173 K)</b>		<2.0 mm Hg		
<b>Surface tension (for 66.9-33.1 mol% composition):</b>		$g=128.13 - 0.04548T$ , T range: 1020-1135 K [93]		
<b>Phase diagram:</b>		See Figure 5-27 [83].		
	Density (g/cm <sup>3</sup> )	Heat capacity (volumetric) (cal/cm <sup>3</sup> -°C)	Viscosity (cP)	Thermal conductivity (W/m-K)
Value (at 973 K)	1.66	0.46	1.40	0.40
Correlation	$2.25458 - 0.000474 \times T^*$ (additive molar volume method)	—	—	—
Error (if applicable)	—	—	—	—
Reference: [83]				
*For 67-33 mol% composition.				

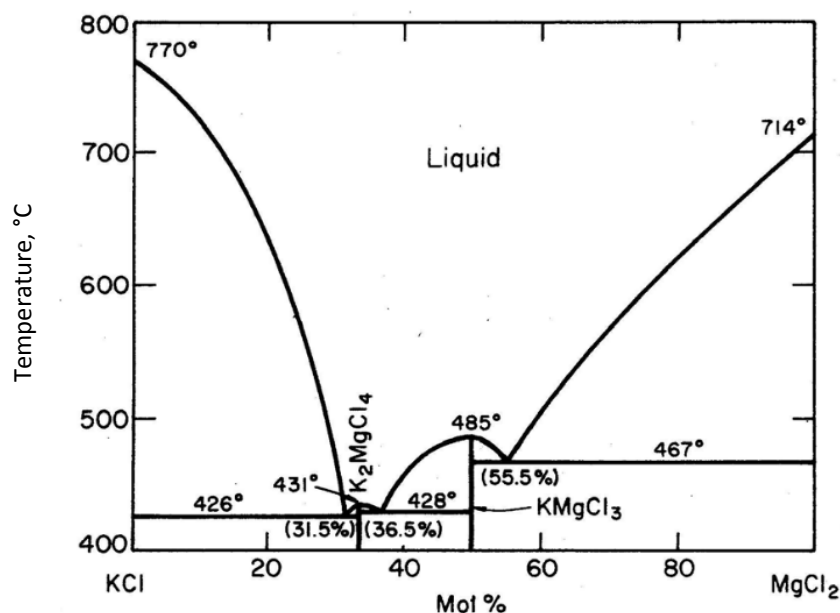


Figure 5-27. KCl-MgCl<sub>2</sub> system.

### 5.3.5 Fluoroborate Salts

#### *NaF-NaBF<sub>4</sub> System*

Table 5-27. NaF-NaBF<sub>4</sub> (8-92 mol%).

<b>Melting point:</b>		658 K		
<b>Vapor pressure (at 1173 K):</b>		9,500 mm Hg		
<b>Volume expansivity, <math>\beta</math> (at 973K):</b>		4.25E-04 (1/°C) [84]		
<b>Prandtl number (at 973 K):</b>		2.640 $C_p \cdot \mu / k$ [84]		
<b>Phase diagram:</b>		See Figure 5-28 [83].		
	Density (g/cm <sup>3</sup> )	Heat capacity (cal/cm <sup>3</sup> -°C)	Viscosity (cP)	Thermal conductivity (W/m-K)
Value (at 973 K)	1.754	0.63	0.90*	0.40**
Correlation	2.2521-0.000711×T (additive molar volume method)	—	—	—
Error (if applicable)	—	—	—	—
Reference: [83]				
*0.88 cP (at 973 K) [84]				
**0.50 W/m-K (at 973 K) [84]				

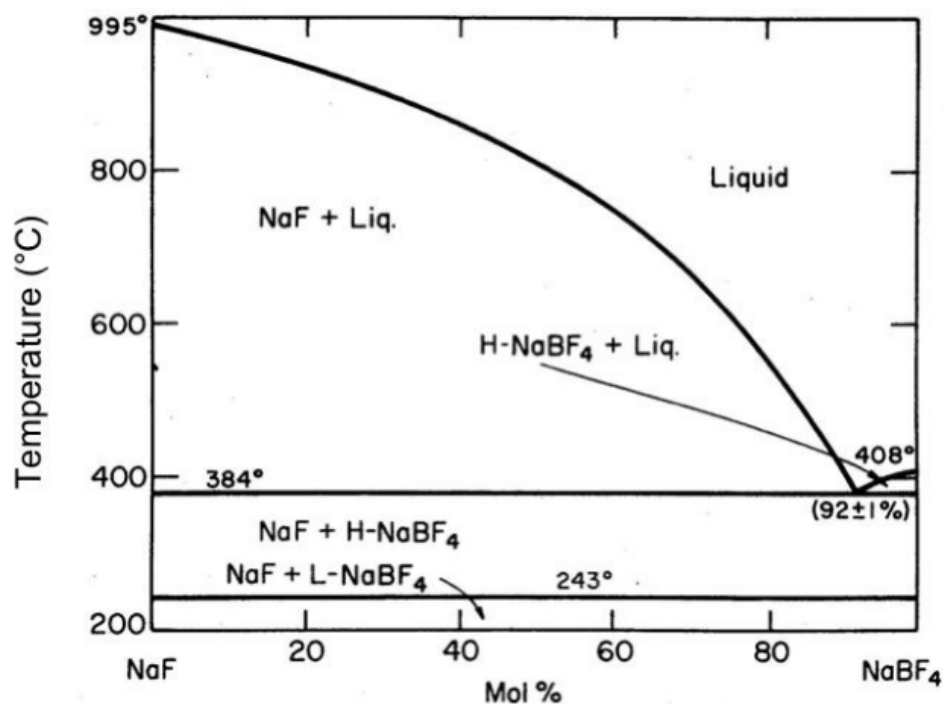


Figure 5-28. NaF-NaBF<sub>4</sub> system.

### KF-KBF<sub>4</sub> System

Table 5-28. KF-KBF<sub>4</sub> (25-75 mol%).

<b>Melting point:</b> 733 K				
<b>Vapor pressure (at 1173 K):</b> 100 mm Hg				
<b>Phase diagram:</b> See Figure 5-29 [83].				
	Density (g/cm <sup>3</sup> )	Heat capacity (cal/cm <sup>3</sup> -°C)	Viscosity (cP)	Thermal conductivity (W/m-K)
Value (at 973 K)	1.696	0.53	0.90	0.38
Correlation	2.258– 0.0008026×T (additive molar volume method)	–	–	–
Error (if applicable)	–	–	–	–
Reference: [83]				

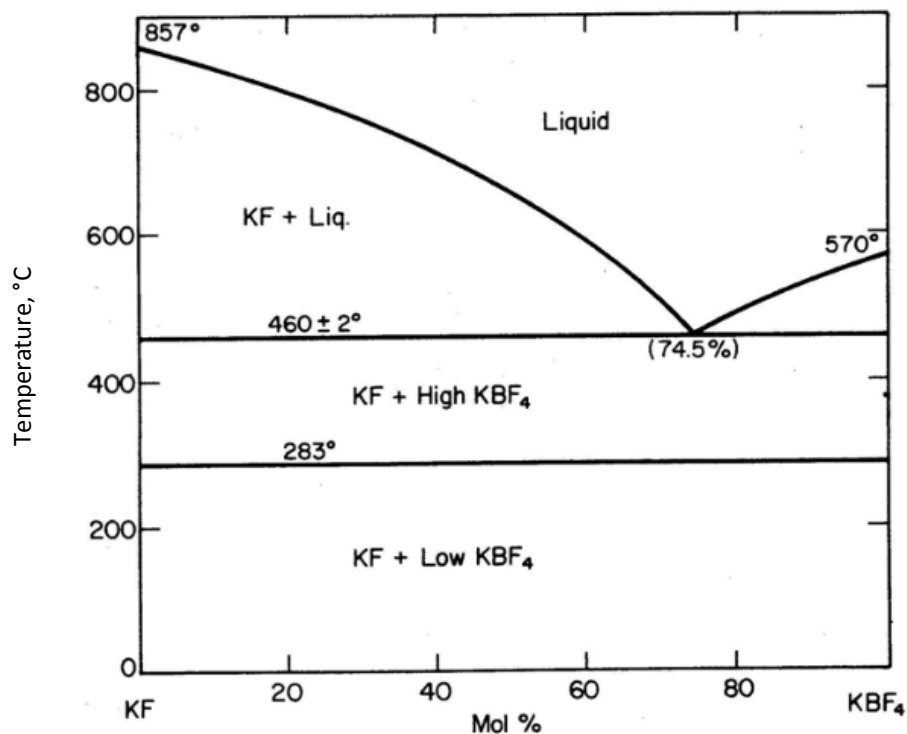


Figure 5-29. KF-KBF<sub>4</sub> system.

### RbF-RbBF<sub>4</sub> System

Table 5-29. RbF-RbBF<sub>4</sub> (31-69 mol%).

<b>Melting point:</b> 715 K				
<b>Vapor pressure (at 1773 K):</b> <100 mm Hg				
<b>Phase diagram:</b> See Figure 5-30 [83].				
	Density (g/cm <sup>3</sup> )	Heat capacity (cal/cm <sup>3</sup> -°C)	Viscosity (cP)	Thermal conductivity (W/m-K)
Value (at 973 K)	2.213	0.48	0.90	0.28
Correlation	2.946-0.001047×T (additive molar volume method)	—	—	—
Error (if applicable)	—	—	—	—
Reference: [83]				

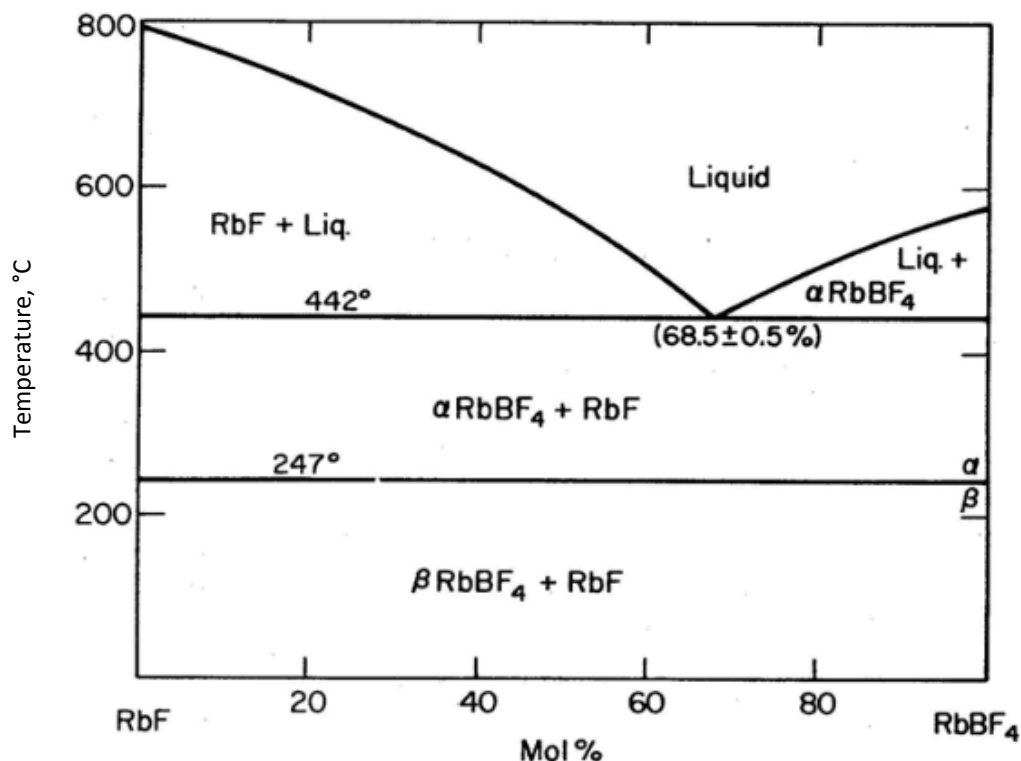


Figure 5-30. RbF-RbBF<sub>4</sub> system.

## 5.4 Conclusions

Property	Database		Knowledge gap/Future efforts needed
Phase diagram	Extensive database available for most of binary and ternary salt-mixtures, of interest for MSR technologies		Very little need to pursue estimation techniques
	<b>Value/s (at molten state)</b>	<b>Temperature Correlation</b>	
Density	Density is known for most of the salt-mixtures, at molten state	Temperature correlations based on experimental data are limited to few systems; most of the correlations are based on predicted methods (an example is additive molar volume method)	Temperature correlations based on experimental techniques (for temperature range of interest for MSRs)
Heat Capacity	Fairly extensive database available for most of the salt-mixtures, at molten state	Temperature correlations not available for all systems	Can be improved with modern instrumentation and techniques available; temperature correlations based on experimental techniques (for temperature range of interest for MSRs)

Viscosity	Viscosity is known for most of the salt-mixtures at molten state	Temperature correlations not available for all systems of interest	Temperature correlations based on experimental techniques (for temperature range of interest for MSRs)
Thermal conductivity	Most difficult property to measure; most uncertain and scattered database	Temperature correlation available for very few systems	Better estimation techniques needed



## 6. APPLICATION OF ELECTROCHEMICAL TECHNIQUES FOR EMERGING MOLTEN SALT REACTOR SYSTEMS

*Tae-Sic Yoo*

### 6.1 Introduction

There is a category of MSRs that uses molten salt for fuel (thermal energy source) and coolant (thermal energy carrier). The versatility of the single molten salt in this system simplifies the reactor system design; however, the salt requires many desirable physical and chemical properties including the following [126]:

- Low melting temperature to keep the salt molten
- Low vapor pressure to keep the system unpressurized
- Low viscosity to transfer the salt effectively
- High heat capacity and conductivity to transfer heat effectively
- High stability with respect to common structural materials to minimize corrosion
- High solubility of the actinide salts to allow the use of fast neutron spectrum.

In this system, the reactor discharges a slip-stream of its molten salt inventory to a chemical reprocessing plant for treatment. Treatment options include the separation of undesirable constituents such as fission and corrosion products, and the reconstitution of the fuel salt. From the perspective of managing the separations chemistries within the chemical reprocessing plant, the relative stabilities of the various salt species play an important role. Ideally, one would want to have a salt system in which the least stable species are those that need to be separated (e.g., neutron poisoning fission products). Thus, for a reactor system requiring chemical reprocessing to maintain reactor performance, the selection of a salt system allowing for the simplest separations processes should be an important criteria. This requirement can be systematically approached by examining the relative stabilities of the candidate salt expressed by the standard state Gibbs free energy of formation.

This section aims to assess the application feasibility of electrochemical techniques to MSR systems by jointly considering the constraints imposed by other components of the MSR system. To this end, the next section gives the standard state Gibbs free energies of formation for various fluoride and chloride species along with its implication to the MSR system. The final section gives relevant literature results regarding the salt treatment options for the MSR system and argues the pertinent challenges associated with the treatment of molten salt in supporting of the MSR operation. Section 7 lists the references.

### 6.2 Chemical Stability of Fluoride and Chloride Species

Figure 6-1 is an Ellingham diagram for various fluoride species normalized to 1 mole of fluorine gas,  $F_2(g)$ . The plot is generated with the HSC Version 6.0 software.<sup>a</sup> For the fluoride system, typical fuel salt candidates for the MSR system include the alkali and alkali metal fluoride species, LiF, NaF, KF, BeF<sub>2</sub>, and CaF<sub>2</sub>. The Ellingham diagram indicates the following.

- CaF<sub>2</sub> is the most stable salt (the lowest standard state Gibbs free energy of formation) among these species. Given the large gap between CaF<sub>2</sub> and other species in Figure 6-1, CaF<sub>2</sub> is likely to remain as salt species throughout the salt treatment process. The melting temperature of CaF<sub>2</sub> is 1418°C, and the

---

a. HSC Version 6.0, a chemistry process calculation software, enables users to simulate chemical or physical processes. It contains 21 calculation modules and 11 databases for reaction, equilibrium, heat balance, heat transfer, petrological and simulation applications.

eutectic melting temperature of LiF-CaF<sub>2</sub> is 767°C. A high melting temperature is a barrier to adopt CaF<sub>2</sub> as a base salt in MSR, which typically is proposed to be operated around 700°C. Regardless of the mentioned operating temperature shortfall barring the usage of CaF<sub>2</sub> as the base fuel salt in MSR, CaF<sub>2</sub> is frequently mentioned as a base salt candidate for the salt treatment process due to its excellent chemical stability [127, 128, 129, 130, 131].

- LiF is the second most stable salt species. Given a large gap between LiF and other species in Figure 6-1, LiF is likely to remain as salt species throughout the salt treatment process. However, LiF enriched in <sup>7</sup>Li is desired to minimize the production of <sup>3</sup>H in the reactor. Regardless of this constraint, the fluoride mixtures including LiF (e.g., FLiBe and FLiNaK) are the most preferred option for constructing a fluoride-based MSR system [126].
- Below 700°C, CeF<sub>3</sub>, a representative species for lanthanides, is more stable than NaF and KF. Thus, designing a simple electrochemical reduction process for removing lanthanides from molten fluoride salt is not trivial. Note that NaF and KF are slightly more stable than PaF<sub>3</sub> indicating that Pa reduction should precede the reduction of Na and K. However, the close proximity of the stability levels among these species can cause nontrivial level of Na and K partitioning with Pa, especially considering that the concentrations of NaF and KF are much higher than the concentration of PaF<sub>3</sub> in the fluoride salt. Regardless of this constraint, the fluoride mixture including NaF and KF, namely FLiNaK, is an emerging option for constructing a fluoride-based MSR system in particular for a fast reactor concept due to its high solubility of the actinide salts [132]. In this option, a treatment of the salt to remove lanthanides is not as critical as the thermal reactor counterpart due to the small lanthanide cross-sections of fast neutron and the removal of lanthanides may not be necessary or can be performed with a significant lanthanide concentration build up in the salt [133].
- All other species are more stable than Be in the fluoride salt except U. Thus, from the salt treatment perspective, the inclusion of BeF<sub>2</sub> in the fuel salt is to add process complexity and not desirable. A remedy for adopting Be is to use molten Bi as a solvent and prevent Be partition to molten Bi by taking advantage of a low solubility of Be to molten Bi [134] (see Figure 6-2). BeF<sub>2</sub> enjoys a low eutectic melting point with LiF, 364°C.
- Assuming that lanthanides behave similarly as Ce, among actinides and lanthanides, lanthanides are more stable than the actinides in the fluoride system. Figure 6-1 indicates that the smallest stability gap to CeF<sub>3</sub> comes with PaF<sub>3</sub>. However, given the fast decay of Pa isotopes to U isotopes, designing a simple electrochemical process separating the two groups (lanthanides and actinides) seems feasible.

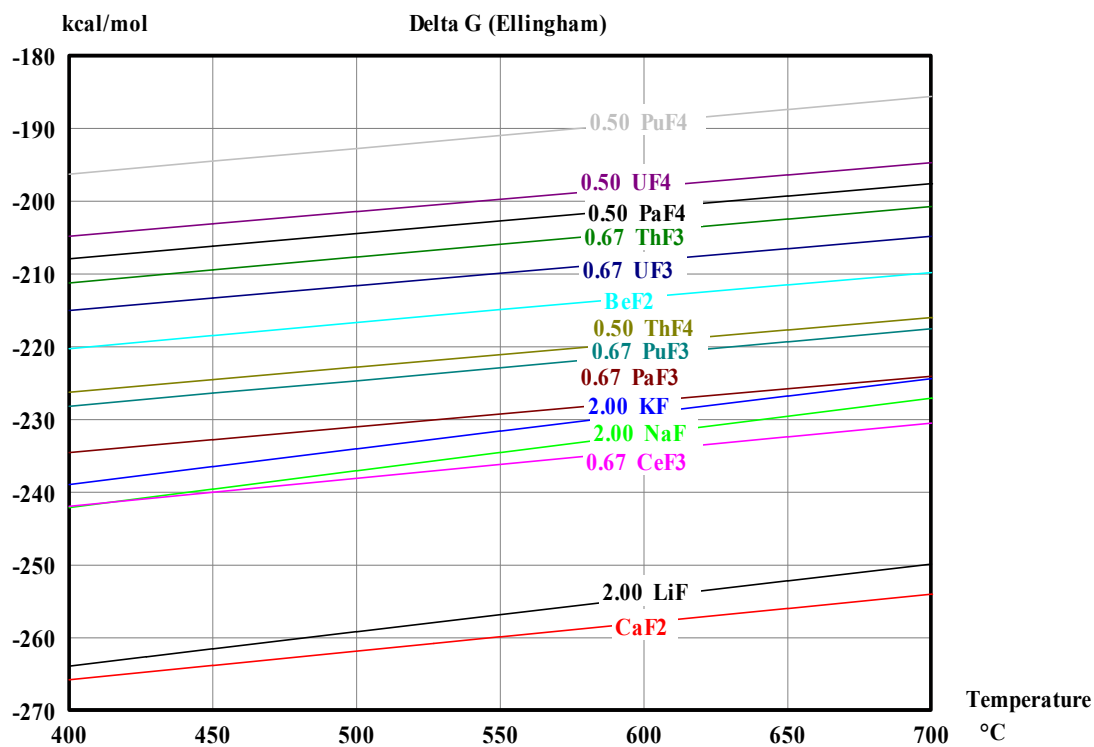


Figure 6-1. Ellingham diagram of fluoride species.

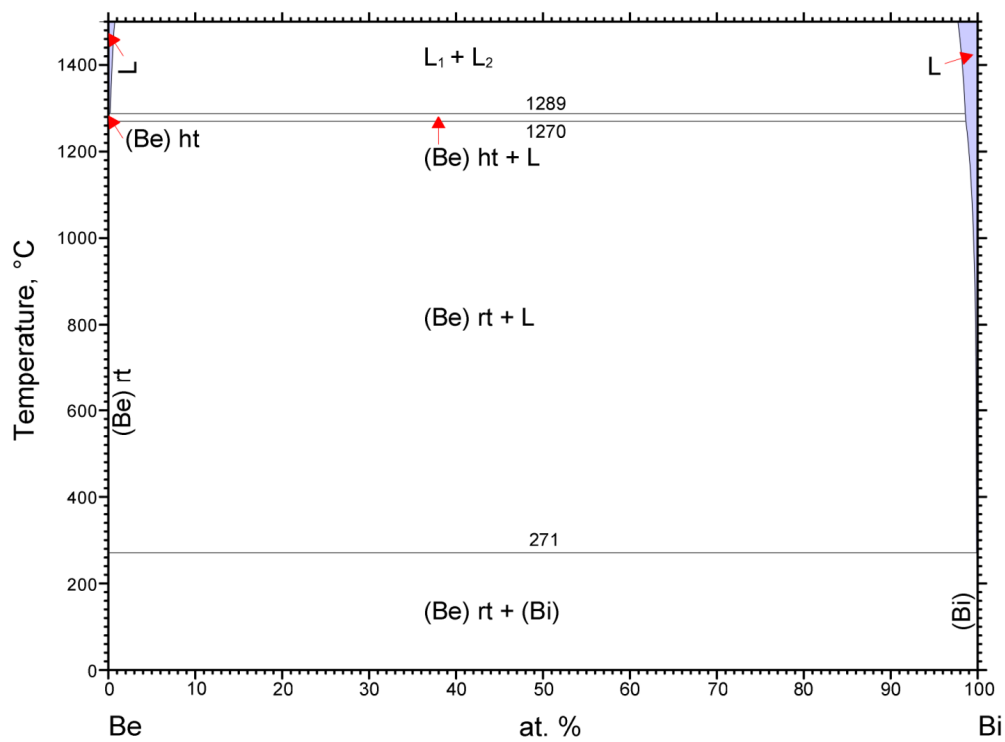


Figure 6-2. Bi-Be phase diagram.

One of the primary deterrents for adopting the chloride system in the MSR system is the most abundant chlorine isotope  $^{35}\text{Cl}$  produces  $^{36}\text{Cl}$ , a long-lived energetic beta source, in the reactor. Thus, an isotope separation process rejecting  $^{35}\text{Cl}$  and enriching  $^{37}\text{Cl}$  is necessary to minimize the production of  $^{36}\text{Cl}$ . Even with this shortfall, the chloride salt system has received attentions primarily for fast reactor application including TerraPower's MCFR due to its higher solubility for actinides and excellent breeding capability compared to the fluoride salt system. To examine the chemical stability of the chloride salt species, Figure 6-3 gives an Ellingham diagram for various chloride species normalized to 1 mole of chlorine gas,  $\text{Cl}_2(\text{g})$ . The plot is generated with the HSC Version 6.0 software. For the chloride system, typical fuel salt candidates for the MSR system include alkali and alkali metal chloride species. The Ellingham diagram indicates the following.

- $\text{NaCl}$  is stable relative to the lanthanide and actinide chlorides. Given a large gap between  $\text{NaCl}$  and the lanthanide and actinide species in Figure 6-3,  $\text{NaCl}$  is likely to remain as salt species throughout the salt treatment process. Being abundant and chemically and neutronically stable,  $\text{NaCl}$  is preferred in constructing a chloride-based MSR system [135, 136].
- $\text{LiCl}$  is the second most stable species. Given a large gap between  $\text{LiCl}$  and other species in Figure 6-3,  $\text{LiCl}$  is likely to remain in the salt phase throughout the salt treatment process. However,  $\text{LiCl}$  is not preferred in the chloride-salt MSR system.  $\text{LiCl}$  enriched in  $^7\text{Li}$  is desired to minimize the production of  $^3\text{H}$  in the reactor. The  $\text{LiCl}$ - $\text{NaCl}$  eutectic melting temperature is  $554^\circ\text{C}$ .
- $\text{KCl}$  is the most stable species among those in Figure 6-3. Given a large gap between  $\text{KCl}$  and other species,  $\text{KCl}$  is likely to remain as salt species throughout the salt treatment process. However,  $\text{KCl}$  is not preferred in the MSR system, because the most abundant isotope  $^{39}\text{K}$  can produce  $^{36}\text{Cl}$  in the reactor. The  $\text{NaCl}$ - $\text{KCl}$  eutectic melting temperature is  $657^\circ\text{C}$ . The  $\text{LiCl}$ - $\text{KCl}$  eutectic melting temperature is  $353^\circ\text{C}$ .
- $\text{CaCl}_2$  is stable relative to the lanthanide and actinide chlorides. Given a large gap between  $\text{CaCl}_2$  and the lanthanide and actinide species in Figure 6-3,  $\text{CaCl}_2$  is likely to remain as salt species throughout the salt treatment process. The  $\text{NaCl}$ - $\text{CaCl}_2$  eutectic melting temperature is  $504^\circ\text{C}$ . The  $\text{LiCl}$ - $\text{CaCl}_2$  eutectic melting temperature is  $475^\circ\text{C}$ . A relatively low eutectic melting temperature with  $\text{NaCl}$  is also advantageous. Though  $\text{CaCl}_2$  seems promising as the base salt species, literature on MSR engaging  $\text{CaCl}_2$  seems lacking.
- With  $\text{MgCl}_2$ , no element in Figure 6-3 is amenable to be reduced prior to  $\text{Mg}$  besides uranium. Thus, from the salt treatment perspective, the inclusion of  $\text{MgCl}_2$  in the fuel salt is to add process complexity and not desirable.  $\text{MgCl}_2$  enjoys a relatively low eutectic melting point with  $\text{NaCl}$ ,  $459^\circ\text{C}$ .  $\text{MgCl}_2$  is proposed as an option for the base salt in constructing a chloride-based MSR system [137, 138].
- With  $\text{BeCl}_2$ , no element in Figure 6-3 is amenable to be reduced prior to  $\text{Be}$ . Thus, from the salt treatment perspective, the inclusion of  $\text{BeCl}_2$  in the fuel salt is to add process complexity and not desirable. Also, a high volatility of  $\text{BeCl}_2$  discourages further the inclusion of  $\text{BeCl}_2$  in the fuel salt.
- Assuming that lanthanides behave similarly as  $\text{Ce}$ , among actinides and lanthanides, lanthanides are more stable than the actinides in the chloride system. The smallest gap to  $\text{CeCl}_3$  comes with  $\text{PaCl}_3$ . However, with fast decay of  $\text{Pa}$  isotopes to  $\text{U}$  isotopes, the separation between the two groups (lanthanides and actinides) seems feasible given a sufficient time to decay  $\text{Pa}$  isotopes to  $\text{U}$  isotopes prior performing a separation operation.

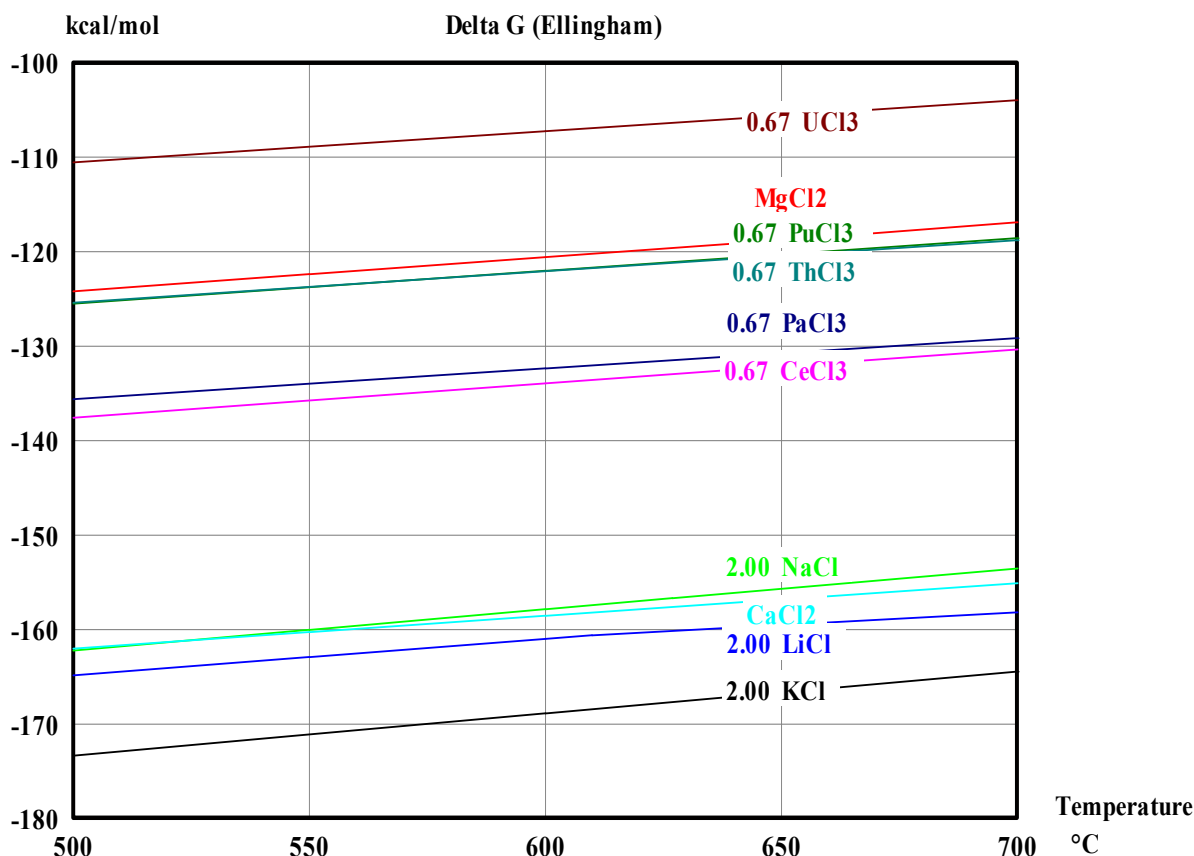


Figure 6-3. Ellingham diagram of chloride species.

### 6.3 Related Literature Results and Challenges

A well designed electrochemical separation process for the treatment of the involved salt in the MSR can be beneficial in terms of cost, simplicity, and waste minimization. As an alternative to the molten salt/molten metal reductive extraction process, the application of an electrochemical process for the treatment of the molten salt in the MSR system was discussed under the Generation Four International Forum. An example of these efforts is given in Figure 6-4 depicting a conceptual flowsheet proposed for treating LiF–BeF<sub>2</sub>–ThF<sub>4</sub>–UF<sub>4</sub> electrochemically [139]. In this system, the molten fluoride salt is intended for a single-fluid MSR. Note that molten Bi is adopted for non-selective material extraction prior to selective material separation. As asserted in the previous section, this is to take advantage of a low solubility of Be to Bi and relative stability of LiF to other salt species and afford the preservation of LiF–BeF<sub>2</sub> in the flowsheet. Another notable option is the adoption of LiF–CaF<sub>2</sub> system for selectively removing rare earth species. As asserted in the previous section, a large electrochemical window induced from excellent LiF and CaF<sub>2</sub> chemical stabilities to other salt species preserves LiF–CaF<sub>2</sub> in the flowsheet while allowing separation processes for other salt species. The flowsheet aligns well with the arguments laid in the previous section regarding the fluoride system. Depending on the choice of the base fuel salt composition (e.g., exclusion of BeF<sub>2</sub>), the flowsheet has a potential to be further simplified.

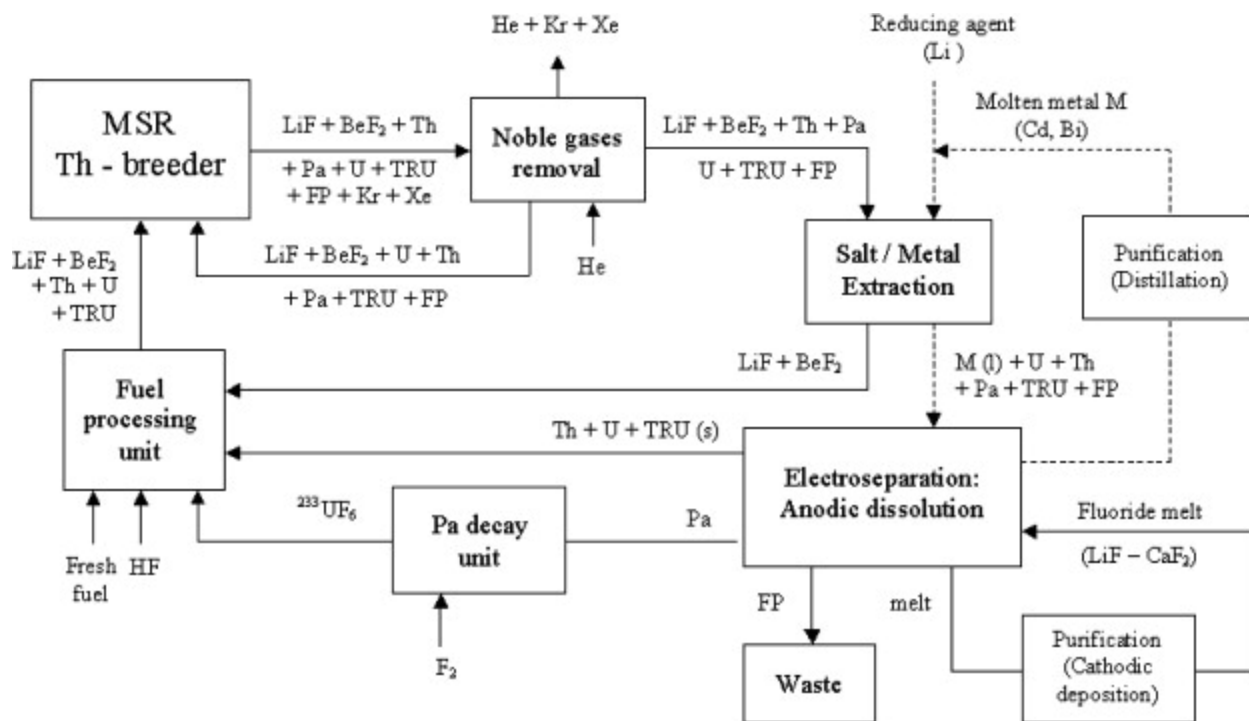


Figure 6-4. Conceptual salt treatment flowsheet of a single-fluid MSR [139].

Compared to fluoride based MSR systems, less effort has been directed to the development of the chloride based MSR system. The corrosion process associated with chloride molten salt is argued to be more complicated than the fluoride counterpart [137]. We note that the chloride based MSR system is typically targeted as a fast reactor concept, and the trichloride actinide species (much less corrosive than tetrachloride counterpart) are considered as the fuel salt, while the fluoride based MSR system typically engages the tetrafluoride actinides. Thus, the corrosive nature of these two systems should be compared carefully. As the research and development for the MSR system were focused primarily on the fluoride salt system, the identification of the structural materials that can survive a harsh chemical and physical environment induced from the reactor operation were deterred. Also insufficient basic research regarding the chloride based reactor system resulted in the immature overall investigations regarding the chloride based MSR system. Though the chloride system is superior to the fluoride system with regards to the neutronics performance in fast spectrum operations, the maturity of the chloride based system in terms of the overall development and knowledge base is considered to be inferior to that of the fluoride counterpart in the context of the MSR system. However, abundant results regarding the nuclear application of the molten chloride salts are available in the context of metal fuels pyroprocessing for the integral fast reactor concept. A flowsheet given in Figure 6-5 [137] is an example of the efforts attempting to extend the knowledge base of the integral fast reactor experience to the MSR system. Though intriguing, the nature of the flowsheet seems speculative and requires further investigations.

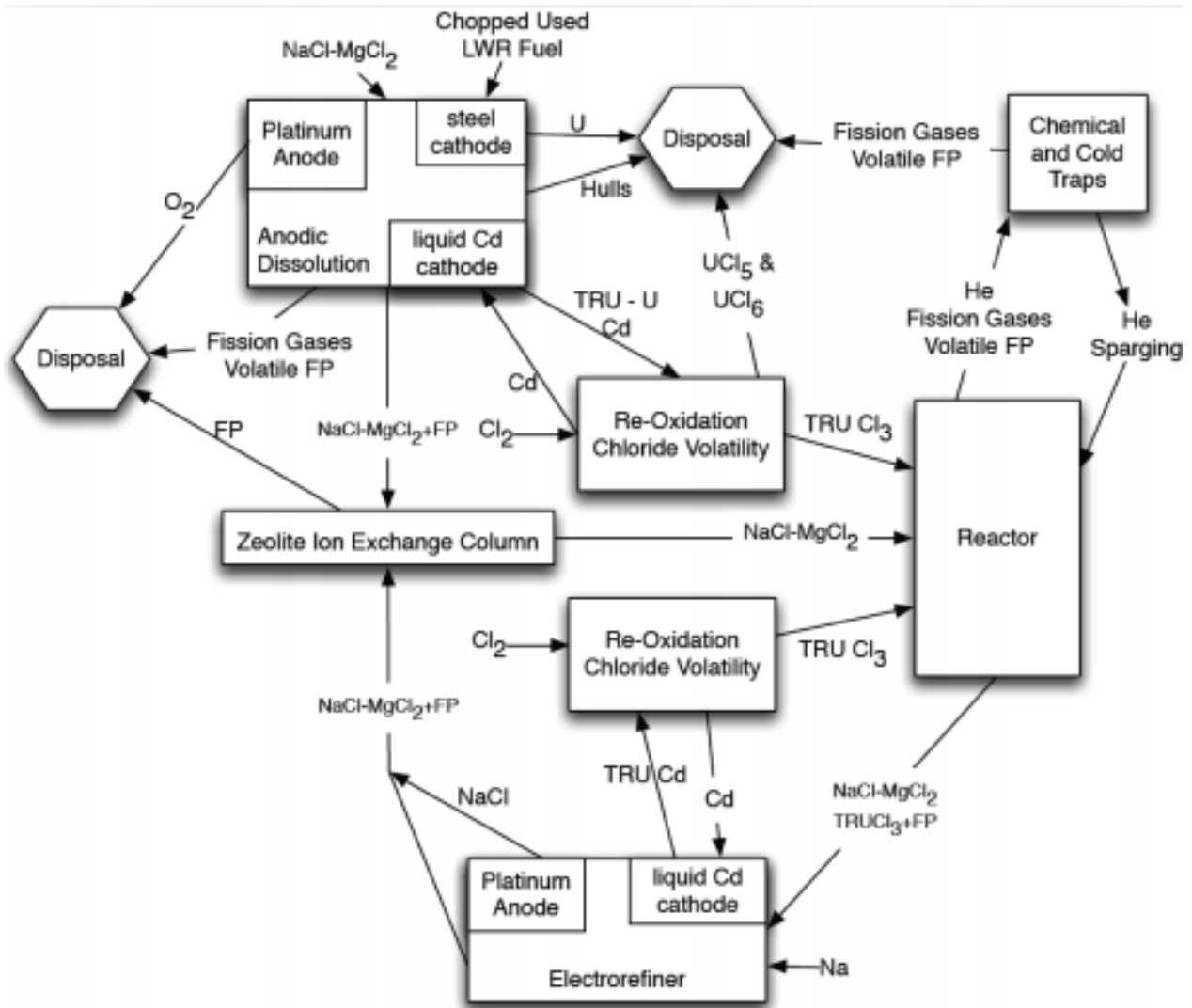


Figure 6-5. Conceptual fuel cycle scenario for a fast spectrum molten chloride salt reactor [137].

## 7. REFERENCES

1. ORNL-4528, 1970, *Two-Fluid Molten-Salt Breeder Reactor Design Study (Status as of January 1, 1968)*, Oak Ridge National Laboratory.
2. ORNL-4541, 1971, *Conceptual Design Study of a Single-Fluid Molten-Salt Breeder Reactor*, Oak Ridge National Laboratory.
3. International Atomic Energy Agency, 2007, *Liquid Metal Cooled Reactors: Experience in Design and Operation*, IAEA-TECDOC-1569.
4. Westinghouse Electric Company, 2003, *The Westinghouse AP1000 Advanced Nuclear Plant: Plant Description*.
5. D. G. Ginnings, T. B. Douglas, and A. F. Ball, 1950, "Heat Capacity of Sodium Between 0° and 900°C, the Triple Point and Heat of Fusion," U.S. Department of Commerce, National Bureau of Standards, Research Paper RP2110, Vol. 45, pp. 23–33.
6. HSC Chemistry Software, Version 9, Outotec.
7. M. J. Huijben, H. Klaucke, J. Hennephof, W. van der Lugt, 1975, "Density of Liquid Sodium-Cesium Alloys," *Scripta Metallurgia*, Vol. 9, No. 653-656, ORNL-4541, pp. 31.
8. ORNL-3791, 1966, *Preliminary Design Study of a Continuous Fluorination-Vacuum-Distillation System for Regenerating Fuel and Fertile Streams in a Molten Salt Breeder Reactor*, Oak Ridge National Laboratory.
9. ORNL-TM-3137, 1971, *Engineering Development Studies for Molten-Salt Breeder Reactor Processing No. 2*, Oak Ridge National Laboratory.
10. ORNL-3996, 1966, *Design Studies of 1000-Mw(e) Molten-Salt Breeder Reactors*, Oak Ridge National Laboratory.
11. ORNL-TM-3258, 1972, *Engineering Development Studies for Molten-Salt Breeder Reactor Processing No. 8*, Oak Ridge National Laboratory.
12. ORNL-5176, 1977, *Engineering Tests of the Metal Transfer Process for Extraction of Rare-Earth Fission Products from a Molten-Salt Breeder Reactor Fuel Salt*, Oak Ridge National Laboratory.
13. ORNL-TM-3259, 1972, *Engineering Development Studies for Molten-Salt Breeder Reactor Processing No. 9*, Oak Ridge National Laboratory.
14. J. Uhler, 2017, "Chemical processing of liquid fuel," book chapter in *Molten Salt Reactors and Thorium Energy*, Elsevier Ltd.
15. M. Ragheb, 2018, "Isotope Separation and Enrichment," book chapter available at <http://mragheb.com/NPRE%20402%20ME%20405%20Nuclear%20Power%20Engineering/Isotopic%20Separation%20and%20Enrichment.pdf>.
16. P. Souček et al., 2017, "Synthesis of UF<sub>4</sub> and ThF<sub>4</sub> by HF gas fluorination and re-determination of the UF<sub>4</sub> melting point," *Journal of Fluorine Chemistry*, Vol. 200, pp. 33–40.
17. M. Iwasaki and T. Sakurai, 1972, "Fluorination of UO<sub>2</sub> and U<sub>3</sub>O<sub>8</sub> by gaseous bromine trifluoride," *J. Inorg. Nucl. Chem*, Vol. 34, pp. 2189–2200.
18. S. Ogata, et al., 2004, "Fluorination reaction of uranium dioxide by fluorine," *Journal of Nuclear Science and Technology*, Vol. 41, No. 2, pp. 135–141.



19. O. Amano, 2002 “FLUOREX Reprocessing Technology with Uranium Removal from Spent Fuel by Fluorination -Volatilization Reaction of Uranium,” *Journal of Nuclear Science and Technology*, Supplement 3, pp. 890–893.
20. J. Uhlir, et al., 2007, “Development of fluoride reprocessing technologies devoted to molten salt reactor systems,” *Global 2007*, September 9–13, 2007.
21. J. Uhlir, 2008, “Current progress in R&D on MSR fuel cycle technology in the Czech Republic,” *OECD-NEA 10th IEM on Actinides and Fission products P&T*, Mito, Japan, October 6–10, 2008.
22. J. Uhlir, et al., 2007, “R&D on Fluoride Volatility Method for Reprocessing of LWR and FR Oxide-type Fuels,” *Proceedings of ICAPP 2007*, Nice, France, May 13–18, 2007.
23. J. Uhlir and M. Marecek, 2009, “Fluoride volatility method for reprocessing of LWR and FR fuels,” *Journal of Fluorine Chemistry*, Vol. 130, pp. 89–93.
24. N. M. Levitz, 1969, “Production of Plutonium Hexafluoride by Fluorination in a Fluidized Bed,” *Nuclear Applications*, Vol. 6.
25. D. Watanabe, et al., 2016, “Experimental study on elemental behaviors in fluorination of nuclear spent fuel with flame reactor,” *Journal of Nuclear Science and Technology*, Vol. 53, No. 4, pp. 513–520.
26. K. Fujiwara, et al., 2003, “Development of fluorination decontamination technique for uranium bearing waste,” *Proceedings of ICEM’03: The 9th international conference on environmental remediation and radioactive waste management*, September 21–25, 2003, Examination Schools, Oxford, England.
27. M. Iwasaki and T. Sakurai, 1972, “Fluorination of  $\text{UO}_2$  and  $\text{U}_3\text{O}_8$  by gaseous bromine trifluoride,” *J. Inorg. Nucl. Chem*, Vol. 34, pp. 2189–2200.
28. B. Claus, et al., 2016, “On the fluorination of plutonium dioxide by ammonium hydrogen fluoride,” *Journal of Fluorine Chemistry*, Vol. 183, pp. 10–13.
29. R. D. Scheele, et al., 2013, “Thermal  $\text{NF}_3$  fluorination/oxidation of cobalt, yttrium, zirconium, and selected lanthanide oxides,” *Journal of Fluorine Chemistry*, Vol. 146, pp. 86–97.
30. J. T. Holmes, et al., 1968, *Engineering development of fluid-bed fluoride volatility processes, part 13, Pilot –plant studies of the fluorination of uranium oxide with bromine pentafluoride*, ANL-7370, Argonne National Laboratory.
31. R. Scheeles, 2012, “On the use of thermal  $\text{NF}_3$  as the fluorination and oxidation agent in treatment of used nuclear fuels,” *Journal of Nuclear Materials*, Vol. 424, pp. 224–236.
32. B. Claus, et al., 2016, “On the fluorination of plutonium dioxide by ammonium hydrogen fluoride,” *Journal of Fluorine Chemistry*, Vol. 183, pp. 10–13.
33. R. Benz, et al., 1963, “Preparation and properties of several ammonium uranium (IV) and ammonium plutonium (IV) fluorides,” *Inorg. Chem.*, Vol. 2, pp. 799–803.
34. B. N. Wani, et al., 1995, “Fluorination of  $\text{Sr}_2\text{CuO}_3$  by  $\text{NH}_4\text{HF}_2$ ,” *Appl. Supercond.*, Vol. 3, pp. 321–325.
35. H. A. Friedman, *Preparation, purification, and properties of the uranium trichlorides: a literature survey*. ORNL Central Files Number 63-11-5, Oak Ridge National Laboratory.
36. P. A. Hass, 1992, *Literature Information Applicable to the Reaction of Uranium Oxides with Chlorine to Prepare Uranium Tetrachloride*, ORNL/TM-11955, Oak Ridge National Laboratory.
37. S. Kitawaki, et al., 2013, “Chlorination of uranium oxides with  $\text{CCl}_4$  using a mechanochemical method,” *Journal of Nuclear Materials*, Vol. 439, Issue 1–3, pp. 212–216.

38. M. D. Ferran and M. H. West, 1993, *The synthesis of plutonium oxide by chlorination of plutonium oxide with phosgene*, LA-12361-MS.
39. H. C. Eun et al., 2017, "A study on chlorination of uranium metal using ammonium chloride," *J Radioanal Nucl Chem*, Vol. 314, pp. 533–537.
40. H. C. Eun, 2018, "A study on recovery of uranium in the anode basket residues delivered from the pyrochemical process of used nuclear fuel," *Journal of Nuclear Materials*, Vol. 501, pp. 8–12.
41. J. P. LaPlante, et al., 1962, *Chlorination of uranium and fission product oxides in molten halide media*, ANL-654, Argonne National Laboratory.
42. K. Uozumi, 2008, "Demonstration of pyropartitioning technology by denitration and chlorination experiment using real high level liquid waste," *International Workshop for Asian Nuclear Prospect*, October 21, 2008, Kobe, Japan.
43. T. Sato, et al., 2015, "Chlorination of  $\text{UO}_2$  and  $(\text{U, Zr})\text{O}_2$  solid solution using  $\text{MoCl}_5$ ," *Journal of Nuclear Science and Technology*, Vol. 52, No. 10, pp. 1253–1258.
44. Y. Sakamura, et al., 2005, "Chlorination of  $\text{UO}_2$ ,  $\text{PuO}_2$  and rare earth oxides using  $\text{ZrCl}_4$  in  $\text{LiCl-KCl}$  eutectic melt," *Journal of Nuclear Materials*, Vol. 340 pp. 39–51.
45. <http://www.elysiumindustries.com/>
46. R. Meier, et al., 2018, "Recovery of actinides from actinide-aluminum alloys by chlorination: Part III - Chlorination with  $\text{HCl(g)}$ ," *Journal of Nuclear Materials*, pp. 213–220.
47. V. A. Lebedev, et al., 2008, "Potentialities of Low-Temperature Chlorination of Aluminum and Its Alloys with Uranium," *Russian Journal of Applied Chemistry*, Vol. 81, No. 11, pp. 1904–1908.
48. E. R. Meier, et al., 2012, "Recycling of Uranium from Uranium-Aluminum alloys by Chlorination with  $\text{HCl(g)}$ ," *Procedia Chemistry*, Vol. 7, pp. 785–790.
49. C. F. Baes, Jr., 1974, "The chemistry and thermodynamics of molten salt reactor fuels," *Journal of Nuclear Materials*, Vol. 51, 1974.
50. J. H. Shaffer, 1962, *Preparation and handling of salt mixtures for the molten salt reactor experiment*, ORNL-4616, Oak Ridge National Laboratory.
51. P. Calderoni, 2010, *An experimental Test plan for the Characterization of Molten Salt Thermochemical Properties in Heat Transport Systems*, INL/EXT-10-19921, Idaho National Laboratory.
52. V. Ignatiev and A. Surekov, 2017, "Corrosion phenomena induced by molten salts in Generation IV nuclear reactors," book chapter in *Structural Materials for Generation IV Nuclear Reactors*, Elsevier Ltd.
53. R. D. Scheele, et al., 2017, "Use of Nitrogen Trifluoride To Purify Molten Salt Reactor Coolant and Heat Transfer Fluoride Salts," *Ind. Eng. Chem. Res.*, Vol. 56, pp. 5505–5515.
54. S. Delpech, et al., 2010, "Molten fluoride for nuclear applications," *Materials Today*, Vol. 13, No. 12.
55. K. Sridharan and T. R. Allen, 2013, "Corrosion in Molten Salts," book chapter in *Molten Salts Chemistry*, Elsevier Ltd.
56. EVOL FINAL REPORT (Project No. 249696), available at <https://cordis.europa.eu/docs/results/249/249696/final1-final-report-f.pdf>, accessed on August 11, 2018.
57. Development of Molten Salt Breeder Reactors, ORNL/TM-4812, August 1972.

58. D. F. Williams, 2017, "Molten Salt Chemistry workshop: technology and applied R&D needed for molten salt chemistry," Resource Document for the *Molten Salt Chemistry Workshop: Innovative Approaches to Accelerate Molten Salt Reactor Technology Deployment*, ORNL/LTR-2017/135, Oak Ridge National Laboratory, available from <https://www.ornl.gov/content/molten-salt-workshop>.
59. D. F. Williams, L. M. Toth, and K. T. Clarno, 2006, *Assessment of Candidate Molten Salt Coolants for the Advanced High-Temperature Reactor (AHTR)*, ORNL/TM-2006/12, Oak Ridge National Laboratory.
60. M. S. Sohal, et al., 2013, *Engineering Database of liquid Salt Thermophysical and Thermochemical Properties*, INL/EXT-10-18297, Idaho National Laboratory.
61. W. Ren, et al., 2011, "Considerations of Alloy N for fluoride salt –cooled high temperature reactor applications," proceedings of the *ASME 2011 Pressure Vessel and Piping Division Conference PVP 2011*, July 17–21, 2011, Baltimore, Maryland.
62. G. Cao et al., 2013, "Fluoride-Salt-Cooled High Temperature Reactor (FHR) Materials, Fuels and Components White Paper," Idaho National Laboratory.
63. S. Guo et al., 2018, "Corrosion in the Molten Fluoride and Chloride Salts and Materials Development for Nuclear Applications," *Progress in Materials Science*, Vol. 97, No. 448–487.
64. G. Zheng, et al., 2015, "Corrosion of 316 stainless steel in high temperature molten  $\text{Li}_2\text{BeF}_4$  (FLiBe) salt," *Journal of Nuclear Materials*, Vol. 461.
65. G. Zheng and K. Sridharan, 2018, "Corrosion of Structural Alloys in High-Temperature Molten Fluoride Salts for Applications in Molten Salt Reactors," *JOM*, Vol. 70, No. 8.
66. K. Chan et al., 2018, "Carburization effects on the corrosion of Cr, Fe, Ni, W, and Mo in fluoride-salt cooled high temperature reactor (FHR) coolant," *Annals of Nuclear Energy*, Vol. 120, pp. 279–285.
67. D. F. Williams, 2006, *Assessment of candidate molten salt coolants for the NGNP/NHI Heat Transfer Loop*, ORNL/TM-2006/69, Oak Ridge National Laboratory.
- A. M. Kruizenga, 2012, *Corrosion Mechanisms in Chloride and Carbonate Salts*, SAND 2012-7594, Sandia National Laboratories.
68. J. Ambrosek, 2011, "Molten Chloride Salt for Heat Transfer in Nuclear Systems," Ph.D. Thesis, University of Wisconsin-Madison.
69. D. E. Holcomb, et al., 2011, *Fast Spectrum Molten Salt Reactor Options*, ORNL/TM-2011/105, Oak Ridge National Laboratory.
70. J. Jackson and M. LaChance, 1954, "Resistance of cast Fe-Ni-Cr alloys to corrosion in molten neutral heat treating salts," *Trans. ASM*, Vol. 45.
71. Vigrarooban et al., 2014, Corrosion resistance of Hastelloys in molten metal-chloride heat-transfer fluids for concentrating solar power applications, *Solar Energy*, Vol. 103, pp. 62–69.
72. K. Sridharan, 2009, *Liquid Salts as Media for Process Heat Transfer from VHTRs: Forced Convective Channel Flow Thermal Hydraulics, Materials, and Coatings*, NERI 07-030, NERI Project Review, Panel No. 3, University of Wisconsin, WI.
73. M. Anderson and K. Sridharan, 2010, *Liquid salt heat exchanger technology for VHTR-based applications*, University of Wisconsin-Madison Quarterly Progress Report.
74. H. Sun et al., 2018, "Corrosion behavior of 316SS and Ni-based alloys in a ternary NaCl-KCl-MgCl<sub>2</sub> molten salt," *Solar Energy*, Vol. 171, pp. 320–329.

75. H. Sun et al., 2017, "Research status and progress of molten salt corrosion for concentrated solar thermal power," *Corrosion Science and Protection Technology*, Vol. 29.
76. B. A. T. Mehrabadi, et al., 2017, "Modeling the Effect of Cathodic Protection on Superalloys Inside High Temperature Molten Salt Systems," *Journal of The Electrochemical Society*, Vol. 164, No. 4, pp. C171-C179.
77. B. A. Tavakoli Mehrabadi, J. W. Weidner, B. Garcia-Diaz, M. Martinez-Rodriguez, L. Olson, and S. Shimpalee, 2016, "Multidimensional Modeling of Nickel Alloy Corrosion Inside High Temperature Molten Salt Systems," *J. Electrochem. Soc.*, Vol. 163, No. 14, pp. C830.
78. B. A. Tavakoli Mehrabadi, S. Shimpalee, J. W. Weidner, B. Garcia-Diaz, M. Martinez-Rodriguez, and L. Olson, 2016, "The Effect of Nickel Alloy Corrosion Under Cathodic Protection Inside High Temperature Molten Salt Systems," *ECS Trans*, Vol. 72, No. 17, pp. 151.
79. H. Cho, J. W. Van Zee, S. Shimpalee, B. A. Tavakoli, J. W. Weidner, B. L. Garcia-Diaz, M. J. Martinez-Rodriguez, L. Olson, and J. Gray, 2016, "Dimensionless Analysis for Predicting Fe-Ni-Cr Alloy Corrosion in Molten Salt Systems for Concentrated Solar Power Systems," *Corrosion*, Vol. 72, No. 6, pp. 742.
80. D. Holcomb, 2017, "Overview of Fuel and Coolant Salt Chemistry and Thermal Hydraulics," Presentation for U.S. Nuclear Regulatory Commission Staff Washington DC, November 7-8, 2017.
81. Moltex Energy, 2018, *An Introduction to the Moltex Energy Technology Portfolio*.
82. D. F. Williams, 2006, *Assessment of candidate molten salt coolants for the NGNP/NHI Heat-Transfer Loop*, ORNL/TM-2006/69, Oak Ridge National Laboratory.
83. D. F. Williams, L. M. Toth, and K. T. Clarno, 2006, *Assessment of Candidate Molten Salt Coolants for the Advanced High-Temperature Reactor (AHTR)*, ORNL/TM-2006/12, Oak Ridge National Laboratory.
84. W. R. Grimes and D. R. Cuneo, 1960, "Molten salts as reactor fuels," In C. R. J. Tipton (Ed.), *Reactor Hand Book* (Second, Vol. I). Interscience Publishers, Inc.
85. W. D. Powers, S. I. Cohen, and N. D. Greene, 1963, "Physical Properties of Molten Reactor Fuels and Coolants," *Nuclear Science and Engineering*, Vol. 71, pp. 200–211.
86. S. I. Cohen, W. D. Powers, and N. D. Greene, 1956, *A Physical Property Summary for ANP Fluoride Mixtures*, ORNL-2150, Oak Ridge National Laboratory.
87. R. C. Robertson et al., 1970, *Two-Fluid Molten-Salt Breeder Reactor Design Study*. ORNL-4528, Oak Ridge National Laboratory.
88. J. P. M. van der Meer, R. J. M. Konings, and H. A. J. Oonk, 2006, "Thermodynamic assessment of the LiF-BeF<sub>2</sub>-ThF<sub>4</sub>-UF<sub>4</sub> system," *Journal of Nuclear Materials*, Vol. 357, No. 1–3, pp. 48–57.
89. L. G. Alexander, W. L. Carter, W. Craven, D. B. Janney, T. W. Kerlin, and R. Van Winkle, 1965, *Molten Salt Converter Reactor*, ORNL-TM-1060, Oak Ridge National Laboratory.
90. E. Bettis, L. G. Alexander, and H. L. Watts, 1972, *Design studies of a Molten-salt Reactor Demonstration Plant*, ORNL-TM-3832, Oak Ridge National Laboratory.
91. R. C. Robertson, 1971, *Conceptual Design Study of a Single-Fluid Molten-Salt Breeder Reactor*, ORNL-4541, Oak Ridge National Laboratory.
92. G. J. Janz, 1988, "Thermodynamic and Transport properties for molten salts: Correlation equations for critically evaluated density, surface tension, electric conductance, and viscosity data," *Journal of Physical and Chemical Reference Data*, Vol. 17 (Supplement No. 2).

93. D. F. Williams and L. M. Toth, 2005, "Chemical Considerations for the Selection of the Coolant for the Advanced High-Temperature Reactor," ORNL/GEN4/LTR-05-011, Oak Ridge National Laboratory.
94. G. J. Janz, 1979, *Physical Properties Data Compilations Relevant to Energy Storage, Part II. Molten Salts: Data on Single and Multi-Component Salt Systems*, NSRDS-NBS 61, Part II, U.S. Department of Commerce.
95. M. V. Smirnov, V. A. Khokhlov, and E. S. Filatov, 1986, "Thermal conductivity of molten alkali halides and their mixtures," *Electrochimica Acta*, Vol. 32, No. 7, pp. 1019–1026.
96. R. E. Thoma, 1975, "Phase Diagrams of Binary and Ternary Fluoride Systems," *Advances in Molten Salt Chemistry, Volume 3*, pp. 275–455.
97. R. E. Thoma, 1959, *Phase Diagrams of Nuclear Reactor Materials*, ORNL-2548, Oak Ridge National Laboratory.
98. G. J. Janz, G. L. Gardner, U. Krebs, and R. P. T. Tomkins, 1974, "Molten Salts: Volume 4, Part 1, Fluorides and Mixtures Electrical Conductance, Density, Viscosity, and Surface Tension Data," *J. Phys. Chem.*, Vol. 4, No. 1.
99. S. Cantor, et al., 1968, *Physical Properties of Molten-Salt Reactor Fuel, Coolant, and Flush Salts*, ORNL-TM-2316, Oak Ridge National Laboratory.
100. H. W. Hoffman and J. Lones, 1955, *Fused salt heat transfer Part II: Fused convection heat transfer in circular tubes containing NaF-KF-LiF eutectic*, ORNL-1777, Oak Ridge National Laboratory.
101. C. N. A. C. Z. Bahri, W. M. Al-Areqi, M. F. Mohd Ruf, and A. A. Majid, 2017, "Characteristic of molten fluoride salt system LiF-BeF<sub>2</sub> (Flibe) and LiF-NaF-KF (Flinak) as coolant and fuel carrier in molten salt reactor (MSR)," in *AIP Conf. Proc. 1799*, Vol. 4, pp. 040008-1-040008-8.
102. D. T. Ingersoll, C. W. Forsberg, P. E. Macdonald, M. Farmer, and F. Dunn, 2007, *Trade Studies for the Liquid-Salt-Cooled Very High-Temperature Reactor : Fiscal Year 2006 Progress Report*, ORNL/TM-2006/140, Oak Ridge National Laboratory.
103. B. Vriesema, 1979, Aspect of molten fluorides as heat transfer agents for power generation.
104. M. Chrenkova, V. Danek, R. Vasiljev, A. Silny, V. Kremenetsky, and E. Polyakov, 2003, "Density and viscosity of the (LiF-NaF-KF)eut -KBF<sub>4</sub>-B<sub>2</sub>O<sub>3</sub> melts," *Journal of Molecular Liquids*, Vol. 102, No. 1–3, pp. 213–226.
105. J. Cibulkova, M. Chrenkova, R. Vasiljev, V. Kremenetsky, and M. Boca, 2006, "Density and viscosity of (LiF+NaF+KF)eut(1) + K<sub>2</sub>TaF<sub>7</sub>(2) + Ta<sub>2</sub>O<sub>5</sub>(3) Melts," *Journal of Chemical and Engineering Data*, Vol. 51, pp. 984–987.
106. R. R. Romatoski and L. W. Hu, 2017, "Fluoride salt coolant properties for nuclear reactor applications: A review," *Annals of Nuclear Energy*, Vol. 109, pp. 635–647.
107. M. Salanne, C. Simon, P. Turq, and P. A. Madden, 2009, "Heat-transport properties of molten fluorides: Determination from first-principles," *Journal of Fluorine Chemistry*, Vol. 130, No. 1, pp. 38–44.
108. L. J. Chapdelaine, 2017, *Experimental and Computational Study of Static Solidification of Molten Fluoride Salts for Reactor Coolant Application*, University of Wisconsin-Madison.
109. J. Ambrosek, M. Anderson, K. Sridharan, and T. Allen, 2009, "Current Status of Knowledge of the Fluoride Salt (FLiNaK) Heat Transfer CURR," *Nuclear Technology*, Vol. 165, No. 2, pp. 166–173.

110. Y. Kato, K. Furukawa, N. Araki, and K. Kobayasi, 1983, "Thermal diffusivity measurement of molten salts by use of a simple ceramic cell," In *8 ETPC Proceedings High Temperatures - High Pressures*, Vol. 15, pp. 191–198.
111. V. Khokhlov, V. Ignatiev, and V. Afonichkin, 2009, "Evaluating physical properties of molten salt reactor fluoride mixtures," *Journal of Fluorine Chemistry*, Vol. 130, No. 1, pp. 30–37.
112. O. Beneš and R. J. M. Konings, 2013, "Thermodynamic assessment of the LiF-CeF<sub>3</sub>-ThF<sub>4</sub> system: Prediction of PuF<sub>3</sub> concentration in a molten salt reactor fuel," *Journal of Nuclear Materials*, Vol. 435, No. 1–3, pp. 164–171.
113. D. J. Rogers, T. Yoko, and G. J. Janz, 1982, "Fusion properties and heat capacities of the eutectic lithium fluoride-sodium fluoride-potassium fluoride melt," *Journal of Chemical & Engineering Data*, Vol. 27, No. 3, pp. 366–367.
114. L. Z. Jinhui, A. Xuehui, Z. Peng, W. Kun, Z. Yong, and T. Zhongfeng, 2014, "Experimental investigation on the thermal physical properties and thermal stability of FKZr," *Nucl. Energy Sci. and Engr.*, Vol. 37, pp. 1–4.
115. H. F. McDuffie, et al., 1969, *Assessment of molten salts as intermediate coolants for LMFBR'S*, ORNL-TM-2696, Oak Ridge National Laboratory.
116. M. S. Sohal, M. A. Ebner, P. Sabharwall, and P. Sharpe, 2010, *Engineering Database of Liquid Salt Thermophysical and Thermochemical Properties*, INL/EXT-10-18297, Idaho National Laboratory, pp. 1–70.
117. O. Beneš and R. J. M. Konings, 2009, "Thermodynamic properties and phase diagrams of fluoride salts for nuclear applications," *Journal of Fluorine Chemistry*, Vol. 130, No. 1, pp. 22–29.
118. P. Gierszewski, B. Mikic, and N. Todreas, 1980, *Property correlations for lithium, sodium, helium, flibe and water in fusion reactor applications*, PFC-RR-80-12, Massachusetts Insitute of Technology.
119. B. C. Blanke, 1956, *Density and Viscosity of Fused Mixtures of Sodium Fluoride, Beryllium Fluoride and Uranium Fluoride*, MLM-1086, Mound Laboratory.
120. S. Cantor, 1973, *Density and Viscosity of Several Molten Fluoride Mixtures*, ORNL-TM-4308, Oak Ridge National Laboratory.
121. M. W. Rosenthal, 1970, *Molten Salt Reactor Program Progress Report*, ORNL-4676, Oak Ridge National Laboratory.
122. M. R. Zaghloul, D. K. Sze, and A. R. Raffray, 2003, "Thermo-physical properties and equilibrium vapor-composition of lithium fluoride-beryllium fluoride (2LiF/BeF<sub>2</sub>) molten salt," *Fusion Science and Technology*, Vol. 44, No. 2, pp. 344–350.
123. S. Cantor, W. T. Ward, and C. T. Moynihan, 1969, "Viscosity and Density in Molten BeF<sub>2</sub> – LiF Solutions," *Journal of Chemical Physics*, Vol. 50, No. 7.
124. S. I. Cohen and T. N. Jones, 1957, *Viscosity Measurements on Molten Fluoride Mixtures*, ORNL-2278, Oak Ridge National Laboratory.
125. T. J. Dolan, ed., 2017, *Molten Salt Reactors and Thorium Energy*, Woodhead Publishing Series in Energy, Elsevier Ltd.
126. P. Chamelot, L. Massot, L. Cassayre, and P. Taxil, 2010, "Electrochemical behaviour of thorium (IV) in molten LiF–CaF<sub>2</sub> medium on inert and reactive electrodes," *Electrochimica Acta* Vol. 55, No. 16, pp. 4758–4764.

127. P. Chamelot, L. Massot, C. Hamel, C. Nourry, and P. Taxil, 2007, "Feasibility of the electrochemical way in molten fluorides for separating thorium and lanthanides and extracting lanthanides from the solvent." *Journal of Nuclear Materials*, Vol. 360, No. 1, pp. 64-74.
128. M. Numakura, N. Sato, C. Bessada, Y. Okamoto, H. Akatsuka, A. Nezu, Y. Shimohara et al. 2011, "Structural investigation of thorium in molten lithium–calcium fluoride mixtures for salt treatment process in molten salt reactor," *Progress in Nuclear Energy*, Vol. 53, No. 7, pp. 994-998.
129. P. Souček, F. Lisý, R. Tuláčková, J. Uhlíř, and R. Mraz, 2005, "Development of electrochemical separation methods in molten LiF–NaF–KF for the molten salt reactor fuel cycle." *Journal of nuclear science and technology*, Vol. 42, No. 12, pp. 1017-1024.
130. C. Nourry, P. Souček, L. Massot, R. Malmbeck, P. Chamelot, and J-P. Glatz, 2012, "Electrochemistry of uranium in molten LiF–CaF<sub>2</sub>," *Journal of Nuclear Materials*, Vol. 430, No. 1–3, pp. 58–63.
- A. Degtyarev, A. Myasnikov, and L. Ponomarev, 2015, "Molten salt fast reactor with U–Pu fuel cycle." *Progress in Nuclear Energy*, Vol. 82, pp. 33–36.
131. L. Mathieu, D. Heuer, E. Merle-Lucotte, R. Brissot, C. Le Brun, E. Liatard, J-M. Loiseaux, O. Méplan, A. Nuttin, and D. Lecarpentier, 2009, "Possible configurations for the thorium molten salt reactor and advantages of the fast nonmoderated version," *Nuclear Science and Engineering*, Vol. 161, No. 1, pp. 78–89.
132. L. M. Ferris, J. C. Mailen, J. J. Lawrence, F. J. Smith, and E. D. Nogueira, 1970, "Equilibrium distribution of actinide and lanthanide elements between molten fluoride salts and liquid bismuth solutions." *Journal of Inorganic and Nuclear Chemistry*, Vol. 32, No. 6, pp. 2019–2035.
133. L. G. Alexander, 1963, "Molten-salt fast reactors," In *Proc. Conf. Breeding, Economics and Safety in Large Fast Power Reactors*, pp. 553.
134. M. Taube and J. Ligou, 1974, "Molten plutonium chlorides fast breeder reactor cooled by molten uranium chloride," *Annals of Nuclear Science and Engineering* 1, No. 4 (1974): pp. 277–281.
135. D. E. Holcomb, G. F. Flanagan, B. W. Patton, J. C. Gehin, R. L. Howard, and T. J. Harrison, 2011, *Fast spectrum molten salt reactor options*, ORNL/TM-2011/105.
136. O. Beneš and R. J. M. Konings, 2008, "Thermodynamic evaluation of the NaCl–MgCl<sub>2</sub>–UCl<sub>3</sub>–PuCl<sub>3</sub> system," *Journal of Nuclear Materials*, Vol. 375, No. 2, pp. 202–208.
137. J. Uhlíř, "Chemistry and technology of Molten Salt Reactors—history and perspectives." *Journal of nuclear materials*, Vol. 360, No. 1, pp. 6–11.

## Appendix A Citation Tables

Table A-1. ORNL technical reports for the Aircraft Nuclear Propulsion Program.

Date	Report Number	Report Title
May-46	Event	USAF-AEC Initiates the Nuclear Energy for Propulsion of Aircraft Project (NEPA)
Sep-49	Event	Beginning of the Aircraft Nuclear Propulsion (ANP) Program
Mar-51	ORNL-980	Dry Fluoride Process Status Report
Feb-52	ORNL-1252	General Information Concerning Fluorides
Feb-52	ORNL-1490	General Information Concerning Fluorides (follow-on to ORNL-1252)
Jun-52	ORNL-1234	Reactor Program of the Aircraft Nuclear Propulsion Project
Sep-52	ORNL-1491	Corrosion by Molten Fluorides
Feb-53	ORNL-1463	Methods of Fabrication of Control and Safety Element Components for the Aircraft and Homogenous Reactor Experiments
Mar-53	ORNL-1287	A Design Study of a Nuclear-Powered Airplane in which Circulating Fuel is Piped Directly to the Engine Air Radiators
Aug-53	ORNL-1535	Thermodynamic and Heat Transfer Analysis of the Aircraft Reactor Experiment
Aug-53	CF-53-9-84	A Reflector Moderated, Circulating Fuel, Aircraft Reactor
Sep-53	ORNL-1517	The Moderator Cooling System for the Reflector-Moderated Reactor
Oct-53	ORNL-1615	Critical Experiments on Direct Cycle Aircraft Reactor
Oct-53	ORNL-1634	Preliminary Critical Assembly for the Aircraft Reactor Experiment
Nov-54	ORNL-1721	ORNL Aircraft Nuclear Power Plant Designs
Nov-54	Event	Aircraft Reactor Experiment (2.5 MWt) Operated November 3 to 12, 1954
Jan-55	ORNL-1835	Aircraft Reactor Test Hazards Summary Report
Sep-55	ORNL-1845	Operation of the Aircraft Reactor Experiment
Jan-56	ORNL-1956	Enthalpies and Heat Capacities of Solid and Molten Fluoride Mixtures
Feb-56	ORNL-1976	Steady State Control Characteristics of Chemical Nuclear Aircraft Power Plants
May-56	ORNL-2095	Design Report on the Aircraft Reactor Test (60 MWt)
Aug-56	ORNL-2150	A Physical Property Summary for ANP Fluoride Mixtures
Feb-57	CF-57-2-130	The Physics of the Fused-Salt Reactor Experiment
Jun-57	ORNL-2295	Phase Equilibrium Diagrams for Fused Salt Systems
Aug-57	ORNL-2373	Effect of Radiation on Corrosion of Structural Materials by Molten Fluorides
Aug-57	ORNL-2374	Some Aspects of the Behavior of Fission Products in Molten Fluoride Reactor Fuels
Sep-57	Event	Work on Aircraft Reactor Test is Suspended
Oct-57	Event	Cancellation of Circulating-Fuel Reactors (including Aircraft Reactor Test), Aircraft Nuclear Propulsion Program Continues
Dec-57	ORNL-2376	Aircraft Reactor Test Fuel Pump and Xenon Removal System Development, Test Evaluation, and Aircraft Application
Mar-58	ORNL-2442	Thermal Stress Analysis of the Aircraft Reactor Test Heat Exchanger Channels and Header Pipes
Apr-58	ORNL-1868	Disassembly and Postoperative Examination of the Aircraft Reactor Experiment
Apr-58	ORNL-2199	Investigation of Fluid Flow in the Aircraft Reactor Test and other Reflector-Moderated Reactor Cores



Date	Report Number	Report Title
Nov-58	ORNL-2465	Termination Report for Construction of the Aircraft Reactor Test Facility
Mar-59	ORNL-2337	Interim Report on Corrosion by Alkali-Metal Fluorides; Work to May 1, 1953
Mar-60	ORNL-2464	Aircraft Reactor Test Removal and Disassembly
Jan-61	ORNL-2338	Interim Report on Corrosion by Zirconium-Based Fluorides; July 1952 to June 1956
Apr-57	CF-57-4-18	Engineering Design Features of the ORNL Fluoride Volatility Pilot Plant
Dec-57	CF-57-12-29	Declassification of Molten Salt Reactors
Dec-57	ORNL-2349	Aircraft Reactor Experiment - Metallurgical Aspects
Jan-58	CF-58-1-36	Some Aspects of the Behavior of Fission Products in Molten Fluoride Reactor Fuels
Feb-58	ORNL-2348	Components of the Fused-Salt and Sodium Circuits of the Aircraft Reactor Experiment
Apr-58	ORNL-1868	Disassembly and Postoperative Examination of the Aircraft Reactor Experiment
May-59	CF-59-5-108	Reprocessing of ARE Fuel, Volatility Pilot Plant Runs E-1 and E-2
Aug-59	CF-59-8-73	Reprocessing of ARE Fuel, Volatility Pilot Plant Runs E-3 through E-6
Jun-61	Event	Aircraft Nuclear Propulsion Program Cancelled

Table A-2. ORNL progress reports for the Aircraft Nuclear Propulsion Program.

<b>Report Number</b>	<b>Report Title</b>
ORNL-528	Aircraft Nuclear propulsion Project, Quarterly Progress Report, For Period Ending November 30, 1949
ORNL-629	Aircraft Nuclear propulsion Project, Quarterly Progress Report, For Period Ending February 28, 1950
ORNL-768	Aircraft Nuclear propulsion Project, Quarterly Progress Report, For Period Ending May 31, 1950
ORNL-858	Aircraft Nuclear propulsion Project, Quarterly Progress Report, For Period Ending August 31, 1950
ORNL-919	Aircraft Nuclear propulsion Project, Quarterly Progress Report, For Period Ending December 10, 1950
ANP-60	Aircraft Nuclear propulsion Project, Quarterly Progress Report, For Period Ending March 10, 1951
ANP-65	Aircraft Nuclear propulsion Project, Quarterly Progress Report, For Period Ending June 10, 1951
ORNL-1154	Aircraft Nuclear propulsion Project, Quarterly Progress Report, For Period Ending September 10, 1951
ORNL-1170	Aircraft Nuclear propulsion Project, Quarterly Progress Report, For Period Ending December 10, 1951
ORNL-1227	Aircraft Nuclear propulsion Project, Quarterly Progress Report, For Period Ending March 10, 1952
ORNL-1294	Aircraft Nuclear propulsion Project, Quarterly Progress Report, For Period Ending June 10, 1952
ORNL-1375	Aircraft Nuclear propulsion Project, Quarterly Progress Report, For Period Ending September 10, 1952
ORNL-1439	Aircraft Nuclear propulsion Project, Quarterly Progress Report, For Period Ending December 10, 1952
ORNL-1515	Aircraft Nuclear propulsion Project, Quarterly Progress Report, For Period Ending March 10, 1953
ORNL-1556	Aircraft Nuclear propulsion Project, Quarterly Progress Report, For Period Ending June 10, 1953
ORNL-1609	Aircraft Nuclear propulsion Project, Quarterly Progress Report, For Period Ending September 10, 1953
ORNL-1649	Aircraft Nuclear propulsion Project, Quarterly Progress Report, For Period Ending December 10, 1953
ORNL-1692	Aircraft Nuclear propulsion Project, Quarterly Progress Report, For Period Ending March 10, 1954
ORNL-1729	Aircraft Nuclear propulsion Project, Quarterly Progress Report, For Period Ending June 10, 1954
ORNL-1771	Aircraft Nuclear propulsion Project, Quarterly Progress Report, For Period Ending September 10, 1954

<b>Report Number</b>	<b>Report Title</b>
ORNL-1816	Aircraft Nuclear propulsion Project, Quarterly Progress Report, For Period Ending December 10, 1954
ORNL-1864	Aircraft Nuclear propulsion Project, Quarterly Progress Report, For Period Ending March 10, 1955
ORNL-1896	Aircraft Nuclear propulsion Project, Quarterly Progress Report, For Period Ending June 10, 1955
ORNL-1947	Aircraft Nuclear propulsion Project, Quarterly Progress Report, For Period Ending September 10, 1955
ORNL-2012	Aircraft Nuclear propulsion Project, Quarterly Progress Report, For Period Ending December 10, 1955
ORNL-2061	Aircraft Nuclear propulsion Project, Quarterly Progress Report, For Period Ending March 10, 1956
ORNL-2106	Aircraft Nuclear propulsion Project, Quarterly Progress Report, For Period Ending June 10, 1956
ORNL-2157	Aircraft Nuclear propulsion Project, Quarterly Progress Report, For Period Ending September 10, 1956
ORNL-2221	Aircraft Nuclear propulsion Project, Quarterly Progress Report, For Period Ending December 10, 1956
ORNL-2274	Aircraft Nuclear propulsion Project, Quarterly Progress Report, For Period Ending March 31, 1957
ORNL-2340	Aircraft Nuclear propulsion Project, Quarterly Progress Report, For Period Ending June 30, 1957
ORNL-2387	Aircraft Nuclear propulsion Project, Quarterly Progress Report, For Period Ending September 30, 1957
ORNL-2440	Aircraft Nuclear propulsion Project, Quarterly Progress Report, For Period Ending December 31, 1957
ORNL-2517	Aircraft Nuclear propulsion Project, Quarterly Progress Report, For Period Ending March 31, 1958
ORNL-2599	Aircraft Nuclear propulsion Project, Semiannual Progress Report, For Period Ending September 30, 1958
ORNL-2711	Aircraft Nuclear propulsion Project, Semiannual Progress Report, For Period Ending March 31, 1959
ORNL-2840	Aircraft Nuclear propulsion Project, Semiannual Progress Report, For Period Ending October 31, 1959
ORNL-2942	Aircraft Nuclear propulsion Project, Semiannual Progress Report, For Period Ending April 30, 1960
ORNL-3029	Aircraft Nuclear propulsion Project, Semiannual Progress Report, For Period Ending October 31, 1960
ORNL-3144	Aircraft Nuclear propulsion Project, Semiannual Progress Report, For Period Ending April 30, 1961
ORNL-3226	Aircraft Nuclear propulsion Project, Progress Report, For Period of May 1, 1961 to June 30, 1961

Table A-3. General Electric Company comprehensive technical reports for the Aircraft Nuclear Propulsion Program.

Date	Report Number	Report Title
Jun-62	APEX-901	Comprehensive Technical Report, General Electric Direct-Air-Cycle Aircraft Nuclear Propulsion Program, Program Summary and References
	APEX-902	Comprehensive Technical Report, General Electric Direct-Air-Cycle Aircraft Nuclear Propulsion Program, P-1 Nuclear Turbojet
	APEX-903	Comprehensive Technical Report, General Electric Direct-Air-Cycle Aircraft Nuclear Propulsion Program, Reactor Core Test Facility
	APEX-904	Comprehensive Technical Report, General Electric Direct-Air-Cycle Aircraft Nuclear Propulsion Program, Heat Transfer Reactor Experiment No. 1
	APEX-905	Comprehensive Technical Report, General Electric Direct-Air-Cycle Aircraft Nuclear Propulsion Program, Heat Transfer Reactor Experiment No. 2
Jun-62	APEX-906	Comprehensive Technical Report, General Electric Direct-Air-Cycle Aircraft Nuclear Propulsion Program, Heat Transfer Reactor Experiment No. 3
	APEX-907	Comprehensive Technical Report, General Electric Direct-Air-Cycle Aircraft Nuclear Propulsion Program, XMA-1 Nuclear Turbojet
	APEX-908	Comprehensive Technical Report, General Electric Direct-Air-Cycle Aircraft Nuclear Propulsion Program, XNJ140E Nuclear Turbojet
	APEX-909	Comprehensive Technical Report, General Electric Direct-Air-Cycle Aircraft Nuclear Propulsion Program, Aircraft Nuclear Propulsion System Studies
	APEX-910	Comprehensive Technical Report, General Electric Direct-Air-Cycle Aircraft Nuclear Propulsion Program, Aircraft Nuclear Propulsion Application Studies
	APEX-911	Comprehensive Technical Report, General Electric Direct-Air-Cycle Aircraft Nuclear Propulsion Program, Remote Handling Equipment
	APEX-912	Comprehensive Technical Report, General Electric Direct-Air-Cycle Aircraft Nuclear Propulsion Program, Control and Instrumentation
Jun-62	APEX-913	Comprehensive Technical Report, General Electric Direct-Air-Cycle Aircraft Nuclear Propulsion Program, Metallic Fuel Element Materials
	APEX-914	Comprehensive Technical Report, General Electric Direct-Air-Cycle Aircraft Nuclear Propulsion Program, Ceramic Reactor Materials
	APEX-915	Comprehensive Technical Report, General Electric Direct-Air-Cycle Aircraft Nuclear Propulsion Program, Shield Materials
	APEX-916	Comprehensive Technical Report, General Electric Direct-Air-Cycle Aircraft Nuclear Propulsion Program, Moderator Materials
	APEX-917	Comprehensive Technical Report, General Electric Direct-Air-Cycle Aircraft Nuclear Propulsion Program, Organic, Structural, and Control Materials
May-62	APEX-918	Comprehensive Technical Report, General Electric Direct-Air-Cycle Aircraft Nuclear Propulsion Program, Reactor and Shield Physics
Dec-61	APEX-919	Comprehensive Technical Report, General Electric Direct-Air-Cycle Aircraft Nuclear Propulsion Program, Aerothermodynamics
	APEX-920	Comprehensive Technical Report, General Electric Direct-Air-Cycle Aircraft Nuclear Propulsion Program, Applied Mechanics
	APEX-921	Comprehensive Technical Report, General Electric Direct-Air-Cycle Aircraft Nuclear Propulsion Program, Nuclear Safety

Table A-4. ORNL progress reports for the homogeneous reactor experiment/project/program.

Report Number	Report Title
ORNL-630	Homogenous Reactor Experiment, Report for the Quarter Ending February 28, 1950
	Homogenous Reactor Experiment, Quarterly Progress Report for Period Ending May 1950
ORNL-826	Homogenous Reactor Experiment, Quarterly Progress Report for Period Ending August 31, 1950
	Homogenous Reactor Experiment, Quarterly Progress Report for Period Ending November 1950
ORNL-990	Homogenous Reactor Experiment, Quarterly Progress Report for Period Ending February 28, 1951
ORNL-1057	Homogeneous Reactor Project, Quarterly Progress Report for the Period Ending May 15, 1951
ORNL-1121	Homogeneous Reactor Project, Quarterly Progress Report for the Period Ending August 15, 1951
ORNL-1221	Homogeneous Reactor Project, Quarterly Progress Report for the Period Ending November 15, 1951
ORNL-1280	Homogeneous Reactor Project, Quarterly Progress Report for the Period Ending March 15, 1952
ORNL-1318	Homogeneous Reactor Project, Quarterly Progress Report for the Period Ending July 1, 1952
ORNL-1424	Homogeneous Reactor Project, Quarterly Progress Report for the Period Ending October 1, 1952
ORNL-1478	Homogeneous Reactor Project, Quarterly Progress Report for the Period Ending January 1, 1953
ORNL-1554	Homogeneous Reactor Project, Quarterly Progress Report for the Period Ending March 31, 1953
ORNL-1605	Homogeneous Reactor Project, Quarterly Progress Report for the Period Ending July 31, 1953
ORNL-1658	Homogeneous Reactor Project, Quarterly Progress Report for the Period Ending October 31, 1953
ORNL-1678	Homogeneous Reactor Project, Quarterly Progress Report for the Period Ending January 31, 1954
ORNL-1753	Homogeneous Reactor Project, Quarterly Progress Report for the Period Ending April 30, 1954
ORNL-1772	Homogeneous Reactor Project, Quarterly Progress Report for the Period Ending July 31, 1954
ORNL-1813	Homogeneous Reactor Project, Quarterly Progress Report for the Period Ending October 31, 1954
ORNL-1853	Homogeneous Reactor Project, Quarterly Progress Report for the Period Ending January 31, 1955
ORNL-1895	Homogeneous Reactor Project, Quarterly Progress Report for the Period Ending April 30, 1955
ORNL-1943	Homogeneous Reactor Project, Quarterly Progress Report for the Period Ending July 31, 1955
ORNL-2004	Homogeneous Reactor Project, Quarterly Progress Report for the Period Ending October 31, 1955
ORNL-2057	Homogeneous Reactor Project, Quarterly Progress Report for the Period Ending January 31, 1956
ORNL-2096	Homogeneous Reactor Project, Quarterly Progress Report for the Period Ending April 30, 1956
ORNL-2148	Homogeneous Reactor Project, Quarterly Progress Report for the Period Ending July 31, 1956
ORNL-2222	Homogeneous Reactor Project, Quarterly Progress Report for the Period Ending October 31, 1956

<b>Report Number</b>	<b>Report Title</b>
ORNL-2272	Homogeneous Reactor Project, Quarterly Progress Report for the Period Ending January 31, 1957
ORNL-2331	Homogeneous Reactor Project, Quarterly Progress Report for the Period Ending April 30, 1957
ORNL-2379	Homogeneous Reactor Project, Quarterly Progress Report for the Period Ending July 31, 1957
ORNL-2432	Homogeneous Reactor Project, Quarterly Progress Report for the Period Ending October 31, 1957
ORNL-2493	Homogeneous Reactor Project, Quarterly Progress Report for the Period Ending January 31, 1958
ORNL-2561	Homogeneous Reactor Project, Quarterly Progress Report for the Period Ending April 30 and July 31, 1958
ORNL-2654	Homogeneous Reactor Project, Quarterly Progress Report for the Period Ending October 31, 1958
ORNL-2696	Homogeneous Reactor Project, Quarterly Progress Report for the Period Ending January 31, 1959
ORNL-2743	Homogeneous Reactor Project, Quarterly Progress Report for the Period Ending April 30, 1959
ORNL-2879	Homogeneous Reactor Program, Progress Report for the Period from May 1 through October 31, 1959
ORNL-2920	Homogeneous Reactor Program, Quarterly Progress Report for the Period Ending January 31, 1960
ORNL-2947	Homogeneous Reactor Program, Quarterly Progress Report for the Period Ending April 30, 1960
ORNL-3004	Homogeneous Reactor Program, Quarterly Progress Report for the Period Ending July 31, 1960
ORNL-3061	Homogeneous Reactor Program, Progress Report for the Period from August 1 to November 30, 1960
ORNL-3167	Homogeneous Reactor Program, Progress Report for the Period from December 1, 1960 to May 31, 1961

Table A-5. ORNL technical reports for the early development of molten salt power reactors.

Date	Report Number	Report Title
Sep-50	LA-1156	Lithium Isotope Separation by Electrolysis
Jul-53	ORNL-1592	Chemical Methods for the Separation of Lithium Isotopes
Sep-53	CF-53-10-25	Oak Ridge School of Reactor Technology: Study of a Fused Salt Breeder Reactor for Power Production
Oct-53	ORNL-1567	Heavy Isotope Build-Up in Core of U233 Breeder
May-54	CF-54-4-198 (Rev.)	Reactor Chemistry
Jul-54	ORNL-1702	A Summary of Density Measurements on Molten Fluoride Mixtures and a Correlation for Predicting Densities of Fluoride Mixtures
Sep-55	ORNL-1885	A Fused Salt - Fluoride Volatility Process for Recovery and Decontamination of Uranium
Oct-55	ORNL-1810	Some Economic Aspects of Thorium Breeder Reactors
Feb-56	ORNL-1924	A Theoretical Study of Xe135 Poisoning Kinetics in Fluid-Fueled, Gas-Sparged Nuclear Reactors
Aug-56	CF-56-8-204	Fused Salt Fast Breeder: Reactor Design and Feasibility Study (chloride salt)
Aug-56	CF-56-8-208	600 MW Fused Salt Homogeneous Reactor Power Plant: Reactor Design and Feasibility Study (fluoride salt)
Mar-57	ORNL-2265	An Analysis of Power Reactor Fuel Reprocessing
Apr-57	CF-57-4-27	A Preliminary Study of Molten Salt Power Reactors
Jun-57	ORNL-2264	Inconel as a Structural Material for a High-Temperature Fused-Salt Reactor
Jun-57	ORNL-2278	Viscosity Measurements on Molten Fluoride Mixtures
Jun-57	ORNL-2295	Phase Equilibria Diagrams for Fused Salt Systems
Oct-57	CF-57-10-41	Molten Salts for Civilian Power
Jan-58	ORNL-2421	Solubility Relations Among Some Fission Product Fluorides in NaF-ZrF <sub>4</sub> -UF <sub>4</sub> (50-46-4 mole %)
Feb-58	CF-58-2-46	A Molten Salt Natural Convection Reactor System
Jun-58	ORNL-2530	Solubility and Stability of PuF <sub>3</sub> in Fused Alkali Fluoride-Beryllium Fluoride Mixtures
Oct-58	CF-58-10-37	U233 Breeders - Commentary and General Remarks
Oct-58	CF-58-10-49	Cost Comparisons of Capital Investment in Various Nuclear Power Plants for Central Station Applications
Oct-58	CF-58-10-60	Survey of Low Enrichment Molten-Salt Reactors
Oct-58	ORNL-2605	Gas Cooled, Molten Salt Heat Exchanger - Design Study
Nov-58	ORNL-2396	Guide to the Phase Diagrams of the Fluoride Systems
Dec-58	CF-58-12-79	The Need for U233 Breeding
Jan-59	CF-59-1-26	A Preliminary Study of a Graphite Moderated Molten Salt Reactor
Feb-59	CF-59-1-13	Fuel Cycle Costs in a Graphite Moderated Slightly Enriched Fused Salt Reactor
Feb-59	CF-58-2-59	Results of X-Ray Diffraction Phase Analyses of Fused Salt Mixtures
Apr-59	CF-59-4-86	The Economics of Nuclear Power
Apr-59	CF-59-2-61	Processing of Molten Salt Power Reactor Fuel
Apr-59	ORNL-2661	The Fused Salt-Fluoride Volatility Process for Recovering Uranium
Jun-59	CF-59-6-89	Internally Cooled Molten-Salt Reactors

Date	Report Number	Report Title
Aug-59	CF-59-8-133	Molten Salt-Graphite Compatibility Test. Results of Physical and Chemical Measurements
Aug-59	ORNL-2719	Phase Equilibria in the Systems $\text{UF}_4\text{-ThF}_4$ and $\text{LiF-UF}_4\text{-ThF}_4$
Sep-59	ORNL-2751	Nuclear Characteristics of Spherical, Homogenous, Two-Region, Molten-Fluoride-Salt Reactors
Oct-59	ORNL-2749	Solubility Relations Among Rare-Earth Fluorides in Select Molten Fluoride Solvents
Nov-59	ORNL-2548	Phase Diagrams of Nuclear Reactor Materials
Jan-60	CF-59-12-64	Molten-Salt Breeder Reactors
Mar-60	CF-60-3-31	Interim Report on Fluid-Fuel Thermal Breeder Reactors
Mar-60	CF-60-3-31 (Rev.)	Interim Report on Fluid-Fuel Thermal Breeder Reactors
Mar-60	ORNL-2796	Experimental Molten-Salt-Fueled 30-MW Power Reactor
Jun-60	CF-60-6-97	Molten-Salt Reactors: Report for 1960 Ten-Year-Plan Evaluation
Sep-60	ORNL-2985	The Feasibility of an Unattended Nuclear Power Plant
Dec-60	ORNL-2896	Phase Equilibria in Molten Salt Breeder Reactor Fuels. I. The System $\text{LiF-BeF}_2\text{-UF}_4\text{-ThF}_4$
Dec-60	CF-60-12-111	Homogenous Molten Salt Reactor
May-61	CF-61-3-9	Thorium Breeder Reactor Evaluation. Part I. Fuel Yield and Fuel Cycle Costs in Five Thermal Breeders
May-61	CF-61-3-9	Thorium Breeder Reactor Evaluation. Part I. Fuel Yield and Fuel Cycle Costs in Five Thermal Breeders (Appendices)
Jun-61	CF-61-6-83	Economics of Thorium Fuel Cycles
Jun-61	ORNL-3124	INOR-8-Graphite-Fused Salt Compatibility Test
May-62	ORNL-TM-201	Conceptual Design of the Pebble Bed Reactor Experiment
Jul-62	ORNL-TM-241	Thorium Utilization Program: A Survey of Processing Methods for Thorium Reactor Fuels
Oct-62	ORNL-3293	Thermodynamic Properties of Molten-Salt Solutions



Table A-6. ORNL technical reports on fluorination and fluoride volatility processes.

Date	Report Number	Report Title
Apr-54	CF-54-4-217	Recovery of Uranium from Reduction Bomb Slag by Direct Fluorination
Jun-54	ORNL-1709	Recovery and Decontamination of Uranium from Fused Fluoride Fuels by Fluorination
Sep-55	ORNL-1885	A Fused Salt - Fluoride Volatility Process for Recovery and Decontamination of Uranium
Jun-56	CF-56-6-100	Feed Materials Status Report
Apr-57	CF-57-4-18	Engineering Design Features of the ORNL Fluoride Volatility Pilot Plant
May-58	CF-58-5-113	A Series of Seven Flowsheet Studies with Nonradive Salt, Volatility Pilot Plant Runs C-9 through C-15
Jun-58	CF-58-6-86	Volatility Studies of Some Fission Product Fluorides
Jul-58	CF-58-7-98	The Problem of Scrubbing the Hydrofluorination Off Gas with Liquid HF
Sep-58	ORNL-2550	Equipment Decontamination Methods for the Fused Salt - Fluoride Volatility Process
Dec-58	CF-58-12-50	Volatility Pilot Plant: Design of Hydrofluorinator for Dissolution of U-Zr Fuel Elements
Dec-58	CF-58-12-55	Volatility Pilot Plant Modifications - Hydrogen Fluoride Condensers, FV-2004, FV-2005
Apr-59	ORNL-2661	The Fused Salt-Fluoride Volatility Process for Recovering Uranium
Apr-59	CF-59-2-61	Processing of Molten Salt Power Reactor Fuel
May-59	CF-59-5-89	Volatility: Fluorinator Design FV-100, Zr-U Fuel Element Processing Phase
May-59	CF-59-5-108	Reprocessing of ARE Fuel, Volatility Pilot Pant Runs E-1 and E-2
Aug-59	CF-59-8-73	Reprocessing of ARE Fuel, Volatility Pilot Pant Runs E-3 through E-6
Sep-59	CF-59-9-5	Plutonium Behavior in the Fluoride Volatility Process
Nov-59	CF-59-11-110	Thermodynamics in the Fused Salt Dissolution Process for Zirconium Fuel
Jul-60	CF-60-3-74 (Rev.)	Volatility Pilot Plant - Hazards Review Report
Sep-60	CF-60-7-65	Engineering Evaluation of Volatility Pilot Plant Equipment
Jun-61	ORNL-2832	Corrosion Associated with Fluorination in the Oak Ridge National Laboratory Fluoride Volatility Process
Nov-61	ORNL-2833	Corrosion Associated with Fluorination in the Oak Ridge National Laboratory Fluoride Volatility Process
Dec-61	ORNL-TM-80	Laboratory-Scale Demonstration of the Fused Salt Volatility Process
Feb-62	ORNL-3253	Corrosion of Volatility Pilot Plant Mark I INOR-8 Hydrofluorinator and Mark III L Nickel Fluorinator after Fourteen Dissolution Runs
Sep-62	ORNL-3280	Use of Fused Salt Fluoride Volatility Process with Irradiated Urania Decayed 15-30 Days
Sep-62	ORNL-3298	Recovery of PuF <sub>6</sub> by Fluorination of Fused Fluoride Salts
Oct-62	ORNL-TM-522	Design Studies and Cost Estimates of Two Fluoride Volatility Plants
Jan-63	ORNL-3371	Evaluation of Automatic Data Processing in the Fluoride Volatility Pilot Plant
Oct-63	ORNL-TM-717	Process Developments in the ORNL Fluoride Volatility Program, October 1962 - September 1963
Jun-64	ORNL-3596	Adaptation of the Fused-Salt Fluoride-Volatility Process to the Recovery of Uranium from Aluminum-Uranium Alloy Fuel

Date	Report Number	Report Title
Aug-64	ORNL-3594	Molten-Salt Solvents for Fluoride Volatility Processing of Aluminum-Matrix Nuclear Fuel Elements
Oct-64	ORNL-TM-972	Proposed Design of a Fluidized-Bed Fluoride-Volatility Pilot Plant for Installation at Oak Ridge National Laboratory
Jul-65	ORNL-TM-1206	Fluidized Bed Volatility - Process for BrF <sub>5</sub> Fluorination and UF <sub>6</sub> Recovery
Jan-66	ORNL-3791	Preliminary Design Study of a Continuous Fluorination-Vacuum-Distillation System for Regenerating Fuel and Fertile Streams in a Molten Salt Breeder Reactor
Jul-67	ORNL-TM-1849	Fluoride Volatility Processing Semiannual Progress Report for Period Ending November 30, 1966
Jan-68	ORNL-TM-2058	Measurement of the Relative Volatilities of Fluorides of Ce, La, Pr, Nd, Sm, Eu, Ba, Sr, Y and Zr in Mixtures of LiF and BeF <sub>2</sub>
Jan-68	ORNL-4251	Molten-Salt Fluoride Volatility Pilot Plant: Equipment Performance During Processing of Aluminum-Clad Fuel Elements
Nov-68	ORNL-4224	Fluorination of Falling Droplets of Molten Fluoride Salt as a Means of Recovering Uranium and Plutonium
Jan-69	ORNL-4414	Disposal of Solid Waste from the Reprocessing of Nuclear Fuels by the Fluidized-Bed Fluoride-Volatility Process: Evaluation of the Canning of Waste Powders
Apr-69	ORNL-TM-2170	Hot-Cell Studies of the Fluidized Bed Fluoride Volatility Process for Recovering Uranium and Plutonium from Spent UO <sub>2</sub> Fuels
Jun-69	ORNL-4415	Liquid-Vapor Equilibria in LiF-BeF <sub>2</sub> and LiF-BeF <sub>2</sub> -ThF <sub>4</sub> Systems
Apr-71	ORNL-4574	Molten-Salt Fluoride Volatility Pilot Plant: Recovery of Enriched Uranium from Aluminum-Clad Fuel Elements

Table A-7. ORNL technical reports for the two-fluid molten salt breeder reactor.

Date	Report Number	Report Title
May-61	CF-61-5-62	Xenon Poisoning in Molten Salt Reactors
Aug-61	CF-61-8-86	Thorium Breeder Reactor Evaluation. Part 1. Fuel Yields and Fuel Cycle Costs of a Two-Region, Molten Salt Breeder Reactor
Dec-62	ORNL-3373	Thermal Analysis and Gradient Quenching Apparatus and Techniques for the Investigation of Fused Salt Phase Equilibria
May-63	ORNL-TM-528	Design and Operation of a Forced-Circulation Corrosion Test Loops with Molten Salt
Aug-63	ORNL-3691	Mixtures of Metals with Molten Salts
Aug-63	ORNL-3411	Review of Electronic Absorption Spectra of Molten Salts
Jan-64	ORNL-3544	Reduction of Uranium Hexafluoride Retention on Beds of Magnesium Fluoride used for Removal of Technetium Hexafluoride
Mar-65	ORNL-TM-1051	Reconstitution of MSR Fuel by Reducing $UF_6$ Gas to $UF_4$ in a Molten Salt
May-65	ORNL-3804	Rare-Earth Halides
Mar-66	ORNL-TM-1467	Summary of Molten-Salt Breeder Reactor Design Studies
Aug-66	ORNL-3996	Design Studies of 1000-MWe Molten-Salt Breeder Reactors
Mar-67	ORNL-TM-1730	Considerations of Low Pressure Distillation and Its Application to Processing of Molten Salt Breeder Reactor Fuels
Aug-67	ORNL-TM-1946	Review of Molten Salt Reactor Physics Calculations
Sep-67	ORNL-TM-1545	Design Study of a Heat-Exchanger System for One MSBR Concept
Nov-67	ORNL-TM-2047	Containers for Molten Fluoride Spectroscopy
Jan-68	ORNL-TM-2058	Measurement of the Relative Volatilities of Fluorides of Ce, La, Pr, Nd, Sm, Eu, Ba, Sr, Y and Zr in Mixtures of LiF and $BeF_2$
Mar-68	ORNL-TM-2180	Electrical Conductivity of Molten Fluorides: A Review
Apr-68	ORNL-TM-2213	Design of an Engineering-Scale Vacuum Distillation Experiment for Molten-Salt Reactor Fuel
Jun-68	ORNL-TM-2256	Chemical Feasibility of Fueling Molten Salt Reactors with $PuF_3$
Dec-68	ORNL-4327	Mechanical Properties of Artificial Graphites - A Survey Report
Aug-70	ORNL-4528	Two-Fluid Molten-Salt Breeder Reactor Design Study (Status as of January 1, 1968)

Table A-8. Special series of ORNL technical reports for the two-fluid molten salt breeder reactor.

Date	Report Number	Report Title
Jun-67	ORNL-TM-1851	Summary of the Objectives, the Design, and a Program of Development of Molten-Salt Breeder Reactors
Jun-67	ORNL-TM-1852	Fuel and Blanket Processing Development for Molten Salt Breeder Reactors
Jun-67	ORNL-TM-1853	Chemical Research and Development for Molten-Salt Breeder Reactors
Jun-67	ORNL-TM-1854	Materials Development for Molten-Salt Breeder Reactors
Jun-67	ORNL-TM-1855	Components and Systems Development for Molten-Salt Breeder Reactors
May-67	ORNL-TM-1856	Instrumentation and Controls Development for Molten-Salt Breeder Reactors
Aug-71	ORNL-TM-3303	Further Discussion of Instrumentation and Controls Development Needed for the Molten Salt Breeder Reactor (follow-on to ORNL-TM-1856)
Jun-67	ORNL-TM-1857	Physics Program for Molten-Salt Breeder Reactors
Jun-67	ORNL-TM-1858	Safety Program for Molten-Salt Breeder Reactors
Jun-67	ORNL-TM-1859	Maintenance Development for Molten-Salt Breeder Reactors

Table A-9. ORNL technical reports for the Molten Salt Reactor Experiment.

Date	Report Number	Report Title
Jul-60	CF-60-7-96	Reactor Physics Calculations for the MSRE
Sep-60	CF-60-9-55	MSRE Drain Tank - Heat Removal Studies
Nov-60	CF-60-11-108	MSRE Radiator Design
Feb-61	CF-61-2-46	Molten-Salt Reactor Experiment Preliminary Hazards Report
Aug-61	CF-61-2-46(1st Add.)	Addendum to ORNL CF-61-2-46, Molten-Salt Reactor Experiment Preliminary Hazards Report
May-62	CF-61-2-46(2nd Add.)	Molten-Salt Reactor Experiment Preliminary Hazards Report, Addendum No. 2 to ORNL CF-61-2-46
Apr-61	CF-61-4-62	MSRE Preliminary Physics Report
Feb-62	ORNL-TM-128	Development of Freeze Valve for Use in the MSRE
May-62	ORNL-TM-251	Safety Calculations for MSRE
Sep-62	ORNL-TM-328	Corrosion Behavior of Reactor Materials in Fluoride Salt Mixtures
Nov-63	ORNL-3500	Fabrication of the Heat Exchanger Tube Bundle for the Molten-Salt Reactor Experiment
Aug-64	ORNL-3661	Influence of Several Metallurgical Variable on the Tensile Properties of Hastelloy N
Feb-65	ORNL-TM-1017	Tensile and Creep Properties of INOR-8 for the Molten-Salt Reactor Experiment
Feb-65	ORNL-TM-1023	Tube Plugging in the Molten-Salt Reactor Experiment Primary Heat Exchanger
Jun-65	Event	MSRE Beginning of Phase I Program U235 Operations
Dec-65	ORNL-TM-1070	Stability Analysis of the Molten-Salt Reactor Experiment
Aug-66	ORNT-TM-497	Analysis of Filling Accidents in MSRE
Oct-66	ORNL-TM-1626	Period Measurements on the Molten Salt Reactor Experiment During Fuel Circulation: Theory and Experiment
Oct-66	ORNL-TM-1647	Experimental Dynamic Analysis of the Molten-Salt Reactor Experiment
Jun-67	ORNL-4069	Development of a Model for Computing $^{135}\text{Xe}$ Migration in the MSRE
Jul-67	ORNL-4123	MSRE Control Elements: Manufacture, Inspection, Drawings, and Specifications
Aug-67	CF-67-8-10	Program Plan for the Molten Salt Reactor Experiment
Aug-67	ORNL-TM-1127 (Rev.)	Description of Facility Radiation and Contamination Systems Installed in the Molten Salt Reactor Experiment, Bldg. 7503
Sep-67	ORNL-4148	Gas Transport in MSRE Moderator Graphite. I. Review of Theory and Counterdiffusion Experiments
Nov-67	ORNL-TM-1997	An Evaluation of the Molten Salt Reactor Experiment Hastelloy N Surveillance Specimens - First Group
Feb-68	ORNL-4233	Zero-Power Physics Experiments on the Molten-Salt Reactor Experiment
Mar-68	Event	MSRE End of Phase I Program U235 Operations
Jul-68	ORNL-4257	An EMF Study of $\text{LiF-BeF}_2$ Solutions
Aug-68	Event	U235 Removed from the Fuel Salt and Replaced with U233
Aug-68	ORNL-TM-2316	Physical Properties of Molten-Salt Reactor Fuel, Coolant, and Flush Salts
Oct-68	Event	MSRE Beginning of Phase II Program U233 Operations
Feb-69	ORNL-TM-2359	An Evaluation of the Molten-Salt Reactor Experiment Hastelloy N Surveillance Specimens - Second Group
Mar-69	ORNL-TM-2478	Design, Construction, and Testing of a Large Molten Salt Filter

Date	Report Number	Report Title
Mar-69	ORNL-4371	Preparation of Enriching Salt $7\text{LiF}\cdot 233\text{UF}_4$ For Refueling the Molten Salt Reactor
May-69	ORNL-4389	Gas Transport in MSRE Moderator Graphite. II. Effects of Impregnation. III. Variation of Flow Properties
Jun-69	ORNL-4397	Analysis of Transients in the MSRE System with $233\text{U}$ Fuel
Aug-69	ORNL-TM-2578	Processing of the MSRE Flush and Fuel Salts
Dec-69	Event	MSRE End of Phase II Program $\text{U}233$ Operations
Jan-70	ORNL-TM-2647	An Evaluation of the Molten-Salt Reactor Experiment Hastelloy N Surveillance Specimens – Third Group
Apr-70	ORNL-TM-2974	Plans for Post-Operation Examination of the Molten-Salt Reactor Experiment
Apr-70	ORNL-TM-2999	Quality-Assurance Practices in Construction and Maintenance of the Molten-Salt Reactor Experiment
Sep-70	ORNL-CF-70-9-3	Critique of the Molten-Salt Reactor Experiment: A Collection of Comments Submitted by Persons Associated with the Reactor
Sep-70	ORNL-TM-3144	Fluorine Production and Recombination in Frozen MSR Salts After Reactor Operation
Oct-70	ORNL-TM-2987	Development of Fuel and Coolant-Salt Centrifugal Pumps for the Molten-Salt Reactor Experiment
Jan-71	ORNL-4434	Low-Pressure Distillation of Molten Fluoride Mixtures: Nonradioactive Tests for the MSRE Distillation Experiment
Jan-71	ORNL-4616	Preparation and Handling of Salt Mixtures for the Molten Salt Reactor Experiment
Aug-71	ORNL-4577	Low-Pressure Distillation of a Portion of the Fuel Carrier Salt from the Molten Salt Reactor Experiment
Oct-71	ORNL-TM-3524	Operation of the Sampler-Enricher in the Molten Salt Reactor Experiment
Dec-71	ORNL-4658	Chemical Aspects of MSRE Operations
Feb-72	ORNL-4674	Reactivity Balance Calculations and Long-Term Reactivity Behavior with $235\text{U}$ in the MSRE
Aug-72	ORNL-TM-3151	A Study of Fission Products in the Molten-Salt Reactor Experiment by Gamma Spectroscopy
Nov-72	ORNL-4829	Intergranular Cracking of INOR-8 in the MSRE
Dec-72	ORNL-TM-4174	Post Irradiation Examination of Materials from the MSRE
Jun-73	ORNL-TM-3039	MSRE Systems and Components Performance
Aug-73	ORNL-TM-3041	MSRE Operator Training and Operating Techniques
Oct-75	ORNL-4865	Fission Product Behavior in the Molten Salt Reactor Experiment

Table A-10. Special series of ORNL technical reports for the Molten Salt Reactor Experiment.

Date	Report Number	Report Title
Jan-65	ORNL-TM-728	MSRE Design and Operations Report, Part I, Description of Reactor Design
Feb-68	ORNL-TM-729	MSRE Design and Operations Report, Part II-A, Nuclear and Process Instrumentation
Sep-72	ORNL-TM-729	MSRE Design and Operations Report, Part II-B, Nuclear and Process Instrumentation
Feb-64	ORNL-TM-730	MSRE Design and Operations Report, Part III, Nuclear Analysis
Not Published	ORNL-TM-731	MSRE Design and Operations Report, Part IV, Chemistry and Materials
Aug-64	ORNL-TM-732	MSRE Design and Operations Report, Part V, Reactor Safety Analysis Report
Feb-68	ORNL-TM-2111	MSRE Design and Operations Report, Part V-A, Safety Analysis of Operation with 233U
Apr-65	ORNL-TM-733	MSRE Design and Operations Report, Part VI, Operating Safety Limits for the Molten-Salt Experiment
Aug-65	ORNL-TM-733 (Rev.)	MSRE Design and Operations Report, Part VI, Operating Safety Limits for the Molten-Salt Reactor Experiment
Jul-69	ORNL-TM-733 (Rev. 3)	MSRE Design and Operations Report, Part VI, Operating Safety Limits for the Molten-Salt Reactor Experiment
May-65	ORNL-TM-907	MSRE Design and Operations Report, Part VII, Fuel Handling and Processing Plant
Dec-67	ORNL-TM-907 (Rev.)	MSRE Design and Operations Report, Part VII, Fuel Handling and Processing Plant
Jan-65	ORNL-TM-908	MSRE Design and Operations Report, Part VIII, Operating Procedures, Volume I
Jan-66	ORNL-TM-908	MSRE Design and Operations Report, Part VIII, Operating Procedures, Volume II
Jun-65	ORNL-TM-909	MSRE Design and Operations Report, Part IX, Safety Procedures and Emergency Plans
Jun-68	ORNL-TM-910	MSRE Design and Operations Report, Part X, Maintenance Equipment and Procedures
Nov-66	ORNL-TM-911	MSRE Design and Operations Report, Part XI, Test Program
Sep-68	ORNL-TM-2304	MSRE Design and Operations Report, Part XI-A, Test Program for 233U Operation

Table A-11. ORNL technical reports for the MSR experiment decommissioning.

Date	Report Number	Report Title
Feb-71	ORNL-TM-3253	MSRE Procedures for the Periods Between Examination and Ultimate Disposal (Phase III of Decommissioning Program)
Jan-72	CF-72-1-1	Consideration of Possible Methods of Disposal of MSRE Salts
Aug-77	ORNL-CF-77-391	Decommissioning Study for the ORNL Molten-Salt Reactor Experiment (MSRE)
Sep-84	X-OE-231, Vol. 5	Preliminary Decommissioning Study Reports, Volume 5: Molten Salt Reactor Experiment
Dec-85	ORNL-TM-9756	Extended Storage-in-Place of MSRE Fuel Salt and Flush Salt
Jan-88	ORNL-RAP-17	Decommissioning of the Molten Salt Reactor Experiment a Technical Evaluation
Jan-96	ORNL-TM-13142	A Descriptive Model of the Molten Salt Reactor Experiment After Shutdown: Review of FY 1995 Progress
Sep-96	INEL-96-0329	Evaluation of Potential for MSRE Spent Fuel and Flush Salt Storage and Treatment at the INEL
Nov-96	ORNL-M-5506	Chemical Interactions During Melting of the MSRE Fuel Salt
Jun-98	DOE/OR/02-1671&D2	Record of Decision for Interim Action to Remove Fuel and Flush Salts from the Molten Salt Reactor Experiment Facility at the Oak Ridge National Laboratory, Oak Ridge, Tennessee
Jan-00	ORNL-TM-1999-287	System Requirement Document for the Molten Salt Reactor Experiment 233U Conversion System

Table A-12. ORNL technical reports for the MSCR.

Date	Report Number	Report Title
Jun-62	SL-1954	Capital Cost Evaluation, 1000 MWe Molten Salt Converter Reactor Power Plants
Oct-62	ORNL-TM-522	Design Studies and Cost Estimates of Two Fluoride Volatility Plants (to support converter reactor)
Jan-65	ORNL-3686	A Comparative Evaluation of Advanced Converters (not molten-salt reactors)
Sep-65	ORNL-TM-1060	Molten Salt Converter Reactor Design Study and Power Cost Estimates for a 1000 MWe Station

Table A-13. ORNL technical reports for the molten salt breeder experiment.

Date	Report Number	Report Title
Aug-69	ORNL-TM-2643	Conceptual System Design Description of the Salt Pump Test Stand for the Molten Salt Breeder Experiment
Dec-69	ORNL-TM-2780	Preliminary Systems Design Description (Title I Design) of the Salt Pump Stand for the Molten Salt Breeder Experiment
Nov-70	ORNL-TM-3177	Molten Salt Breeder Experiment Design Basis (150 MWth)

Table A-14. ORNL technical reports for the MSR demonstration.

Date	Report Number	Report Title
Jun-72	ORNL-TM-3832	Design Studies of a Molten-Salt Reactor Demonstration Plant (350 MWe)

Table A-15. ORNL technical reports for the single-fluid molten salt breeder reactor.

Date	Report Number	Report Title
Apr-69	ORNL-TM-2490	Compatibility of Hastelloy N and Croloy 9M with NaBF <sub>4</sub> -NaF-KBF <sub>4</sub> (90-4-6 mole %) Fluoroborate Salt
Aug-69	ORNL-3391	Mixtures of Metals with Molten Salts
Jun-69	ORNL-TM-2489	MSBR Control Studies
Feb-70	ORNL-4473	Encapsulation of Noble Fission Product Gases in Solid Media Prior to Transportation and Storage
May-70	ORNL-TM-2927	Control Studies of a 1000 MWe MSBR
Jul-70	ORNL-4451	Siting of Fuel Reprocessing Plants and Waste Management Facilities
Nov-70	ORNL-MIT-117	Removal of Tritium from the Molten Salt Breeder Reactor Fuel
Mar-71	ORNL-4575, Vol. 1	Corrosion in Polythermal Loop Systems. I. Mass Transfer Limited by Surface and Interfacial Resistance as Compared with Sodium-Inconel Behavior
May-71	ORNL-TM-3102	MSBR Control Studies: Analog Simulation Program
Jun-71	ORNL-4541	Conceptual Design Study of a Single-Fluid Molten-Salt Reactor
Jun-71	ORNL-4575, Vol. 2	Corrosion in Polythermal Loop Systems II. A Solid-State Diffusion Mechanism with and without Liquid Film Effects
Dec-71	EIS-71:022	Technical Report of the Molten Salt Group, Part 1, Evaluation of a 1000 MWe Molten-Salt Breeder Reactor
Dec-71	EIS-71:023	Technical Report of the Molten Salt Group, Part 2, Evaluation of a 1000 MWe Molten-Salt Breeder Reactor
Feb-72	TID-26156	1000 MWe Molten Salt Breeder Reactor Conceptual Design Study, Final Report - Task 1
May-72	ORNL-TM-3579	Design and Cost Study of a Fluorination - Reductive Extraction - Metal Transfer Processing Plant for the MSBR
Aug-72	ORNL-4812	The Development Status of Molten-Salt Breeder Reactors
Dec-72	ORNL-TM-4122	Development of a Venturi Type Bubble Generator for Use in the Molten-Salt Reactor Xenon Removal System
Dec-72	ORNL-TM-4188	Effect of FeF <sub>2</sub> Addition on Mass Transfer in a Hastelloy N - LiF-BeF <sub>2</sub> -UF <sub>4</sub> Thermal Convection Loop System
Dec-72	ORNL-4874	Development and Construction of a Molybdenum Test Stand
Jan-73	ORNL-TM-3863	Design and Operation of a Forced-Circulation Corrosion Test Facility (MSR-FCL-1) Employing Hastelloy N Alloy and Sodium Fluoroborate Salt
Feb-73	ORNL-4831	Development of the Variable-Gap Technique for Measuring the Thermal Conductivity of Fluoride Salt Mixtures
May-73	ORNL-4628	ORIGEN - The ORNL Isotope Generation and Depletion Code
May-73	ORNL-TM-4179	Improved Representation of Some Aspects of Circulating-Fuel Reactor Kinetics
Mar-73	ORNL-TM-4308	Density and Viscosity of Several Molten Fluoride Mixtures
Mar-74	ORNL-TM-4533	Development of an Axial-Flow Centrifugal Gas Bubble Separator for Use in MSR Xenon Removal Systems
Dec-74	ORNL-5018	Program Plan for Development of Molten-Salt Breeder Reactors
Apr-75	ORNL-TM-4804	A Method for Calculating the Steady-State Distribution of Tritium in a Molten-Salt Breeder Reactor Plant
Jun-75	ORNL-TM-4802	The Molten-Salt Reactor Information System
Sep-76	ORNL-TM-4210	MRPP - Multiregion Processing Plant Code



Date	Report Number	Report Title
Apr-76	ORNL-TM-5325	Evaluation of Alternate Secondary (and Tertiary) Coolants for the Molten-Salt Breeder Reactor
Jul-76	ORNL-TM-5253	Conceptual Design of a Continuous Fluorinator Experimental Facility (CFEF)
Nov-76	ORNL-TM-5503	Temperature Gradient Compatibility Tests of Some Refractory Metals and Alloys in Bismuth and Bismuth-Lithium Solutions
Nov-76	ORNL-5143	Measurement of Mass Transfer Coefficients in a Mechanically Agitated, Nondispersing Contactor Operating with a Molten Mixture of LiF-BeF <sub>2</sub> -ThF <sub>4</sub> and Molten Bismuth
Feb-77	ORNL-5176	Engineering Tests of the Metal Transfer Process for Extraction of Rare-Earth Fission Products from a Molten-Salt Breeder Reactor Fuel Salt
Apr-77	ORNL-TM-5759	Distribution and Behavior of Tritium in the Coolant-Salt Technology Facility
May-77	ORNL-TM-5783	Compatibility Studies of Potential Molten-Salt Breeder Reactor Materials in Molten Fluoride Salts
Oct-77	ORNL-TM-6002	Status of Tellurium-Hastelloy N Studies in Molten Fluoride Salts
Jan-78	ORNL-TM-5920	Status of Materials Development for Molten Salt Reactors

Table A-16. Special series of ORNL technical reports for the single-fluid molten salt breeder reactor.

Report Number	Report Title
ORNL-TM-3053	Engineering Development Studies for Molten-Salt Breeder Reactor Processing No. 1, Period Ending December 1968
ORNL-TM-3137	Engineering Development Studies for Molten-Salt Breeder Reactor Processing No. 2, Period Ending March 1969
ORNL-TM-3138	Engineering Development Studies for Molten-Salt Breeder Reactor Processing No. 3, Period Ending June 1969
ORNL-TM-3139	Engineering Development Studies for Molten-Salt Breeder Reactor Processing No. 4, Period Ending September 1969
ORNL-TM-3140	Engineering Development Studies for Molten-Salt Breeder Reactor Processing No. 5, Period Ending December 1969
ORNL-TM-3141	Engineering Development Studies for Molten-Salt Breeder Reactor Processing No. 6, Period Ending March 1970
ORNL-TM-3257	Engineering Development Studies for Molten-Salt Breeder Reactor Processing No. 7, Period Ending June 1970
ORNL-TM-3258	Engineering Development Studies for Molten-Salt Breeder Reactor Processing No. 8, Period Ending September 1970
ORNL-TM-3259	Engineering Development Studies for Molten-Salt Breeder Reactor Processing No. 9, Period Ending December 1970
ORNL-TM-3352	Engineering Development Studies for Molten-Salt Breeder Reactor Processing No. 10, Period Ending March 1971
ORNL-TM-3774	Engineering Development Studies for Molten-Salt Breeder Reactor Processing No. 11 (cancelled 2/14/1979)
ORNL-TM-3775	Engineering Development Studies for Molten-Salt Breeder Reactor Processing No. 12 (cancelled 4/6/1976)
ORNL-TM-3776	Engineering Development Studies for Molten-Salt Breeder Reactor Processing No. 13 (cancelled 4/6/1976)
ORNL-TM-4018	Engineering Development Studies for Molten-Salt Breeder Reactor Processing No. 14 (cancelled 4/6/1976)
ORNL-TM-4019	Engineering Development Studies for Molten-Salt Breeder Reactor Processing No. 15 (cancelled 4/6/1976)
ORNL-TM-4020	Engineering Development Studies for Molten-Salt Breeder Reactor Processing No. 16 (cancelled 4/6/1976)
ORNL-TM-4178	Engineering Development Studies for Molten-Salt Breeder Reactor Processing No. 17 (cancelled 4/6/1976)
ORNL-TM-4698	Engineering Development Studies for Molten-Salt Breeder Reactor Processing No. 18, Period January through June 1974
ORNL-TM-4863	Engineering Development Studies for Molten-Salt Breeder Reactor Processing No. 19, Period July through September 1974
ORNL-TM-4870	Engineering Development Studies for Molten-Salt Breeder Reactor Processing No. 20, Period October through December 1974
ORNL-TM-4894	Engineering Development Studies for Molten-Salt Breeder Reactor Processing No. 21, Period January through March 1975
ORNL-TM-5041	Engineering Development Studies for Molten-Salt Breeder Reactor Processing No. 22, Period April through June 1975

Table A-17. ORNL technical reports for the denatured MSR.

Date	Report Number	Report Title
Feb-77	ORNL-TM-5750	Preliminary Report on the Promise of Accelerator Breeding and Converter Reactor Symbiosis (ABACS) as an Alternative Energy System
Aug-78	ORNL-TM-6413	Molten-Salt Reactors for Efficient Nuclear Fuel Utilization without Plutonium Separation
Mar-79	ORNL-TM-6415	Development Status and Potential Program for Development of Proliferation-Resistant Molten-Salt Reactors
Dec-79	ORNL-5388	Interim Assessment of the Denatured 233U Fuel Cycle: Feasibility and Nonproliferation Characteristics
Dec-79	ORNL-5388-R1	Interim Assessment of the Denatured 233U Fuel Cycle: Feasibility and Nonproliferation Characteristics
Dec-79	ORNL-5388-Summary	Interim Assessment of the Denatured 233U Fuel Cycle: Feasibility and Nonproliferation Characteristics
Dec-79	ORNL-5388-ERATTA	Interim Assessment of the Denatured 233U Fuel Cycle: Feasibility and Nonproliferation Characteristics
Jul-80	ORNL-TM-7207	Conceptual Design Characteristics of a Denatured Molten-Salt Reactor with Once-Through Fueling

Table A-18. Recent ORNL technical reports on MSR technologies.

Date	Report Number	Report Title
Oct-94	ORNL-M-2733-R1	R. L. Jolley, R. K. Genung, L. E. McNeese, J. E. Mrochek; The ORNL Chemical Technology Division 1950-1994
Feb-95	ORNL-TM-12925	J. R. DiStefano, J. H. DeVan, J. R. Keiser, R. L. Klueh, W. P. Eatherly; Materials Considerations for Molten Salt Accelerator-Based Plutonium Conversion Systems
Mar-95	ORNL-TM-12925-R1	J. R. DiStefano, J. H. DeVan, J. R. Keiser, R. L. Klueh, W. P. Eatherly; Materials Considerations for Molten Salt Accelerator-Based Plutonium Conversion Systems
Sep-99	ORNL-6952	C. W. Forsberg, L. C. Lewis; Uses for Uranium-233: What Should Be Kept for Future Needs?
Sep-00	ORCA-7	A. S. Quist; A History of Classified Activities at Oak Ridge National Laboratory
Dec-05	ORNL-TM-2005-556	W. R. Corwin, et al.; Updated Generation IV Reactors Integrated Materials Technology Program Plan, Revision 2
Mar-06	ORNL-TM-2006-12	D. F. Williams, L. M. Toth, K. T. Clarno; Assessment of Candidate Molten Salt Coolants for the Advanced High-Temperature Reactor (AHTR)
Jun-06	ORNL-TM-2006-69	D. F. Williams; Assessment of Candidate Molten Salt Coolants for the NGNP/NHI Heat-Transfer Loop
Aug-08	ORNL-TM-2008-129	W. R. Corwin, et al.; Generation IV Reactors Integrated Materials Technology Program Plan: Focus on Very High Temperature Reactor Materials
Mar-10	ORNL-TM-2009-181	M. W. Rosenthal; An Account of Oak Ridge National Laboratory's Thirteen Nuclear Reactors
Jul-11	ORNL-TM-2011-105	D. E. Holcomb, G. F. Flanagan, B. W. Patton, J. C. Gehin, R. L. Howard, T. J. Harrison; Fast Spectrum Molten Salt Reactor Options
Dec-13	ORNL-TM-2013-543	B. Ade, A. Worrall, J. Powers, S. Bowman, G. Flanagan, J. Gehin; Safety and Regulatory Issues of the Thorium Fuel Cycle
May-16	ORNL-TM-2016-199	K. R. Robb, P. K. Jain, T. J. Hazelwood; High-Temperature Salt Pump Review and Guidelines - Phase I Report

Apr-17	ORNL-LTR-2017-135	D. F. Williams, P. F. Britt, Editors; Molten Salt Chemistry Workshop, Technology and Applied R&D Needs for Molten Salt Chemistry: Innovative Approaches to Accelerate Molten Salt Reactor Technologies Deployment
--------	-------------------	---

Table A-19. ORNL progress reports for the MSR Program.

Report Number	Report Title
ORNL-2378	Molten-Salt Reactor Program Quarterly Progress Report, For Period Ending September 1, 1957
ORNL-2431	Molten-Salt Reactor Program Quarterly Progress Report, For Period Ending October 31, 1957
ORNL-2474	Molten-Salt Reactor Program Quarterly Progress Report, For Period Ending January 31, 1958
ORNL-2551	Molten-Salt Reactor Program Quarterly Progress Report, For Period Ending June 30, 1958
ORNL-2626	Molten-Salt Reactor Program Quarterly Progress Report, For Period Ending October 31, 1958
ORNL-2684	Molten-Salt Reactor Program Quarterly Progress Report, For Period Ending January 31, 1959
ORNL-2723	Molten-Salt Reactor Program Quarterly Progress Report, For Period Ending April 30, 1959
ORNL-2799	Molten-Salt Reactor Program Quarterly Progress Report, For Period Ending July 31, 1959
ORNL-2890	Molten-Salt Reactor Program Quarterly Progress Report, For Period Ending October 31, 1959
ORNL-2973	Molten-Salt Reactor Program Quarterly Progress Report, For Periods Ending January 31 and April 30, 1960
ORNL-3014	Molten-Salt Reactor Program Quarterly Progress Report, For Period Ending July 31, 1960
ORNL-3122	Molten-Salt Reactor Program Semiannual Progress Report, For Period Ending February 28, 1961
ORNL-3215	Molten-Salt Reactor Program Semiannual Progress Report, For Period Ending August 31, 1961
ORNL-3282	Molten-Salt Reactor Program Semiannual Progress Report, For Period Ending February 28, 1962
ORNL-3369	Molten-Salt Reactor Program Semiannual Progress Report, For Period Ending August 31, 1962
ORNL-3419	Molten-Salt Reactor Program Semiannual Progress Report, For Period Ending January 31, 1963
ORNL-3529	Molten-Salt Reactor Program Semiannual Progress Report, For Period Ending July 31, 1963
ORNL-3626	Molten-Salt Reactor Program Semiannual Progress Report, For Period Ending January 31, 1964
ORNL-3708	Molten-Salt Reactor Program Semiannual Progress Report, For Period Ending July 31, 1964
ORNL-3812	Molten-Salt Reactor Program Semiannual Progress Report, For Period Ending February 28, 1965

Report Number	Report Title
ORNL-3872	Molten-Salt Reactor Program Semiannual Progress Report, For Period Ending August 31, 1965
ORNL-3936	Molten-Salt Reactor Program Semiannual Progress Report, For Period Ending February 28, 1966
ORNL-4037	Molten-Salt Reactor Program Semiannual Progress Report, For Period Ending August 31, 1966
ORNL-4119	Molten-Salt Reactor Program Semiannual Progress Report, For Period Ending February 28, 1967
ORNL-4191	Molten-Salt Reactor Program Semiannual Progress Report, For Period Ending August 31, 1967
ORNL-4254	Molten-Salt Reactor Program Semiannual Progress Report, For Period Ending February 29, 1968
ORNL-4344	Molten-Salt Reactor Program Semiannual Progress Report, For Period Ending August 31, 1968
ORNL-4396	Molten-Salt Reactor Program Semiannual Progress Report, For Period Ending February 28, 1969
ORNL-4449	Molten-Salt Reactor Program Semiannual Progress Report, For Period Ending August 31, 1969
ORNL-4548	Molten-Salt Reactor Program Semiannual Progress Report, For Period Ending February 28, 1970
ORNL-4622	Molten-Salt Reactor Program Semiannual Progress Report, For Period Ending August 31, 1970
ORNL-4676	Molten-Salt Reactor Program Semiannual Progress Report, For Period Ending February 28, 1971
ORNL-4728	Molten-Salt Reactor Program Semiannual Progress Report, For Period Ending August 31, 1971
ORNL-4782	Molten-Salt Reactor Program Semiannual Progress Report, For Period Ending February 29, 1972
ORNL-4832	Molten-Salt Reactor Program Semiannual Progress Report, For Period Ending August 31, 1972
Not Published	Molten-Salt Reactor Program Semiannual Progress Report, For Period Ending February 28, 1973
Not Published	Molten-Salt Reactor Program Semiannual Progress Report, For Period Ending August 31, 1973
Not Published	Molten-Salt Reactor Program Semiannual Progress Report, For Period Ending February 28, 1974
ORNL-5011	Molten-Salt Reactor Program Semiannual Progress Report, For Period Ending August 31, 1974
ORNL-5047	Molten-Salt Reactor Program Semiannual Progress Report, For Period Ending February 28, 1975
ORNL-5078	Molten-Salt Reactor Program Semiannual Progress Report, For Period Ending August 31, 1975

Report Number	Report Title
ORNL-5132	Molten-Salt Reactor Program Semiannual Progress Report, For Period Ending February 29, 1976
Not Published	Molten-Salt Reactor Program Semiannual Progress Report, For Period Ending August 31, 1976

Table A-20. ORNL progress reports for the Chemical Technology Division, Unit Operations Section.

Report Number	Report Title
CF-55-1-94	Chemical Technology Division, Unit Operations Section, Monthly Progress Report, January 1955
CF-55-2-185	Chemical Technology Division, Unit Operations Section, Monthly Progress Report, February 1955
CF-55-3-190	Chemical Technology Division, Unit Operations Section, Monthly Progress Report, March 1955
CF-55-4-164	Chemical Technology Division, Unit Operations Section, Monthly Progress Report, April 1955
CF-55-5-176	Chemical Technology Division, Unit Operations Section, Monthly Progress Report, May 1955
CF-55-6-180	Chemical Technology Division, Unit Operations Section, Monthly Progress Report, June 1955
CF-55-7-138	Chemical Technology Division, Unit Operations Section, Monthly Progress Report, July 1955
CF-55-8-157	Chemical Technology Division, Unit Operations Section, Monthly Progress Report, August 1955
CF-55-9-150	Chemical Technology Division, Unit Operations Section, Monthly Progress Report, September 1955
CF-55-10-110	Chemical Technology Division, Unit Operations Section, Monthly Progress Report, October 1955
CF-55-11-176	Chemical Technology Division, Unit Operations Section, Monthly Progress Report, November 1955
CF-55-12-154	Chemical Technology Division, Unit Operations Section, Monthly Progress Report, December 1955
CF-56-1-175	Chemical Technology Division, Unit Operations Section, Monthly Progress Report, January 1956
CF-56-2-154	Chemical Technology Division, Unit Operations Section, Monthly Progress Report, February 1956
CF-56-3-116	Chemical Technology Division, Unit Operations Section, Monthly Progress Report, March 1956
CF-56-4-210	Chemical Technology Division, Unit Operations Section, Monthly Progress Report, April 1956
CF-56-5-197	Chemical Technology Division, Unit Operations Section, Monthly Progress Report, May 1956
CF-56-6-177	Chemical Technology Division, Unit Operations Section, Monthly Progress Report, June 1956
CF-56-7-150	Chemical Technology Division, Unit Operations Section, Monthly Progress Report, July 1956
CF-56-8-157	Chemical Technology Division, Unit Operations Section, Monthly Progress Report, August 1956
CF-56-9-127	Chemical Technology Division, Unit Operations Section, Monthly Progress Report, September 1956
CF-56-10-83	Chemical Technology Division, Unit Operations Section, Monthly Progress Report, October 1956
CF-56-11-143	Chemical Technology Division, Unit Operations Section, Monthly Progress Report, November 1956



<b>Report Number</b>	<b>Report Title</b>
CF-56-12-128	Chemical Technology Division, Unit Operations Section, Monthly Progress Report, December 1956
ORNL-2251	Chemical Technology Division, Monthly Progress Report, January 1957
ORNL-2270	Chemical Technology Division, Monthly Progress Report, February 1957
ORNL-2307	Chemical Technology Division, Monthly Progress Report, March 1957
ORNL-2324	Chemical Technology Division, Monthly Progress Report, April 1957
ORNL-2361	Chemical Technology Division, Monthly Progress Report, May 1957
ORNL-2362	Chemical Technology Division, Monthly Progress Report, June 1957
ORNL-2385	Chemical Technology Division, Monthly Progress Report, July 1957
ORNL-2400	Chemical Technology Division, Monthly Progress Report, August 1957
ORNL-2416	Chemical Technology Division, Monthly Progress Report, September 1957
ORNL-2417	Chemical Technology Division, Monthly Progress Report, October 1957
ORNL-2447	Chemical Technology Division, Monthly Progress Report, November 1957
ORNL-2468	Chemical Technology Division, Monthly Progress Report, December 1957
CF-58-1-137	Chemical Technology Division, Unit Operations Section, Monthly Progress Report, January 1958
CF-58-2-139	Chemical Technology Division, Unit Operations Section, Monthly Progress Report, February 1958
CF-58-3-71	Chemical Technology Division, Unit Operations Section, Monthly Progress Report, March 1958
CF-58-4-123	Chemical Technology Division, Unit Operations Section, Monthly Progress Report, April 1958
CF-58-5-50	Chemical Technology Division, Unit Operations Section, Monthly Progress Report, May 1958
CF-58-6-85	Chemical Technology Division, Unit Operations Section, Monthly Progress Report, June 1958
CF-58-7-126	Chemical Technology Division, Unit Operations Section, Monthly Progress Report, July 1958
CF-58-8-59	Chemical Technology Division, Unit Operations Section, Monthly Progress Report, August 1958
CF-58-9-62	Chemical Technology Division, Unit Operations Section, Monthly Progress Report, September 1958
CF-58-10-90	Chemical Technology Division, Unit Operations Section, Monthly Progress Report, October 1958
CF-59-5-1	Chemical Technology Division, Unit Operations Section, Monthly Progress Report, November 1958
CF-59-5-2	Chemical Technology Division, Unit Operations Section, Monthly Progress Report, December 1958
CF-59-1-74	Chemical Technology Division, Unit Operations Section, Monthly Progress Report, January 1959
CF-59-2-45	Chemical Technology Division, Unit Operations Section, Monthly Progress Report, February 1959
CF-59-3-61	Chemical Technology Division, Unit Operations Section, Monthly Progress Report, March 1959

<b>Report Number</b>	<b>Report Title</b>
CF-59-4-47	Chemical Technology Division, Unit Operations Section, Monthly Progress Report, April 1959
CF-59-5-47	Chemical Technology Division, Unit Operations Section, Monthly Progress Report, May 1959
CF-59-6-63	Chemical Technology Division, Unit Operations Section, Monthly Progress Report, June 1959
CF-59-7-58	Chemical Technology Division, Unit Operations Section, Monthly Progress Report, July 1959
CF-59-8-76	Chemical Technology Division, Unit Operations Section, Monthly Progress Report, August 1959
CF-59-9-69	Chemical Technology Division, Unit Operations Section, Monthly Progress Report, September 1959
CF-59-10-77	Chemical Technology Division, Unit Operations Section, Monthly Progress Report, October 1959
CF-59-11-54	Chemical Technology Division, Unit Operations Section, Monthly Progress Report, November 1959
CF-59-12-49	Chemical Technology Division, Unit Operations Section, Monthly Progress Report, December 1959
CF-60-1-49	Chemical Technology Division, Unit Operations Section, Monthly Progress Report, January 1960
CF-60-2-56	Chemical Technology Division, Unit Operations Section, Monthly Progress Report, February 1960
CF-60-3-61	Chemical Technology Division, Unit Operations Section, Monthly Progress Report, March 1960
CF-60-4-37	Chemical Technology Division, Unit Operations Section, Monthly Progress Report, April 1960
CF-60-5-58	Chemical Technology Division, Unit Operations Section, Monthly Progress Report, May 1960
CF-60-6-11	Chemical Technology Division, Unit Operations Section, Monthly Progress Report, June 1960
CF-60-7-46	Chemical Technology Division, Unit Operations Section, Monthly Progress Report, July 1960
CF-60-8-86	Chemical Technology Division, Unit Operations Section, Monthly Progress Report, August 1960
CF-60-9-43	Chemical Technology Division, Unit Operations Section, Monthly Progress Report, September 1960
CF-60-10-49	Chemical Technology Division, Unit Operations Section, Monthly Progress Report, October 1960
CF-60-11-38	Chemical Technology Division, Unit Operations Section, Monthly Progress Report, November 1960
CF-60-12-28	Chemical Technology Division, Unit Operations Section, Monthly Progress Report, December 1960
CF-61-1-27	Chemical Technology Division, Unit Operations Section, Monthly Progress Report, January 1961
CF-61-2-65	Chemical Technology Division, Unit Operations Section, Monthly Progress Report, February 1961

<b>Report Number</b>	<b>Report Title</b>
CF-61-3-67	Chemical Technology Division, Unit Operations Section, Monthly Progress Report, March 1961
ORNL-TM-32	Chemical Technology Division, Unit Operations Section, Monthly Progress Report, Period Ending April 1961
ORNL-TM-33	Chemical Technology Division, Unit Operations Section, Monthly Progress Report, Period Ending May 1961
ORNL-TM-34	Chemical Technology Division, Unit Operations Section, Monthly Progress Report, Period Ending June 1961
ORNL-TM-35	Chemical Technology Division, Unit Operations Section, Monthly Progress Report, Period Ending July 1961
ORNL-TM-65	Chemical Technology Division, Unit Operations Section, Monthly Progress Report, Period Ending August 1961
ORNL-TM-112	Chemical Technology Division, Unit Operations Section, Monthly Progress Report, Period Ending September 1961
ORNL-TM-121	Chemical Technology Division, Unit Operations Section, Monthly Progress Report, Period Ending October 1961
ORNL-TM-122	Chemical Technology Division, Unit Operations Section, Monthly Progress Report, Period Ending November 1961
ORNL-TM-136	Chemical Technology Division, Unit Operations Section, Monthly Progress Report, Period Ending December 1961
ORNL-TM-150	Chemical Technology Division, Unit Operations Section, Monthly Progress Report, Period Ending January 1962
ORNL-TM-157	Chemical Technology Division, Unit Operations Section, Monthly Progress Report, Period Ending February 1962
ORNL-TM-222	Chemical Technology Division, Unit Operations Section, Monthly Progress Report, Period Ending March 1962
ORNL-TM-292	Chemical Technology Division, Unit Operations Section, Monthly Progress Report, Period Ending April 1962
ORNL-TM-297	Chemical Technology Division, Unit Operations Section, Monthly Progress Report, Period Ending May 1962
ORNL-TM-313	Chemical Technology Division, Unit Operations Section, Monthly Progress Report, Period Ending June 1962
ORNL-TM-343	Chemical Technology Division, Unit Operations Section, Monthly Progress Report, Period Ending July 1962
ORNL-TM-355	Chemical Technology Division, Unit Operations Section, Monthly Progress Report, Period Ending August 1962
ORNL-TM-410	Chemical Technology Division, Unit Operations Section, Monthly Progress Report, Period Ending September 1962
ORNL-TM-412	Chemical Technology Division, Unit Operations Section, Monthly Progress Report, Period Ending October 1962
ORNL-TM-441	Chemical Technology Division, Unit Operations Section, Monthly Progress Report, Period Ending November 1962
ORNL-TM-453	Chemical Technology Division, Unit Operations Section, Monthly Progress Report, Period Ending December 1962
ORNL-TM-541	Chemical Technology Division, Unit Operations Section, Monthly Progress Report, Period Ending January 1963

<b>Report Number</b>	<b>Report Title</b>
ORNL-TM-581	Chemical Technology Division, Unit Operations Section, Monthly Progress Report, Period Ending February 1963
ORNL-TM-586	Chemical Technology Division, Unit Operations Section, Monthly Progress Report, Period Ending March 1963
ORNL-TM-608	Chemical Technology Division, Unit Operations Section, Monthly Progress Report, Period Ending April 1963
ORNL-TM-613	Chemical Technology Division, Unit Operations Section, Monthly Progress Report, Period Ending May 1963
ORNL-TM-628	Chemical Technology Division, Unit Operations Section, Monthly Progress Report, Period Ending June 1963
ORNL-TM-642	Chemical Technology Division, Unit Operations Section, Monthly Progress Report, Period Ending July 1963
ORNL-TM-776	Chemical Technology Division, Unit Operations Section, Monthly Progress Report, Period Ending August 1963
ORNL-TM-785	Chemical Technology Division, Unit Operations Section, Monthly Progress Report, Period Ending September 1963
ORNL-TM-823	Chemical Technology Division, Unit Operations Section, Monthly Progress Report, Period Ending October 1963
ORNL-TM-756	Chemical Technology Division, Unit Operations Section, Monthly Progress Report, Period Ending November 1963
ORNL-TM-775	Chemical Technology Division, Unit Operations Section, Monthly Progress Report, Period Ending December 1963
ORNL-TM-798	Chemical Technology Division, Unit Operations Section, Monthly Progress Report, Period Ending January 1964
ORNL-TM-836	Chemical Technology Division, Unit Operations Section, Monthly Progress Report, Period Ending February 1964
ORNL-TM-887	Chemical Technology Division, Unit Operations Section, Monthly Progress Report, Period Ending March 1964
ORNL-TM-886	Chemical Technology Division, Unit Operations Section, Monthly Progress Report, Period Ending April 1964
ORNL-TM-937	Chemical Technology Division, Unit Operations Section, Monthly Progress Report, Period Ending May 1964
ORNL-TM-963	Chemical Technology Division, Unit Operations Section, Monthly Progress Report, Period Ending June 1964
	Chemical Technology Division, Unit Operations Section, Monthly Progress Report, Period Ending July 1964
ORNL-TM-1027	Chemical Technology Division, Unit Operations Section, Monthly Progress Report, Period Ending August 1964
ORNL-TM-1027	Chemical Technology Division, Unit Operations Section, Monthly Progress Report, Period Ending September 1964
ORNL-TM-1069	Chemical Technology Division, Unit Operations Section, Monthly Progress Report, Period Ending October 1964
ORNL-TM-1090	Chemical Technology Division, Unit Operations Section, Monthly Progress Report, Period Ending November 1964
ORNL-TM-1091	Chemical Technology Division, Unit Operations Section, Monthly Progress Report, Period Ending December 1964

<b>Report Number</b>	<b>Report Title</b>
ORNL-TM-1092	Chemical Technology Division, Unit Operations Section, Monthly Progress Report, Period Ending January 1965
ORNL-TM-1094	Chemical Technology Division, Unit Operations Section, Monthly Progress Report, Period Ending February 1965
ORNL-TM-1103	Chemical Technology Division, Unit Operations Section, Monthly Progress Report, Period Ending March 1965
ORNL-3868	Chemical Technology Division, Unit Operations Section, Quarterly Progress Report, Period Ending June 1965
ORNL-3916	Chemical Technology Division, Unit Operations Section, Quarterly Progress Report, Period Ending September 1965
ORNL-3958	Chemical Technology Division, Unit Operations Section, Quarterly Progress Report, Period Ending December 1965
ORNL-3995	Chemical Technology Division, Unit Operations Section, Quarterly Progress Report, Period Ending March 1966
ORNL-4074	Chemical Technology Division, Unit Operations Section, Quarterly Progress Report, Period Ending June 1966
ORNL-4075	Chemical Technology Division, Unit Operations Section, Quarterly Progress Report, Period Ending September 1966
ORNL-4094	Chemical Technology Division, Unit Operations Section, Quarterly Progress Report, Period Ending December 1966
ORNL-4139	Chemical Technology Division, Unit Operations Section, Quarterly Progress Report, Period Ending March 1967
ORNL-4204	Chemical Technology Division, Unit Operations Section, Quarterly Progress Report, Period Ending June 1967
ORNL-4234	Chemical Technology Division, Unit Operations Section, Quarterly Progress Report, Period Ending September 1967
ORNL-4235	Chemical Technology Division, Unit Operations Section, Quarterly Progress Report, Period Ending December 1967
ORNL-4364	Chemical Technology Division, Unit Operations Section, Quarterly Progress Report, Period Ending March 1968
ORNL-4365	Chemical Technology Division, Unit Operations Section, Quarterly Progress Report, Period Ending June 1968
ORNL-4366	Chemical Technology Division, Unit Operations Section, Quarterly Progress Report, Period Ending September 1968

Table A-21. Annual progress reports for the ORNL Chemical Technology Division.

Report Number	Report Title
ORNL-2788	Chemical Technology Division, Annual Progress Report, Period Ending August 31, 1959
ORNL-2993	Chemical Technology Division, Annual Progress Report, Period Ending August 31, 1960
ORNL-3153	Chemical Technology Division, Annual Progress Report, Period Ending May 31, 1961
ORNL-3314	Chemical Technology Division, Annual Progress Report, Period Ending June 30, 1962
ORNL-3452	Chemical Technology Division, Annual Progress Report, Period Ending May 31, 1963
ORNL-3627	Chemical Technology Division, Annual Progress Report, Period Ending May 31, 1964
ORNL-3830	Chemical Technology Division, Annual Progress Report, Period Ending May 31, 1965
ORNL-3945	Chemical Technology Division, Annual Progress Report, Period Ending May 31, 1966
ORNL-4145	Chemical Technology Division, Annual Progress Report, Period Ending May 31, 1967
ORNL-4272	Chemical Technology Division, Annual Progress Report, Period Ending May 31, 1968
ORNL-4422	Chemical Technology Division, Annual Progress Report, Period Ending May 31, 1969
ORNL-4572	Chemical Technology Division, Annual Progress Report, Period Ending May 31, 1970
ORNL-4682	Chemical Technology Division, Annual Progress Report, Period Ending March 31, 1971
ORNL-4794	Chemical Technology Division, Annual Progress Report, Period Ending March 31, 1972
ORNL-4883	Chemical Technology Division, Annual Progress Report, Period Ending March 31, 1973
ORNL-4966	Chemical Technology Division, Annual Progress Report, Period Ending March 31, 1974
ORNL-5050	Chemical Technology Division, Annual Progress Report, Period Ending March 31, 1975
ORNL-5172	Chemical Technology Division, Annual Progress Report, Period Ending March 31, 1976
ORNL-5295	Chemical Technology Division, Annual Progress Report, Period Ending March 31, 1977
ORNL-5383	Chemical Technology Division, Annual Progress Report, Period Ending March 31, 1978
ORNL-5542	Chemical Technology Division, Annual Progress Report, Period Ending March 31, 1979

Table A-22. Annual progress reports for the ORNL Reactor Chemistry Division.

<b>Report Number</b>	<b>Report Title</b>
ORNL-2931	Reactor Chemistry Division Annual Progress Report, For Period Ending January 31, 1960
ORNL-3127	Reactor Chemistry Division Annual Progress Report, For Period Ending January 31, 1961
ORNL-3262	Reactor Chemistry Division Annual Progress Report, For Period Ending January 31, 1962
ORNL-3417	Reactor Chemistry Division Annual Progress Report, For Period Ending January 31, 1963
ORNL-3591	Reactor Chemistry Division Annual Progress Report, For Period Ending January 31, 1964
ORNL-3789	Reactor Chemistry Division Annual Progress Report, For Period Ending January 31, 1965
ORNL-3913	Reactor Chemistry Division Annual Progress Report, For Period Ending December 31, 1965
ORNL-4076	Reactor Chemistry Division Annual Progress Report, For Period Ending December 31, 1966
ORNL-4229	Reactor Chemistry Division Annual Progress Report, For Period Ending December 31, 1967
ORNL-4400	Reactor Chemistry Division Annual Progress Report, For Period Ending December 31, 1968
Not Published	Reactor Chemistry Division Annual Progress Report, For Period Ending December 31, 1969
ORNL-4586	Reactor Chemistry Division Annual Progress Report, For Period Ending May 31, 1970
ORNL-4717	Reactor Chemistry Division Annual Progress Report, For Period Ending May 31, 1971
ORNL-4801	Reactor Chemistry Division Annual Progress Report, For Period Ending May 31, 1972

Table A-23. Reports evaluating nuclear reactor technologies.

Date	Report Number	Report Title
Feb-59	TID-8507	Report of the Fluid Fuel Reactors Task Force to the Division of Reactor Development United States Atomic Energy Commission
Oct-59	ATL-A-102	An Evaluation of Mercury Cooled Breeder Reactors
May-61	ANL-6360	Organic Nuclear Reactors: An Evaluation of Current Development Programs
1962	1962-RTP-USAEC	Civilian Nuclear Power: A Report to the President - 1962, U.S. Atomic Energy Commission
1967	1967-RTP-USAEC	Civilian Nuclear Power: The 1967 Supplement to the 1962 Report to the President, U.S. Atomic Energy Commission
Jan-67	ORNL-3921	An Evaluation of Heavy Water-Moderated Organic-Cooled Reactors
Jan-67	1967-ARTC-AEC	Annual Report to Congress of the Atomic Energy Commission
Jun-67	AI-CE-87	Heavy Water Organic Cooled Reactor: Status and Potential
Jan-68	1968-ARTC-AEC	Annual Report to Congress of the Atomic Energy Commission
Apr-68	WASH-1083	An Evaluation of Heavy Water-Moderated Organic-Cooled Reactors (OUO Draft)
Dec-69	WASH-1085	An Evaluation of High Temperature Gas-Cooled Reactors
	WASH-1086	An Evaluation of Heavy Water-Moderated Boiling Light Water-Cooled Reactors
Apr-69	WASH-1087	An Evaluation of Advanced Converter Reactors
Apr-69	WASH-1088	An Evaluation of Steam-Cooled Fast Breeder Reactors
Apr-69	WASH-1090	An Evaluation of Alternate Coolant Fast Breeder Reactors
Jun-69	WASH-1097	The Use of Thorium in Nuclear Power Reactors
	WASH-1098	Potential Nuclear Power Growth Patterns
Apr-69	WASH-1126	Cost-Benefit Analysis of the U.S. Breeder Reactor Program
Jan-72	WASH-1184	Updated (1970) Cost-Benefit Analysis of the U.S. Breeder Reactor Program
Sep-72	WASH-1222	An Evaluation of the Molten Salt Breeder Reactor
Jul-75	ORNL-4995	An Assessment of Industrial Energy Options Based on Coal and Nuclear Systems
Jan-77	ORNL-TM-5565	Assessment of the Thorium Fuel Cycle in Power Reactors
Mar-08	RS22542	CRS Report to Congress: Nuclear Fuel Reprocessing: U.S. Policy Development



Table A-24. External publications on MSR technologies by ORNL research staff.

E. S. Bettis, R. W. Schroeder, G. A. Cristy, H. W. Savage, R. G. Affel, L. F. Hemphill; The Aircraft Reactor Experiment-Design and Construction; Nuclear Science and Engineering: 2, 804-825 (1957).
W. K. Ergen, A. D. Callihan, C. B. Mills, D. Scott; The Aircraft Reactor Experiment-Physics; Nuclear Science and Engineering: 2, 826-840 (1957).
E. S. Bettis, W. B. Cottrell, E. R. Mann, J. L. Meem, G. D. Whitman; The Aircraft Reactor Experiment-Operation; Nuclear Science and Engineering: 2, 841-853 (1957).
R. C. Briant, A. M. Weinberg; Molten Fluoride as Power Reactor Fuels; Nuclear Science and Engineering: 2, 797-803 (1957).
G. I. Cathers; Uranium Recovery from Spent Fuel by Dissolution in Fused Salt and Fluorination; Nuclear Science and Engineering: 2, 768 (1957).
J. A. Lane, H. G. MacPherson, F. Maslan, Editors; Fluid Fuel Reactors; Addison-Wesley Publishing Company, Inc., Reading, Massachusetts (1958).
W. H. Carr; Volatility Processing of the ARE Fuel; Chemical Engineering Symposium Series: 56, 28 (1960).
C. J. Barton, R. A. Strehlow; Phase Relations in the System LiF-PuF <sub>3</sub> ; Journal of Inorganic and Nuclear Chemistry: 18, 143-147 (1961).
C. J. Barton, J. D. Redman, R. A. Strehlow; Phase Equilibria in the Systems NaF-PuF <sub>3</sub> and NaF-CeF <sub>3</sub> ; Journal of Inorganic and Nuclear Chemistry: 20, 45-52 (1961).
W. D. Powers, S. I. Cohen, N. D. Greene; Physical Properties of Molten Reactor Fuels and Coolants; Nuclear Science and Engineering: 71, 200-211 (1963).
L. G. Alexander; Molten-Salt Fast Reactors; Conference Proceedings, Economics and Safety in Large Fast Power Reactors, Argonne National Laboratory, ANL-6792, October 7-10, 1963.
M. J. Kelly; Removal of Rare Earth Fission Products from Molten-Salt Reactor Fuels by Distillation; Transactions of the American Nuclear Society: 8, 171 (1965).
H. F. Bauman, P. R. Kasten; Fuel-Cycle Analysis of Molten-Salt Breeder Reactors; Nuclear Applications: 2, 287-293 (1966).
J. M. Chandler, R. B. Lindauer; Preparation and Processing of MSRE Fuel; Symposium on Reprocessing of Nuclear Fuels, The Metallurgical Society of AIME, Iowa State University, Ames, Iowa, August 25-27, 1969; Nuclear Metallurgy: 15, 97-120 (1969).
M. E. Whatley, L. E. McNeese, W. L. Carter, L. M. Ferris, E. L. Nicholson; Engineering Development of the MSBR Fuel Cycle; Symposium on Reprocessing of Nuclear Fuels, The Metallurgical Society of AIME, Iowa State University, Ames, Iowa, August 25-27, 1969; Nuclear Metallurgy: 15, 121-122 (1969).
R. G. Ross, W. R. Grimes, C. J. Barton, C. E. Bamberger, C. F. Baes; The Reductive Extraction of Protactinium and Uranium from Molten LiF-BeF <sub>2</sub> -ThF <sub>4</sub> Mixtures into Bismuth; Symposium on Reprocessing of Nuclear Fuels, The Metallurgical Society of AIME, Iowa State University, Ames, Iowa, August 25-27, 1969; Nuclear Metallurgy: 15, 363-374 (1969).
J. H. Shaffer, D. M. Moulton, W. R. Grimes; The Reductive Extraction of Rare Earths from Molten LiF-BeF <sub>2</sub> -ThF <sub>4</sub> Mixtures into Bismuth; Symposium on Reprocessing of Nuclear Fuels, The Metallurgical Society of AIME, Iowa State University, Ames, Iowa, August 25-27, 1969; Nuclear Metallurgy: 15, 375-384 (1969).
M. W. Rosenthal, P. R. Kasten, R. B. Briggs; Molten-Salt Reactors - History, Status, and Potential; Nuclear Applications & Technology: 8, 107-117 (1970).
P. N. Haubenreich, J. R. Engel; Experience With the Molten-Salt Reactor Experiment; Nuclear Applications & Technology: 8, 118-136 (1970).
W. R. Grimes; Molten-Salt Reactor Chemistry; Nuclear Applications & Technology: 8, 137-155 (1970).

H. E. McCoy, et al.; New Development in Materials for Molten-Salt Reactor; Nuclear Applications & Technology: 8, 156-169 (1970).
M. E. Whatley, L. E. McNeese, W. L. Carter, L. M. Ferris, E. L. Nicholson; Engineering Development of the MSBR Fuel Recycle; Nuclear Applications & Technology: 8, 170-178 (1970).
E. P. Eatherly, D. Scott; Graphite and Xenon Behavior and Influence on MSBR Design; Nuclear Applications & Technology: 8, 179-189 (1970).
E. S. Bettis, R. C. Robertson; The Design and Performance Features of a Single-Fluid Molten-Salt Reactor; Nuclear Applications & Technology: 8, 190-207 (1970).
A. M. Perry, H. F. Bauman; Reactor Physics and Fuel-Cycle Analyses; Nuclear Applications & Technology: 8, 208-219 (1970).
L. M. Ferris, J. C. Mailen, J. J. Lawrence, F. J. Smith, E. D. Nogueira; Equilibrium Distribution of Actinide and Lanthanide Elements Between Molten Fluoride Salts and Liquid Bismuth Solution; Journal of Inorganic Nuclear Chemistry: 32, 2019-2035 (1970).
J. C. Mailen, F. J. Smith, L. M. Ferris; Solubility of $\text{PuF}_3$ in Molten $2 \text{ LiF-BeF}_2$ ; Journal of Chemical and Engineering Data: 16, 68-69 (1971).
L. E. McNeese, L. M. Ferris; Molten-Salt Breeder Reactor Fuel Processing; Transactions of the American Nuclear Society: 14, 84-85 (1971).
L. E. McNeese, L. M. Ferris, E. L. Nicholson; Molten-Salt Breeder Reactor Fuel Processing; 72 <sup>nd</sup> National Meeting of the American Institute of Chemical Engineers, St. Louis, Missouri, May 21, 1972.
A. M. Perry, A. M. Weinberg; Thermal Breeder Reactors; Annual Review of Nuclear and Particle Science: 22, 317-354 (1972).
P. N. Haubenreich; Molten-Salt Reactors - Concepts and Technology; Journal of the British Nuclear Energy Society: 12, 145-152 (1973).
R. G. Ross, C. E. Bamberger, C. F. Baes; The Oxide Chemistry of Protactinium in Molten Fluorides; Journal of Inorganic Nuclear Chemistry: 35, 433-449 (1973).
C. F. Baes; The Chemistry and Thermodynamics of Molten Salt Reactor Fuels; Journal of Nuclear Materials: 51, 149-162 (1974).
M. R. Bennett, L. M. Ferris; Formation of U(V) in a Molten Fluoride Salt at 550-650°C by Reaction of Gaseous $\text{UF}_6$ with Dissolved $\text{UF}_4$ ; Journal of Inorganic & Nuclear Chemistry: 36, 1285-1290 (1974).
J. W. Koger; Corrosion Product Deposition in Molten Fluoride Salt Systems; Corrosion: 30, 125-130 (1974).
J. R. Hightower; Process Technology for the Molten-Salt Reactor $^{233}\text{U}$ -Th Cycle; ANS 1975 Winter Meeting, San Francisco, California, November 16-21, 1975.
C. F. Baes, R. P. Wichner, C. E. Bamberger, B. F. Freasier; Removal of Iodine from $\text{LiF-BeF}_2$ Melts by $\text{HF-H}_2$ Sparging - Application to Iodine Removal from Molten-Salt Breeder Reactor Fuel; Nuclear Science and Engineering: 56, 399-410 (1975).
J. R. Engel, H. T. Kerr, E. J. Allen; Nuclear Characteristics of a 1000-MW(e) Molten-Salt Breeder Reactor; Transactions of the American Nuclear Society: 22, 705-706 (1975).
A. M. Perry; Molten-Salt Converter Reactors; Annals of Nuclear Energy: 2, 809-818 (1975).
J. R. Engel, I Spiewak; Molten-Salt Reactors for Efficient Nuclear-Fuel Utilization Without Plutonium Separation; Transactions of the American Nuclear Society: 27, 431-432 (1977).
W. R. Grimes; Molten Fluoride Mixtures as Possible Fission Reactor Fuels; The Electrochemical Society Meeting, Oak Ridge, Tennessee, May 21-25, 1978.
L. M. Toth, B. F. Hitch; Telluride Ion Chemistry in Molten-Salts; Inorganic Chemistry: 17, 2207-2211 (1978).

J. R. Engel, W. A. Rhoades, W. R. Grimes, J. F. Dearing; Molten-Salt Reactors for Efficient Nuclear Fuel Utilization without Plutonium Separation; Nuclear Technology: 46, 30-43 (1979).
J. R. Keiser, J. H. Devan, E. J. Lawrence; Compatibility of Molten-Salts with Type 316 Stainless Steel and Lithium; Journal of Nuclear Materials: 85-6, 295-298 (1979).
H. G. MacPherson; The Molten Salt Reactor Adventure; Nuclear Science and Engineering: 90, 374-380 (1985).
U. Gat, J. R. Engel; Molten-Salt Reactors for Burning Dismantled Weapons Fuel; Nuclear Technology: 100, 390-394 (1992).
L. M. Toth, U. Gat, G. D. Del Cul, S. Dai, D. F. Williams; Review of ORNL's MSR Technology and Status; International Conference on Accelerator-Driven Transmutation Technologies and Applications, Kalmar, Sweden, June 3-7, 1996.
D. F. Hallenbach, C. M. Hopper; Criticality Safety Considerations for MSRE Fuel Drain Tank Uranium Aggregation; Conference Proceedings, Topical Meeting on Criticality Safety Challenges in the Next Decade, Chelon, Washington, September 7-11, 1997.
U. Gat, H. L. Dodds; Molten Salt Reactors - Safety Options Galore; International Topical Meeting on Advanced Reactors Safety (ARS 97), Orlando, Florida, June 1-5, 1997.
U. Gat; Safe Actinide Disposition in Molten Salt Reactors; International Topical Meeting on Advanced Reactors Safety (ARS 97), Orlando, Florida, June 1-5, 1997.
U. Gat, J. R. Engel; Non-Proliferation Attributes of Molten Salt Reactors; Nuclear Engineering and Design: 201, 327-334 (2000).
G. D. Del Cul, A. S. Icenhour, D. W. Simmons, L. D. Trowbridge, D. F. Williams, L. M. Toth, S. Dai; Overview of the Recovery and Processing of <sup>233</sup> U from the Oak Ridge Molten Salt Reactor Experiment (MSRE) Remediation Activities; Global 2001, Paris, France, September 9-13, 2001.
G. D. Del Cul, A. S. Icenhour, D. W. Simmons; Development of the Process for the Recovery and Conversion of (UF <sub>6</sub> )-U <sup>233</sup> in NaF Traps from the Molten Salt Reactor Remediation Project; Nuclear Technology: 136, 89-98 (2001).
M. H. Haghighi, M. K. Ford, R. M. Szozda, and M. R. Jugan; Waste Stream Generated and Waste Disposal Plans for Molten Salt Reactor Experiment at Oak Ridge National Laboratory; WM'02 Conference, Tucson, Arizona, February 24-28, 2002.
D. F. Williams, D. F. Wilson, J. E. Keiser, L. M. Toth, J. Caja; Research on Molten Fluorides as High Temperature Heat Transfer Agents; Global 2003, New Orleans, Louisiana, November 16-20, 2003.
C. W. Forsberg; Molten-Salt Cooled Advanced High-Temperature Reactor for Production of Hydrogen and Electricity; Nuclear Technology: 144, 289-302 (2003).
C. W. Forsberg, P. F. Peterson, H. Zhao; An Advanced Molten Salt Reactor Using High-Temperature Reactor Technology; 2004 International Congress on Advances in Nuclear Power Plants (ICAPP '04), Pittsburgh, Pennsylvania, June 13-17, 2004.
C. Forsberg; The Advanced High-Temperature Reactor: High-Temperature Fuel, Liquid Salt Cooled, Liquid-Metal Reactor Plant; Progress in Nuclear Energy: 47, 32-43 (2005).
C. W. Forsberg; Molten Salt Reactor Technology Gaps; 2006 International Congress on Advances in Nuclear Power Plants (ICAPP '06), Reno, Nevada, June 4-8, 2006.
C. W. Forsberg; Thermal and Fast-Spectrum Molten Salt Reactors for Actinide Burning and Fuel Production; Proceedings of Global 07, Boise, Idaho, September 9-13, 2007.
D. F. Williams, K. T. Clarno; Evaluation of Salt Coolants for Reactor Applications; Nuclear Technology: 163, 330-343 (2008).
J. Serp, et al.; The Molten Salt Reactor (MSR) in Generation IV: Overview and Perspective; Progress in Nuclear Energy: 77, 308-319 (2014).

J. C. Gehin, J. J. Powers; Liquid Fuel Molten Salt Reactors for Thorium Utilization; Nuclear Technology: 194, 152-161 (2016).
B. R. Betzler, J. J. Powers, A. Worrall; Molten Salt Reactor Neutronics and Fuel Cycle Modeling and Simulation with SCALE; Annals of Nuclear Energy: 101, 489-503 (2017).
N. R. Brown, B. R. Betzler, J. J. Carbajo, A. J. Wysocki, M. S. Greenwood, C. Gentry, A. L. Qualls; Preconceptual Design of a Fluoride High Temperature Salt-Cooled Engineering Demonstration Reactor: Core Design and Safety Analysis; Annals of Nuclear Energy: 103, 49-59 (2017).
A. L. Qualls, B. R. Betzler, N. R. Brown, J. J. Carbajo, M. S. Greenwood, R. Hale, T. J. Harrison, J. J. Powers, K. R. Robb, J. Terrell; Preconceptual Design of a Fluoride High Temperature Salt-Cooled Engineering Demonstration Reactor: Motivation and Overview; Annals of Nuclear Energy: 107, 144-155 (2017).

Table A-25. Bibliographies related to MSR technologies.

Date	Report Number	Report Title
Mar-57	CF-57-3-153	Bibliography-Nuclear Reactor Fuel Processing
Jul-57	CF-57-7-110	Bibliography on Radiochemical Processing of Irradiated Fuel Elements
Oct-58	CF-58-10-60	Survey of Low Enrichment Molten-Salt Reactors
Feb-59	CF-59-2-46	Summary Statement and Bibliography of Liquid-Metal Technology Developed at the Oak Ridge National Laboratory
Sep-63	CF-63-9-20	A Literature Survey of Thermal and Physical Properties of Molten Fluoride and Chloride Salt Mixtures (EOMSR-2)
Apr-64	ORNL-TM-800	Bibliography of Rover Fuel Processing and Molten Salt Fluoride Volatility Process Development Studies at Oak Ridge National Laboratory
Sep-65	ANL-7092	Catalog of Nuclear Reactor Concepts. Part I. Homogenous and Quasi-Homogenous Reactors. Section III. Reactors Fueled with Molten-Salt Solutions
Dec-71	ORNL-TM-3595	Indexed Abstracts of Selected References on Molten-Salt Reactor Technology
Mar-74	ORNL-TM-4497	Heat Transfer and Fluid Flow Bibliography
May-96		B. J. Snyder; Aircraft Nuclear Propulsion: An Annotated Bibliography; Prepared for the United States Air Force History and Museums Program